Point-of-Care medical device development for high sensitivity multiplexed detection of blood biomarkers for health care management of cardiac patients

Mathilde Aubret

THÈSE

Pour obtenir le grade de

DOCTEUR DE L'UNIVERSITÉ GRENOBLE ALPES

École doctorale : PHYS - Physique
Spécialité : Physique pour les Sciences du Vivant
Unité de recherche : Laboratoire d'Electronique et de Technologie de l'Information (LETI)

Développement d'un dispositif médical pour la détection simultanée haute sensibilité de biomarqueurs sanguins pour la prise en charge terrain des patients en souffrance cardiaque

Point-of-Care medical device development for high sensitivity multiplexed detection of blood biomarkers for health care management of cardiac patients

Présentée par :

Mathilde AUBRET

Direction de thèse :

Arnaud BUHOT DIRECTEUR DE RECHERCHE, CEA CENTRE DE GRENOBLE	Directeur de thèse
Myriam CUBIZOLLES	Co-encadrant de thèse

Rapporteurs :

MAGALIE FAIVRE
CHARGEE DE RECHERCHE HDR, CNRS DELEGATION RHONE AUVERGNE
FRANCK MOLINA
DIRECTEUR DE RECHERCHE, CNRS DELEGATION OCCITANIE EST

Thèse soutenue publiquement le **5 octobre 2023**, devant le jury composé de :

MAGALIE FAIVRE CHARGEE DE RECHERCHE HDR, CNRS DELEGATION RHONE AUVERGNE	Rapporteure
FRANCK MOLINA DIRECTEUR DE RECHERCHE, CNRS DELEGATION OCCITANIE EST	Rapporteur
EMMANUEL DELAMARCHE SENIOR SCIENTIST, SPIDEN	Examinateur
FRANZ BRUCKERT PROFESSEUR DES UNIVERSITES, GRENOBLE INP	Président
CORINNE RAVELET PROFESSEURE DES UNIVERSITES, UNIVERSITE GRENOBLE ALPES	Examinatrice

Invités :

JEAN-BAPTISTE BOUCHET
CHU DE SAINT ETIENNE

Contents

Remerciements

Pour commencer, je souhaite remercier toutes les personnes qui ont fait partie de l'aventure de ces trois dernières années.

Je remercie sincèrement les membres du jury qui ont accepté d'évaluer ce travail de thèse. Madame Faivre et Monsieur Molina qui ont accepté d'être rapporteurs de ce travail de thèse, pour votre lecture attentive du manuscrit, vos retours éclairés et nos discussions passionnantes. Madame Ravelet et Monsieur Bruckert pour l'intérêt que vous avez porté à ce projet et son suivi durant les trois années, ainsi que tous les conseils et discussions pertinentes que nous avons pu avoir. Enfin, Monsieur Delamarche pour le fort intérêt que vous portez à ce projet.

Tous les travaux présentés dans ce manuscrit n'auraient pas pu voir le jour sans tout l'aide et le travail des équipes et techniciens du DTBS et du SyMMES, en particulier les laboratoires LSMB, PRISM et CREAB. Je tiens donc à remercier Fabrice Navarro, chef du service SEMIV, Jean-Maxime Roux, chef du laboratoire LSMB et Yanxia Hou, cheffe du laboratoire CREAB, pour leurs accueils dans les laboratoires respectifs, pour m'avoir fourni les moyens matériels et financier et pour avoir veillé au bon déroulement de ce projet.

Je remercie très sincèrement mes encadrants Arnaud Buhot et Myriam Cubizolles pour leur accompagnement de grande qualité durant ces trois ans de travail. Votre soutien sans faille m'a fait continuellement explorer de nouvelles pistes et donné de l'enthousiasme pour toujours aller plus loin dans mes recherches. Vous avez donné du sens et de l'humanité à ce projet pas toujours facile à mener. Je vous remercie de m'avoir transmis vos nombreuses connaissances et partagé votre savoir faire et curiosité pour la recherche scientifique et technologique. Je suis consciente de la chance que j'ai eu de réaliser ce projet de thèse à vos côtés et je vous remercie sincèrement.

Je remercie personnelement le docteur Jean-Baptiste Bouchet du CHU de Saint-Etienne pour la collaboration sur ce projet, l'opportunité de se confronter aux besoins et aux usages cliniques, et toutes ces discussions passionantes sur les pratiques en terme de diagnostic des maladies cardiaques. Je remercie également Jean Breton et le groupe d'étudiants du master GEM diagnostic in vitro pour leur implication sur la partie applicative du projet.

Je remercie chaleureusement toutes les personnes avec qui j'ai pu travailler durant ces trois années au CEA. Un grand merci à Christine Saint-Pierre, Yoann Roupioz, Patricia Laurent, Charlotte Parent et Yves Fouillet pour leur implication sur ce projet de thèse. Votre aide et vos conseils avisés m'ont permis d'élargir mon champ de compétences et de connaissances et de faire avancer mon projet. Merci également à Hélène Jousset et Jessica VanDesteen pour vos contributions pour ce projet. Hélène tu as posé les premières briques de l'intégration microfluidique qui ont mené sur la fin du projet à de très beaux résultats, merci.

Merci Christine pour ton accueil sur la plateforme BioMade, et ton aide précieuse dans les différentes manips pas toujours faciles à mettre en place, ta patience et ta persévérance. J'ai appris énormément à tes cotés et je t'en remercie. Merci également pour toutes ces pauses déjeuners et café discussion. Je remercie Anne-Gaëlle Bourdat, Mélissa Baque et Hugo Ben-

detricth pour vos conseils avisés sur les protocoles LAMP et votre intérêt pour cette partie du projet. Un grand merci à Yves Fouillet et Charlotte Parent pour votre expertise en microfluidique qui ont permis de développer une grande partie ambitieuse de ce projet de thèse. Merci pour toute votre aide, vos conseils et discussions techniques et autre qui ont permis l'intégration des protocoles. Merci également pour les discussions techniques vélos, randonnée ou ski et les sorties associées. Vous avez été d'un grand et précieux soutien sur ces trois années.

Je tiens également à remercier Patricia avec qui nous avons mené de longues investigations sur ces protocoles biologiques longs et complexes. Je n'aurais pu espérer une meilleure aide et un meilleur soutien même dans les moments difficiles. Ces moments en manip ont également été des moments de partage, de conseils en biologie, mais aussi en tout genre (ski, ballade, voyage...). Merci pour ton enthousiasme, tous ces sms envoyés à 18h pour se tenir au courant des derniers résultats resteront gravés. Merci aussi de m'avoir fait confiance et prêté ta maison pendant deux semaines à Autrans, je pense que ce fut les deux meilleures semaines de ma période de rédaction. Merci également à Xavier qui a toujours été moteur pour apporter des idées pour améliorer mon montage optique.

Merci à toute l'équipe microfabrication du laboratoire PRISM (SEMIV). Merci à Nicolas Verplanck pour toute la formation microfluidique, depuis la conception et standardisation jusqu'à la fabrication. Merci à François et Romain, d'avoir consacré du temps pour la fabrication des cartes parfois à partir de CAO loufoques.... Merci à Joris pour les formations et conseils en dessin Solidworks, il faut dire que je n'ai pas toujours été une élève irréprochable. Merci également pour les conseils en dessin au sens plus large du terme, des graphes aux aquarelles. Merci également de m'avoir remis dans le droit chemin quand, en avril 2023, à 6 mois de la fin de la thèse et avec un manuscrit à rédiger, je demandais la production de 10 nouvelles cartes microfluidiques... qui ont finalement donné de très beaux résultats !

Un grand merci à Charly pour toute l'aide apportée, que ce soit dans le montage du banc, dans les moments de détresse technique, ta réactivité exceptionnelle etc... Mais surtout toutes ces discussions et rigolades au café ou à l'atelier méca. Et par-dessus tout, ton rôle d'acteur dans mon film de thèse ! Un des meilleurs souvenirs de la thèse.

Lors de mes rares passages en salle blanche pour assembler les cartes microfluidiques, je voudrais remercier Mahfod pour avoir mis un peu d'ambiance en salle. Bien sur la musique, mais aussi toutes les discussions, sur Cannes, le cinéma, les pâtisseries algériennes.... Merci ensuite pour ton accueil dans "l'open space de l'austérité" pour ma longue période de rédaction, ces pauses cafés et ces encouragements quotidiens.

Un grand merci également à tous les partenaires de paillasse, en 147 avec Marie G, Anne-Carey, Charlotte, Léna, Katell, Marie H, Patricia, Aurélien, Thomas, Paul, Remco, Nico S. et au L2 avec Séverine, Nathalie, Clément, Matei, Emma, Camille. Un grand merci aux membres du T-gang qui furent un grand soutien durant cette thèse : Léna, Marie H, Katell et Hélène. Merci Marie G. pour avoir suivi la thèse de A à Z entre Lyon et Grenoble et avoir été un fort soutien dans les bons comme les mauvais moments.

Je tiens à remercier tous les membres de l'open space 309 pour leur accueil chaleureux et les propositions de pauses café. Je tiens tout particulièrement à remercier les membres du carré de l'ambiance, tout d'abord Louis, puis Séverine et enfin Léna. Cette atmosphère chaleureuse pour travailler a été un grand atout pour la réussite de cette thèse (même si il a fallu que je m'isole dans l'austérité pour rédiger). Séverine, la voie de la raison, toujours présente pour discuter de tout et de rien... face à trois doctorants, il en faut de la patience, merci d'avoir toujours été présente. Merci à Léna qui a su ponctuer ces deux dernières années de thèse d'un grain de folie et de rébellion. Nos soirées diners/Bastille du jeudi soir ont souvent été une bonne porte de décompression. Enfin Louis, un coloc extraordinaire, merci pour cette consommation journalière de ricorée, de maté en période de rédaction, les sorties ski, vélo, trail... Un des

meilleurs partenaires de thèse que l'on ne peut espérer.

Merci également à toutes les personnes que j'ai rencontré au CEA qui m'ont fait passé trois années extraordinaires : Bastien, Adrien, Morgane, Mélissa, Aude, Marie-Line, Hugo, Samir, Aurélien, Paul, Thomas... Tous ces déjeuners à H3, ces courses à la Bastille et les sorties au bistrot. Merci aux personnes qui ont contribué de près ou de loin à la relecture du manuscrit : Arnaud, Myriam, Alix, Mélanie et Joris. Merci à Alix qui m'a beaucoup encouragé sur cette dernière année de thèse, et toujours appris et aidé à monter jusqu'aux sommets des Alpes.

Quand j'ai commencé mes études à Lyon en 2014, je me souviens d'un professeur de physique qui avait dit "Si vous voulez faire de la physique plus tard, vous vivrez surement à Grenoble". 9 ans plus tard me voilà en train de finir mon doctorat sur la presqu'île scientifique de Grenoble. Ces années à Grenoble ont été riches en apprentissages et rencontres, et je voudrais remercier toutes les personnes qui ont participé de près comme de loin au bon déroulement de ces années.

Merci donc à mes amis qui m'ont toujours soutenu durant ces trois années de thèse. Merci à Sofia, Mélanie et Célia pour le soutien dans les bons comme dans les mauvais moments, les escapades dans les alpes Françaises ou Suisses, et jusqu'en Inde. Merci à mes amis de plus longue date, Rouchouze, Ludivine et Damien en particulier, votre amitié m'est précieuse. Merci à mes amis de Phelma, l'équipe Spark, pour tous ces moments partagés au fil des années, l'entraide et les rigolades en continu, en particulier Ali, Rose, Léa, Jules, Hubert, Hugo, Clément, Guilhem, Guillaume, Valentin, Fiona, Maxime... Merci à Jean, partenaire d'escapades toujours plus loufoques, de la Bastille à Tokyo, et à Marie, ma coloc éternelle qui bien que maintenant exilée dans le sud tu es toujours très présente auprès de moi. Merci à Margot pour l'amitié de la rue ampère et la joie de vivre. Merci à Charlotte et Giro, avec qui il est toujours possible de faire aussi bien du triathlon qu'un gratin de ravioles. Merci Sophia, mon amie grenobloise qui n'était jamais très loin du batiment 42, pour toutes ces escapades escalade, alpinisme ou même plongée qui m'ont fait un grand bien pendant ces trois années de thèse.

Je souhaiterais particulièrement remercier mes proches qui me soutiennent depuis très longtemps. Clara, tu as suivi cette thèse et bien plus depuis tant d'années, toujours avec de l'enthousiasme, merci de toujours me permettre de trouver refuge auprès de toi. Merci à toutes les personnes qui ont porté de l'intérêt pour mes études et m'ont toujours soutenu, Laurence, Philippe, et Rolland. Un grand merci à Solina pour nos 10 ans d'amitité franco-américaine. Merci de faire partie de la famille et d'être toujours présente et proche de nous. Merci à mes grands parents pour m'avoir donné la rigueur et la patience nécessaires à la conduite d'un projet scientifique. Adriane et Enzo, merci pour votre joie de vivre et votre ouverture d'esprit propre à la famille qui me donnent de l'énergie et de la confiance. Enfin, merci à mes parents pour votre amour et votre soutien dans mes projets. Merci maman de m'avoir conduis à l'école depuis 26 ans en me disant "amuse toi bien".

Abstract

Cardiovascular diseases are the leading cause of death in the world and several biomarkers are clinically used to diagnose patients. Cardiac troponin is currently the gold standard for the diagnostic of acute myocardial infarction (AMI). In hospital emergency departments, testing patient blood for cardiac troponin is crucial to rule-in or rule-out patients. Conventional methods to detect cardiac troponin and other biomarkers are usually performed in central medical laboratories with costly equipment and long analysis time. Point-of-Care devices propose on-site and rapid testing, but these devices currently lack sensitivity. We propose an innovative quantification assay for cardiac biomarkers integrated into a portable and automated instrument for rapid and high sensitivity testing.

We developed a method based on isothermal nucleic acids amplification (LAMP) using an original structure called dumbbell. For the quantification of biomarkers, the sample is incubated with this dumbbell structure containing various types of molecular probes such as aptamers or antibodies. Complete detection protocols are derived for various types of targets and integrated on a portable and automated platform. This latter contains microfluidic cartridges including a network of fluidic chambers used for the discrete manipulation of fluids. The cartridge architecture is designed specifically for the developed assay based on dumbbell amplification, and allow carrying out all the assay steps, from the sample recovery to the result.

We validated the isothermal amplification of the dumbbell structure with various types of molecular probes. We used thrombin as a model protein and included a specific thrombin aptamer in the dumbbell structure to obtain sensitive (100 pM) and antibody-free detection using this aptameroLAMP method. It is however limited to targets for which a double aptamer sandwich is available. For the troponin cardiac biomarker, we derived the method with antibodies coupled with the dumbbell structure for its exponential amplification, named immunoLAMP. We tested this method on human plasma samples and reached a limit of detection of 100 pg/mL, a relevant concentration for physio-pathological testing. Then, each step of the detection assay was successfully integrated in microfluidic cartridges on a portable instrument. Two main architectures were designed. The first one allowed the sample preparation on magnetic beads to sandwich capture the target. Troponin was detected down to 1 ng/mL in this cartridge using the fully automated instrument. The second architecture proposes the LAMP reaction integration. The microfluidic cartridge is therefore placed on a thermal actuation system associated with an optical module to record the real-time fluorescence. The quantification of the dumbbell using LAMP in this second architecture was possible down to 10 pM.

Our detection method using LAMP is generic and opens many perspectives for its application to other types of cardiac biomarkers (NTproBNP, miRNA...). The versatility of the microfluidic technology and the instrument developed should allow the multiplexed detection of cardiac biomarkers on this platform using this generic detection method, and should improve cardiovascular diseases diagnostic.

Acronyms

ACS Acute Coronary Syndrom 32, 33, 41

AMI Acute Myocardial Infarction 24, 32, 33, 35–41, 43, 66, 69, 71, 146, 147

ANP Atrial Natriuretic Peptide 39

AOC antibody-oligonucleotide conjugate 126–128

AOCs antibody-oligonucleotide conjugates 126

APTES (3-Aminopropyl)triethoxysilane 63, 146, 152

AST Aspartate Transaminase 35

BIP Backward Inner Primer 80, 81, 83, 84, 91, 92, 95, 96, 100, 118, 119, 133

BNP Brain Natriuretic Peptide 19, 34, 36, 39, 40, 53, 69

BSA Bovine Serum Albumine 108, 161, 182, 185, 189

CAD Computer Aided Design 24, 151, 152

CAGR Compound Annual Growth Rate 46

CEA Commissariat à l'énergie nucléaire et aux énergies alternatives 24, 144, 148, 152, 153

CHU Centre Hospitalier Universitaire 210, 211

CK Creatine Kinase 35

COC cyclo-olefin copolymer 24, 66, 67, 148, 150–152, 164, 165

CRP C reactive protein 53, 146

Ct Cycle Threshold 76

cTnC Cardiac Troponin C 115

cTnI Cardiac Troponin I 23, 24, 36, 38, 53–55, 64, 65, 67, 70, 115, 119, 131–134, 136, 146, 147

cTnT Cardiac Troponin T 20, 36, 48, 53, 59, 61, 67, 68, 115, 146

CVD Cardiovascular Diseases 30–32, 34, 35, 39–41, 43, 45, 47, 48, 146

DB Dumbbell Buffer 133, 134, 186

ddLAMP digital droplet LAMP 209, 210

ddPCR digital droplet PCR 77, 209

DNA Deoxyribonucleic acid 25, 51, 58, 76–82, 86, 99–103, 105, 108, 111, 114, 116, 120, 122–128, 130, 131, 139–141, 161–163, 168, 177, 178, 181, 182, 184, 185, 189–192, 194, 195, 197, 199

dNTPs Desoxiribonuclease Triphosphate 81, 92, 94, 97, 99, 189

DPV Differential Pulse Voltammetry 53

DSS Disuccinimidyl suberate 127

ECG Electrocardiogram 32, 34, 41

ECL Electrochemiluminescence 24, 146, 147

ECS European Society of Cardiology 32

ED Emergency Department 37, 42, 43, 145

EDTA Ethylenediaminetetraacetic acid 69, 130

EFS Etablissement Français du Sang 106, 109, 135, 137, 187

ELASA enzyme-linked aptamer-sorbent assay 56

ELISA Enzyme Linked ImmunoSorbent Assay 24, 34, 39, 53, 54, 56, 58, 59, 66, 72, 101, 118, 119, 122, 124, 133–137, 150, 153, 158, 173, 182, 207

ELONA Enzyme Linked Oligonucleotide Assay 54, 115

EMC electrochemically-driven microfluidic chip 178, 180

ESC European Society of Cardiology 33, 37, 39, 45

EWOD Electrowetting On Dielectric 65

EXPAR Exponential amplification reaction 79

FET Field Effect Transistor 24, 66, 146, 147

FIP Forward Inner Primer 80, 81, 83, 84, 91, 92, 95, 96, 100, 118, 119, 133

GEM Grenoble Ecole de Management 43

H-FABP heart-type fatty acid binding protein 146

H5N1 Influenza A virus subtype H5N1 124

HB Hybridization Buffer 105, 117, 182, 183

HF Heart Failure 34, 39

HPLC High Performance Liquid Chromatography 131

HRP horseradish peroxidase 53, 119

hs-cTnI high-sensitivity cTnI 37

IB Incubation Buffer 129, 133, 185–187

ICU Intensive Care Unit 41, 210

iLAMP ImmunoLAMP 23, 27, 123, 128, 134–141, 143, 154, 159, 161, 172–176, 180, 181, 184, 185, 189, 191, 201–203, 205, 208, 209

ISO International Organization for Standardization 148

Kd Dissociation constant 111, 115, 121, 136

LAMP Loop Mediated Isothermal Amplification 5, 21, 25, 26, 28, 58, 59, 75–81, 83–85, 87–92, 94, 95, 97, 99, 100, 102–105, 108, 109, 111, 114, 117, 119, 122–125, 134, 135, 137, 140, 154, 155, 157, 158, 161–163, 167–172, 174, 176–183, 186, 188–197, 200–205, 207, 209

LD Lactate Dehydrogenase 35

LDLR low-density lipoprotein receptor 128

LED Light Emitting Diode 24, 155, 156, 173, 189, 203

Leti Laboratoire d'Electronique et Technologie de l'Information 24, 144, 153

LFIA Lateral Flow ImmunoAssay 3, 55, 60, 61, 67–69

LOD Limit of Detection 37, 56, 57, 62, 64, 65, 69, 70, 106, 113, 121–123, 136, 138–141, 146, 177, 178, 180, 184, 187, 190, 192, 200–202

LSMB Laboratory of Microfluidic Systems and Bioengineering 24, 137, 144, 149–152, 156, 157, 161, 173

MB Magnetic beads storage buffer 119, 133

MI Myocardial Infarction 32, 115

microTAS micro Total Analysis System 148

miRNA micro Ribonucleic Acid 40, 41, 48, 80, 140, 205, 207, 208

MIT Massachusetts Institute of Technology 146

mRNA messenger RNA 40

MRSA Methicillin-resistant *Staphylococcus aureus* 178, 180

MSSA Methicillin-sensitive *Staphylococcus aureus* 178, 180

MW Molecular Weigth 126

MWCO Molecular Weigth Cut Off 130, 131

N-STEMI Non ST Segment Elevation Myocardial Infarction 32

NASBA Nucleic Acid Sequence-Based Amplification 76, 79

NHS N-Hydroxysuccinimide 130

NP Natriuretic Peptide 34, 39

NTproBNP N-terminal Prohormone of Brain Natriuretic Peptide 19, 34–36, 39, 40, 44, 45, 48, 53, 70, 140, 146, 205, 207, 208

OAR oligonucleotide to antibody ratio 127, 130

PBE Phosphate Buffer EDTA 130

PBS Phosphate Buffer Saline 105, 108, 130, 131, 133, 161, 170, 182, 185, 189

PCR Polymerase Chain Reaction 51, 52, 58, 59, 76–79, 82, 101, 102, 122–125, 176

PDMS Polydimethylsiloxane 63, 66, 67, 146, 148, 178, 180

PEG Polyethylene glycol 139

PID proportional–integral–derivative 154

PLA proximity ligation assay 123

PMMA Poly(methyl methacrylate) 63, 67, 146, 148, 177, 180

POC Point of Care 20, 24, 29, 38, 41–49, 56, 60, 61, 67–72, 140, 143, 145–148, 150, 173, 175, 176, 179, 202, 207, 208, 210

POCT Point of Care Testing 42, 44, 46

proBNP Prohormone of Brain Natriuretic Peptide 39, 68

qPCR Quantitative Polymerase Chain Reaction 76, 77, 123

RCA Rolling Cycle Amplification 76, 79

redox reduction–oxidation 69

RNA Ribonucleic Acid 40, 76, 79, 103, 124, 141, 176–178

RNAs Ribonucleic Acids 40, 102

RPA Recombinant Polymerase Amplification 58, 79

RS Rinsing Solution 105, 117, 182

RT Room Temperature 119, 133

RT-LAMP Reverse transcription loop-mediated isothermal amplification 79, 103, 123, 176, 178

SELEX Systematic Evolution of Ligands by EXponential enrichment 51, 52, 115

skTnI Skeletal Troponin I 119, 133, 135

SPR Surface Plasmon Resonance 54, 55, 115, 118, 119

STEMI ST-Segment Elevation Myocardial Infarction 32

SyMMES Systèmes Moléculaires et nanoMatériaux pour l'Énergie et la Santé 130

TAB Troponin Aptamer Buffer 119

TBE Tris-borate-EDTA 95

TCEP tris(2-carboxyethyl)phosphine 130

THAB Thrombin Aptamer Buffer 108, 109

TMB Tetramethylbenzidine 135

Tp Time-to-positive 82, 111, 113, 120, 129, 137, 167, 184, 187, 190, 191, 199–201

UGA Université Grenoble Alpes 43

UN United Nations 29, 30, 34, 41

URL Upper Reference Limit 38

WB Washing Buffer 119, 133, 134, 160, 161, 185

WHO World Health Organization 30, 32, 34, 35, 76

List of Figures

Chapter 1

State of the Art: Cardiovascular Diseases Diagnosis

Objectives

- The cardiovascular diseases diagnosis stakes and current clinical trends are exposed
- For cardiovascular diseases diagnosis, different cardiac biomarkers emerging from the literature and clinical practices are presented
- The need for cardiac POC devices is highlighted, and a market study for ultra-sensitive and portable detection of cardiac biomarkers is presented
- Different biosensing methods are exposed for the development of cardiac biomarker tests
- Different technologies to design portable and autonomous systems to integrate biological assays are exposed
- Lastly, several commercialized cardiac POC devices are presented

This chapter introduces the stakes of cardiovascular diseases diagnosis. As cardiovascular diseases are the leading cause of death worldwide [1], this chapter exposes the different diseases, cardiac biomarkers, and the importance of diagnosis through cardiac biomarkers testing. The potential of portable devices such as POC is highlighted. Different testing solutions are explored through a thorough state-of-the-art review of the biosensing methods and existing integrated and portable technologies. Some commercialized devices for cardiac biomarkers sensing are exposed, with their performances and limitations, which lead to the definition of this PhD project goal.

1.1 Context: cardiovascular diseases

Ensuring good health and well-being is placed amongst the 17 sustainable development goals defined by the United Nations (UN) in the last decades [2]. Major progress have been made lately in the health sector, improving the health of many people, but the recent Covid-19 pandemic highlighted our vulnerability to health threats.

1.1.1 Cardiovascular diseases

Cardiovascular diseases represent the major cause of death worldwide, with about 45% of death [3]. According to World Health Organization (WHO), this number is due to increase by 2030 [3]. Heart attacks and strokes represent 85% of Cardiovascular Diseases (CVD) deaths. They are the most acute events and are caused by a blockage that prevents blood from flowing into the heart or brain.

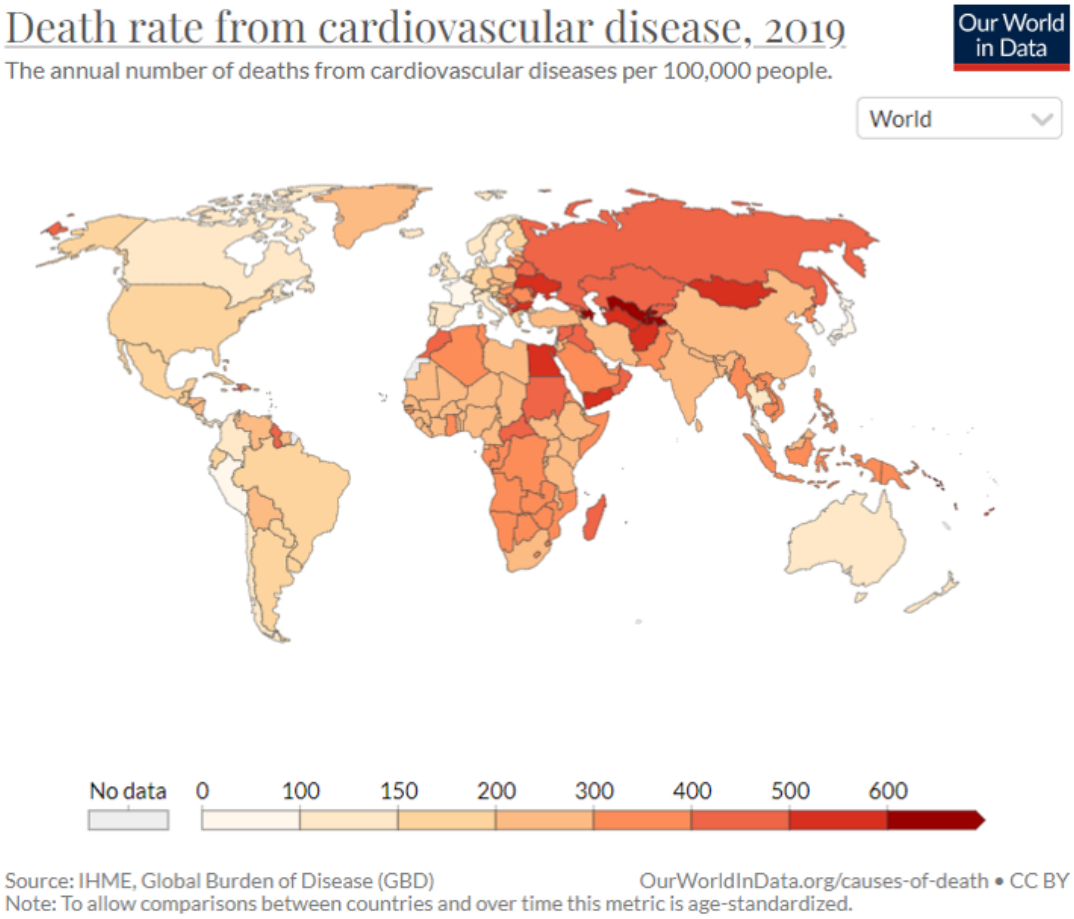

Figure 1.1: World map of death rate for cardiovascular diseases in 2019. Values show the annual number of deaths from cardiovascular diseases per 100,000 people [1]

Figure 1.1 shows the death rate worldwide for CVD, overlooked by stroke and myocardial infarction, also called heart attacks [1]. Amongst other cardiovascular diseases, one can find hypertension, heart failure and acute coronary syndrome. However, with myocardial infarction representing about one-third of total death [1], it has become WHO major public health priority. In addition, acute coronary syndrome and heart failure are the second priority and catch the attention of scientists and clinicians worldwide [4] [1] [5]. As cardiovascular diseases are a global burden and a major threat to public health, it becomes a key sector to address in order to meet the UN development goals for the next decades.

The important risk factors of heart diseases are unhealthy diet, physical inactivity, tobacco and alcohol consumption [3]. Therefore, aware and responsible individual behavior on these factors can have a positive impact on the prevalence of CVD. Public health policies are also essential to drive people to adopt and sustain healthy lifestyles and therefore reduce CVD risks. More-

over, clinically identifying people with a high risk of CVD and providing them with appropriate treatment can reduce the risk of CVD [5].

Cardiovascular diseases death rate is very heterogeneous geographically, as exposed in figure 1.1. The highest death rate of CVD is found in the Middle Eastern, Asian and African parts of the world. Indeed, over 75% of CVD deaths occur in low and middle-income countries [3].

Cardiovascular diseases generally represent an important cost in the health system of a country. We studied specifically two countries and the distribution of the different diseases in terms of total annual cost for the health system. From figure 1.1, we chose to focus on France and China since the two countries show great differences in death rate from CVD. In France, where the CVD death rate is relatively low, CVD represents an annual cost of 11.2 billion euros, with hypertension representing the highest expense. In comparison, in China, where the CVD death rate is rather important, the total global annual cost is 108 billion euros, and heart failure represents the highest cost. For these two countries, if we scale up these numbers regarding the population numbers, we find that CVD expenses in France represent about 150€ per inhabitant, whilst in China it represents about 75€, so about half of France.

These findings can be explained considering that in France, CVD leading to heavy and costly medical care are prevalent, with for example stroke, myocardial infarction and acute coronary syndrome representing about half of the costs, whilst in China, these three diseases represent about 1/4 of the total costs. Moreover, in regards to figure 1.2, France's burden of CVD in terms of death rate is lower than the one of China, so the higher expenses in France likely lead to better patient care and reduced mortality.

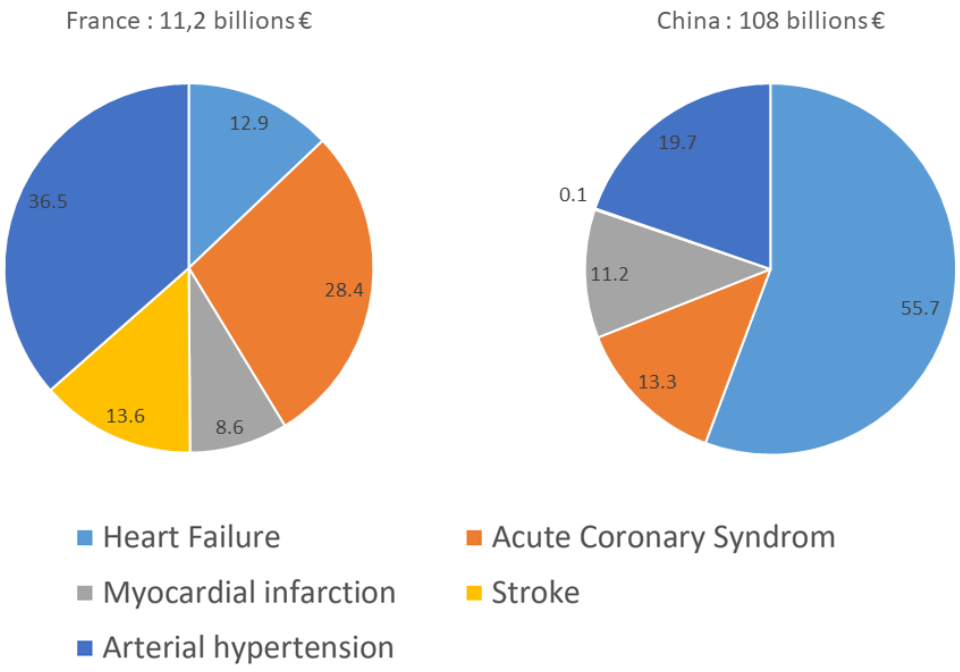

Figure 1.2: Cardiac diseases global total annual cost for France (2018) and China (2008) [6]

Cardiovascular diseases represent a major health threat globally. Geographically, major heterogeneities are observed, with different prevalence of CVD death rates and cost to the

health system. CVD often leads to heavy medical care and are important expense for the health system. In a global effort to reduce the burden of cardiovascular diseases, one must first understand what are these diseases, and how they are diagnosed and treated medically. The next section will detail three major CVD: Acute Coronary Syndrome, Myocardial Infarction and Heart Failure.

1.1.1.1 Acute Coronary Syndrome and Myocardial infarction

Acute Coronary Syndrom (ACS) is a syndrome due to the decreased blood flow in the coronary arteries. The most common symptom is chest pain and in a few hours it leads to the inability of the heart muscle to function properly, therefore leading in most cases to myocardial infarction [1]. There are two scenarios for the diagnosis of ACS, depending on the duration of symptoms, Electrocardiogram (ECG) shape and blood test result. In half of the cases, when symptoms are of short duration, the ACS is an unstable angina. In the other half of cases, the diagnosis is Myocardial Infarction (MI).

MI has been defined as WHO's major priority when it comes to addressing CVD threat. It is defined by the European Society of Cardiology (ECS) as "the cardiomyocyte necrosis in a clinical setting consistent with acute myocardial ischemia" [5]. Between 5 to 20 % of patients arriving at the hospital emergency department present symptoms of myocardial infarction, mainly chest pain.

The diagnosis of MI is based on a combination of criteria [5], including the detection of an increase or decrease of a reference cardiac biomarker, preferably troponin I, and one of the following :

- Symptoms of myocardial ischemia
- New ischaemic ECG changes
- Development of pathological Q-waves on ECG
- Imaging evidence of loss of viable myocardium or new regional wall motion abnormality in a pattern consistent with an ischaemic aetiology
- Intracoronary thrombus detected on angiography or autopsy

Overcrowding of the emergency department being a major problem worldwide, a key challenge in the management of patients with suspected AMI is to be able to rule-in or rule-out patients in regards to the risk of AMI [1]. The main symptoms of patients with suspected AMI is chest pain, but it is not sufficient itself to diagnose myocardial infarction [7]. After admission in the hospital, an electrocardiography is performed. If the electrocardiogram presents an elevation of the ST segment, it describes an irregular heart rate and is therefore proof for myocardial dysfunction. This type of infarctus is called ST-Segment Elevation Myocardial Infarction (STEMI). However, this ST elevation is visible on the electrocardiogram only in 20-40 % of the cases [5]. In the other cases, called Non ST Segment Elevation Myocardial Infarction (N-STEMI), a biomarker assay is ordered by the clinician in order to give additional information for the diagnosis. Different groups of experts [5] and clinicians recommend that the diagnosis of N-STEMI infarction must be based on:

1. The variation of cardiac biomarkers concentration such as cardiac troponins due to their high specificity and sensitivity
2. A clinical symptom amongst the list defined above

Troponin has been thoroughly validated scientifically and used clinically as the reference biomarker for the diagnosis of AMI. The variation of its concentration in blood at different times from the accident gives precise information about the infarction risk. At the beginning of the 21^{st} century, the European Society of Cardiology and the American College of Cardiology decided to add cardiac troponin levels shifts to the universal definition of myocardial infarction [1]. Therefore, cardiac troponins are currently the gold standard biomarkers for myocardial infarction, as recommended in the latest report of European Society of Cardiology (ESC) for the management of acute coronary syndromes in patients without persistent ST-segment elevation [5]. An example of decision algorithm and triage rules for ACS patient can be found in figure 1.3.

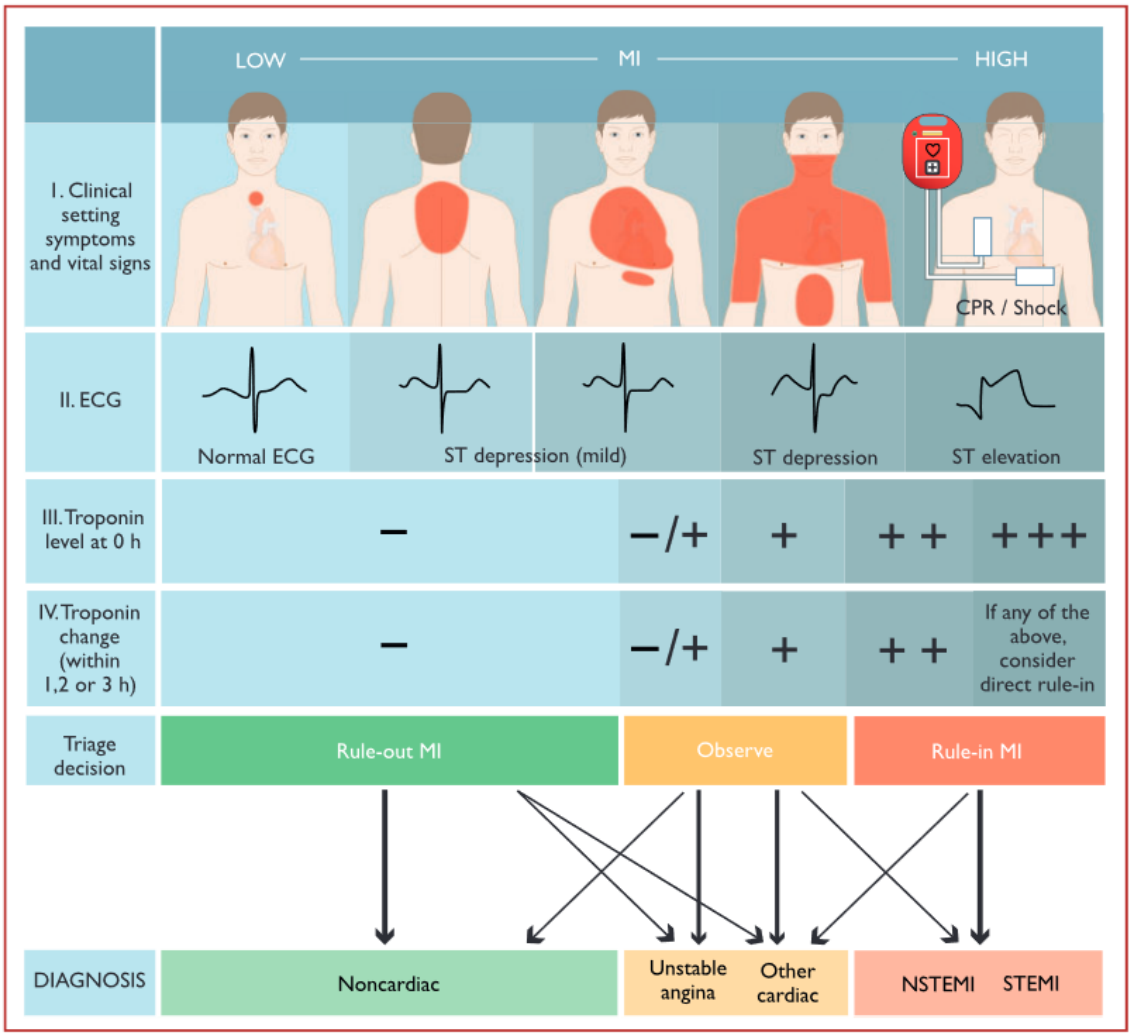

Figure 1.3: Diagnostic algorithm and triage in acute coronary syndrome [5]

1.1.1.2 Heart Failure

Heart Failure (HF) is a major problem worldwide affecting about 26 million people worldwide and with increasing prevalence [8]. Heart failure is the inability of the heart to pump enough blood around the body and at the right pressure, which occurs when the heart muscle becomes weak. It is a complex clinical syndrome of different cardiac conditions, as the final stage of a disease that results in the decompensation of the heart's ability to contract or relax. Symptoms include shortness of breath, intense tiredness, and leg swelling. The common causes of heart failure are coronary artery disease, heart attack, high blood pressure, atrial fibrillation, valvular heart disease, infection, and cardiomyopathy. All these factors cause heart failure by changing the structure or function of the heart. The diagnosis of HF is based on symptoms and echocardiography. As the patho-physiological system involves the release of hormones and proteins into the bloodstream, this latter can also be used as diagnostic biomarkers [9]. There are multiple biomarkers useful for the diagnosis of HF, such as BNP, NTproBNP, mid-regional pro-adrenomedullin (MR-proADM) or C-reactive protein [10]. The most common biomarker for HF belongs to the Natriuretic Peptide (NP) family and plays an important role in the diagnosis, prognosis and treatment of HF patients [9].

1.1.1.3 Towards better patient care: cardiovascular diseases diagnosis

In the scope of the UN sustainable development goals targeting "good health and well-being for all", it is precised to "Strengthen the capacity of all countries, in particular developing countries, for early warning, risk reduction and management of national and global health risks" [2]. Early warning and detection of diseases appear as a major strategy for global healthcare improvement. With cardiovascular diseases being the major cause of death worldwide, this field of healthcare appears strategic for future developers. WHO recommends to reduce the risk of heart diseases through early prevention [10].

The diagnosis of CVD in clinical settings is composed of several tools. The first stage is a physical examination, followed by electrocardiogram, electrocardiography (Xrays, ultrasound) and echocardiogram (figure 1.4). These methods are time-consuming and require heavy medical equipment. Moreover, the results obtained through these methods are not entirely reliable in diagnosing cardiac diseases. Indeed, about 70 % of patients suspected with a CVD showed a normal ECG at their admission to the emergency department [7].

Cardiac biomarkers are molecules released into the bloodstream in the case of heart muscle damage and give valuable information on the onset of a cardiac accident [1]. In particular, levels of cardiac troponins give precise information about the risk of myocardial infarction. In clinical settings, ELISA are the gold standard for the quantification of proteins, and therefore are the reference test for cardiac biomarkers. They provide a good accuracy of the result, but rely on heavy equipment, trained staff, expensive biological reagents and are time-consuming.

For the case of CVD diagnosis through cardiac biomarker testing, there is a high demand for rapid and sensitive tests, as the variation of troponin levels are very low. Current guidelines recommend a blood analysis time of less than one hour from patient admission in the hospital to blood test result [5]. To meet this criterion, there is an important ongoing research and development in the field of portable devices called Point-of-Care for cardiac biomarker sensing.

1.1.2 Cardiac biomarkers

Blood tests represent a major diagnostic tool for cardiovascular diseases and a guide for practitioner's decision-making. There are several markers released in the blood [11], but recently troponin and natriuretic peptides appeared as the most clinically relevant biomarkers to test for heart damages [5]. A review of the historical trends in cardiac biomarkers testing will be

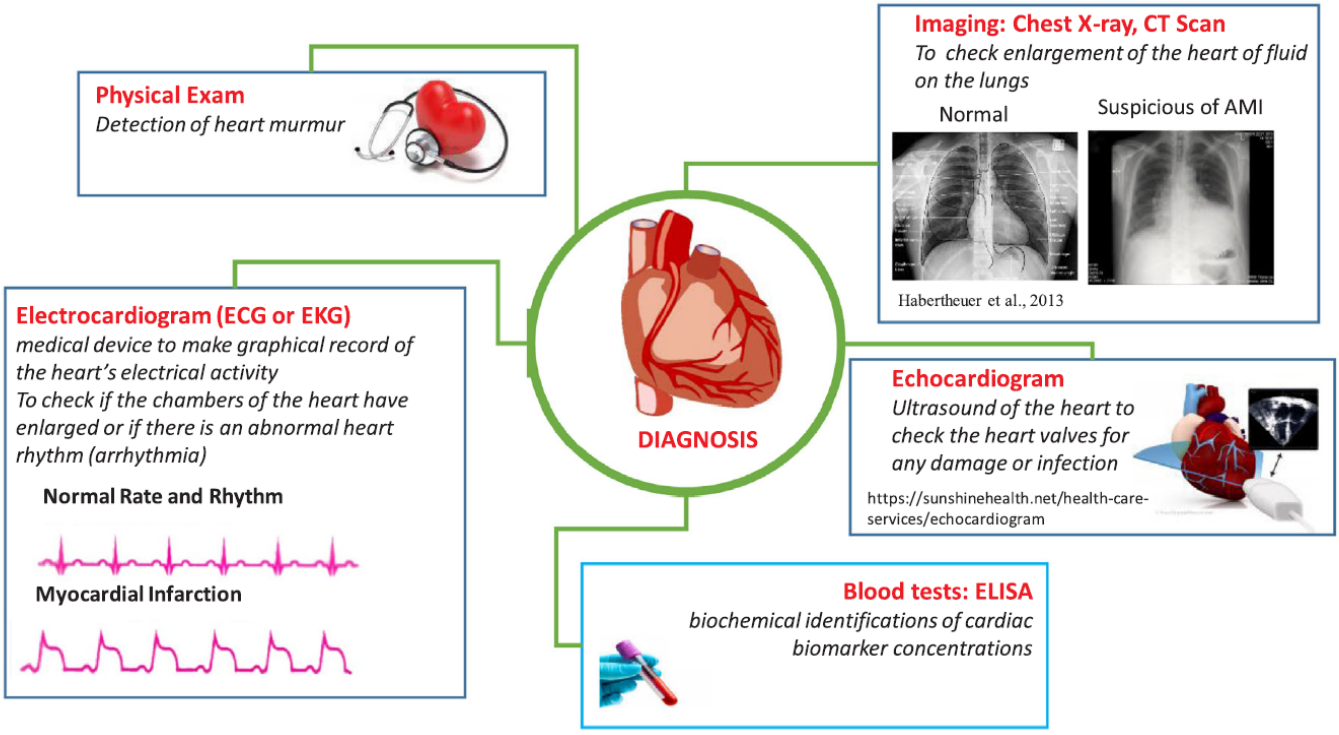

Figure 1.4: Current diagnostic tool to detect cardiovascular diseases in clinical settings [7]

given, the description of the two most used biomarkers (troponin and NTproBNP), and lastly an emerging category of cardiac biomarker will be exposed in this section.

1.1.2.1 History of clinically-used cardiac biomarkers

Circulating blood biomarkers are becoming increasingly important for the diagnosis of cardiovascular diseases. There has been long ongoing research on their characteristics and utility in clinical practice, with several reviews on the matter. According to [12], a biomarker is "an objectively measured parameter that is an indicator of normal biological processes, pathogenic process or as a response to pharmacological therapy". Figure 1.5A highlights the variety of biomarkers that have been studied in the scope of CVD diagnosis. A graph of some biomarker's temporal variations during a cardiac accident is exposed in figure 1.5B.

The first biomarker ever used for the diagnosis of AMI was introduced by WHO in the AMI definition in 1960 was Aspartate Transaminase (AST). However, it was shortly found to be unspecific to cardiac muscle alteration, and soon after, in the years 1970, Lactate Dehydrogenase (LD) and Creatine Kinase (CK) were introduced as more specific than AST. Their activity also increased in liver, kidney and skeletal muscle diseases, therefore altering their specificity for CVD diagnosis. However, a derivative from CK enzyme called CK-MB was found to provide a more reliable and specific diagnosis for cardiac diseases. In 1978, myoglobin, a small oxygen-carrying protein, was proposed as a new biomarker for AMI. It is freed within one hour after tissue damage occurred and can provide a reliable diagnosis. However, its rapid clearance from blood and its increasing levels in case of renal failure, myopathies or traumas are limiting factors for its wide use clinically. In the early 2000, a global scientific and clinical consensus defined the troponin as the reference biomarker for the diagnosis of myocardial infarction. Its high specificity for AMI and its concentration variation in the blood are strong arguments to define this protein as the gold standard for AMI diagnosis. Later, another class of cardiac biomarkers was introduced and

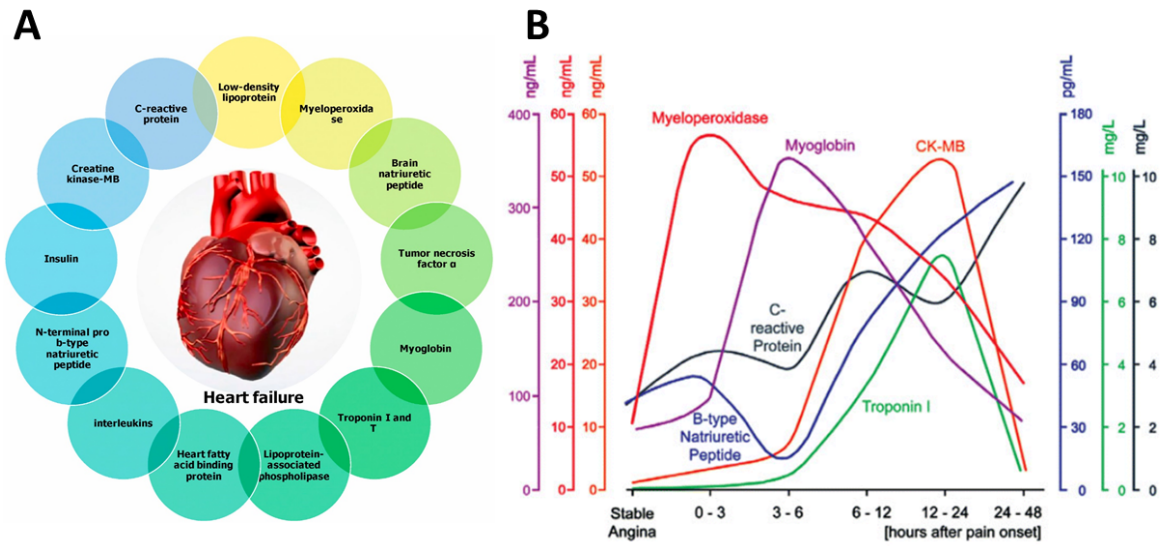

Figure 1.5: Schematic of the most commonly used CVD biomarkers and time variation (A) The most commonly used cardiovascular biomarkers for the detection of CVD according to [13]. (B) Time-dependent change in biomarkers concentration after chest pain onset [11]. The troponin range is in μg/L.

clinically validated: natriuretic peptides. Two important biomarkers for heart failure are Brain Natriuretic Peptide BNP and N-terminal proBNP NTproBNP. C-reactive protein, an acute phase protein with plasma levels increasing up to 10,000 times upon cardiac events, has also been added to the list of validated cardiac biomarkers. However, the C-reactive protein is an inflammatory marker, therefore its use for early diagnosis was ruled out and this marker is mostly used for prognosis [11]. Finally, several other cardiac biomarkers have been discovered and are currently under study for their potential relevance and use in clinical practices: myeloperoxidase (MPO), TnF-α, the heart fatty acid binding protein (H-FABP) or ?? [14] [15] [1].

1.1.2.2 Troponin I: the gold standard for myocardial infarction

Since the beginning of the 21^{st} century, troponin has emerged as the favorite biomarker for the diagnosis of myocardial infarction [1], [5]. As it is the most sensitive and specific biomarker for AMI, it is considered nowadays as the gold standard biomarker.

Troponin is a complex of three proteins in the myocardial contractile system (Fig 1.6A). The three subunits are troponin I, troponin T and troponin C [1]. The troponin C binds calcium ions for muscle contraction and is similarly expressed in the skeletal muscle and in myocardium, therefore is not specific to heart damage. It is not used in cardiology practices. Troponin T has a molecular weight of 37 kDa and is a marker of renal disease and skeletal muscle injury. Lastly, troponin I has a molecular weight of 24 kDa and exists in skeletal muscle and myocardium. It prevents muscle fiber from contracting without calcium. Cardiac troponins regulate muscular contraction based on intracellular calcium. After myocardial infarction, the damaged cells release cardiac troponin I into the bloodstream. During the infarction, the concentration of cTnI is lower than that of cTnT, but the kinetics of variation are similar for both proteins. During myocardial infarction, a part of the myocardium undergoes necrosis due to hypoxia (meaning $PaO2 < 60mmHg$) and the interruption of blood flow in the coronary arteries. Hence, an increase in troponin levels in the blood indicates a cardiac muscle injury. Cardiac troponins are therefore a biomarker of high interest for myocardial infarction diagnosis, especially troponin I

which is the subject of many research and developed blood tests [16].

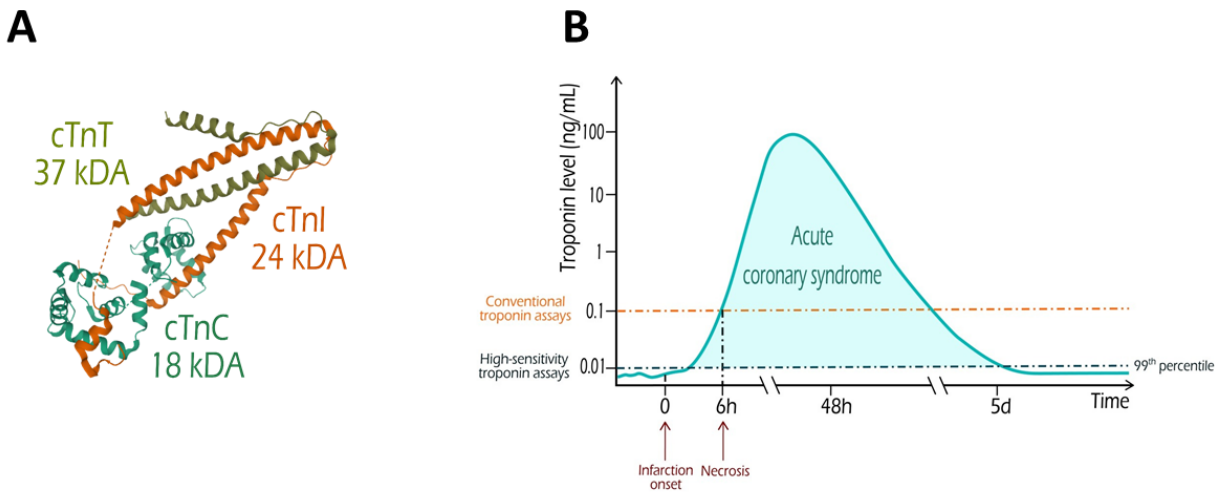

Figure 1.6: Troponin for ACS and AMI diagnosis (A) Schematic of troponin complex [17] and (B) Evolution of troponin levels over time during myocardial infarction [1]

Nowadays in clinical practices, troponin I level measurement represents a common diagnostic procedure, as recommended by the ESC [5]. Troponin I basal concentration in bloodstream is very low, about 10 ng/L (Fig 1.6B), and its increase in concentration should be observed at the beginning of the symptoms and three hours after [5]. A few hours after the infarction onset, the troponin I level increase is about 50 %, whilst six hours after it reaches about 10 times. This variation poses major challenges for the biological tests used to quantify cardiac troponin levels in blood. Indeed, detecting a biomarker variation of about 50 % in blood requires the use of high-sensitivity immunoassays. Moreover, as troponin is a small protein (24 kDa) in a complex medium (blood), immunoassays used must also present a high specificity.

Over the last decades, there was many improvements in biological test methods and we observed a shift in the sensitivity of the assays, which were necessary to validate and use troponin as an AMI biomarker [5] (Fig 1.7)

The first troponin I immunoassay was described in 1987 [18] and required two days to perform the test with a limit of detection of 10 μg/L, which was far away from the sensitivity required (Fig 1.7). After many developments, conventional troponin assays proposed a Limit of Detection (LOD) in the range 10 ng/L, which is already above the basal troponin concentration. In 2010, the transition to high-sensitivity troponin assays occurred, with ?? in the ng/L range, and are now recommended in clinical practices. Compared to conventional assays, the detection limit is lowered by a factor of 10, and the test time is significantly reduced and presents an improved accuracy. These high-sensitive tests are very effective at the beginning of the infarction onset when troponin levels are low in blood, and they allow the identification of early necrosis.

Moreover, it is recommended to monitor the kinetics of troponin concentration in blood with at least two measurements separated by 3h. In 2019, a panel of experts [19] wrote recommendations for institutional transitioning to high-sensitivity troponin testing. Based on the fact that high-sensitivity cTnI (hs-cTnI) tests currently have a high analytical precision at lower concentrations resulting in great clinical sensitivity, they can now accurately indicate small changes in troponin I concentration within a short time frame. The experts drew the conclusion that the delay between two troponin measurements can be reduced to 1h, with the first measurement taken at the patient's admission to Emergency Department (ED), and the second one hour after. However, it is important to note that different diagnostic procedures are used in different coun-

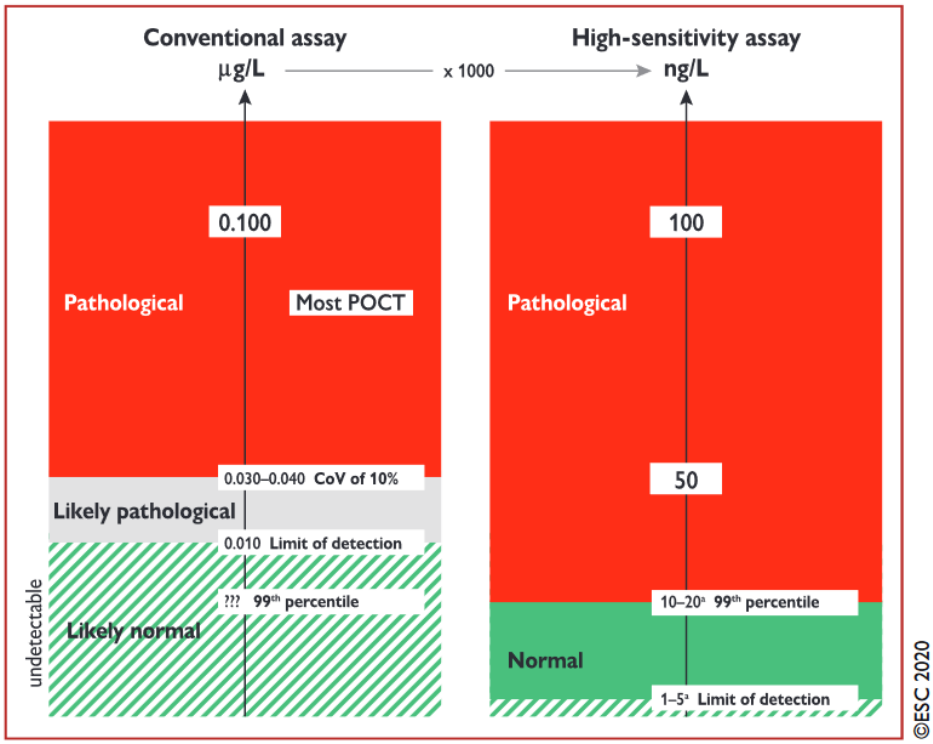

Figure 1.7: Desired troponin assay sensitivity from [5]

tries and it is difficult nowadays to define a general cut-off value to rule-in or rule-out patients with regard to the risk of AMI. Different factors like age or sex influence troponin I values and should be taken into consideration. In the universal definition of myocardial infarction, it is recommended to use the 99^{th} percentile concentration of cardiac troponin in a normal population as part of the decision threshold for AMI [20]. This procedure gives the Upper Reference Limit (URL) and is given by any manufacturer of troponin I test. The implementation of this procedure is a way to reduce geographic and population dependence of troponin levels, but has limits when it comes to hospital dependence [20]. Finally, troponin I was also found to give prognostic information such as the risk of death, and also helps with risk stratification.

Figure 1.7 highlights the challenges when it comes to high-sensitivity troponin sensing. As recommended by the experts, rapid and sensitive detection of cardiac cTnI needs to be obtained in order to ensure better patient care. Portable and autonomous platforms such as POC propose a rapid and on-site testing method but currently lack the required sensitivity. There are important research efforts going on to design and develop cardiac POC platforms with high sensitivity for troponin sensing.

In conclusion, troponin I currently represents the gold standard biomarker of myocardial infarction. Troponin I level measurement in blood few hours before a cardiovascular accident gives precise and valuable information for the clinicians [5]. Conventional laboratory immunoassays currently propose high-sensitivity sensing of troponin I levels, and are widely and commonly used in clinical practices. Portable and autonomous platforms such as POC systems are valuable tools to propose a diagnosis of cardiac troponin I, but current challenges remain with their sensitivity and wide acceptance in clinical practices.

1.1.2.3 Natriuretic Peptides: the reference for heart failure

Natriuretic peptides are hormones synthesized by several organs like the brain and the heart. In the 1980s, several peptidic hormones with known amino acid sequences were identified, such as Atrial Natriuretic Peptide (ANP) or BNP [1] (Fig 1.8A). They are produced by myocardial tissues and by binding to NP receptors they maintain homeostasis in the cardiovascular system. The Prohormone of Brain Natriuretic Peptide (proBNP) precursor is cleaved when the heart suffers from an atrial and ventricular dysfunction. The active BNP and the inactive NTproBNP segments are then secreted into the heart ventricles (Fig 1.8B). In the case of heart dysregulation, concentrations of BNP and NTproBNP in plasma increase. These biomarkers are thus appropriate for the diagnosis of AMI [21] and for the diagnosis of HF [5]. The current guidelines from ESC recommend the measurement of BNP and NTproBNP in plasma for patients with suspected HF [9]. Amongst the two biomarkers, NTproBNP is preferred to BNP due to its longer degradation time in patient blood (Fig 1.8B). Indeed, in plasma BNP half-life is about 20 minutes, therefore giving important challenges for biological testing procedures. In healthy patients, NTproBNP has a basal concentration of 20 ng/L, and for patients with HF, this value rises to 125 ng/L. As for other cardiac biomarkers, these values are multi-parameter dependent (age, sex...). In clinical practices, these biomarkers are tested in patient blood using classical ELISA immunoassay, and include the use of various antibodies that bind different epitopes of the peptide. Therefore, the results vary from one technique to another which leads to difficulties in defining a single threshold value.

Moreover, natriuretic peptides concentration can also change in case of pulmonary pathologies, renal inefficiencies, or diabetes for example. Therefore, their specificity is reduced compared to the one of troponin for example. In order to improve the specificity of these peptides, they should be more thoroughly studied by the scientific community. In particular, ANP lack studies and analysis in the scientific literature and could be a useful indicator for CVD, perhaps in combination with other markers.

Lastly, natriuretic peptides have a prognostic function. During AMI, it is recommended to measure NTproBNP concentration in patient blood to evaluate the risk of death. They also guide clinicians in treatment and are widely used for risk stratification [9].

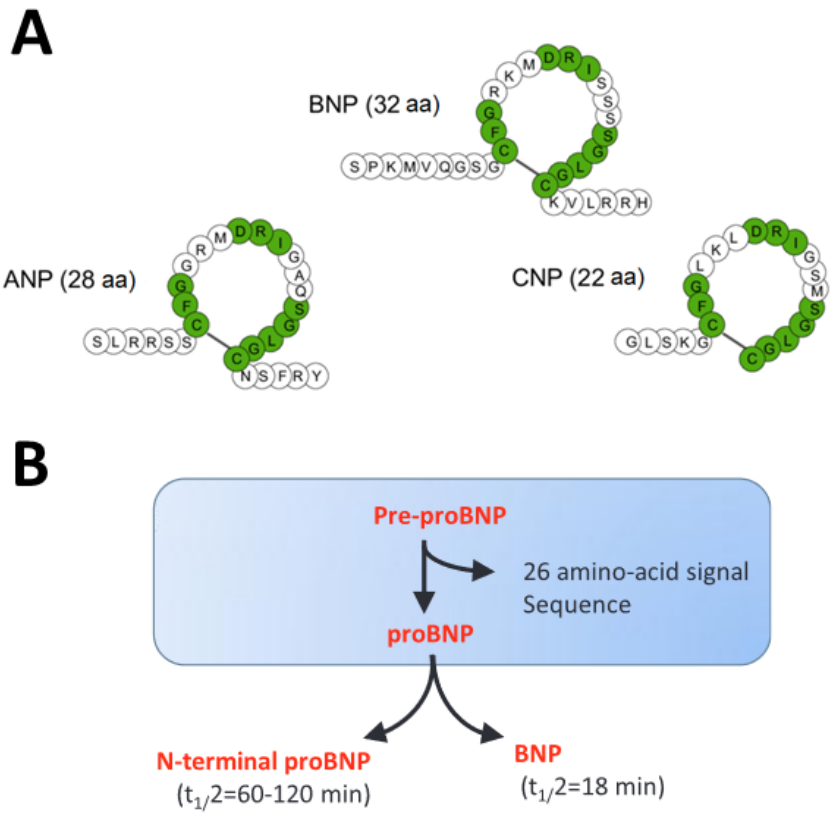

Figure 1.8: Natriuretic peptides. (A) Structures of different natriuretic peptides [17] and (B) Biological pathways of natriuretic peptides leading to the production of BNP and NTproBNP biomarkers [7]

1.1.2.4 miRNAs as emerging biomarkers

microRNAs or micro Ribonucleic Acid (miRNA)s, a small regulatory Ribonucleic Acid (RNA) that modulate translation, is a short (18-22 nucleotides) regulatory Ribonucleic Acids (RNAs) that binds messenger RNA (mRNA) to induce its degradation or prevent its translation into proteins. miRNAs are present in several body fluids such as blood, urine, saliva, and are very robust and chemically stable. Discovered in 2004 [22], they were rapidly identified as a promising biomarker for many diseases [14]. They have been evaluated as a new category of biomarkers for cardiovascular diseases [23].

Some miRNAs are specifically expressed in cardiomyocytes: the myomiR. There have been several studies pointing out a specific group of myomiR specific for CVD: miR-1, miR-133a, miR-208a/b and miR-499 [1]. It has been particularly found that miR-208 is overexpressed in patients with AMI and detectable one hour after onset [24]. miR-499 was also evaluated [14] for its specificity for AMI diagnosis. However, the performances of these biomarkers have not yet reached a consensus in the scientific community and is still a matter of debate regarding their potential to improve the diagnosis of CVD. It is also important to note that there is currently no clinical validation of these biomarkers.

Moreover, miRNAs suffer from technical issues regarding their broad study and use. First, they are very much dependent on patient's parameters, and there is currently a lack of investi-

gations on this matter. Secondly, there is no established standard measurement method, which brakes the ongoing clinical research on the matter. Therefore, there is an important need to standardize protocols in order to produce reliable miRNAs research results. Cardiac miRNAs have a huge potential in the field of cardiovascular diseases biomarkers. They could become powerful biomarkers for CVD, but more studies and standardization methods need to be obtained before their acceptability and use in clinical practice becomes a reality [14].

In conclusion, in the crowded field of cardiac biomarkers, there have been different trends historically with different biomarkers used during different time spans. Lately, cardiac troponin I has emerged as the reference marker for ACS and AMI diagnosis [5]. In the last twenty years, it went through a thorough scientific validation and is now widely used in clinical practice. The second relevant category of biomarkers are natriuretic peptides. They give precious information for the diagnosis of patients with heart failure, and can also be used in combination with troponin for patients with suspected AMI [21]. Lastly, miRNAs are an emerging category of cardiac biomarkers that draw the attention of the scientific community [14]. They are currently understudied and the lack of standardization is a brake to their entry into the clinical practice.

Cardiac biomarkers are of great importance for cardiovascular diseases diagnosis. In combination with other diagnosis methods (ECG, physical examination, medical imaging), they give reliable information to the practitioners for the diagnosis of CVD.

1.1.3 Diagnostic of cardiovascular diseases with Point-of-Care systems

Amongst current clinical guidelines regarding the diagnostic of cardiovascular diseases, it is recommended to test in patient blood some of the cardiac biomarkers described above. There are nowadays several conventional laboratory methods used to test the biomarkers, with various methodologies and technical characteristics. Most of these methods provide a good accuracy and sensitivity of the test results, but rely on heavy equipment, trained staff, expensive biological reagents and are time-consuming. To meet the criteria of rapid testing, Point-of-Care devices have been under important developments lately and are promising tools to assist and enhance medical diagnosis.

The UN defined the parameters to consider in order to ensure a good medical diagnosis through the acronym REASSURED: Real-time connectivity, Ease of specimen collection and environmental friendliness, Affordability, Sensitivity, Specificity, User-Friendliness, Rapidity, Equipment-Free, Delivered [25]. Point-of-Care devices are a category of diagnostic devices that meets all of these criteria. Such devices perform on-site testing and allow a major reduction of test time in critical situations, in which the risk needs to be determined quickly [26]. Besides their fast turnaround time, POC devices have many other benefits for patients and healthcare systems. Several studies have been conducted in different countries pointing out their potential to improve healthcare. In 2017, Nayak et al [26] categorized POC devices into 4 categories depending on the infrastructure and the budget (Fig 1.9). Cardiovascular disease testing devices are mostly used in clinics, and the budget can vary from moderate in the case of hospitals or Intensive Care Unit (ICU) to constrained for primary care clinics with reduced medical equipment. Therefore, cardiac POC devices fall predominantly in use case 1, and in some cases in use case 2 (Fig 1.9). Such devices have the major advantage of proposing a triage of patients, to rule-in or rule-out patients actually presenting a risk of cardiovascular diseases. However, for cardiac diseases diagnostic, POC are rather recent devices and use potentially disruptive technologies, so their acceptance in clinical practice is not always obvious. Several clinical studies have been conducted to evaluate the acceptance and usefulness of such devices in the context of CVD diagnosis enhancement.

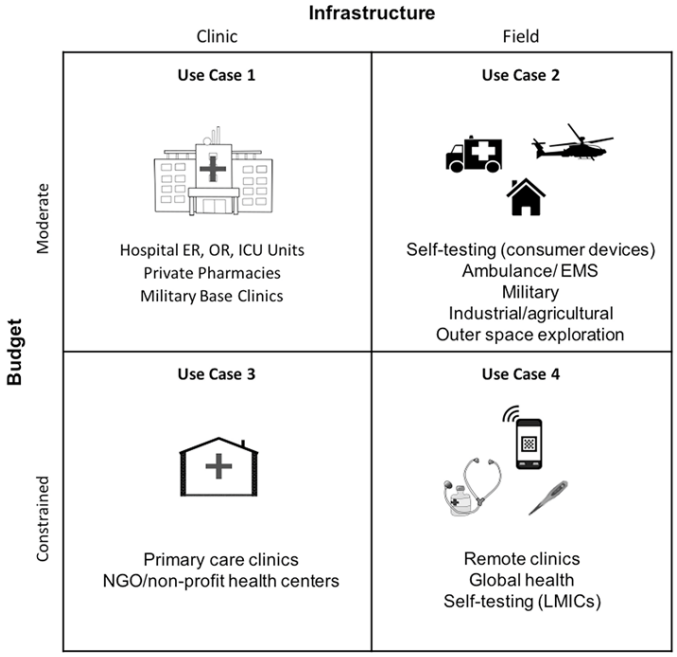

Figure 1.9: Representative POC diagnostic devices from Nayak et al [26]

In 2004, a study was conducted in the UK in order to analyze the impact of POC tests used in coronary care units [27]. Researchers conducted a prospective randomized study on 263 admissions in coronary care units and compared Point of Care Testing (POCT) with central laboratory testing for troponin T tests. Diagnostic accuracy and mortality were found to be similar for both testing systems, and there was no difference in length of stay in the coronary care unit. However, there was a significant reduction in non-coronary units stays and overall hospital stays. Therefore, they drew the main conclusion that rapid biochemical diagnosis and structured decision-making reduce the length of stay in the hospital overall, but the study results were less obvious for the specific coronary care unit under study. It is important to note that this study was conducted in the early 2000, a time in which the conventional troponin assays had a rather low sensitivity compared to the sensitivity that can be obtained with nowadays modern high-sensitivity troponin assays. Particularly for POC devices, the sensitivity was very likely lower than the one of the central laboratories. Moreover, in 2004, POC devices use in healthcare was very recent, and their acceptance in clinical practice was incomplete, which is coherent with the poor visible improvement in the study.

More recently, a study was conducted in 2020 by Hopital Pitié Salpétrière in Paris with the objective of examining a panel of cardiac POC solutions and their potential to decrease the length of stay of patients in the ED [28]. Researchers handled a prospective, controlled cluster-randomized study, with troponin T blood tests either performed in the hospital central laboratory or on POC implemented in the ED and included around 20,000 patients. Their main conclusion was a reduction of about 9 minutes for the length of stay in the ED and a significant shorter time to get the result from the POC device compared to the central laboratory (51 minutes). However, the over-cost for using POC device was estimated at 4.70 per patient. Governmental organizations will need to examine carefully these results in order to weigh the potential advantages of POC devices for the complete healthcare system. The study highlights the potential of POC devices to improve the flow of patients in the ED, but also points out that the benefits of POC to shorten the length of stay in the ED needs to be coupled to a broader

acceptance and training of clinical staff.

POC devices have a huge potential to improve healthcare practices. However, they will only show all their advantages if the healthcare system actually easily includes them in their practices. There is a need for staff training in order to improve trust in such systems. There is also a strong need for engineers to develop systems that give a biological result equivalent to one obtained in a central laboratory.

Current guidelines for the diagnosis of CVD with biomarkers recommend a total analysis time of less than one hour from patient admission in the hospital to the blood test result [5]. Therefore, important key challenges remain in biological tests used to quantify cardiac biomarkers' presence in blood. Indeed, the low basal concentration and slow increase in concentration over time require the development of high-sensitivity assays. Moreover, in order to obtain a rapid answer on the risk of AMI for a patient arriving with chest pain in the ED, the test result needs to be obtained in the shortest time span possible. Such criteria can be met through the development of portable devices.

During the development of cardiac Point-of-Care devices, we will pay attention to the importance of the different parameters defined in the acronym REASSURED [25]. A summary of the priorities we attribute for cardiac POC development can be found in table 1.1.

Priority	**Parameter**	**Considerations for cardiac POC**
1	Sensibility and specificity	Very low target concentration, complex medium (blood), reduce false positive
2	Time-to-result	Situation of cardiac emergency Reduce sample-to-answer time
3	Equipment-free	Portability (ambulances, offices...)
4	User-Friendly, Delivered	Easy and ready to use for non-trained staff
5	Connectivity	Real-time test results in the ED
6	Ease of specimen collection	Hospital settings in which blood tests are common
7	Affordability	Moderate cost because vital situation

Table 1.1: Order of priority for the different parameters in cardiac POC development

1.1.4 Market for cardiac POC devices

In order to highlight the potential for cardiac POC devices, global market information are presented. The aim is to understand the importance of such devices in the *in vitro* diagnostic industry, the major trends and actors, and the potential for new breakthrough innovations.

This market study was conducted with a student group from Université Grenoble Alpes (UGA) and Grenoble Ecole de Management (GEM) enrolled in a master in *In vitro* Diagnostic. They conducted a project work on "Innovation in In Vitro Diagnostic" and were asked to define the market for ultra-sensitive and portable detection systems (POC) for cardiac biomarkers. Their main results and findings are exposed in this section. The methods used include study and sampling (questionnaire on specific medical groups), data collection (internet, papers, libraries, interviews) and data estimation (for missing data based on verified data). Their study and main conclusions are summarized here and will orientate technical solutions proposed in the scope of this PhD project.

1.1.4.1 Market definition and sizing

The cardiac POC market is defined as the category of portable detection devices that are used to quantify cardiac biomarkers in blood when a patient is suffering from chest pain. Such devices can be used in ambulances, medical homes, retirement homes, hospitals, or doctor's offices.

In order to define this market size, data from the French healthcare system were used [29]. 21 million of cardiac biomarkers tests are performed each year in France since 2016 and it represents about 330 million euros. According to the French health insurance data [29], the most used cardiac biomarker is NTproBNP, with 14.3 million tests prescribed in 2020, compared to about 6.5 million troponin tests prescribed (Fig 1.10A). The two other most used biomarkers are myoglobin and creatine kinase but they represent only a few percent of the market share and price (Fig 1.10A). Similar trends are observed for the market prices, with NTproBNP representing the highest expense, followed by troponin tests (Fig 1.10B).

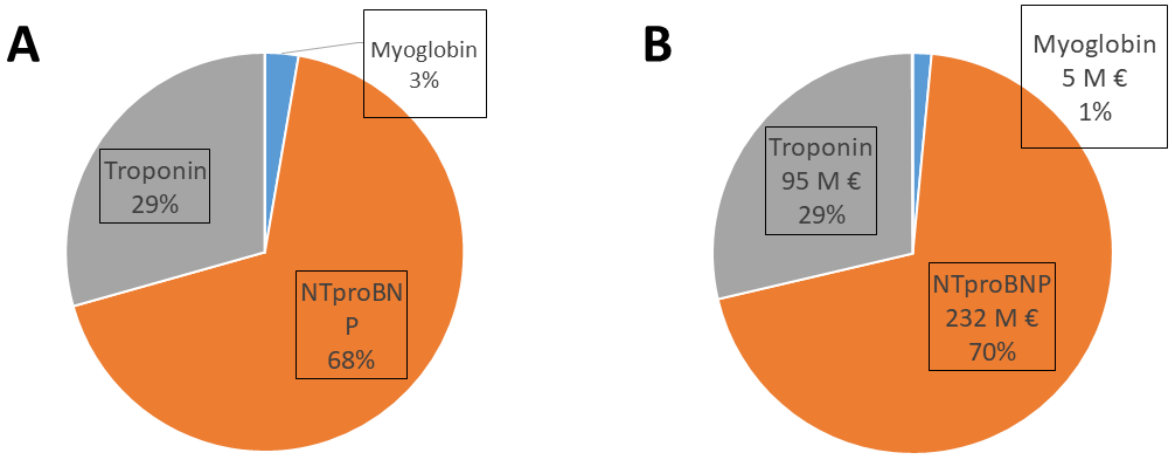

Figure 1.10: French cardiac tests markets in 2020. (A) Market share in number of tests performed and (B) Market price in expenses (millions) per biomarker

These data are extended to Europe which then represents annually a market of about 3.2 billion euros and 250 million tests performed (Fig 1.11). In a similar fashion, it is extended worldwide and represents annually a market of 8.5 billion euros. This market value defines the Total Available Market for cardiac biomarkers. This market is narrowed down to the Serviceable Available Market with the 3.2 billion euros that represents the cardiac biomarker European market. Lastly, to define the market share of cardiac POCT in Europe, we evaluated the POC testing as about 30 % of the tests performed. Therefore, the yearly cardiac POC testing market in Europe is estimated at 950 million euros (Fig 1.12). This share of 30 % for POC testing in Europe was found by estimating the number of ambulances, medical homes and nursing facilities that could use POC devices, and is confirmed in the literature [30]. From this Target Market for European cardiac POC device, we can evaluate the market share that a company proposing a new cardiac POC device could hope to reach in France, and this share was estimated at 1 %, representing a market share of 9.5 million euros for a new cardiac POC device.

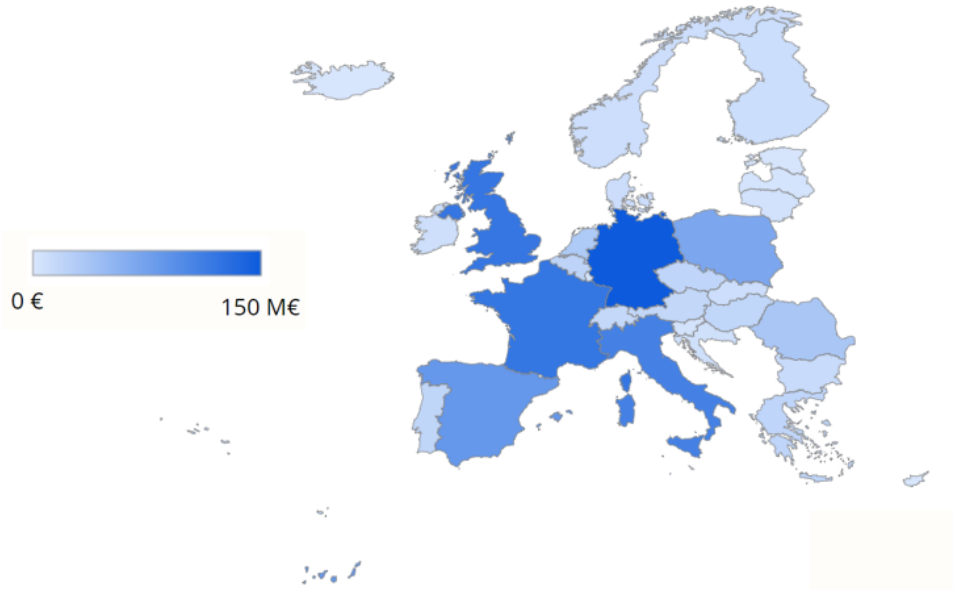

Figure 1.11: Estimated annual market size of POCT for cardiac biomarkers in European countries

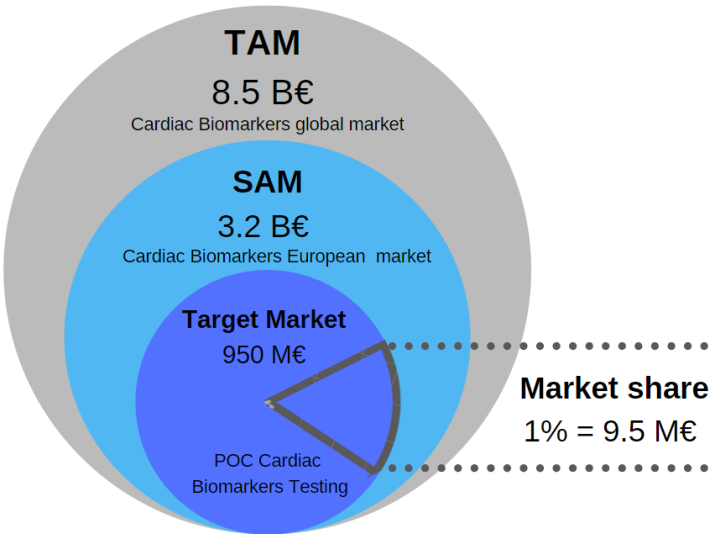

Figure 1.12: Diagram of the market sizing with TAM (Total Available Market), SAM (Serviceable Available Market) and Target Market for cardiac POC tests in Europe.

Figure 1.13 shows the trend in terms of growth for the four main cardiac biomarkers in France from 2016 to 2020. It shows that over the past five years, troponin and NTproBNP have grown the most in terms of tests prescribed in France. It is in accordance with recent guidelines from the ESC [5] and shows the adaptation of medical practices. Moreover, in the last decades, several studies have highlighted that myoglobin and creatine kinase were less specific and sensitive for CVD diagnostic [11], leading to a rather important decrease in their use as cardiac biomarkers.

The cost of cardiac tests on POC devices is very heterogeneous, and several technologies are available on the market for hospitals and practitioners to choose from. Worldwide, the total cardiac biomarkers testing market is estimated at 8.5 billion euros. The study in the scope of this project will be narrowed down to the European Point of Care market for CVD, reducing it

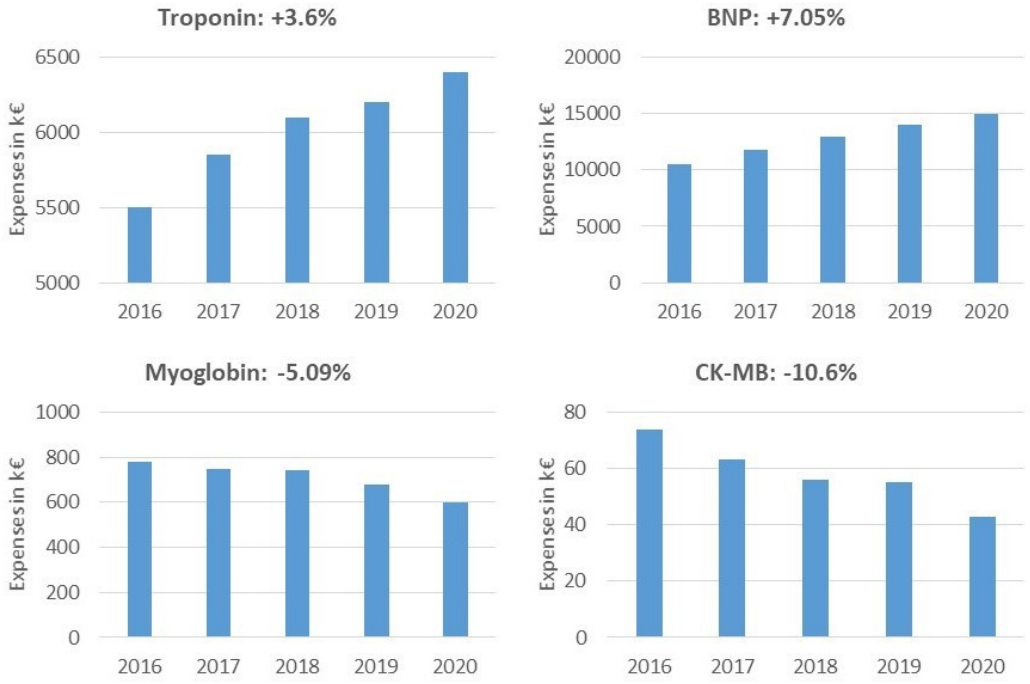

Figure 1.13: Annual growth of the four main cardiac biomarkers in euros in France from 2016 to 2020. Market price (total test annual cost) is represented over the years.

to a total share of 950 million euros for a new POC device.

1.1.4.2 Market growth

In France, the cardiac biomarker market is growing every year with a Compound Annual Growth Rate (CAGR) of 2.4 %. More precisely, the estimation of cardiac biomarkers testing growth in POC is approximately 11 % over the 5 past years (Fig 1.14). This trend shows the growth of this sector with the adoption of more POC devices by healthcare professionals. Therefore this market is growing due to the cardiac biomarker test demand and the POCT devices demand. It is also important to note that the number of tests for cardiac biomarkers has greatly increased in 2020. This increase is due to the COVID-19 pandemic. Infection with Sars-Cov2 can lead to cardiovascular disorders, including myocardial injury, arrhythmia and acute coronary syndrome. Therefore, the increase number of patients with COVID-19 and pre-existing medical conditions such as cardiovascular diseases has amplified the worldwide demand for cardiac biomarker testing.

1.1.4.3 Major players and competitors

The market for cardiac point-of-care devices is dominated by North America as the leader with 40 % of the market share, followed by Europe with 32 % of the market shares, and Pacific Asia with 20 %. To study thoroughly the ongoing technological development in the field, eight companies in the medical technology sector were selected. It was intended to have a heterogeneous mix of small and larger companies, as well as companies that have been in the field for a long time or possible market disruptors. A general overview of the company's financial situation is given, as well as their strategic developments, in the scope of their operations and products

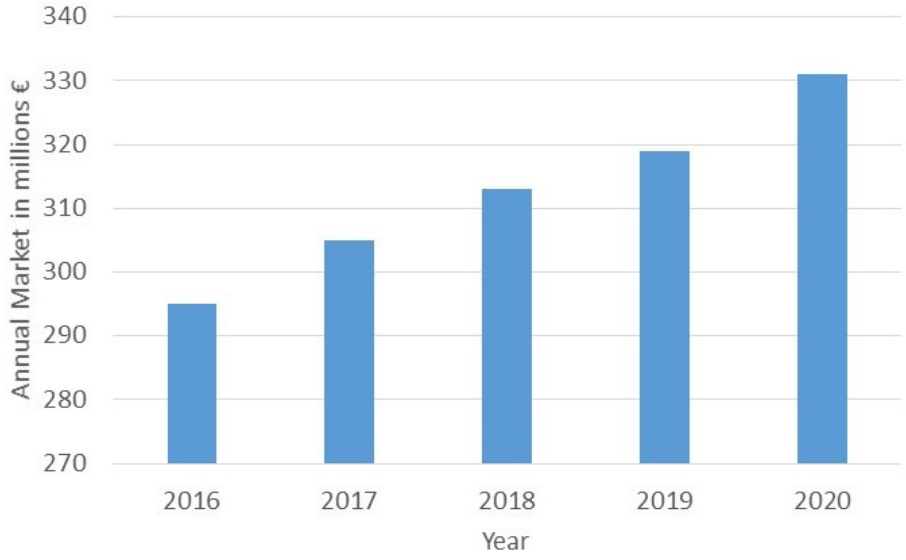

Figure 1.14: Evolution of the annual market of cardiac biomarkers testing in France

in the segment of cardiac point of care.

The eight companies' financial profiles are presented in table 1.2, sorted by their revenues in descending order. It already highlights that the companies operate under different conditions and have different possibilities to enter the cardiac Point-of-Care market. It is important to note that no differentiation is made between the operating segments of each company, even though all of them are major competitors in the cardiac POC market.

Company	Origin	Revenue*	Cost of Sales*	R&D expenses*	Cost of sale /revenue	R&D expenses /revenue
Roche	Swiss	41.8	7.6	9.9	18 %	24 %
Thermo Fischer	US	32.2	24.2	1.2	75 %	3.6 %
Abbot	US	29.8	14.8	2.1	49 %	6.9 %
Philips	German	19.5	10.6	1.9	55 %	9.8 %
Siemens Healthineers	German	14.6	8.9	1.3	61 %	9.2 %
Biomerieux	French	3.1	1.3	399	43 %	12 %
BioRad	US	2.4	1.1	226	45 %	9 %
Quidel	US	1.7	312	84	19 %	5 %

Table 1.2: Financial overview of major players (retrieved from 2020 annual report). ** in million euros*

First, BioRad and ThermoFischer are both worldwide Life Science companies but have no offers for cardiac POC systems. ThermoFischer has for example many high-sensitivity immunoassays for CVD markers but only one POC system for hemoglobin. Therefore those two competitors are currently not part of the race for cardiac POC. Two companies notably develop competitive troponin POC systems. Siemens Healthineers offers a troponin POC system giving result in 8 minutes. The company's 2020 annual report states that it focuses its efforts on POC developments. Abbott offers the only troponin test on the market with gender-specific values. The US-based company Quidel offers a broad portfolio for CVD testing, with different immunoassays and multiplexed platforms.

Finally, Biomérieux and Roche both propose a portable platform for the detection of multiplex cardiac biomarkers in less than half an hour. Biomérieux has the highest ratio of R&D expenses to revenue (12%) and a very strong culture of research, but currently, no novel biomarker is under investigation. Roche also has high R&D expenses, and a growth of 54% in the diagnostic division, with a very strong focus on POC systems. Currently, it proposes a reference immunoassay platform for cTnT and NTproBNP testing, and a POC devices for various cardiac biomarkers (Cobas h232 [31]). The variety of products offered by Roche in the field of cardiac biomarkers testing places Roche as the leader for cardiac POC development. Its current product Elecsys targeting troponin and NT-proBNP is currently very competitive and places Roche as the leader for cardiac POC.

The companies developing cardiac POC systems have very various profiles, from small companies with relatively low revenue but broad product portfolio such as Quidel, to market leaders in the field of diagnosis with the example of Roche. With the available commercial and market information about each company, it is difficult to define a market leader, even though Roche appears as the major competitor with the variety of cardiac testing systems it offers on its portfolio. The variety of companies present in the market, opens the way to the introduction of different innovative products, especially with the introduction of new biomarkers and new diagnostic tools and methods.

Acute Coronary Syndrome, Myocardial Infarction and Heart Failure are the three main cardiovascular diseases and represent the leading cause of death in the world. Early and precise diagnosis can reduce the risk of CVD through early prevention. Amongst the conventional clinical diagnostic tools, the scientific literature highlighted the potential of different biomarkers to improve cardiac care [1]. Amongst this, troponin and NT-proBNP particularly drew the attention of the scientific community and clinicians over the last decades. This is confirmed by the market analysis presented in the previous section: troponin and NTproBNP are the most commonly used biomarkers, and their use increased respectively by 3% and 7% over the last 5 years in France. There are also ongoing research efforts for the discovery and evaluation of new cardiac biomarkers. For example, miRNA have a great potential to be used as cardiac biomarkers [14], which, in combination with current biomarkers, would be more sensitive, more specific, and more accurate for cardiac diseases.

Conventional central laboratory methods are mostly used to test cardiac biomarkers in blood but are often long, and require heavy machinery and trained staff. There are many possible improvements in the cardiac testing domain to propose quantitative tests on portable and autonomous platforms. POC devices have a huge potential to improve cardiac disease diagnosis, and in combination with the diversity of biomarkers used, they can become important tools for practitioner's decision-making. The European market share for cardiac POC systems is estimated at 950 billion which highlights the many innovations possibilities in this field. There are many worldwide competitors focusing on research and development efforts to design cardiac POC systems, highlighting the potential of such devices for healthcare systems.

1.2 Cardiac POC systems

Point-of-Care devices have a huge potential to improve the *in vitro* diagnostic industry. There is still a great potential for innovation in cardiac testing devices. The previous section highlighted the main criteria to design cardiac POC systems that can enhance CVD diagnostic. This section will present the technical characteristics of cardiac POC devices, by reviewing the different existing biosensing methods and potential innovations, and the different methods for biological

protocol integration relying on microfluidic technologies. Lastly, to highlight the variety of the technical solutions described, a summary of the main commercialized cardiac POC devices is exposed, as well as potential areas for improvements, to define the Ph.D. project goal.

1.2.1 Biological assay developments

There are different methodologies to detect molecules of interest in a biological sample. This section will summarize the main relevant methods in the case of cardiac biomarkers, but the methods also apply to many other biological species in various application domain such as environmental monitoring, food-processing industry and civil surveillance. The typical elements of a biosensor as exposed in figure 1.15 will be carefully reviewed with specific examples of cardiac biosensors and new emerging methods.

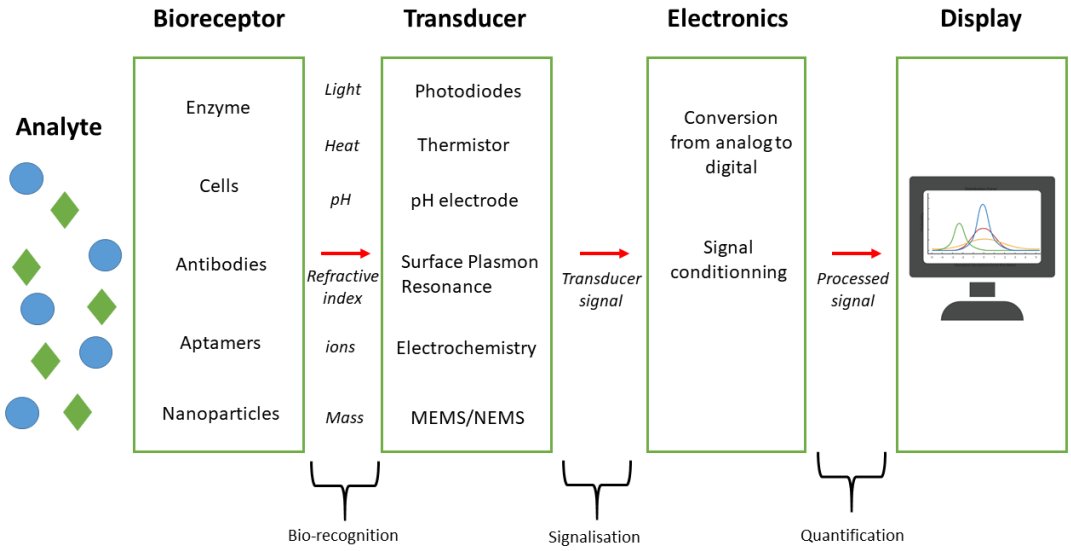

Figure 1.15: Schematic representation of a biosensors adapted from [32]

1.2.1.1 Bio-recognition elements: antibodies and aptamers as molecular probes

Most of the tests used to quantify a biomarker in a sample rely on its capture thanks to a molecular probe. In the context of cardiac biomarkers presented in the previous section, two types of molecular probes are commonly used: antibodies and aptamers. Their schematic representation is given in figure 1.16.

An antibody is a Y-shaped protein of 150 kDa that recognizes a unique molecule called an antigen (Fig 1.16A). These proteins are commonly used in diagnostic procedures for their broad applications to various biomarkers, especially for peptides and proteins. They possess a very strong affinity with their specific target and are designed specifically to bind to an analyte with a very good association coefficient due to strong interactions; like Van Der Waals, H-bonds, or Coulomb. Each tip of the Y-shape is specific to a particular epitope into the antigen, allowing accurate binding of the two structures. There are two main types of antibodies, monoclonal or poly-clonal [33]. Polyclonal antibodies are heterogeneous and recognize several epitopes of the antigen, whilst monoclonal antibodies recognize a single epitope in the antigen [34]. Both are produced *in vivo* with animals during the response to an immunization towards an antigen.

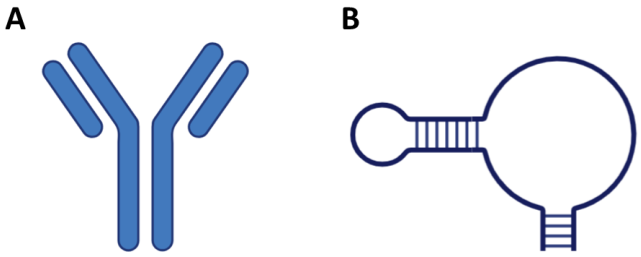

Figure 1.16: Schematic representation of antibodies (A) and aptamers (B)

For monoclonal antibodies, the animal spleen cells are harvested and fused to myeloma cells to produce hybridoma cells. Following clone screening, the selected hybridomas are kept and therefore used to indefinitely produce the monoclonal antibody (Fig 1.17A). The polyclonal antibodies, obtained in 4 to 8 weeks, are necessarily produced *in vivo* since they are withdrawn directly from the animal blood serum (Fig 1.17B).

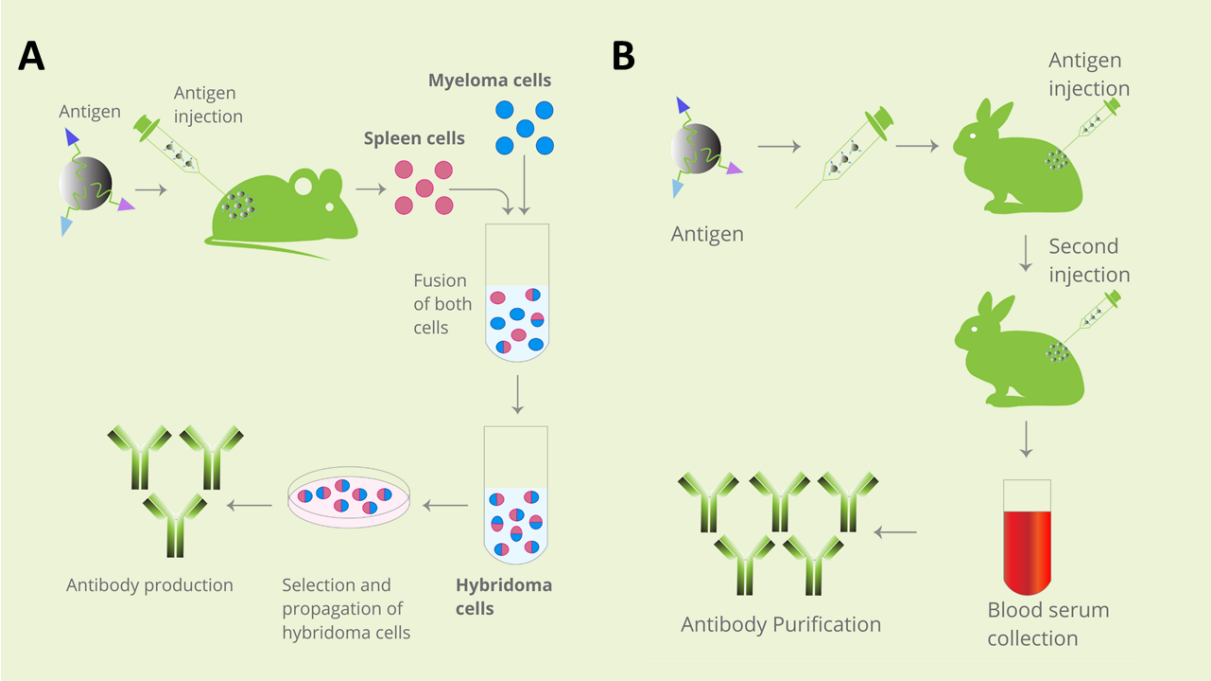

Figure 1.17: Schematic of the different production pathways of antibodies [35]. (A) Production of monoclonal antibodies and (B) Production of polyclonal antibodies

Antibodies are widely used in immunoassays and are therefore important bio-recognition elements for biomarker sensing. However, they present several drawbacks that encouraged the development of alternative molecular probes [36]. They are produced *in vivo* with animals or *in vitro* using cell cultures and are therefore very expensive biological reagents to produce. Moreover, the batch to batch variability can be very high which alters the reproducibility of the developed test. Lastly, they are fragile proteins and are therefore sensitive to temperature variation and present limited shelf storage [37]. Therefore, alternative methods to the use of antibodies have emerged.

Synthetic bio-molecules called aptamers have been discovered in the 1990s' by two inde-

pendent research groups [38] [39]. They are nucleic-acid-based bio-recognition elements, single-stranded with a 3D shape that allows them to bind to a specific target (Fig 1.16B). In the early 1990s', they emerged as a competitor to antibodies [40], especially with the development of the Systematic Evolution of Ligands by EXponential enrichment (SELEX) process which selects specific DNA sequences for the desired target.

The term aptamer was first used in the 1990s' by Tuerk et Gold [38], and comes from the latin *aptus* for "binding" and the suffix *mer* to relate to the base unit of a polymer. An aptamer is a single-stranded nucleic acid structure, rather short (15-60 bases), and has a certain affinity for a target molecule such as organic molecules, proteins, peptides, or cells. The structural characteristics of aptamers give their affinity towards a specific target. Nucleic acid strands display specific conformation folding with loops, G-quadruplex, or stems. Hydrogen bonding between the bases stabilizes the structure, leading to a tri-dimensional compact formation. To interact with a target, an aptamer adopts a specific conformation, and in some cases, the aptamer folding is induced by the target binding.

Aptamers are selected for a specific target through a selection process called SELEX, for "Systematic Evolution of Ligands by EXponential enrichment" [38] [41]. This technique relies on the isolation of target-specific oligonucleotide sequences from a random library of oligonucleotides.

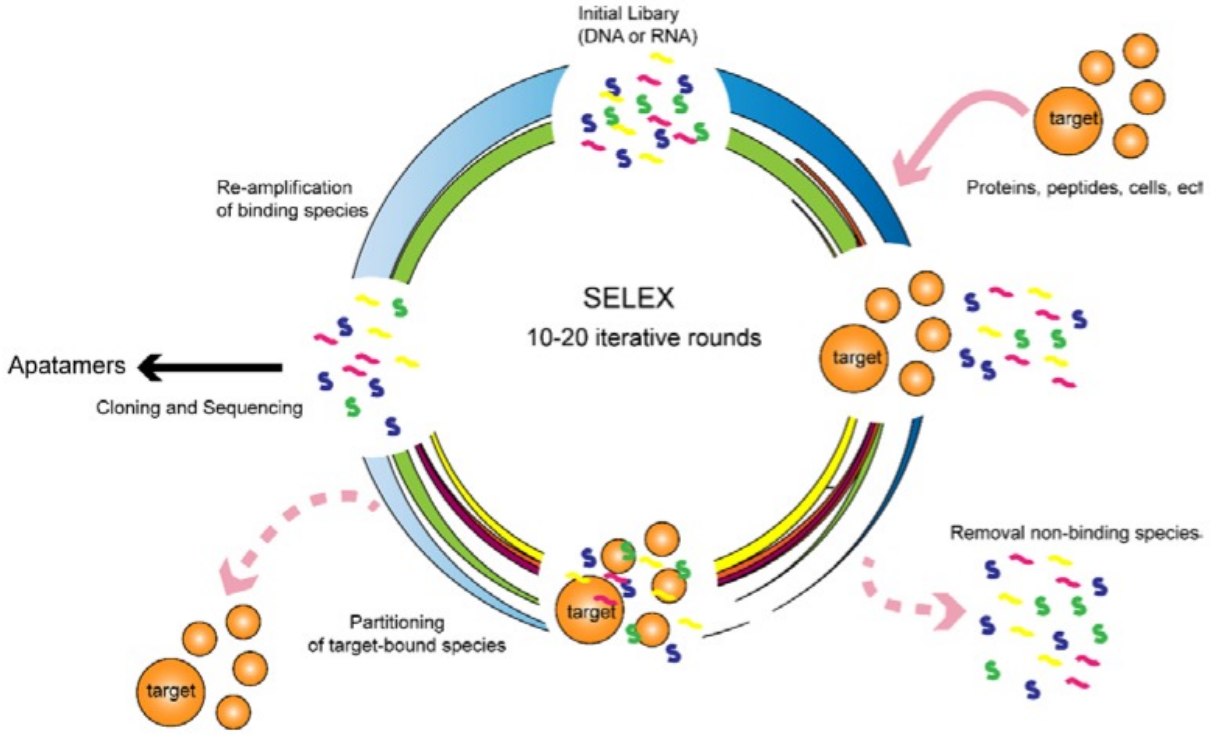

Figure 1.18: Schematic of the different steps of the SELEX process from [41]

The SELEX cycle presented in figure 1.18 consists in screening a large number of random oligonucleotides in an iterative process alternating selection and amplification steps. First, a single stranded DNA library is made of about 10^{14} and 10^{15} random DNA sequences chemically produced. These sequences contain a common area at the 3' and 5' end with primer-specific bases used for downstream Polymerase Chain Reaction (PCR), and a variable area of N nucleotides randomly chosen with the 4 nucleotides A, T, C, G. These sequences are incubated with the target of interest. The experimental conditions such as buffer and reaction temperature are important parameters and therefore reported in the process. A part of the sequences react

with the target, and the rest of the sequences that did not react are eliminated by a physical method (filtration, gel electrophoresis for example). The sequences having an affinity with the target are then isolated and amplified by PCR in order to generate a new library enriched with candidate sequences. Lastly, this new library is put into contact with a new sample and the process is conducted again. The process is repeated in between 8-15 times until the sequences with the highest affinity to the target are obtained. The selected oligonucleotides are sequenced and the obtained sequences are optimized in order to remove all the unnecessary nucleotides present during the process (PCR primers for example). The final optimized aptamer sequences are generally lower than 40 nucleotides. They are functional in the experimental conditions they have been selected into (buffer, temperature).

Generally, the SELEX process takes from weeks to months to obtain a specific aptamer sequence, and the hit rates are rather low. Thus, obtaining high quality aptamer against a specific target remains a challenge, and several modified SELEX method arose lately [41], like negative SELEX [42], capillary electrophoresis SELEX [43] or microfluidic SELEX [44] [45] [46].

Nowadays, several companies offer SELEX process, such as the company *Novaptech* (Bordeaux, France), and several research groups also achieve their own selection of aptamers. The specificity of an aptamer is validated when several international research teams validate its use and share their experimental practices in peer-reviewed journals.

Once an aptamer sequence is selected, it can be synthesized chemically, rapidly and at low cost. In addition, it can be easily modified or functionalized for various downstream applications. Moreover, aptamer's *in vitro* selection enables their animal-free production, compared to antibodies. Smaller than antibodies (5-20 kDa versus 150 kDa), aptamers are very stable over time and less sensitive to temperature variation. Their storage and transport are therefore easier. Their affinity is equivalent to antibodies with a dissociation constant K_d ranging from micromolar to picomolar. Aptamers are often called "synthetic antibodies". Their main properties in regards to antibodies are summarized in table 1.3.

Property	**Antibody**	**Aptamer**
Size	150 kDa	5-20 kDa
Production	*In vivo*	*In vitro*
Development time	Several months	Several weeks/months
Cost	High	Moderate
Targets	Protein, peptides only	Protein, peptides, organic molecules, toxins
Modification	Chemical conjugation	Easy modification in 3' or 5' (biotin, NHS...)
Storage	Several months at +4°C or -20°C	Several years at -20°C
Stability	Temperature sensitive, irreversible denaturation	Temperature robust, reversible denaturation
Type of interaction with targets	Van der Waals, H-bond, hydrophobic, Coulomb	Weak (Van der Waals, H-bond)
Affinity	pM - μM	pM - μM

Table 1.3: Comparative table of antibody and aptamer properties for biosensing applications.

Antibodies and aptamers are two different types of bio-receptors that bind to various types of targets. Antibodies bind only to protein and peptide but present a very strong interaction, whilst aptamers have a wider range of targets (proteins, peptides, toxins, organic molecules...) with weaker interaction, mainly due to a higher dissociation coefficient. Antibodies are produced *in vivo* at a high cost, and aptamers can be produced *in vitro* at relatively low costs. Both products

required long development times, usually several weeks or months.

Aptamers seem to present many advantages over antibodies, mainly low cost production and long stability over time [40] [47]. Aptamers have been the core of many researches to develop competitive antibody-free biosensors [48] [49]. However, to our knowledge, no commercialized biosensor device using aptamer exists, showing the limitation of this compound.

1.2.1.2 Transducers

Next to the choice of analyte capture, there are several types of signal transducers whose roles are to convert the bio-recognition event into a readable and measurable signal. Most transducers provide either electrical or optical signals usually proportional to the amount of the analyte of interest, and must be chosen adequately to ensure minimally invasive, rapid and highly sensitive detection.

Electrical The first scientifically proposed and commercialized biosensors are electrochemical biosensors. They are composed of electrochemical transducers, which use a chemical reaction between the biomolecule and the target analyte to produce or consume ions or electrons which therefore affects the measurable electrical properties in the solution [50]. Their main advantages are robustness, real-time detection and ability to operate on small sample volumes, but they have important limitations such as enzyme saturation, interference of other compounds in solution, influence of pH and slow electron transfer. Electrochemical transducers can be categorized into three main categories:

- Amperometric / Voltammetric
- Potentiometric / Conductometric
- Impedimetric / Capacitive

They are used in a wide spectrum of applications such as food monitoring, agricultural, or clinical diagnosis. There are numerous examples in the literature of electrochemical platforms for the diagnostic of cardiovascular diseases [7] (Fig 1.19). One of the most well-known example is the i-STAT platform from Abbott [1], which is a whole blood amperometric immunoassay. The electrochemical sensor is made of a silicon chip and an alkaline phosphatase enzyme conjugated to the antibody, that produces a readable electrochemical signal. Troponin I is captured in the sample thanks to a two-site ELISA assay. The device is composed of two sensors, the first one containing magnetic beads functionalized with capture antibodies to capture the target, and the second one with antibody-enzyme conjugate. Both sensors are positioned side by side on a substrate composed of a gold micro-array electrode. Below the second electrochemical sensor, a high field magnet attracts the magnetic beads onto the sensor and allow to concentrate the beads during a washing step, thus reducing the number of unbound analyte and improving the signal-to-noise ratio. After complex formation and washing, the substrate is cleaved by the enzyme conjugated to the antibody, producing a readable electrochemical signal.

Another example of amperometric sensor was described by De Avila in 2014 [51] to detect C reactive protein (CRP) and NTproBNP after a redox reaction with the horseradish peroxidase (HRP) enzyme (Fig 1.19A).

Label-free approaches using Electrochemical Impedance Spectroscopy have also been described. They measure the change in the impedance value when a potential is applied to an electrode immersed in an electrolyte. In 2017, Shanmunga et al [53] described a zinc oxide nano-sensor for the detection of cTnI and cTnT in human serum. In 2018, two independent teams made use of Differential Pulse Voltammetry (DPV) to quantify cTnI [52] and BNP [54] with the use of nitrogen-doped reduced graphene oxide and troponin aptamer (Fig 1.19B).

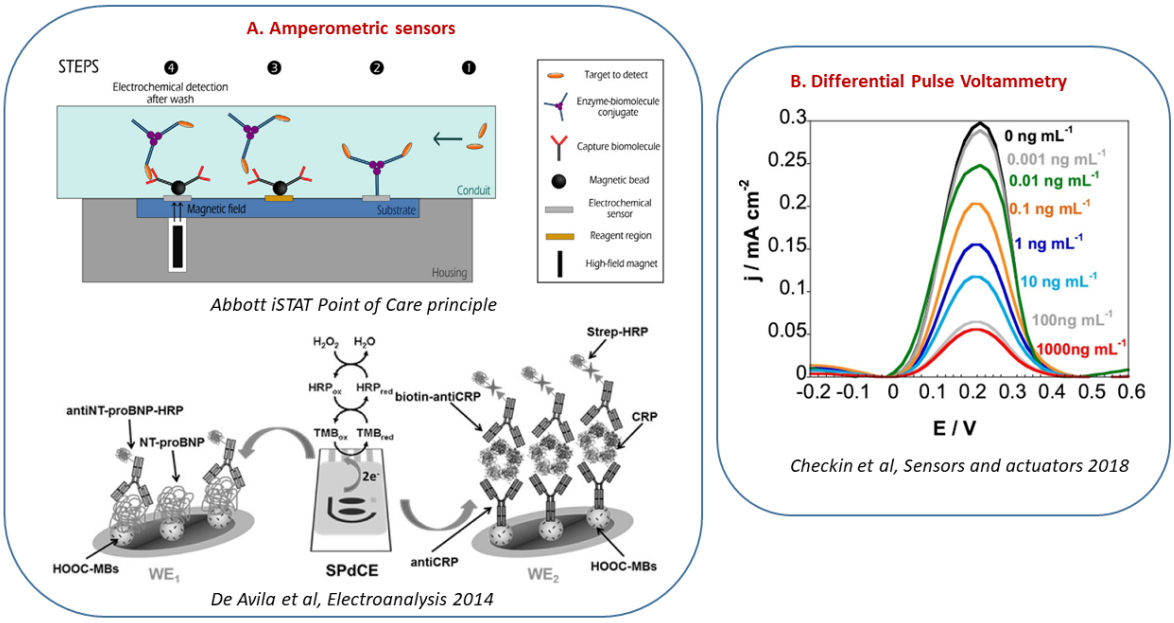

Figure 1.19: Different biosensors for the detection of cardiac biomarkers with electrical readout strategies. (A) Amperometric sensors with iSTAT platform from Abbott [1] and magnetic immuno-sensor for the detection of NTproBNP and CRP [51]. (B) Detection of cTnI using DPV [52]

Optical Another common way to detect an immunoreaction is through optical means, and it is the most common way to detect an immunoreaction in clinical settings. There are several approaches such as colorimetry, fluorescence intensity measurement, luminescence, Surface Plasmon Resonance (SPR), metal-enhanced fluorescence and surface-enhanced Raman spectroscopy.

A very common optical transducer is colorimetry. It relies on a substrate that reacts with an enzyme which induces a change of color in solution. Nowadays, most of the ELISA assays for troponin sensing that meet the requirement in terms of sensitivity use this detection method. Torrini et al in 2019 described a sensor combining aptamers and colorimetry detection for the characterization of troponin T binding aptamer in a so-called innovative Enzyme Linked Oligonucleotide Assay (ELONA) [55] (Fig 1.20A). The colorimetric technique has the advantage of being easy to perform and measure, especially for an integration in a Point-of-Care System [56], but presents the inconvenient of a lack of sensitivity and limited dynamic range.

Fluorescence intensity measurement is another common optical transducer also used in both antibody and aptamer assays. It relies on the emission of light by a substance that absorbs light and re-emits it at a longer wavelength. In assays, the combination of antibodies to a fluorescent probe is a common way to implement fluorescent readout strategy. There have been several innovative sensing techniques shown in the literature, for example with the use of TiO_2 nanotubes for cTnI sensing [57] with fluorescent labeled antibodies. The use of fluorescence has also been combined with aptamers based on graphene oxide sensors that quenches the fluorescence [58] (Fig 1.20B). Moreover, aptamers as short nucleic acids sequences are easily integrated with fluorophore or quenchers and it becomes easy to follow the binding to an analyte through the fluorescence measurement [49]. A substitute to fluorescence intensity measurement is chemiluminescence, the emission of light as a result of a chemical reaction. It has been successfully employed in immunoassays for troponin I sensing with a double antibody sandwich strategy [59].

Chemiluminescence reagents are added at the end of the assay and the luminescence intensity is evaluated by a chemiluminescence detection system, thus removing the need for fluorescence excitation systems.

Optomagnetic measurements combine the optical and magnetic characteristics of particles. It has been successfully applied in a commercialized device with the Philips Minicare [8], [60], [61]. The detection relies on superparamagnetic nanoparticles that bind to the sensor via a sandwich immunoassay and that is detected using the optical technique of frustrated total internal reflection (FITR) [60] (Fig 1.20C).

SPR technology has been recently developed for troponin sensing with a label-free direct assay mode [62] (Fig 1.20D). SPR uses the surface plasmon resonance of metallic surfaces to detect the molecules bound at the surface. This sensing technique gives a rapid response in real-time and can be used for multiple sample analysis by SPR imaging. However, with this technique, the limit of detection is well above the cut-off level of cTnI. This technique is therefore mostly used to characterize the bio-interaction in a biosensor in terms of association and dissociation constant [63].

Lastly, spectroscopy techniques can be used as optical readout strategies through the interpretation of the electromagnetic spectra from the interaction between electromagnetic radiation and matter. For example, Raman spectroscopy, can be used for the detection of cardiac biomarkers as exposed by Zhang et al in 2018 [64] (Fig 1.20E). This technique takes advantage of the Raman scattering of dyes placed in a LFIA system and can detect three different cardiac biomarkers.

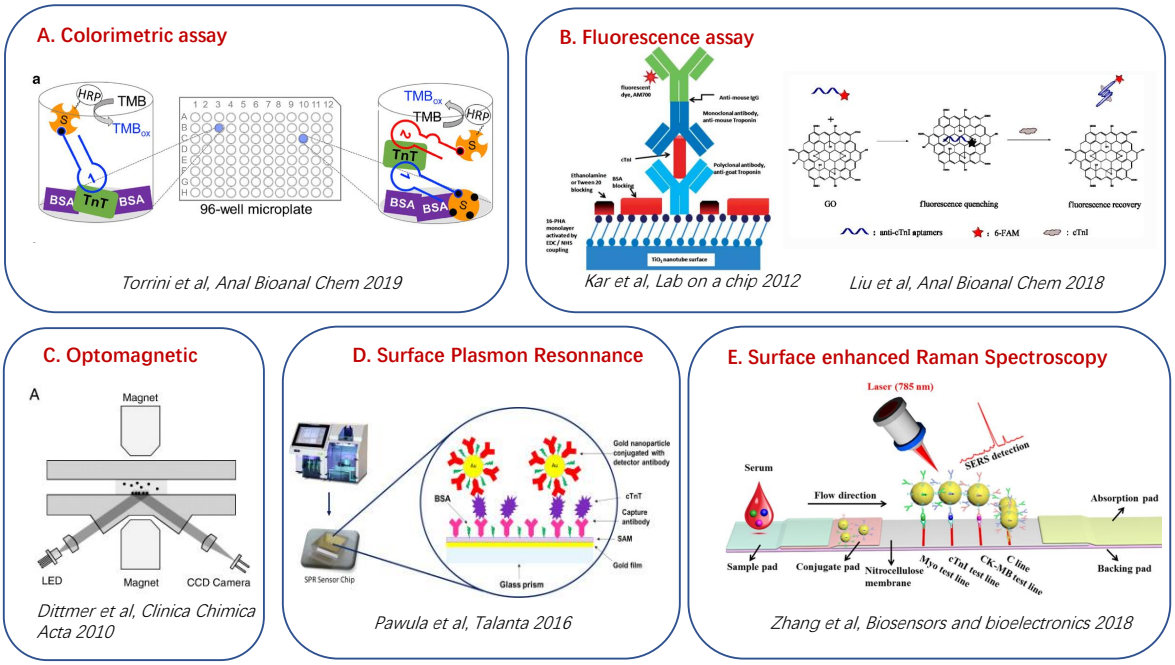

Figure 1.20: Different biosensors for the detection of cardiac biomarkers with optical readout strategies. (A) Colorimetric assay [55]. (B) Fluorescence intensity measurement [58] [57]. (C) Optomagnetic sensors [60]. (D) Surface Plasmon Resonnance sensors [62]. (E) Raman spectroscopy biosensor [64].

Electrochemical detection methods have the advantage of being easy to perform and in most cases label-free, but they present limitations in terms of sensitivity. Moreover, embedded

technology for electrochemical sensing usually requires a complex fabrication process (electrode array). Optical detection usually exhibits high-sensitivity testing and potential for multiplexing, but it requires bulky instrumentation. A trade-off between those two main detection methodologies needs to be determined for each desired application. In the context of cardiac biomarkers testing, the important need for sensitive and portable tests brings the transducer choice to optical transducing options, allowing the quantitative signal readout with minimally invasive technology, and potential real-time monitoring [65].

For the application of cardiac biomarkers, two main bio-recognition elements have been described (antibodies and aptamers) and two main transducing options (electrochemical and optical), with examples of potential implementation for cardiac testing in POC testing devices. Some integrated assays combining both options for bio-recognition and transducers will be exposed in the next section. Their advantages will be highlighted for the detection of cardiac biomarkers.

1.2.1.3 Integrated assays for cardiac biomarkers testing

The conventional assay for cardiac biomarkers testing will be presented: the ELISA assay combining antibody recognition and optical detection. Then, some possible innovations to overcome the drawbacks of this assay will be presented, by changing the bio-recognition elements or the transducing option.

Conventional method: ELISA A well-known and now widely used detection method relying on antibody capture and enzymatic amplification was developed in the early 1970s [66]. This method called ELISA is based on a sandwich of the target with two antibodies followed by an enzymatic amplification. It is a powerful method for detecting and quantifying a specific protein in a complex mixture. There are different versions of this test: direct, sandwich, competitive and extended sandwich assays (Fig 1.21). The key step is the capture of the antigen by a capture antibody attached to the plate. The antigen is then detected directly (labeled primary antibody) or indirectly (labeled secondary antibody). The sandwich ELISA is the most widely used ELISA assay. It indirectly immobilizes and indirectly detects the presence of a target antigen. The very good sensitivity and specificity of ELISA tests makes them widely used. After the enzymatic reaction, the most commonly used detection method is optical, through colorimetry. Alternatives optical methods relying on fluorescent labeled antibodies also exist.

The development of an ELISA test is laborious because it always requires the development of antibodies, and the procedure is dependent on many parameters such as the plate coating and capture of the antigen, plate blocking, choice of detection probe and signal measurement strategies [66] [36]. This quantitative assay is widely used for cardiac biomarker testing and many biosensors have been described [18] [67] [68]. Many companies have worked on the development of ELISA tests and the current commercialized tests can be very competitive in terms of sensitivity and specificity. For example, the Life Science company ThermoFisher offers several ELISA tests for troponin, with a very low LOD of 0.38 pg/mL [69].

Trends in cardiac biomarkers tests In biological assay development, antibodies can be replaced by other molecules such as aptamers. This way, the conventional ELISA method can be called enzyme-linked aptamer-sorbent assay (ELASA). This method can serve either for the quantification of molecules or for validating aptamers [70].

Aptamers can also be used in electrochemical devices for the detection of cardiac biomarkers [71]. The combination of aptamers and electrochemical readout has been under great develop-

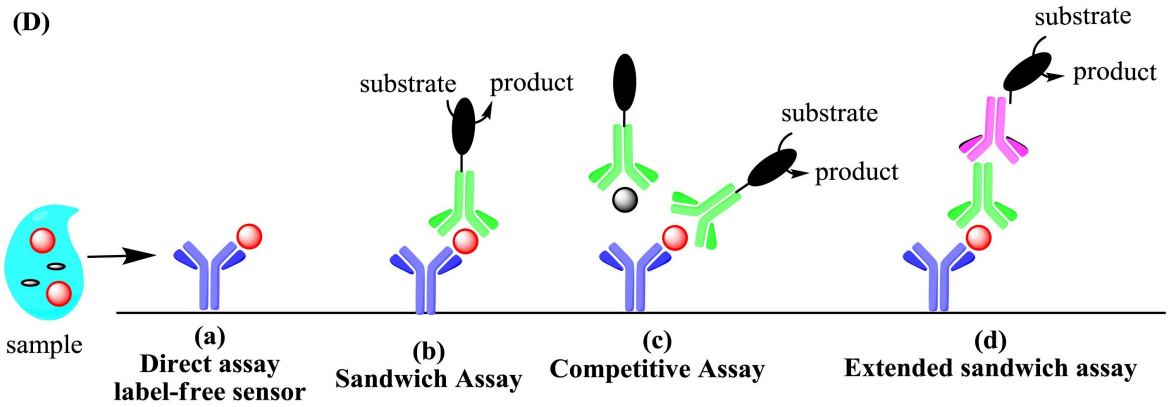

Figure 1.21: Schematic of 4 common ELISA assays [7]: (a) direct assay, label-free in which the analyte binding produces a readable signal, (b) sandwich assay using labeled secondary antibody (c) competitive assay using labeled antibodies and (d) extended sandwich assay using tertiary antibody for sensing.

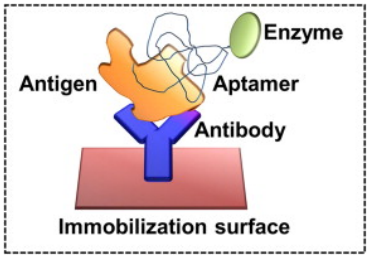

Figure 1.22: Schematic of ELASA principle [47]

ment over the past years, and the trends in the achieved LOD shows that this combination led to a significant reduction from 20 pg/mL down to 0.5 pg/mL (Fig 1.23).

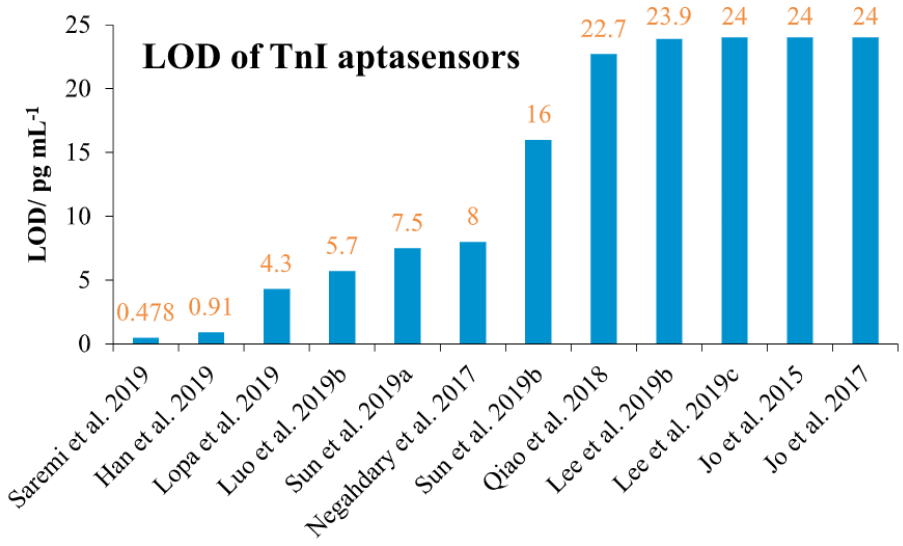

Figure 1.23: Reported LOD for cardiac electrochemical aptasensor [71]

These examples including aptamers in cardiac biosensors, place aptamers as a powerful

alternative to conventional antibodies, eventually able to meet the required sensitivity in the case of antibody-free cardiac biosensors. As observed in figure 1.23, the sensitivity of troponin sensors using aptamers has decreased consequently, down to the required sensitivity of a few pg/mL, being therefore competitive with conventional troponin sensing methods used in central laboratories.

When the analyte is present at a very low concentration in a sample, the conventional ELISA method can be limited or even inefficient. Therefore, another way to achieve high-sensitivity sensing consists in the replacement of the signal amplification strategy, before the signal readout. Immunoassays like ELISA are mostly used for the detection of protein biomarkers, while nucleic acids amplification techniques are considered to detect genes [72]. The innovative integration of immunoassays with nucleic acids amplification techniques combines the direct and rapid performance of an immunoassay with the ultra-sensitivity given by a molecular assay with nucleic acids amplification. There are two main types of nucleic acids amplification techniques. PCR amplification was discovered in the 1980s and allows nucleic acids exponential amplification through nucleic acids synthesis based on temperature cycles. LAMP amplification was discovered in the early 2000s' and allows the isothermal exponential amplification of nucleic acids. It takes advantage of the DNA polymerase with strong strand displacement to perform nucleic acid amplification at a constant temperature of typically 60-65°C. Those two amplification techniques can be combined with immunoassays to improve the assay sensitivity. Those two amplification techniques have the advantage of proposing nucleic acids exponential amplification, but other nucleic acids amplification strategies also exist, such as Recombinant Polymerase Amplification (RPA) that lead to linear amplification.

This methodology is novel and only few examples exist in the literature for such sensors. The most common combines immunoassay and PCR amplification to propose the immunoPCR method [73] [74] [75] [76].

To the extent of our knowledge, only one example combining nucleic acid amplification techniques with immunoassay for the detection of cardiac markers is present in the literature. In 2019, Ivanoc et al described a RPA combined with magnetic nanoparticles for the fluorometric detection of troponin T (Fig 1.24) [77]. The method combines magnetic beads immunoassay with RPA amplification, in a 2 hours integrated assay with a detection limit of 10 pg/mL in serum and plasma, which was enhanced compared to the conventional ELISA or ImmunoPCR methods run with the same reagents [77].

The combination of immunoassays and nucleic acids amplification techniques is promising for the development of sensitive assays. Yet, very few examples exist of such a combination, especially in the case of cardiac biomarker testing. Amongst nucleic acids amplification techniques, isothermal techniques such as LAMP appear as a powerful alternative to PCR mainly due to their isothermal characteristics which gives interesting opportunities for their integration into a portable device. Particularly, it should be of great interest for the detection of proteins through immuno-loop-mediated isothermal amplification [78] (Fig 1.25). Its application to cardiac biomarkers has not yet been studied.

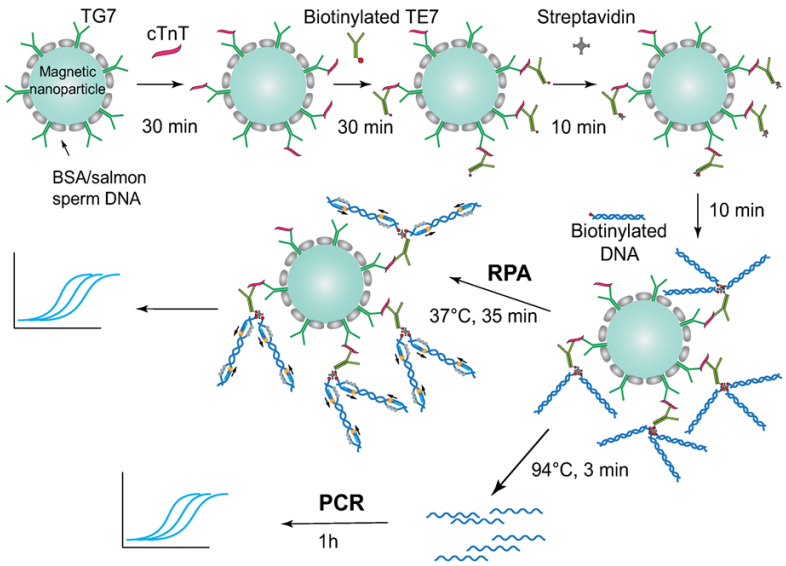

Figure 1.24: Schematic of iRPA cTnT detection method from [77]

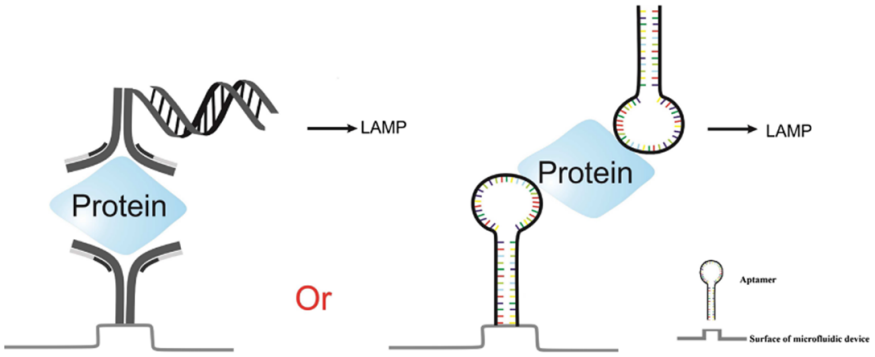

Figure 1.25: Principle of immuno-loop-mediated isothermal amplification and aptamero-loop-mediated isothermal amplification [78]

The conventional method for cardiac biomarkers testing uses the ELISA method. There are many innovations possible, in order to propose alternative detection methodologies for cardiac biomarkers meeting the sensitivity requirements. Aptamers appear as very promising biorecognition synthetic products [48]. Their ease of fabrication, low cost and high stability over time are obvious advantages for their use in biosensors. There are already numerous examples of biosensors using aptamers for cardiac biomarker sensing, on different original platforms [71] [7]. The main challenge for cardiac sensing still remains on the very low limit of detection to obtain in order to design a clinically relevant sensor. This way, nucleic acid amplification techniques such as PCR or LAMP appear as powerful tools to meet the sensitivity requirements [78]. There are several examples in the literature combining nucleic acid amplification methods with either antibody or aptamer sensing, but to the extent of our knowledge only one for cardiac biomarker testing (cTnT) [77]. There seems to be an innovation bridge to build between those two molecular biology tools in order to propose innovative detection methods that could be suitable for high sensitive cardiac biomarkers. Additionally, optical readout strategies allow the real-time detection of analytes in a minimally invasive and rapid way, and are thus suitable transducing

options to develop rapid and portable cardiac detection devices, in combination with original immunoassays.

The biosensing methods exposed in this section all handle a biological fluid (blood, saliva etc...) to perform the medical diagnostic. A diagnostic device that meets the requirements defined in the REASSURED criteria must integrate all the biosensor necessary functions, from sample preparation to sensing and reporting in a single and portable device [25]. Therefore, the development of Point-of-Care devices seems to meet this criterion. Such devices must therefore carry all the operations from the initial fluid to the signal readout and result display, and consequently integrate the biological sensor reagent handling and signal transducer. Microfluidic technologies, the category of science that studies and handles fluid at the microscale, have a great potential to deal with biological fluids in a portable system. Thus, it shows great promises in the design of portable diagnostic systems.

1.2.2 Microfluidic technologies towards Point-of-Care devices development

At the end of the 1990s, the science that studies fluid movements at the micrometer scale emerged. Microfluidic consists of studying fluid motion in micrometer-size channels, size in which the fluid properties fundamentally change. On the contrary to macroscopic fluid handling, surface effects like capillarity are predominant, whilst gravity becomes negligible for example. Microfluidic systems are usually characterized by a low Reynolds number. Therefore viscosity forces are predominant and the flow is laminar. There are several categories of microfluidic methods to guide the flow in geometrical length scales.

The following section will highlight the different microfluidic technologies and their potential use to design cardiac POC. The different microfluidic technologies are categorized based on the material and the actuation principle. Historically, silicon was the first used material for microfluidic chips [79], as a result of long-term expertise in this material processing from the semiconductor industry. Then, other materials such as glass, polymers, paper, metals or ceramics have been used during various microfluidic developments. Amongst them, paper and polymers stood out for their properties and suitability to design chips that are simple, low-cost, disposable and that can be easily processed to create patterns.

1.2.2.1 Paper microfluidic and LFIA immunoassays

Paper-based microfluidic relies on the phenomenon of capillary forces in a porous medium like paper. With its porous structure, paper is an interesting material for fluid handling at the microscale in the paper medium, without drawing any specific channels [80]. Indeed, controlling paper porosity, size and height is usually sufficient to control flow motion and passively transport fluids. Paper is the easiest microfluidic technology, and is already employed in many successful applications for various targets, with then many existing commercialized devices. It is a category of microfluidic technology that perfectly matches the need for portable, cheap and user-friendly diagnosis.

So-called LFIA tests (or test strips) are the most famous example of paper microfluidic implementation into a biosensor. It has successfully been used for the implementation of test strips for pregnancy tests or with the many Sars-Cov2 test strips recently available on the market.

The principle of detection relies on the migration of the target through the paper strip by capillarity (thus without external forces) and its recognition with different sensing molecules (Fig 1.26). The paper strips are composed of different areas to achieve each sensing step:

- Sample pad: area where the liquid sample is deposited. This part is impregnated with surfactant, buffers, salt, etc in order to control the flow rate and facilitate its migration further in the strip.
- Conjugate or probe pad: it contains detection particles (antibodies or aptamers) usually conjugated with gold nanoparticles. It ensures correct conservation of the antibody during the storage but also its release during the sample migration.
- Detection membrane: it contains the test and control lines. Capture antibodies sensitive to the analyte are fixed on the test lines, and antibodies sensitive to the detection antibodies are fixed on the control lines and reveal themselves as the liquid flows. When the sample arrives at the test line, a sandwich complex is formed in the presence of the targets with the capture and detection antibodies. The accumulation of the nanoparticles at the control and test lines produces a color change due to plasmonic effects. The detection membrane is commonly made of nitrocellulose.
- Absorbant pad: it maintains the sample flow in the detection membrane thanks to a natural capillary pump. It has no biological role but it ensures a total liquid flow through the detection membrane.

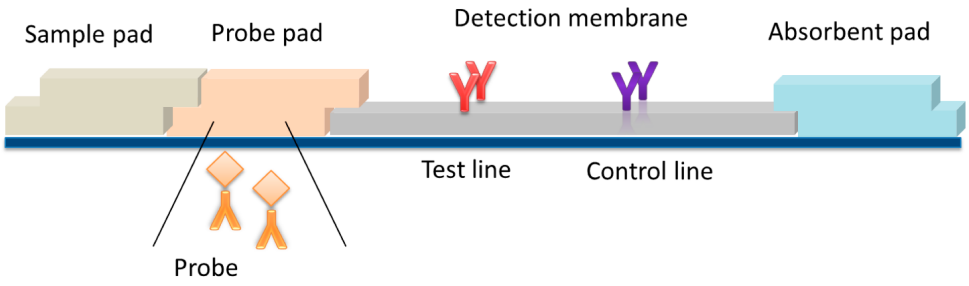

Figure 1.26: Typical Lateral Flow ImmunoAssay strip [23]

Roche commercializes several test strips for cardiovascular diseases (cTnT, CK-MB, D-dimer, proBNP) associated with a portable instrument for the quantitative evaluation of immunoassays using the gold nanoparticles technique. The combination of the test strip and the instrument offers a rapid diagnosis with an enhanced clinical interpretation. There are many *R&D* efforts put into the development of LFIA test strips for troponin and other cardiac biomarker sensing [81], [82], [83], [84].

Other categories of microfluidic paper-based devices are also developed [81], [83], [84]. In such devices, patterns are placed on the paper strip thanks to wax deposition and allow fluid motion control. An example of such a device was used for the multiplex detection of various cardiac biomarkers in a single chip [81]. The paper reaction area is formed of nitrocellulose patterned with wax forming microchannels for fluid motion, and an absorbent pad is used to absorb fluid excess (Fig 1.27). With such a device, researchers reached a sensitivity of about 50 pg/mL for cTnT, and 500 pg/mL for CK-MB and GPBB.

Paper is a very convenient material to be used for microfluidic technologies [80]. The properties of the porous membrane allow for the fluid motion through capillary forces and thus in an autonomous way, without the need for support equipment. It offers many advantages regarding the design of POC devices, such as simple fabrication, low cost and easy disposal [80] [85]. However, due to its simplicity, paper microfluidics only allows the integration of rather simple protocols. Lastly, the simplicity of the technology and integrated assays limits the quantification and sensitivity of such devices.

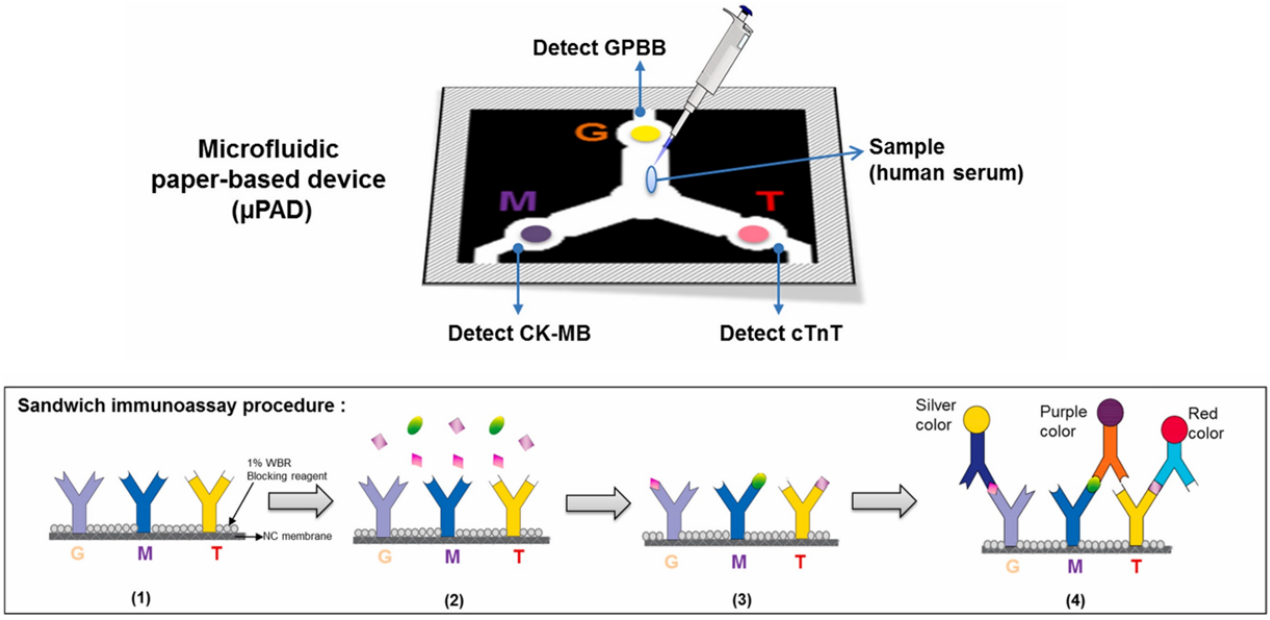

Figure 1.27: Example of microfluidic paper-based device for multiplex detection of cardiac biomarkers. It has a single sample injection zone in the middle and three detection zones for multiplex detection. [81]

1.2.2.2 Polymer-based microfluidic chips

Polymers materials stood out in the design of microfluidic cartridges for their simplicity, low cost, disposability and ease of fabrication with micro-fabrication techniques [79]. From a polymer-based microfluidic chip, there are several actuation techniques to allow fluid movements. Amongst them, capillary, centrifugal forces, digital droplets and pneumatic actuation particularly drew our attention to design portable and autonomous microfluidic chips.

Capillary forces Capillary microfluidic takes advantage of the tension forces at the surface of the microchannel to displace fluid in a controlled manner. It can deliver liquids without peripheral equipment by exploiting surface tension effects and surface chemistry in microchannels. Careful studies of the geometry can therefore allow researchers to deliver liquid in preprogrammed manners [86] [87].

A very successful example of a commercialized device for cardiac diseases diagnosis is the Triage True one-step chip system, commercialized by Quidel [86]. The company produces a simple microfluidic chip that detects cardiac biomarkers in whole blood. The device incorporates a blood filter to separate blood cells from plasma and uses a hydrophobic barrier to control sample incubation time. Capillary microfluidic is used to displace the fluid to different areas such as assay and internal control zones (Fig 1.28A). The laminated microfluidic device provides a quantitative readout with high sensitivity, with a LOD in the range of pg/mL for troponin I detection.

An example of a very simple microfluidic cartridge for the detection of cardiac troponin T uses a single microfluidic channel and gradient-based rapid immunoassay [68]. It is a multizone microfluidic channel functionalized with capture antibodies, and it creates a troponin concen-

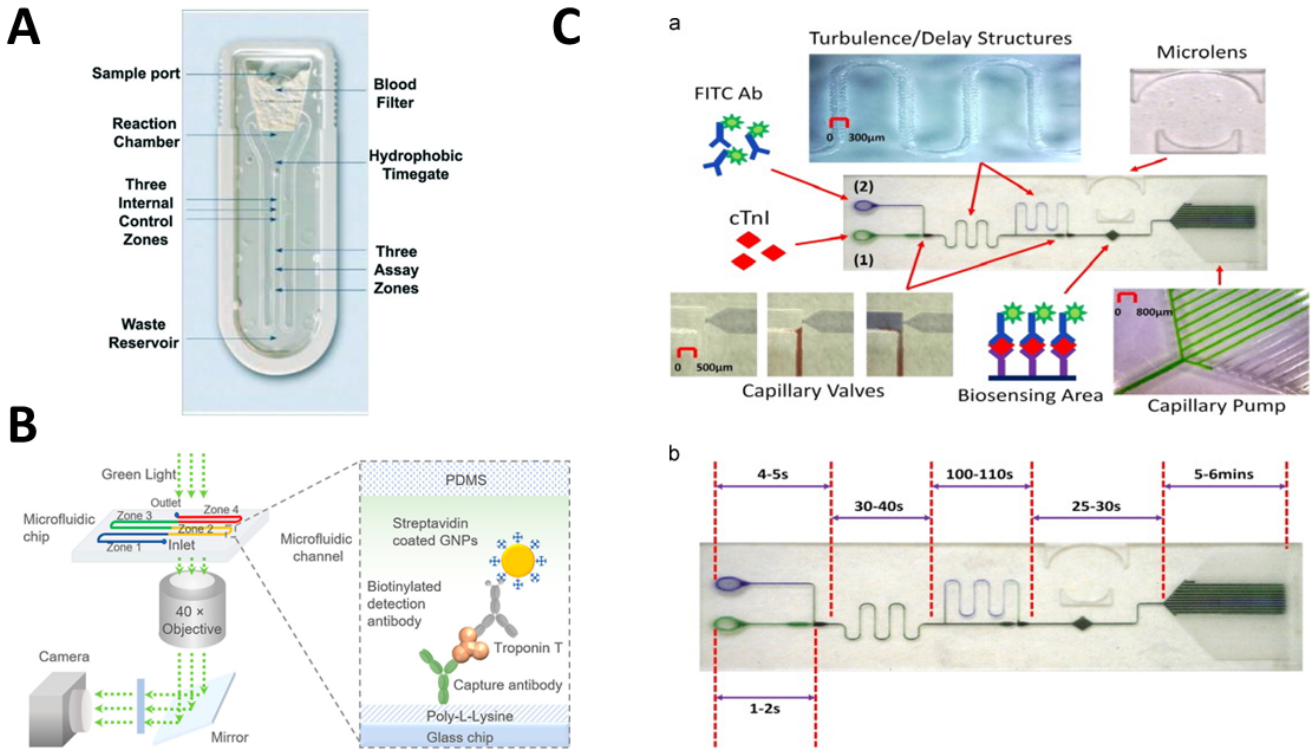

Figure 1.28: (A) Image of the Triage chip for one step immunoassay from whole blood [86]. (B) Schematic of single channel gradient-based rapid digital immunoassay [68]. (C) Image of the complete microfluidic fluoroimmunoassay platform with sample injection, capillary valves, turbulence/delay structures, biosensing area, microlens and capillary pump [88]

tration gradient along the channel because of binding-induced depletion. It counts the quantity of detection antibody bound to the troponin in the different channel areas, and uses differential counting between the zones (Fig 1.28B). The chip is made of Polydimethylsiloxane (PDMS) placed on a glass substrate coated with antibodies. The system reaches a limit of quantification of 6.2 pg/mL with only 1 μL of plasma sample.

Other microfluidic systems also use more complex capillary microfluidic systems to detect cardiac biomarkers. Mohammed et al described in 2014 [88] an autonomous capillary microfluidic system for troponin I detection. They present a new laser engraving technique for prototyping capillary systems with embedded optics and biosensing elements. The chip was made of Poly(methyl methacrylate) (PMMA) and its surface was functionalized using (3-Aminopropyl)triethoxysilane (APTES) chemistry for the antibody coating. It uses capillary action to actuate, stop and trigger delay valves and capillary pumps to provide chip automation (Fig 1.28C). The system reaches a sensitivity of 24 pg/mL in less than 10 minutes in buffer samples.

Capillary microfluidic devices are usually easy to manufacture, have low energy consumption due to passive actuation, and function in a fully automated way, thus reducing operator intervention. They also require minimal equipment since the actuation technique does not require external forces. The various examples of capillary microfluidic technologies for cardiac biomarker testing show their great promises in designing simple, low-cost and small detection devices. However, capillary microfluidic cartridges are often not adapted for the integration of

complex multi-steps assays and parallel reactions. The simplification of the protocol is often needed to constrain it to a few basic steps, that can be integrated into such cartridges.

Centrifugal force Another type of microfluidic chip actuation technique uses centrifugal force. So-called lab-on-a-disc platforms have been under development lately, and several examples of biosensors exist using this method. In such platforms, the fluid is subdivided into discrete volumes in associated chambers. The chamber actuation is achieved through centrifugal force and the controlled actuation of valves.

An original microfluidic device for the simultaneous detection of protein biomarkers for cardiovascular diseases was described by Park et al in 2012 [89]. It uses a centrifugal microfluidic layout (Fig 1.29A) with three connected reaction chambers (Fig 1.29B) and a total process time of 20 minutes. This lab-on-disc platform uses two fluid actuation methods: centrifugation force and ferrowax microvalves (Fig 1.29D) which are switched on and off with laser irradiation. It allows fluid motion in different chip areas during the sensing protocols (Fig 1.29C), until the final detection step of absorbance measurement. For cTnI detection in whole blood, the device achieved a detection range from 0.46 to 37 ng/mL, with a LOD of 0.3 ng/mL.

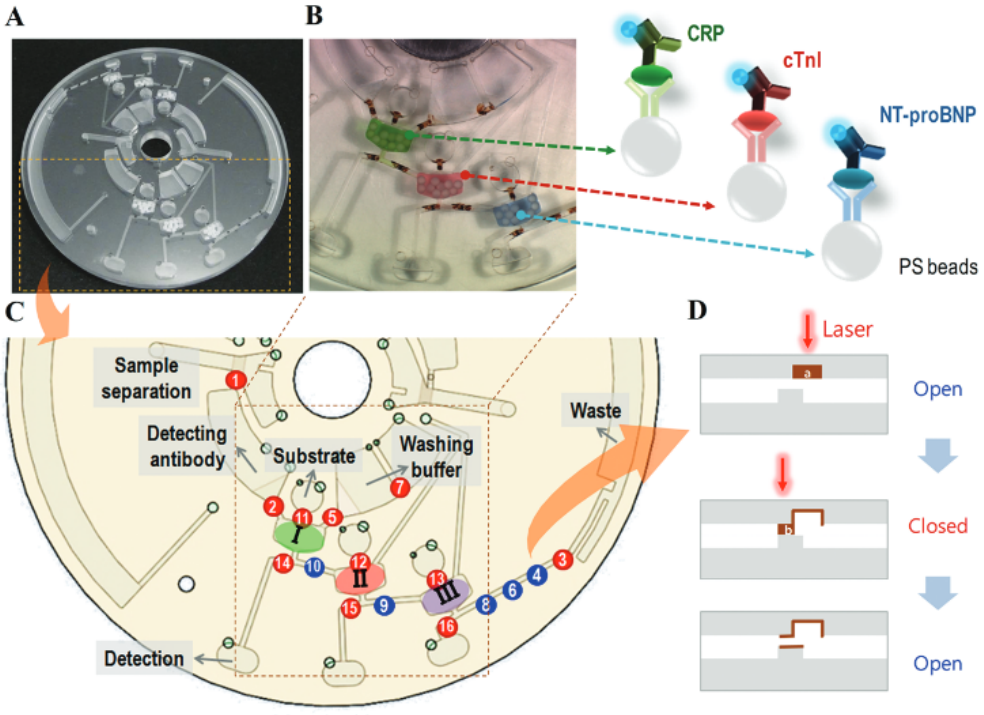

Figure 1.29: Example of the lab-on-disc platform for multiplexed cardiac biomarker immunoassays [89].

Centrifugal microfluidic is an interesting method to perform on-chip fluidic operations. However, the portability of such a system is limited to the need of a platform able to perform centrifugation. Spin programs must be written for the integration of each assay step, which can be complex to implement. Moreover, there are only a few applications of centrifugal force microfluidic devices for cardiac biomarkers sensing, and the sensitivity is limited.

Droplets microfluidic In a similar fashion as lab-on-a-disc platforms, the fluid volume can be partitioned into specific volumes in droplet-based microfluidic devices. This digital microfluidic

technique takes advantage of droplet generation in immiscible flow to partition the fluid into compartments of small volumes. It defines discrete units of volumes and microfluidic functions that can be reduced to a set of repeated basic manipulations for fluid control [90]. It provides good mixing, encapsulation of biological samples, sorting and sensing. This technique requires good understanding of droplet generation through various techniques in order to perform various logical operations such as droplet manipulation, sorting, merging, and breakup [91].

Once formed, the manipulation of discrete droplets is usually achieved on a substrate or open array of insulated electrodes [92]. Its designation as digital comes from the analogy with digital microelectronics. One common actuation method for digital microfluidic is Electrowetting On Dielectric (EWOD) [93].

In 2021, Shen et al [94] described a digital microfluidic chip with multi-channels for the multiplexed detection of cardiac biomarkers myoglobin, CK-BM and cTnI (Fig 1.30A). The assay relies on fluorescence detection embedded in the digital microfluidic platform. Droplets of 1 μm size containing antibody-coated magnetic beads are generated through voltage supply, and mixed with sample droplets, washed, and moved to the chip fluorescent detection area. The device was tested with human serum samples and cTnI was detected with a LOD of 0.15 ng/mL within 30 minutes.

In 2023, Cheng et al described a rapid chemiluminescence immunoassay for cardiac troponin I based on digital microfluidics [59]. It integrates a magnetic beads assay on a digital microfluidic chip with an electrode array pattern (Fig 1.30B). The complete process takes 40 minutes and shows a LOD around 0.34 ng/mL.

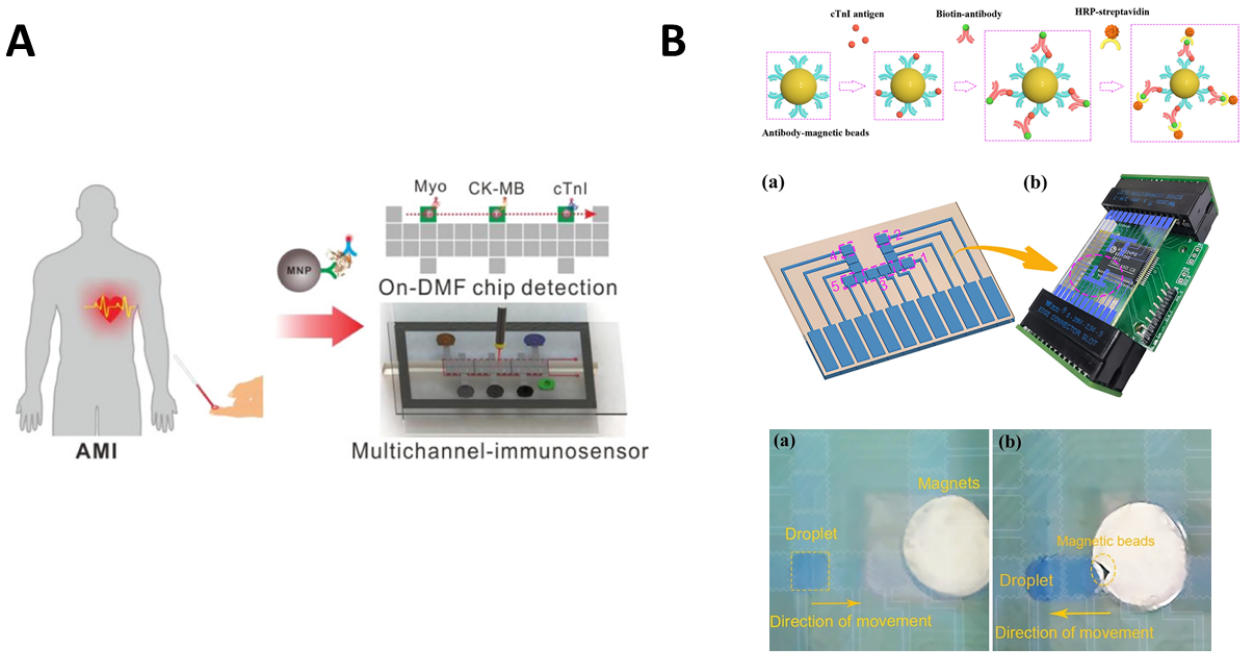

Figure 1.30: Examples of cardiac biosensors using digital microfluidic chips (A) Multi-channel chip for the multiplexed detection of cardiac biomarkers [94] (B) Chemiluminescence assay on digital microfluidic chip [59]

Digital droplets microfluidic allows the discretization of very small volumes of samples. EWOD actuation techniques allow the very fine manipulation of droplets. However, the very

small volume used often limits the sensitivity that can be achieved due to the very low number of targets in a small sample volume. Additionally, the sample preparation is often limited on digital microarrays and often requires additional microfluidic components on the array, thus increasing the complexity of the global chip.

Pneumatic actuation for digital microfluidic In digital microfluidics, the volume discretization can be achieved with pneumatic actuation of chambers and valves. This yields important forces and amplitudes due to the mechanical actuation.

A very famous example of volume digitization on PDMS chips through pneumatic actuation was described in 2002 by Thorsen et al [95] with a high-density microfluidic chip with thousands of micromechanical valves and hundreds of individually addressed chambers. The main advantage of this method is the easy programming due to the analogy with electronic integrated circuits.

Several examples have highlighted the application of pneumatic actuation to cardiac biomarker sensing. In 2019, Sinha et al [96] described an original device combining a microfluidic chip and a FET. The microfluidic chip is composed of several PDMS layers for pneumatic control, liquid flow, tape, and FET substrate. The microfluidic platform is equipped with immobilized target-specific aptamer probes. The fully automated device uses very low fluid consumption (4 μL) and tests 4 cardiac biomarkers very rapidly (5 minutes). Other pneumatic actuation methods have been developed, for example with the use of a stretchable membrane [56]. Shortly, this technique uses two polymeric layers (COC) placed on both sides of the stretchable membrane. The pneumatic actuation of the membrane allows it to move from the fluidic to the pneumatic layer, therefore transporting the fluid through the chip chambers. This technology allows very precise volume calibration, and it has been exemplified with troponin ELISA tests to draw calibration curves on chip [56] [97]. In 2019, a PDMS microfluidic platform was also used for the detection of troponin I with an original assay combining aptamers and enzymatic amplification [98]. The microfluidic chip is composed of an air control layer placed above a liquid channel layer on a glass substrate. The operation principle of the pneumatically controlled chip is the following: the thin PDMS barrier at the top of the fluidic layer forms the barrier between liquid and air channels. Compressed air or vacuum is allowed to flow in the air control layer and leads to fluid flow across the microfluidic chip. The device reaches a limit of detection of 12 pg/mL, which shows that the device could be used for a reliable diagnosis of AMI.

Pneumatic actuation in microfluidic chips is a very robust way to handle fluids. It allows precise, reversible and automated fluid control, giving rise to digital microfluidic technologies that are versatile [95] [56]. However, the pneumatic control requires pressure controllers which need to be connected to vacuum and compressed air which reduces the portability of the system. Moreover, the microfluidic chips using pneumatic actuation are often made of several layers, which can make the chip fabrication rather complex (many layers, micro-machining, assembling, etc...). The pneumatic controllers can also be bulky and reduce the portability of devices using the pneumatic actuation technique.

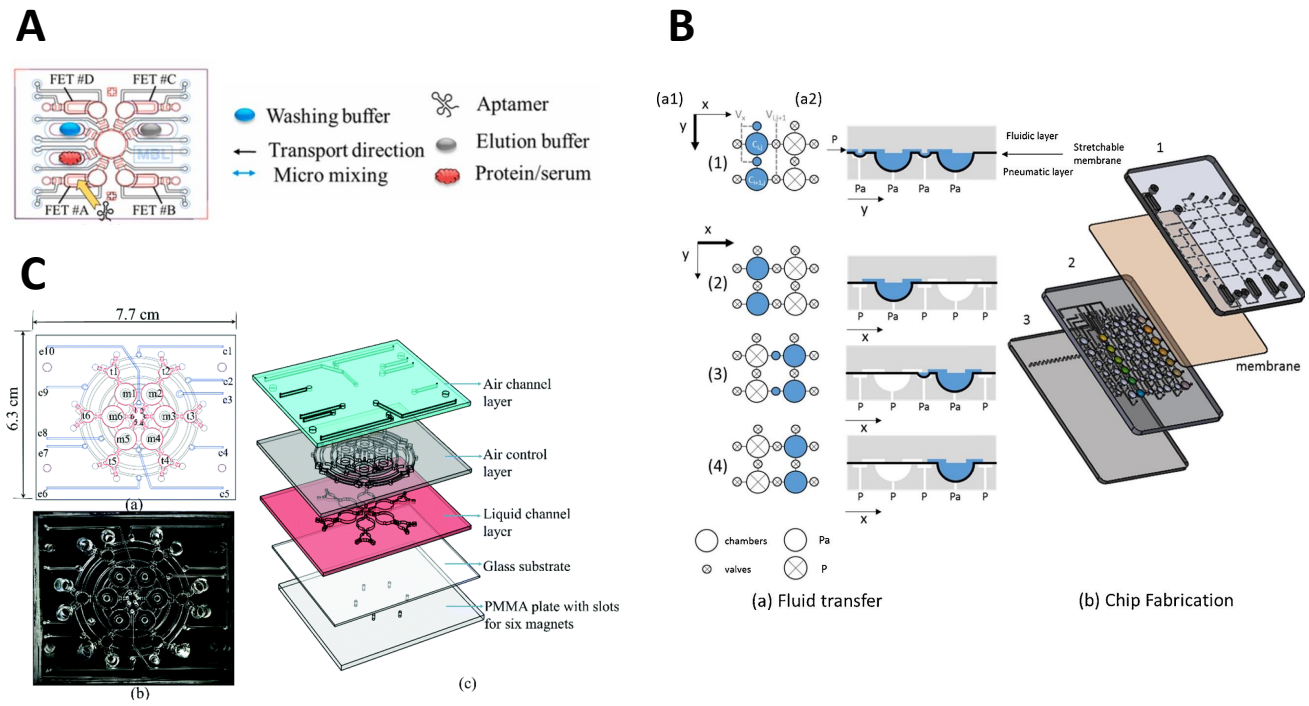

Figure 1.31: (A) Image of the microfluidic chip with FET for multiple cardiovascular marker sensing [96]. (B) Microfluidic chip with stretchable membrane with chambers and microvalves [56]. (C) Microfluidic chip with air channel layer, a liquid channel layer, glass substrate and microfluidic components: micromixers, transportation units, electromagnetic valves and waste collection units [98].

A summary of the various microfluidic technologies exposed in this section and their application to cardiac testing is exposed in table 1.4.

Target	Biosensing method	Chip material	Actuation technique	LOD	Assay time	Reference
cTnT	LFIA	Paper strip	Capillary	40 ng/L	12 min	[31]
cTnT	Sandwich immunoassay	Paper and wax valves	Capillary	50 ng/L	10 min	[81]
cTnI	Fluoroimmunoassay	PMMA	Capillary	24 ng/L	10 min	[88]
cTnI	Immunoassay	COC	Centrifugal force	500 ng/L	20 min	[89]
cTnI	Chemiluminescence Immunoassay	Electrode Array	Digital Microfluidic	340 ng/L	40 min	[59]
cTnI	Enzyme-linked aptamer assay	PDMS	Pneumatic	12 ng/L	30 min	[98]

Table 1.4: Summary of microfluidic technologies for cardiac biomarker testing

Microfluidic technologies have great potential to be used in portable and autonomous diagnostic platforms such as POC systems. The review of the different existing microfluidic technologies and applicability to cardiac biomarker testing highlighted the suitability of each technique for the design of a cardiac POC system, with various assay performances presented in table 1.4.

Paper strips like LFIA are the most obvious examples of portable, low-cost and autonomous devices. However, their performance for biomarker quantification is limited. Capillary microfluidic cartridges are simple and easy to manufacture but their application to long, complex and multi-steps biological assays is limited. Digital microfluidics proposes the partitioning of fluid into discrete volumes and can be implemented in droplet microfluidics or pneumatically actuated chips with chambers and valves. Droplets digital microfluidic is often limited in sensitivity due to very small sample addition into droplets, and the use of electrode arrays often complicates the chip's fabrication. Pneumatic actuation produces important forces and therefore allows the partitioning of broad ranges of discrete volumes giving versatility for assay integration. This technology is therefore versatile for the integration of complex quantitative biological assays with parallelized reactions.

1.2.3 Examples of commercialized POC devices for cardiovascular diseases testing

There are already several examples of commercialized POC devices for cardiac biomarkers. They will be reviewed here, and a special focus will be given to their detection methodology, based on the basic principles exposed in the previous section.

Roche, Cobas LFIA tests (or test strips) are a category of biosensors that can easily meet the criterion of portability and ease of use. Roche develops the Cobas h32 POC device and offers several test strips targeting several cardiac biomarkers: cTnT, CK-MB, D-dimers, proBNP (Fig 1.32A) [31]. The principle of detection is exposed in the previous section with LFIA strips. For the detection of cTnT, two cTnT-specific antibodies are used, one is fixed in the detection membrane, and the other is conjugated with a nanoparticle and bound in the conjugate pad to cTnT. Once the detection antibody and the cTnT reach the test line, a color line is formed and its intensity is proportional to the concentration of cTnT in the sample. In combination with the associated reader, the company proposes a complete cardiac POC device for several cardiac biomarkers.

Figure 1.32: Examples of Lateral Flow Assays. (A) Roche Cobas h232 [31]. (B) Quidel Triage Cardiac

Quidel, TriageTrue Quidel also offers a device able to detect multiple cardiac biomarkers based on LFIA technology: troponin I and NT-proBNP (Fig 1.32B). This device is very competitive since it can detect troponin I at very low concentrations (1.5 ng/L), and in about 20 minutes.

Quidel has a very broad portfolio of cardiac POC systems, with paper and polymer microfluidic devices. Amongst them, TriageTrue is a microfluidic chip for embedded fluorescent immunoassay (Fig 1.33A). The chip is linked with a reader, the Quidel Triage MeterPro system (Fig 1.33B). Amongst the tests available, it offers a troponin test with a very high sensitivity that operates with Ethylenediaminetetraacetic acid (EDTA) blood, with a sample volume of 175 μL, and reaches a LOD of around 1 ng/L, a detection range 0.1 - 1000 ng/L and yields results in less than 20 minutes. The company also provides NTproBNP tests with the same technology, with a detection range of 20 - 35 000 pg/mL, 20 minutes time-to-result and connectivity of the system.

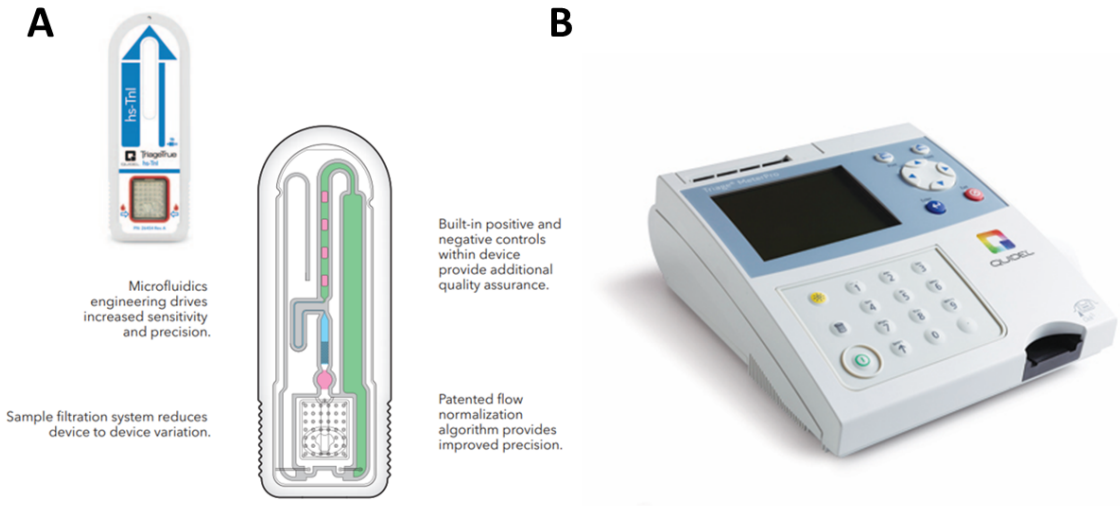

Figure 1.33: Quidel cardiac POC system [99]. (A) Triage true troponin microfluidic chip and (B) Quidel Triage MeterPro system

Abbott, I-STAT Abbott develops a technology for cardiac POC sensing relying on electrochemistry: I-STAT. The method relies on the measurement of an electrical current generated by an electron transfer during a reduction–oxidation (redox) reaction on the detected conjugate. Abbott combined the benefits of labeled antibodies, magnetic beads, and electrochemical sensing into a portable troponin I detection platform that can help to accelerate and improve the diagnosis of AMI (Fig 1.34A). The device reaches a LOD of 20 ng/L in less than 10 minutes. Abbott also offers the same electrochemical platform for BNP sensing but this device is not precise enough to be considered as an improvement compared to other existing methods or devices. It is interesting to note that the Abbott I-STAT system is the first and only device on the market offering gender-specific values for troponin sensing.

Philips, Minicare Philips offers a platform combining magnetic particles and innovative imaging techniques for the measurement of troponin I and other cardiac biomarkers: the Philips Minicare (Fig 1.34B). It consists of a handled instrument and a plastic disposable cartridge. It uses the Philips Magnotech technology [60] which controls precisely the motion of magnetic particles in a small sample volume, and detects the particles using frustrated total internal reflection (FTIR) imaging (Fig **??**B).

The analytical performances were evaluated [61] and the manufacturer states that the device has a sensibility and precision that makes it clinically usable for the determination of cTnI concentrations. The limit of detection obtained is 18 ng/L and it has a very good correlation coefficient with reference laboratory tests such as Beckman Coulter Access.

The company expanded the use of this device for other cardiac marker such as NTproBNP with current developments understudies [67] and has a LOD of 5.8 ng/L. However, this device is currently under development for improvements and is not yet commercialized.

Siemens, Atellica The company Siemens Healthineers released recently in 2021 their competitive cardiac POC device: The Atellica VTLi. It offers an analyzer with a cartridge for the high-sensitivity sensing of cardiac troponin I (Fig 1.34C). It can operate with various sample sizes (100-30 μL) on whole blood or capillary blood, and the time-to-result is around 8 minutes, with a LOD of 1 ng/L. Due to its recent release commercially, no further technical information can be found.

Figure 1.34: Pictures of commercialized cardiac POC systems. (A) I-STAT by Abbott, (B) Minicare by Philips and (C) Atellica VTLi by Siemens

The different cardiac POC commercialized devices performances are summarized in table 1.5. It shows that many companies have managed to develop competitive sensitive cardiac POC devices. All the devices meet the portability and rapidity criteria, but only some devices propose high-sensitivity sensing. The assay usually use small volumes (a few dozens of μL) of complex samples (blood, plasma), and the assay time-to-result is very competitive, 20 minutes or less.

Device	Target	LOD	Detection range	Time-to-result
Cobas h232 (Roche)	cTnT NTproBNP CK-MB D-dimers Myoglobin	NA	40 - 2.000 ng/L 60 - 9.000 pg/L 1.0 - 40 ng/L 0.1 - 4,0 µg/L 30 - 700 ng/L	12 min
Triage (Quidel)	cTnI NTproBNP	1 ng/L NA	0.1 - 1000 ng/L 20 - 35 000 pg/mL	20 min 20 min
iSTAT (Abbott)	cTnI	20 ng/L	20 - 50 000 ng/L	10 min
Minicare (Philips)	cTnI	18 ng/L	NA	10 minutes
Atellica VTLi (Siemens)	cTnI	1.25 ng/L	NA	8 min

Table 1.5: Performances of commercialized cardiac POC systems

The versatility of the method used in the Roche Cobas h232 device gives the possibility to offer a broad range of cardiac biomarkers tests. However, the different tests use different cartridges and their sensitivity is lower than for other cardiac POC platforms. The various detection methodologies in the other examples of commercialized devices lead to various analytical performances, most of them achieving high-sensitivity sensing on their portable device in less than 20 minutes. For some devices, a comparison was made with conventional laboratory methods and the test results were found to be equivalent [61]. Notably, over the past two years, Siemens and Quidel successfully commercialized very high-sensitivity cardiac POC within a very short time. However, none of these devices propose the multiplex detection of several cardiac biomarkers on the same platform.

From the commercialized cardiac POC devices review, it seems that various companies have focused their efforts on designing small devices with high-sensitivity detection. Thus, numerous very competitive cardiac POC devices already exist and are able to achieve high-sensitivity sensing of cardiac biomarkers in a reduced time. However, there are still some drawbacks, such as their high cost and lack of standardization. Indeed, in the case of cardiac troponin tests for the diagnosis of AMI, the cut-off point is a very important value as it defines the number of false positives and false negatives in a test. It is set as the 99^{th} percentile of cardiac troponin in a normal reference population [5], as it depends on parameters such as age and sex. Due to the lack of reproducibility within different POC systems, the definition of the cut-off value with a POC system is challenging. The comparison of POC devices with standard laboratory testing [100] [101] highlights the lack of standardization of such devices. Indeed, since the result depends on the device itself, no universal cut-off value can be defined. The definition of the cut-off value is of great importance for clinicians, and a misconception leads to high false negatives and therefore discharged patients, who actually presented a risk of AMI. To limit this effect, clinicians usually focus on the use of a single diagnosis platform and method, which reduces the broad acceptance and wide use of POC testing devices.

Point-of-care devices are crucial in the *in vitro* diagnostic industry. There are already several commercialized Point of Care devices for cardiac diseases, however, there is still room for improvement in such devices. **The main findings and recommendations of this section are devices that are very sensitive, that propose a multiplex detection of several cardiac biomarkers (such as troponin and NTproBNP, pointed out as promising),**

with a multiparametric detection result (age, sex), a very short test time (less than one hour), and a user-friendly device that delivers readable results for the practitioners.

1.3 PhD project definition

Cardiovascular diseases are the leading cause of death in the world, and patient care can be enhanced through early diagnosis. There are several cardiac biomarkers released in the blood before a cardiovascular accident, and the monitoring of their quantity gives precious information for the medical diagnosis. Amongst them, troponin is the gold standard biomarker for the diagnosis of myocardial infarction. Conventional methods to test troponin in blood usually use central medical laboratories to perform ELISA tests, which are costly and time-consuming methods. The development of Point-of-Care systems aims to propose medical tests on portable and autonomous platforms. There are already several successful commercialized cardiac POC devices, but there are still some gaps to fill in terms of sensitivity and multiplexed detection of several biomarkers on a single portable device.

The main problem addressed during this PhD is to design a point-of-care device for the high-sensitivity multiplexed detection of cardiac biomarkers in blood. To do so, we will design high-sensitivity assays with a method that is versatile enough to address the variety of cardiac biomarkers. We will also design associated microfluidic cartridges to integrate the developed biological assays on a portable and autonomous platform.

The three building blocks of this project are (i) the biological assay development, (ii) the microfluidic integration and (iii) the complete device. Various types of bio-recognition elements will be studied, mainly aptamers and antibodies as molecular probes for biomarkers, and they will be combined with an isothermal amplification method to design complete sensitive biomarker assays. Pneumatically actuated polymer cartridges relying on digital microfluidic technology will be designed to integrate the biological target capture on magnetic beads and the isothermal amplification. A generic platform will be described with adequate hardware modules for microfluidic cartridge actuation and biological assay integration.

To design high sensitive assays, a synthetic oligonucleotide structure called dumbbell will be developed and used in different types of quantification assays. Its suitability for isothermal exponential amplification in combination with various molecular probes will be validated in chapter 2. The incorporation of various probes of different natures will be studied, and the initial steps and hairpin formation during the isothermal amplification will be characterized. This oligonucleotide will serve as a template for nucleic acids amplification during the development of assays for protein sensing described in chapter 3. The combination of aptamers and isothermal amplification will lead to the description of the aptameroLAMP assay with the example of thrombin sensing. For the development of cardiac biomarker assays, we chose the troponin I protein, the gold standard biomarker of myocardial infarction. The combination of immunocapture and isothermal amplification will lead to the development of immunoLAMP assay with the example of cardiac troponin I sensing. A generic platform to integrate biological assays in microfluidic cartridges is presented in chapter 4, and additional hardware components specific to the developed protocols in chapter 3 are presented (thermal, optics). Digital microfluidic cartridge architectures are designed for the on-chip integration of immunoLAMP protocols. Their validation with the developed biological assay is achieved in chapter 5 by order of complexity, with firstly the troponin capture on magnetic beads, and secondly the on-chip dumbbell isothermal amplification. The complete instrumentation and associated microfluidic cartridges should eventually propose a platform for complete protocol integration.

A synthetic schematic of this PhD project can be found in figure 1.35.

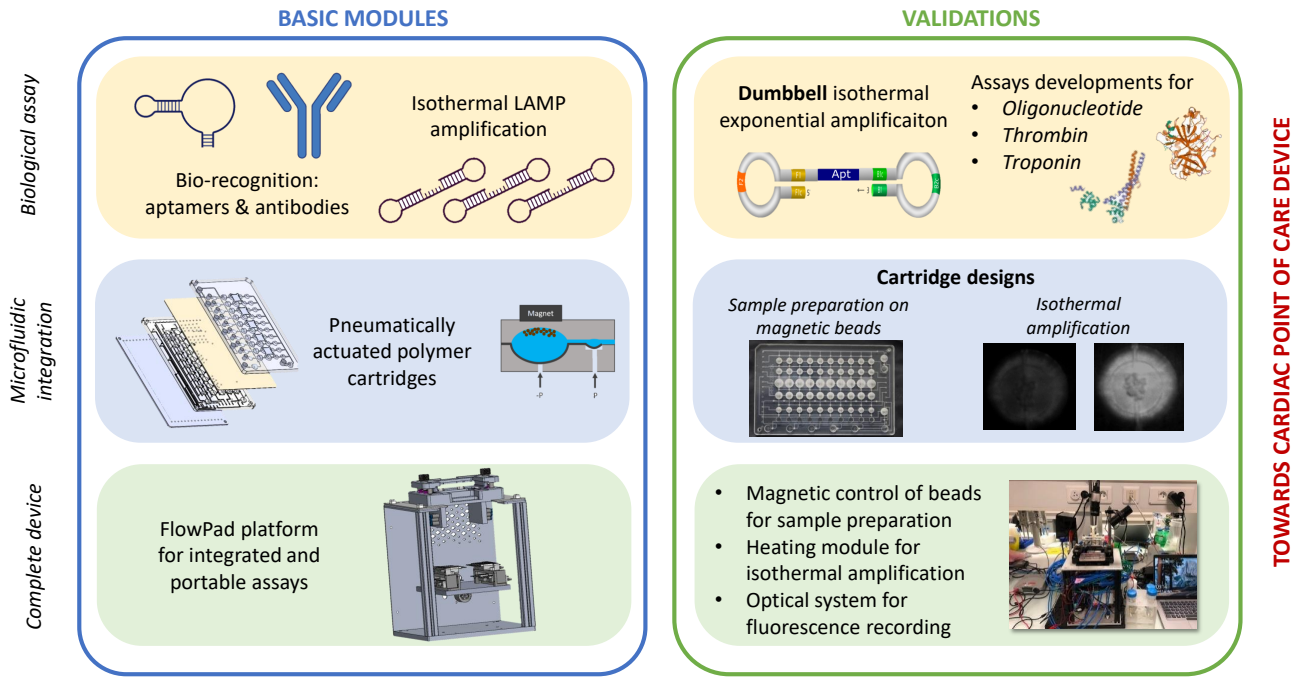

Figure 1.35: Synthesis of PhD project plan

Chapter 2

Development of an oligonucleotide structure for isothermal nucleic acid amplification

Objectives

- Nucleic acids amplification strategies for signal amplification are reviewed
- Based on recent work on isothermal amplification, an oligonucleotide structure suitable for isothermal amplification with only 2 primers is described
- The dumbbell structure's minimal components are described and its suitability for isothermal amplification is demonstrated
- This dumbbell structure is used with different molecular probes incorporated inside the structure for different sensing scenarios
- A theoretical framework for the understanding of the dumbbell isothermal amplification is described with the computation of hairpins lengths

One of the main challenges for the diagnosis of cardiovascular diseases through blood biomarker testing is the assay sensitivity [1]. Amplification strategies can be used to enhance the sensitivity of biomarker assays. Nucleic acids amplification methods are usually used for pathogen or virus detection through their genome amplification, but they can also be incorporated as an amplification strategy for biomarker quantification [72].

This chapter will describe nucleic acids amplification methods, with the development of an oligonucleotide structure suitable for isothermal LAMP amplification and its use for different bioassays. It will highlight the ongoing developments in the literature regarding isothermal amplification and describe a specific oligonucleotide structure called dumbbell. It will exemplify its use when combined with a sensing probe that can have different natures and its potential use in different assays. A theoretical framework is derived to understand the isothermal amplification layout, and experimental and theoretical data are compared. During the scope of this project, all the development on this novel oligonucleotide structure lead to three patent deposition, with numbers FR2109667 (deposited on 2021/09/15) [102], FR2114556 (deposited on 2021/12/27) [103] and FR2214563 (deposited on 2022/12/27) [104].

2.1 State-of-the-Art: Nucleic Acids Amplification methods

The quantification of a target present in a solution at a very low concentration still remains a challenge nowadays. Nucleic acids amplification methods show a great potential to quantify very low amounts of analyte in a complex sample. These methods particularly show their potential with the ongoing research on Sars-Cov2 detection and the need for rapid, sensitive, specific, and on-site testing [105]. To this end, two main nucleic acids amplification methods exist: PCR, the gold standard nucleic acid test, and isothermal amplification methods such as Loop Mediated Isothermal Amplification (LAMP) [106], Rolling Cycle Amplification (RCA), Nucleic Acid Sequence-Based Amplification (NASBA), etc... which were developed over the past decades [107]. The Loop Mediated Isothermal Amplification [106] showed a particular great scientific interest in recent years with the ongoing research on Sars-Cov2 detection methods [108]. They were considered as an alternative to the PCR tests that show a high cost and long time-to-results. The LAMP amplification shows many advantages over PCR such as its simplicity, high sensitivity and strong specificity, its low time-to-result and simple instrument requirements due to its isothermal characteristics, thus cutting the need for thermocycling and heavy equipments. In the scope of this project, LAMP appears as particularly promising because of its high specificity and sensitivity [107].

2.1.1 PCR amplification

In the early 1980s, DNA amplification through the Polymerase Chain Reaction or PCR was discovered [109]. It is a biological enzymatic reaction allowing *in vitro* specific DNA exponential amplification. It relies on the exponential multiplication of an oligonucleotide sequence thanks to two specific primers which recognize the both 3' end of the DNA matrix. An enzyme synthesizes a copy of the DNA strand and the amplification can reach 10^9 copies. This synthesis is based on temperature variation to achieve the necessary steps in each cycle : (i) denaturation of double-stranded DNA at 95°C, (ii) hybridization of the two specific primers at a temperature in the range 50-60°C and (iii) elongation step with the enzyme which synthesizes the complementary DNA strand using the deoxyribonucleotides. The DNA quantity is therefore doubled at each cycle, so it becomes possible to obtain 10^9 copies of DNA after 30 cycles (Fig 2.1A). It is possible to quantify the amount of synthesized DNA at each cycle with a fluorescent intercalating dye, which fixes itself on double-stranded DNA strands formed during the amplification reaction.

The reaction usually takes place in an instrument called a thermocycler which optically measures the fluorescence level over the cycles. Fluorescence kinetic curves can be drawn by plotting the fluorescence level, which is proportional to the number of DNA amplicons, over time (Fig 2.1B). This plot shows three phases: the initiating phase where the reaction settles, the exponential increase phase corresponding to DNA synthesis, and a last phase of fluorescence saturation due to reagents shortage and reaction shutdown. From this curve, a time called Cycle Threshold (Ct) can be defined when the fluorescence level reaches a reference level. It corresponds to the time when the fluorescence level increase becomes significant, especially over noise. By recording the Ct value for different initial DNA samples, it is possible to draw a calibration curve. Ct values can then be drawn over the logarithm of known DNA concentration, allowing the quantification of unknown DNA sample. This method of quantification based on PCR amplification is called Quantitative Polymerase Chain Reaction (qPCR) and is a broadly used method to detect and quantify DNA or RNA in a sample. This method can be employed for pathogen nucleic acids detection, with the well-known example of Sars-Cov2 virus PCR tests [111] [105] which has been defined as the gold standard detection tests by WHO. This method is also widely used for nucleic acids in food matrices, biological fluids, environmental liquids etc...

One important strength of PCR amplification is its ability to quantify an amount of target.

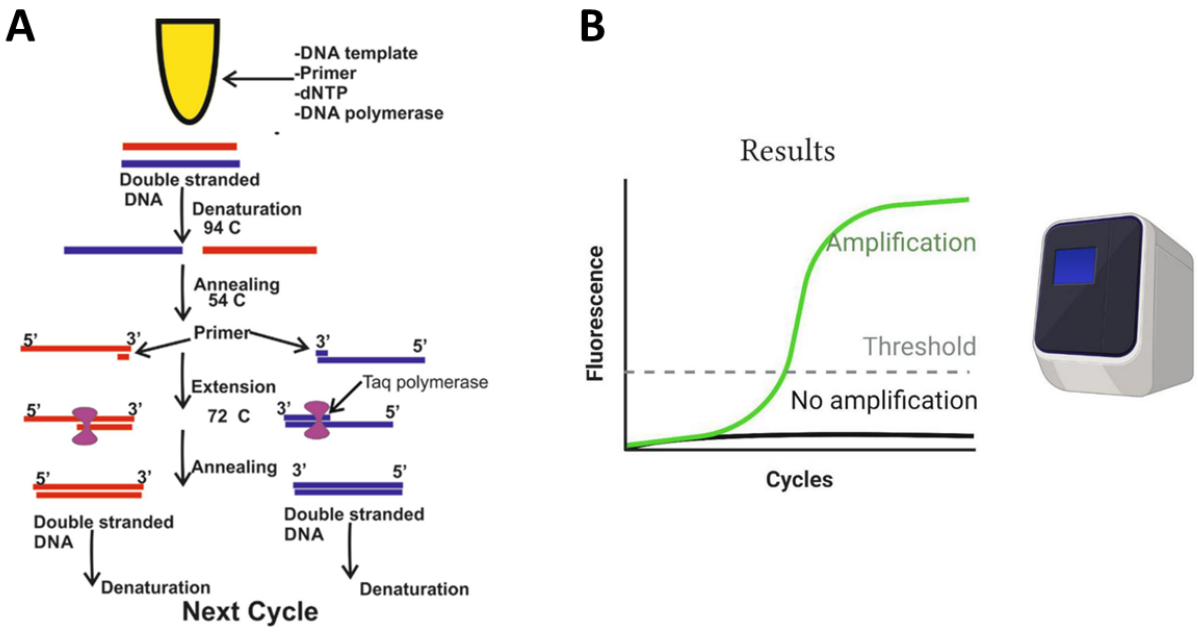

Figure 2.1: (A) Schematic of Polymerase Chain Reaction principle [110]. (B) Plot of fluorescence over cycle number [105]

However, its sensitivity is limited by the virus load. Several alternative methods to counteract this feature have been developed, for example with the digital PCR. This method consists in partitioning the sample into multiple PCR reactions and using statistical analysis to compute the initial DNA concentration from the ratio between negative and positive reactions. Following this principle, digital droplet PCR (ddPCR) has been developed taking advantage of water-in-oil droplets and displays great improvements in clinical diagnosis with a higher detection range and accuracy [105].

Overall, PCR methods and their various alternatives (qPCR, ddPCR...) are suitable for large-scale nucleic acids screening and their efficiency has been shown with the example of COVID-19 tests. It is a very sensitive method that can detect very low amounts of initial DNA so it is widely used when the target is present in a very small quantity and in a very large liquid sample. However, its main limitations are a long reaction time, sophisticated thermal cycling equipment, and trained staff to carry out the operations.

2.1.2 LAMP amplification

Another nucleic acids amplification method called LAMP for Loop Mediated Isothermal Amplification was discovered in the early 2000s by a Japanese team [106], and overcome some limitations of the PCR amplification. It takes advantage of a DNA polymerase with strong strand displacement and has the main advantage of taking place at a constant temperature, typically between 60°C and 65°C. It allows rapid, specific, sensitive, and robust exponential amplification. The main advantages of LAMP over PCR are summarized in table 2.1. Very importantly, its isothermal operation facilitates its integration into a portable platform due to the limited hardware requirements [112] [113].

The LAMP amplification uses 4 or 6 different primers to recognize different areas in the

target DNA. This important number of primers gives a great selectivity for the method, but their design can be rather complex. Indeed, the primers are long (20-50 bases) but must not form any secondary structure and their melting temperature must be adapted for a reaction around 65°C. The Software Primer Explorer helps scientists in the design of LAMP primers for a desired target DNA. Figure 2.2 illustrates the first steps during the LAMP amplification process. Steps 1 to 4 lead to the formation of a dumbbell structure with the help of 4 primers, and steps 5 to 8 create hairpin structure amplicons of increasing size.

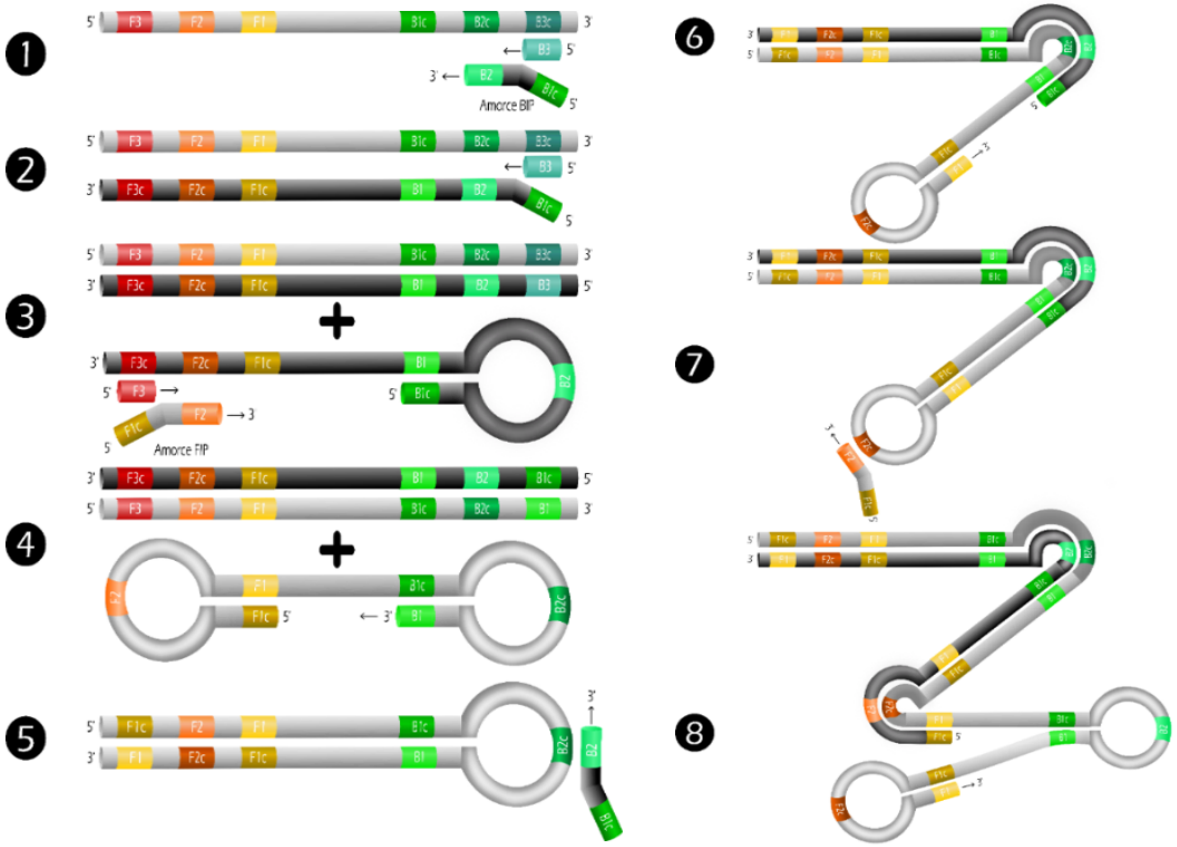

Figure 2.2: Schematic of the first steps of LAMP amplification (adapted from [17])

Recently, LAMP amplification for the detection of viruses appears as a major strategy in the scope of the Sars-Cov2 pandemic, with equivalent detection results as PCR [111]. Thanks to its low cost, ease of implementation, and high sensitivity and specificity, LAMP amplification appears as a powerful diagnostic tool in the scope of the COVID-19 pandemic.

The short reaction time of LAMP reaction, its high specificity and its reduced sensitivity to inhibitors are major advantages of LAMP, especially over PCR reactions. The main limitations are the cross-reactivity due to the important number of primers and the limited possibilities for multiplexed detection implementation [114].

Despite its wide use for many applications [107] [105] and its clinical validation, there are still some remaining challenges to overcome in order to accept the method as a strong alternative to PCR. The current ongoing developments regarding the LAMP amplification methods deal with the reduction of non-specific amplification, the use of the method for target quantification, the simplification of primers design and the introduction of multiplex detection [108] [107] [105] [114].

Property	PCR	LAMP
Temperature	Cycles	Isothermal 60°-65°C
Number of primers	2	4 or 6
Reaction time	1h	30 min
Sensitivity to inhibitors	High	Moderate
Initial step	High temperature denaturation	Enzyme with high strand displacement capacity
Amplification rate	10^9	10^9
Specificity	Less specific than LAMP	High due to the important number of primers

Table 2.1: Comparative table of PCR and LAMP amplification methods.

Alternative methods to LAMP amplification also exist, such as Reverse transcription loop-mediated isothermal amplification (RT-LAMP). An additional reverse transcription phase is achieved to create double-stranded DNA from RNA. Thus, this method can be applied for viral RNA detection [115].

Other isothermal nucleic acids amplification methods exist such as RPA which operates between 37 and 42°C [116], RCA which uses a circular probe as a template to generate long DNA products, or NASBA. Recently, a novel isothermal amplification method was described and named Exponential amplification reaction (EXPAR) [117]. However, these methods are usually less sensitive and specific than LAMP amplification [105].

Isothermal amplification techniques show great interest for nucleic acids amplification mainly due to their isothermal characteristics reducing the need for thermal cycling equipment and thus heavy instrumentation. Amongst such techniques, LAMP amplification developed over the past decades is particularly interesting for its high sensitivity and specificity, but still presents some limitations in primer design and quantification ability. The next section will present the latest developments to simplify the LAMP amplification process with a reduced number of primers, and to propose synthetic tools that serve as a template for isothermal amplification in quantification assays.

2.2 Recent developments on dumbbell structure and LAMP amplification

Amongst nucleic acids amplification strategies, LAMP is chosen for its rapidity, specificity, and ease of integration into portable systems due to its isothermal characteristics. To gather all these advantages, we designed a synthetic oligonucleotide inspired from LAMP products and that serves as a template for isothermal exponential amplification with a reduced number of primers. This way, the LAMP amplification method can be used as a signal amplification strategy in more complex biosensing protocols. The literature already shows several examples of biosensor integrating LAMP amplification [78, 90, 118].

2.2.1 Dumbbell construction

In the recent literature, several teams have highlighted the structures formed during the LAMP amplification process [119, 120]. By deriving the amplification steps from the target oligonucleotide as described by Notomi et al in 2000 [106] (Fig 2.3), one can highlight the formation of dual hairpin structure [119] and the production of dumbbell-shaped amplicons

[120]. Over the past years, several teams took advantage of these specific structures formed during the LAMP amplification to propose innovative detection protocols for the detection of miRNA for example [120].

Originally, the LAMP method is composed of two steps, the first one consists in the transformation of the DNA strands into dumbbell structures with the help of four primers, and the second one consists in the exponential amplification of the dumbbell structure with two primers to form numerous hairpins of increasing lengths [106]. With this pathway, it is possible to propose a generic and synthetic oligonucleotide structure in a dumbbell shape that can be isothermally amplified with the aid of two primers only. Thus, the LAMP amplification process as originally described by Notomi et al [106] (Fig 2.2) can be simplified from step 4 and a generic dumbbell oligonucleotide structure can be described and suitable for exponential isothermal amplification. The principle and methodology behind this simplification of the LAMP process was described in 2020 in the patent number FR3108124 [121].

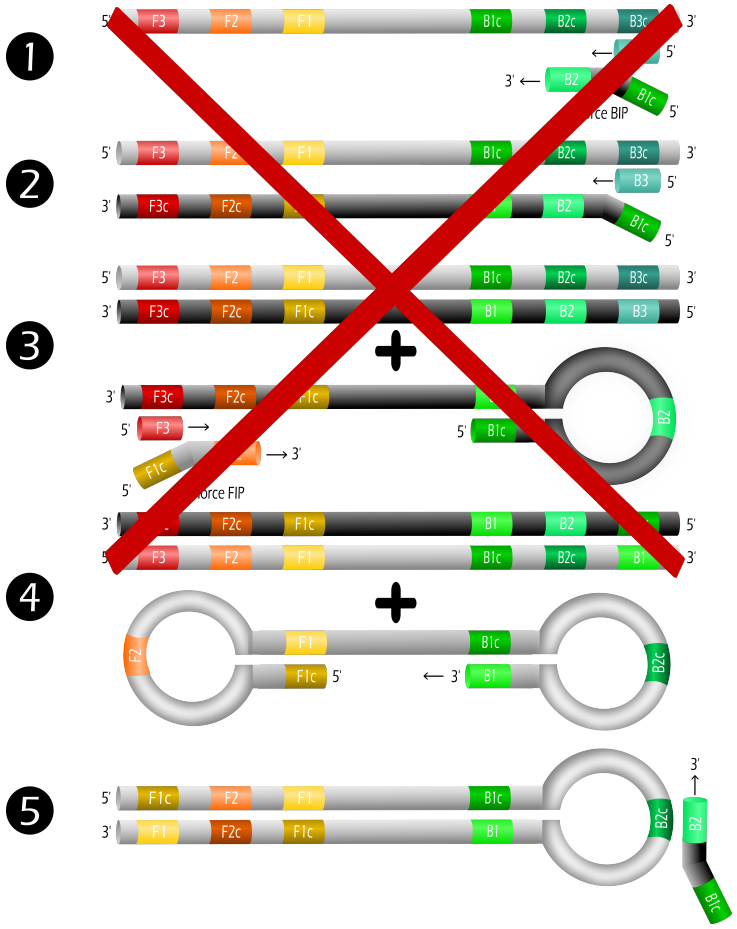

Figure 2.3: Schematic of the first steps of the LAMP amplification process according to [106]. In patent FR3108124 [121], the first three steps of the amplification are removed [17]

From figure 2.2, the generic single-stranded oligonucleotide structure present in step 4 is composed of the following sequence: **5' - F1c - F2 - F1 6 - Int - B1c - B2c - B1 - 3'** or **5' - F1c - F2 - F1 - Int - B1c - B2c - B1 - 3'**. Since each individual sequence F1, F2, B1, B2 and their complementary strands are rather short in length (10-50 bases), the dumbbell's total length is around 100-150 bases. only Backward Inner Primer (BIP) and Forward Inner Primer (FIP) primers are required for the exponential amplification., and the dumbbell structure is composed as follow:

- F1c presents a complementary sequence to F1 and hybridizes with it for the formation of the first hairpin.
- F2 forms the first loop in the dumbbell structure
- B1c presents a complementary sequence to B1 and hybridizes with it for the formation of the first hairpin
- B2c forms the second loop in the dumbbell structure
- The portion Int separates the sequence F1 and B1c and can be a covalent bonding or an oligonucleotide sequence with at least one base.

With this generic sequence, it becomes possible to derive different dumbbells based on different nucleic acids sequences F1, F2 and B1, B2. These sequences are primer-dependent and designed for a specific nucleic acid application. Therefore, generic and synthetic dumbbells can be theoretically described in two possible pathways:

1. Randomly chose a nucleic acid sequence and design F1, F2, B1 and B2 to form the dumbbell structure, with the help of a LAMP primer design software such as Primer Explorer [121, 17].
2. Use an example of detection based on LAMP amplification in the literature and withdraw the F1, F2, B1 and B2 sequences to derive the dumbbell structure from it [103].

These two pathways were used to construct different synthetic dumbbell structures. The methodology behind this construction was described in patents FR3108124 [121] and FR2114556 [103].

First, previous work designed synthetically a dumbbell sequence by choosing a random 200 single-stranded nucleic acids sequence that incorporates the troponin aptamer [17]. The primer sequences F1, F2, B1 and B2 are designed with the specific software Primer Explorer. Several optimizations were carried out to reduce the oligonucleotide length, and allow the dumbbell-shape formation and the correct aptamer folding [17]. This methodology led to the construction of the first dumbbell sequence 1 and its associated primer set FIP1 and BIP1.

Secondly, it is also possible to use LAMP primers designs found in the literature for different target detection and use the F1, F2, B1 and B2 associated sequence description to build a dumbbell structure. With an example from the recent literature, this method was applied to build three other dumbbells: design 2 [122], design 3 [115] and design 4 [114].

The table in figure 2.4 summarizes the different dumbbells and associated primers that are designed and that will be used further on.

2.2.2 Dumbbell isothermal amplification with 2 primers

To check the ability of these described dumbbell sequences to be isothermally amplified and used in subsequent sensing applications, we have tested the amplification of the different dumbbells described above in ranges 10 nM to 10 pM. To this end, dumbbell amplifications were carried out in a 20 μL working volume composed of 18 μL of LAMP mix and 2 μL of the dumbbell samples at fixed and known concentrations [123]. The LAMP reaction solution was composed of several reagents such as FIP and BIP primers at 2.4 μM, 1X isothermal amplification buffer (B0537, NEB France), 1 mM $MgSo_4$, 0.4 U/mL Bst 2.0 DNA polymerase enzyme, 1.4 mM Desoxiribonuclease Triphosphate (dNTPs) and 0.25X EvaGreen Fluorescent dye (EvaGreen, JenaBioscience) (LAMP mix 2 in appendix C). Finally, the solution was placed in the

A

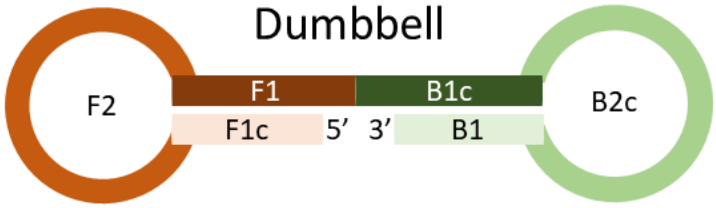

B

Design	Name	Sequence (5'-3')	Length	Reference
Design 1	Dumbbell 1	CGGATCCAAGACGCGGTTTAT CGTGCAGTACGCCAACCTTTCTCA ATAAACCGCGTCTTGGATCCG CATCTCTGAGTTATATCTTTCCCCC CCTCACTGACCCTCCTTCGGGGGAAAGATATAACTCAGAGATG	134	Savonnet *et al* 2022
	FIP1	CGGATCCAAGACGCGGTTTATCGTGCAGTACGCCAACCTTTCTCA	45	
	BIP1	CATCTCTGAGTTATATCTTTCCCCCGAAGGAGGGTCAGTGAGG	43	
Design 2	Dumbbell 2	AGAGCAGCAGAAGTGGCACA GGTGATTGTGAAGAAGAAGAG TGTGCCACTTCTGCTGCTCT TTA TCAACCTGAAGAAGAGCA GGCAGTGAGGACAATCAGTTCT TGCTCTTCTTCAGGTTGA	122	Lamb *et al* 2020
	FIP2	AGAGCAGCAGAAGTGGCACAGGTGATTGTGAAGAAGAAGAG	41	
	BIP2	TCAACCTGAAGAAGAGCAAGAACTGATTGTCCTCACTGCC	40	
Design 3	Dumbbell 3	TCCCCTACTGCTGCCTGGAG TTTTCGGCAGTCAAGCCTCTTC CTCCAGGCAGCAGTAGGGGA TTA TCCTGCTAGAATGGCTGGCAATT TGAACCAGCTTGAGAGCAAAAAA AATTGCCAGCCATTCTAGCAGGA	134	Wang *et al* 2020
	FIP3	TCCCCTACTGCTGCCTGGAGTTTTCGGCAGTCAAGCCTCTTC	42	
	BIP3	TCCTGCTAGAATGGCTGGCAATTTTTTTTGCTCTCAAGCTGGTTCA	46	
Design 4	Dumbbell 4	CTGCCCCGACGATAGGCTTAAT CGTGGTCTGGTGAAGTTCTACGG ATTAAGCCTATCGTCGGGGCAG TGA TCCAGTGCGACCTGCTGGGTG GTACTGGCGGCGAACAATACC CACCCAGCAGGTCGCACTGGA	133	Tanner *et al* 2012
	FIP4	CTGCCCCGACGATAGGCTTAATCGTGGTCTGGTGAAGTTCTACGG	45	
	BIP4	TCCAGTGCGACCTGCTGGGTGGGTATTGTTCGCCGCCAGTAC	42	

Figure 2.4: Dumbbell constructs. (A) Schematic of the dumbbell construct with sequence 5' - F1c - F2 - F1 - B1c - B2c - B1 - 3'. (B) Table of different dumbbell constructs designs inspired from: design 1 [123], design 2 [122], design 3 [115] and design 4 [114].

QuantStudio Real-Time PCR system (Thermo Fischer) and samples were heated at 65°C for one hour. The fluorescence value was recorded every 30 seconds. Experimental amplification duplicates called analytical replicates were systematically achieved for each sample. Figure 2.5 A shows the amplification curve for dumbbell D1.

From the fluorescence data acquired during amplification, the Quant Studio Design and Analysis Software computes Time-to-positive (Tp) values for each sample, defined as the time required for the fluorescence signal to cross a threshold. Calibration curves were drawn with different dumbbell concentrations (in log scale) as a function of the Tp values, and showed the ability of the method to quantify a DNA amount. The response linearity was assessed through a linear regression correlation coefficient [123].

From figure 2.5 A, we can derive the dumbbell D1 calibration curve and associated linear regression with the mean value of normalized fluorescence signal (N=2) (Fig 2.5B). As an illustration, the calibration curves for dumbbell construct D3 and D4 are also plotted in figure 2.5 B. This calibration curve shows that it is possible to quantify the dumbbell quantity present in the solution on three orders of magnitude. All dumbbell DNA sequences were amplified at various concentrations from 10 pM to 10 nM, and in all cases, a clear exponential amplification was observed with larger Tp values for lower concentrations of dumbbells. The linear correlation between the logarithm of the dumbbell concentration and the Tp values was excellent with $R^2 > 0.99$ for dumbbells D1 and D4 shown in this example. Thus, the quantification of

dumbbells D1 and D4 was possible on the 3 orders of magnitude of concentrations in less than 30 minutes. There are notable differences in amplification velocity with these dumbbell constructs. Indeed, construction design D4 appears as very efficient for amplification. The regression slope is similar for both construct designs D1 and D4, giving comparable quantification. Dumbbell design D3 presents a significantly slower amplification velocity, and presents different regression slope.

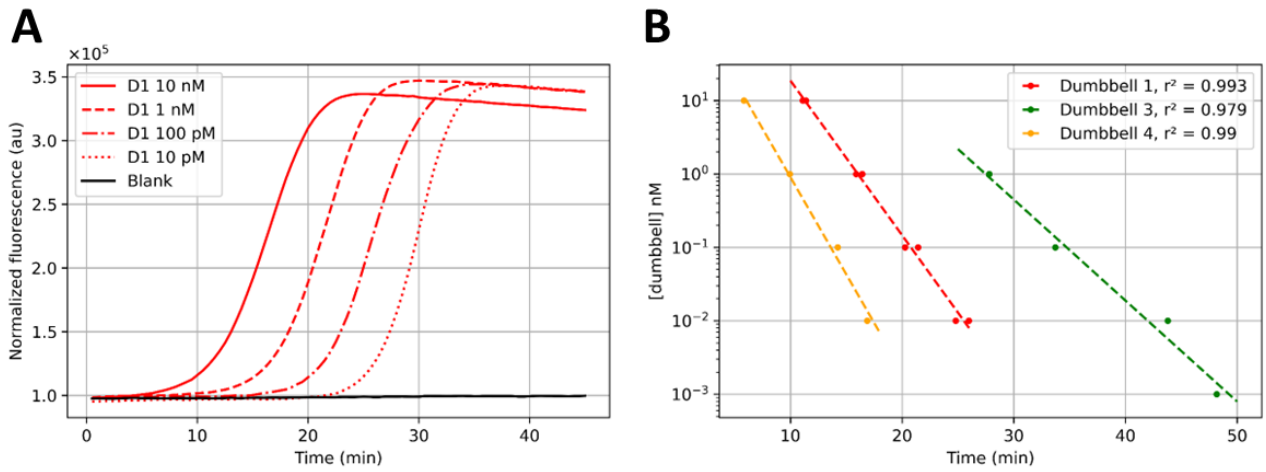

Figure 2.5: (A) Normalized fluorescence data over time for dumbbell D1 in a concentration range from 10 pM to 10 nM along with a blank sample without a dumbbell. (B) Logarithm of the dumbbell concentration as a function of Tp for dumbbells D1, D3 and D4.

From the theoretical description of the LAMP amplification process, we derive a double-stem loop generic oligonucleotide structure called dumbbell and highlighted its suitability for isothermal amplification at 65°C with only two primers FIP and BIP. We implemented several dumbbell designs based on literature examples and validated their quantification through isothermal amplification on three orders of magnitude, with varying amplification velocities.

2.3 Engineering of the dumbbell structure

The previous description of the dumbbell structure gives a very generic oligonucleotide sequence in a double stem-loop shape. The functionality of this sequence for isothermal amplification with only two primers (FIP and BIP) was validated. One of the main advantages of this structure is that it can be chemically synthesized by a standard oligonucleotide manufacturer. However, the synthesis of oligonucleotides is often limited by sequence length and production yield. Therefore, this section will show the sequence engineering to reduce the oligonucleotide length. Moreover, we will show the modification of the structure to incorporate a probe that can be of different natures and for different applications. Thus, the combination of this structure with molecular probes allows the implementation of exponential amplification as a signal amplification strategy in biological assays.

During the subsequent dumbbell isothermal LAMP amplification validation experiments, minor changes in the amplification mixture used were implemented (change in concentration, change in enzyme...). The recap of the different LAMP mixtures can be found in Appendix C, and we will refer to the exact associated mix number in the following sections.

2.3.1 Minimal dumbbell structure

The first approach was to reduce the length of the dumbbell structure, for ease of chemical synthesis. To do so, we removed the double stem-loop in the structure by removing the 5' and 3' ends segments (F1c and B1). The structure becomes a linear oligonucleotide because it does not contain any stem-loop (Fig 2.6D). The sequence is therefore as follow: 5' - F2 – F1 – Int - B1c – B2c – 3'. We can also reduce only one of the loops in the dumbbell structure, and describe a structure either with a left loop (Fig 2.6B) or a right loop ((Fig 2.6C) such as : 5' F1c - F2 – F1 -Int – B1c – B2c – 3' or 5' F2 – F1 -Int – B1c – B2c – B1 3'.

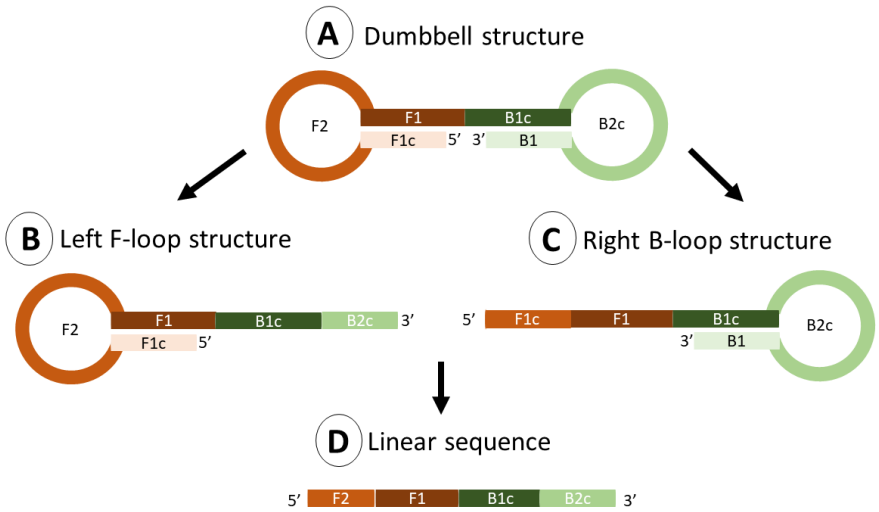

Figure 2.6: (A) Minimal dumbbell (B) F-loop structure. (C) B-loop structure. (D) Linear oligonucleotide structure [103]

Structures B and D (Fig 2.6) were implemented on dumbbell design 1, and their suitability for isothermal amplification was experimentally validated with LAMP amplification with two primers FIP and BIP. With design 1, structure B was called L1-Floop (for linear Floop design 1), and structure D was called L1 (for linear design 1). Their schematic representation can be found in figure 2.7A and their exact nucleic acids sequences can be found in Appendix A. The sequence length is significantly reduced, with 88 bases for L1, and 112 bases for L1-Floop. Sequences D1, L1 and L1-Floop were diluted in the range 10 pM to 10 nM and added into LAMP mix 2 (appendix C) for isothermal amplification.

In figure 2.7B, we show that removing the double stem-loop structure in the dumbbell structure previously described does not inhibit the amplification [103]. Therefore, the so-called linear oligonucleotide is functional for isothermal amplification with the two primers FIP and BIP. However, the amplification is significantly slower than for the original dumbbell structure D1. The linear oligonucleotide L1 presents a very short sequence but it has a very slow amplification (about 45 minutes for the subnanomolar range), whereas the F-loop structure owns a bit longer sequence but its amplification is slightly more rapid. Therefore, when designing dumbbells, there is a trade-off between oligonucleotide length for chemical synthesis yield and amplification velocity. For industrial applications for example, short dumbbells are preferable for mass production (to increase yield and reduce cost) but have long amplification times, but optimal amplification times are found for larger dumbbells.

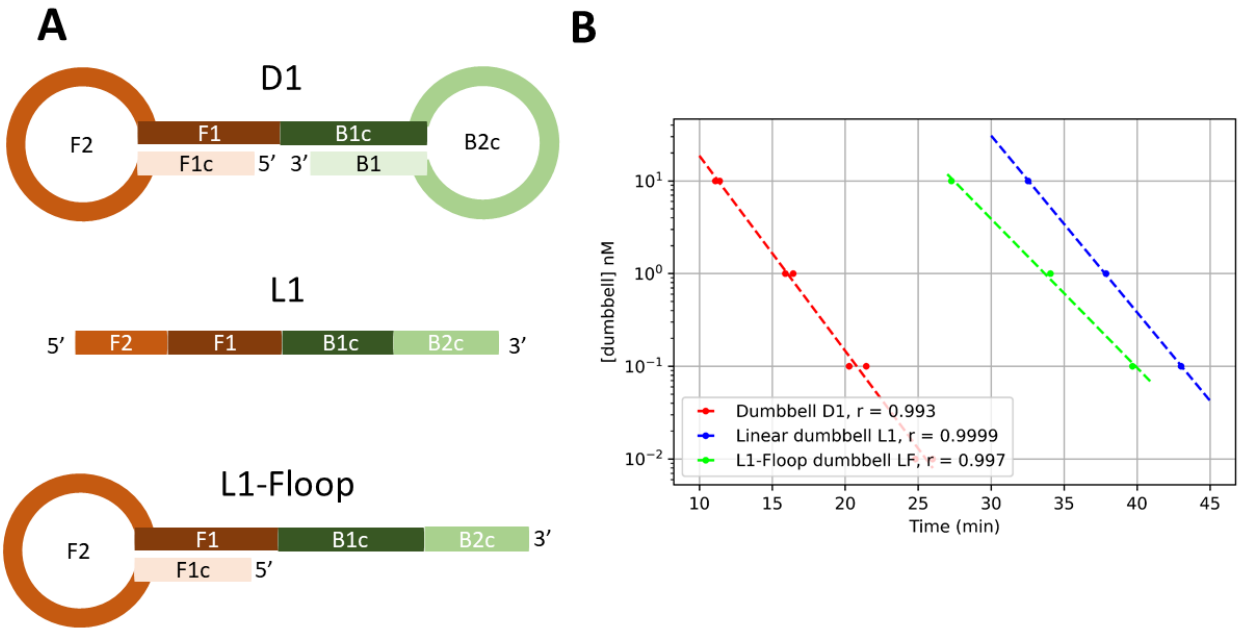

Figure 2.7: LAMP amplification of minimal dumbbells (A) Schematic representation of dumbbell constructs D1 (design A), L1 (design D) and L1-Floop (design B). (B) Logarithm of the dumbbell concentration as function of time-to-positive Tp for dumbbells D1, L1 and L1-Floop.

2.3.2 Extensions of the dumbbell structure

The previous dumbbell and linear oligonucleotide are suitable for isothermal nucleic acids amplification with 2 primers, and we showed that it is possible to quantify their amount in solution through the use of LAMP. Therefore, this structure could be a good candidate for a quantitative signal amplification template in biological assays. Thus, we extended the use of such constructs with the integration of bio-recognition elements. As the structure is made of nucleic acids, the easiest way is to integrate other nucleic acids sequences that can be used as sensing probes. For example, aptamers are nucleic acid-based that can be used as bio-recognition elements. As they are composed of nucleic acids, it appears easy to integrate them into the structure previously described. Therefore, we engineered the structure D1 by incorporating other nucleic acids sequences called S at different positions in the structure. The different positions of the sequence are the following:

- In the middle of the two stem-loops (design E)
- In the F-loop (design F)
- In the B-loop (design G)
- At the 5' dangling end (design H)
- At the 3' dangling end (design I)

The linear structure L1 described in the previous section can also integrate a nucleic acid sequence S at its 5' or 3' end, in a similar fashion to designs H and I with the dumbbell sequence.

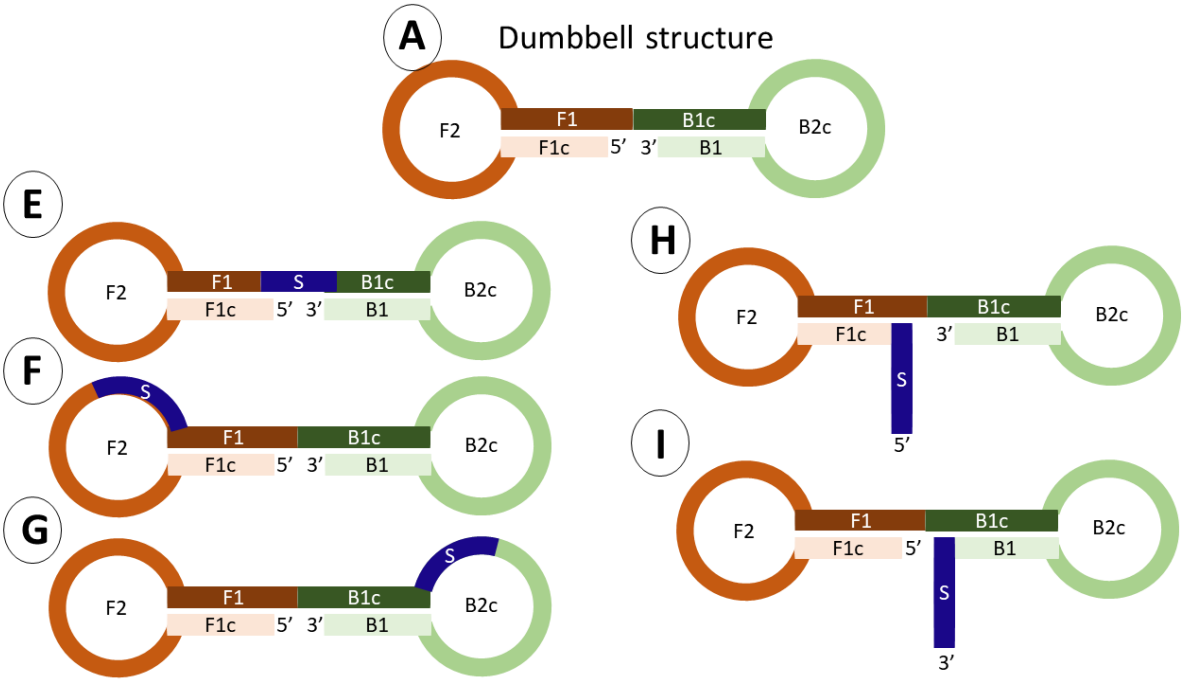

Figure 2.8: Dumbbell original structure (A) incorporating a nucleic acid sequence S at different locations in the sequence (designs E to I): in the middle of the two stem-loops (E), in the F-loop (F), in the B-loop (G), at the 5' end (H) and at the 3' end (I)

Designs E to I will be tested with the integration of various nucleic acid sequences for isothermal amplification and quantification of DNA template. The new sequences created will be named using the following formalism: a sequence will be named D_i-**S-pos** with:

- D_i: the dumbbell design number i
- S: incorporated nucleic acid sequence name
- pos: position of S in the sequence (C = central, L = left loop, R = right loop, DE3 = 3' dangling end, DE5 = 5' dangling end)

2.3.2.1 Integration of thrombin aptamers

The first nucleic acid sequence that was integrated into the dumbbell structure was a thrombin aptamer. This latter was previously described in the literature [63] and two aptamers bind two different epitopes of the protein. We have constructed five different dumbbell structures incorporating the Thr1 aptamer with the following 15-base long sequence: 5'-GGTTGGTGTGGTTGG-3'. Since this aptamer sequence is rather short, it did not significantly elongate the length of the dumbbell from the original construction. This sequence was integrated at the different locations shown in the design E to I (Fig 2.8). This led to the creation of 5 new sequences: D1-THR-C, D1-THR-L, D1-THR-R, D1-THR-DE5 and D1-THR-DE3, with their schematic representations in figure 2.9A. The created dumbbell sequences can be found in Appendix A. All the different dumbbells obtained were tested for isothermal amplifications with primers FIP1 and BIP1 and mix 2 (appendix C). Calibration curves were drawn for dumbbell concentration in the range 10 nM - 10 pM. For designs E to G, therefore dumbbells D1-THR-C, D1-THR-L, D1-THR-R, the comparison was made with dumbbell D1 (Fig 2.9B) and for designs H and I, the comparison was made with a modified version of dumbbell D1 (D1*) containing a intermediate portion of 3 bases between the F1 and B1c portions, since this portion was also present in dumbbells D1-THR-DE5 and D1-THR-DE3 (Fig 2.9C).

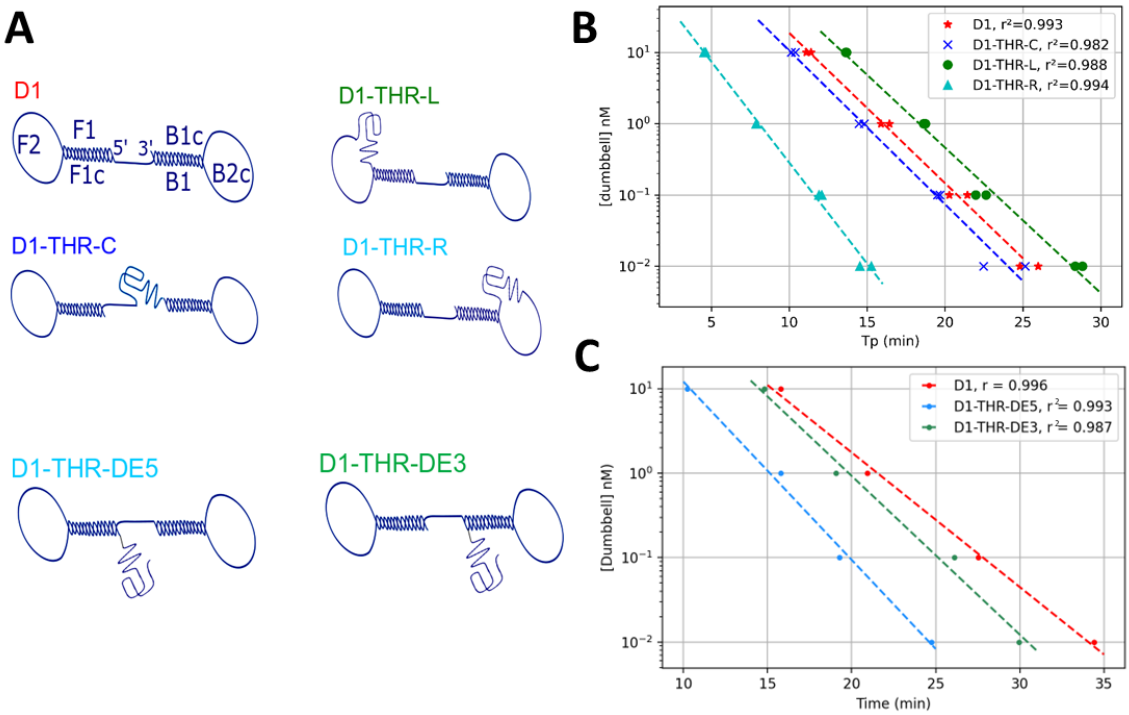

Figure 2.9: LAMP amplification of dumbbells incorporating thrombin aptamers. (A) Schematic representation of dumbbell D1 incorporating the thrombin aptamer Thr1 at different locations. (B) Logarithm of the dumbbell concentration as a function of time for dumbbells D1, D1-THR-C, D1-THR-L and D1-THR-R. (C) Logarithm of the dumbbell concentration as a function of time for dumbbells D1*, D1-THR-DE5 and D1-THR-DE3. In this example, D1 is modified with a 3-base intermediate sequence (TGA) between the F1 and B1c portions.

Interestingly, the integration of the thrombin aptamers does not limit the LAMP amplification. When the Thr1 aptamer is inserted into the dumbbell sequence, its positioning in the B-loop seems to give the fastest amplification, whilst the incorporation in the F-loop seems to

slow down the amplification. There is a trade-off with the thrombin aptamer positioned in the middle for which the amplification time is similar than without any aptamer inserted. Therefore, it seems like the incorporation of an aptamer structure is compatible with LAMP amplification of the structure, and that the incorporation of the aptamer in the middle of the structure seems to have less impact. Secondly, the integration of the aptamer on the 5' or 3' end of the structure seems to speed up the amplification (Fig 2.9C). More interestingly, the integration at the 5' end seems to be more efficient for the amplification velocity. This integration of the aptamer on the 3' or 5' end can be called the "dangling end" and seems favorable for amplification and easiness of structure integration and aptamer conformation. The expression "dangling end" will be used further on to describe this type of structure.

The incorporation of the thrombin aptamer sequence in various positions of the dumbbell highlighted two advantageous locations, the central and the 5' dangling end position, mainly for their amplification velocity.

2.3.2.2 Integration of troponin aptamers

To confirm the suitability of the dumbbell structure for incorporation of nucleic acid sequences such as aptamers, we extended the study with other aptameric sequences. We chose a troponin aptamer, since this target is of high importance in the scope of this project to design sensitive assay for troponin sensing, and the dumbbell sequence incorporating a troponin aptamer could be an interesting template for sensitive assays through the use of isothermal exponential amplification.

Many articles have been found lately in the literature referring to troponin aptamers [49]. The troponin aptamer called Tro4 discovered by Jo et al in 2015 [124] was highly reused in other studies. The aptamer is made of 40 bases, much longer than the thrombin aptamer previously described, which makes the study of this aptamer incorporation into the dumbbell interesting: 5'- CGTGCAGTACGCCAACCTTTCTCATGCGCTGCCCCTCTTA-3'.

Since the study on the incorporation of the thrombin aptamer in the dumbbell structure showed two advantageous incorporation locations (central and dangling end); similarly, we studied the incorporation of the aptamer in the middle of the structure (design E) and in the 5' end of the structure (design H). Since the aptamer sequence is long, in order to limit the structure's total length, we integrated it into the dumbbell design number 2 which is shorter than design number 1. The same formalism was applied to name the created dumbbells, and the lengths of the sequences were still quite important, 159 bases for D2-TROPO-C and 172 bases for D2-TROPO-DE2. The dumbbell schematic representation with the troponin aptamer with a hairpin conformation is shown in figure 2.10 A. These two structures were tested for isothermal amplifications with primers FIP2 and BIP2. Since the sequences are long (over 150 bases), the amplification was enhanced using another enzyme (Bst 3.0 polymerase, M0374, NEB France). The calibration curves after LAMP amplification with mix 3 (appendix C) are shown in figure 2.10 B.

In a similar fashion to the integration of the thrombin aptamer, the integration at the 5' dangling end gives a much faster amplification time. However, both dumbbells are very suitable for isothermal amplification with their two primers FIP2 and BIP2. Moreover, we can think that the incorporation of the troponin aptamer in the dangling end location could be favorable for the Tro4 hairpin shape conformation since it exhibits fewer sterical constraints.

We have studied the integration of aptameric sequences at different locations in the dumbbell structure, and several examples have highlighted that the dangling end location is the most favorable for amplification velocity. This study and the different favorable oligonucleotide structures have been fully described in patent FR2109667 [102].

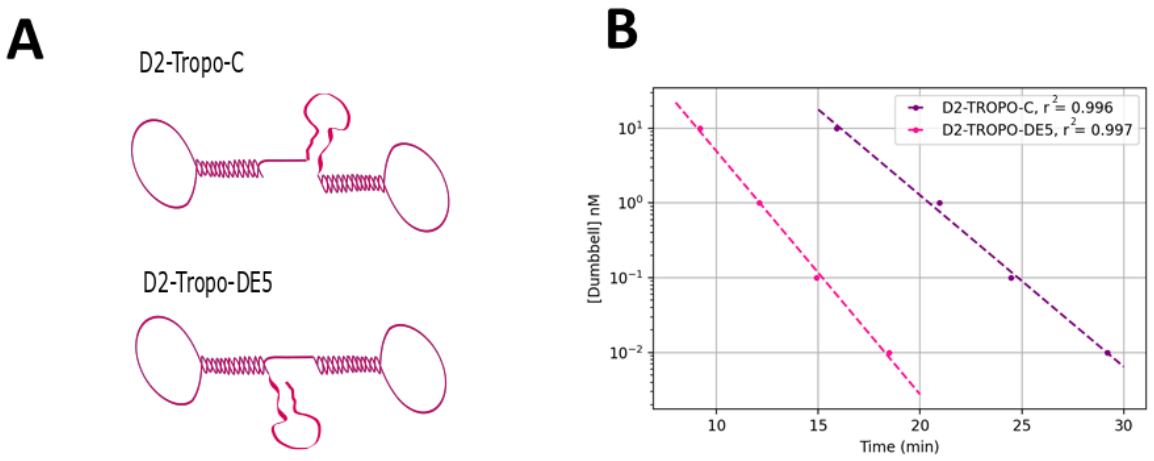

Figure 2.10: LAMP amplification of dumbbells incorporating troponin aptamers. (A) Schematic representation of dumbbell D2 incorporating the troponin aptamer Tro4 at different locations (central and dangling end). The Tro4 aptamer has a hairpin shape. (B) Logarithm of the dumbbell concentration as a function of time for dumbbells D2-TROPO-C and D2-TROPO-DE5.

2.3.2.3 Integration of generic nucleic acid

The integration of nucleic acids sequences such as aptamers in the dumbbell structure is possible and in some cases is even favorable for the velocity of the amplification. However, with the two examples described above, a specific dumbbell has to be designed for each sensing application, for example with the thrombin or troponin aptamers. Thus, to offer a more generic dumbbell structure we extended the dumbbell design by incorporating a generic nucleic acid sequence and the final structure will serve as a template for various sensing applications. The chosen nucleic acid sequence is 24 bases long and is called Zip6, with the following sequence 5'-GACCGGTATGCGACCTGGTATGCG-3'. This short sequence is favorable for dumbbell chemical synthesis with high yield and should not slow down the amplification. With this sequence, we design two new structures based on design number 1: a double stem-loop dumbbell (D1) with the integration of Zip6 at the dangling end 5' end, and a linear dumbbell (L1) with the integration of Zip6 at the dangling end 5' as well. The two structures were tested for amplification in the range 10 nM to 10 pM with mix 2 (appendix C) and compared with other structures (Fig 2.11).

Interestingly, these dumbbell constructs follow the same trend as observed for the previous constructs. The linear dumbbell is shorter in terms of sequence length but has a longer amplification time than the double-stem loop one. For both constructs, there is a trade-off between oligonucleotide sequence length and velocity of LAMP amplification. Both are very interesting constructs since they integrate this generic sequence Zip6 that can be used in various sensing scenarios [102]. For this specific case, the preferred choice of dumbbell will be D1-Zip6-DE since it presents a reasonable sequence length (156 bases), and a rapid amplification (below 30 minutes).

This generic dumbbell incorporating the sequence Zip6 at its 5' dangling end can be used in combination with another oligonucleotide structure including for example an aptamer as a bio-

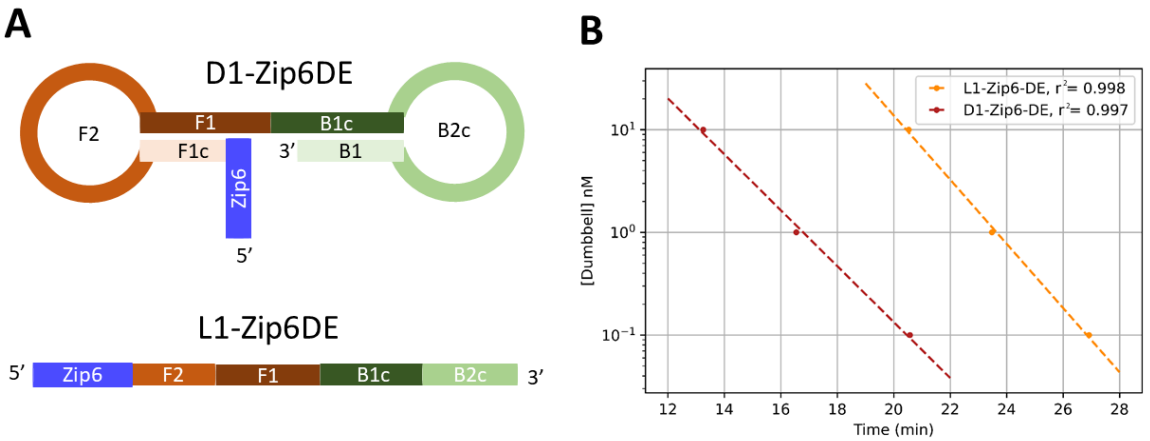

Figure 2.11: (A) Sequences for dumbbells D1 and L1 incorporating sequence Zip6 at the dangling end. (B) Logarithm of the dumbbell concentration as a function of time for dumbbells D1-Zip6-DE and L1-Zip6DE.

recognition element. This second oligonucleotide structure must therefore include a sequence complementary to Zip6, called Zip6c, that will hybridize to the Zip6 sequence contained in the dumbbell (Fig 2.12). This molecular complex will form a bio-recognition element made of the dumbbell containing Zip6 hybridized to the oligonucleotide containing Zip6c and a specific aptamer. This construct is generic because can be easily adapted to any desired aptamer, since only the second sequence of the bio-recognition element has to be replaced. This second sequence is made of the Zip6c sequence (24 bases), eventually a spacing sequence with for example 10 Thymines bases, and then the desired aptamer sequence. With short aptamer sequences, this sequence length will be about 50-80 bases which is reasonable for a chemical synthesis with high yield. This way, the complex will exhibit a specific aptameric sequence S in the additional oligonucleotide hybridized into the dumbbell structure, and this latter will serve as a template for quantitative isothermal LAMP amplification.

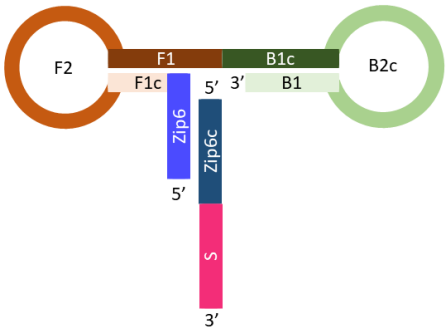

Figure 2.12: Schematic representation of the dumbbell structure D-Zip6-DE for hybridization to another oligonucleotide 5'-Zip6 - S - 3', with S being a sequence of an additional oligonucleotide used as a bio-recognition element.

The use of this dumbbell structure can also be declined with any nucleic acid sequence containing Zip6c that will hybridize on the dumbbell, and that includes any type of bio-recognition element. For example, an antibody can be directly chemically functionalized with the Zip6c strand, and coupled to the dumbbell through hybridization of Zip6-Zip6c.

Last but not least, the generic dumbbell can be chemically functionalized with any function that will allow the binding of other molecules that can be used as bio-sensing elements. For example, the well-known biotin-streptavidin interaction can be used to bind the dumbbell containing a biotin function and any other molecule functionalized with biotin through a free streptavidin, or another molecule functionalized directly with streptavidin.

We have shown that the incorporation of this nucleic acids sequence S does not inhibit the isothermal amplification. We have studied the impact of the sequence position in the structure in terms of amplification times and quantification ability, for different structures S integrated in the dumbbell, in a direct or indirect way.

2.3.3 Conclusion

From the generic oligonucleotide sequence in double stem-loop shape that can be amplified isothermally with the two primers FIP and BIP, we declined its structure and its sequence for various applications. We highlighted the minimal dumbbell structure that removes the two stem-loops and yet remains functional for isothermal amplification [103]. This linear sequence has the advantage of being short in length and therefore can be chemically synthesized with high yield, but it presents a slower amplification time than the double stem-loop structure. Due to its slow amplification time, this structure presents a minor interest in designing rapid biosensing protocols. However, due to its short sequence and the ability to be synthesized with high yield, this structure can be advantageous to use along with other LAMP amplification reactions. Indeed, this short structure represents a very good internal control of any LAMP amplification reaction, since it only contains a short oligonucleotide and only two primers, thus reducing the risk of cross-contamination. Lastly, this structure could be interesting for the implementation of multiplexed detection protocols due to the short length and reduced number of primers [104].

Secondly, the dumbbell structure was extended to include other nucleic acid sequences in it, that can serve as bio-recognition elements, and therefore combine the exponential amplification ability given by the dumbbell structure. For the direct integration, various positions of this sequence were studied, and the dangling end position appeared as the most favorable. This structure was therefore used to integrate thrombin and troponin aptamers, and the functionality of those structures for quantification after isothermal amplification was also validated. Indirect integration of other nucleic acids sequences was also proposed, and a more generic structure including a short nucleic acid sequence that serves as a template to bind different bio-recognition elements was described. This structure is particularly interesting for its versatility and will be used further in the work described in the next chapter.

We propose a generic and synthetic nucleic acid tools that serves as a template for exponential isothermal amplification. In combination with various molecular probes, this tool can be of great use to allow exponential signal amplification. The possibility to quantify its amount in solution through isothermal amplification is very interesting for future biosensor integration.

2.4 Framework for hairpins evolution during isothermal dumbbell exponential amplification

The dumbbell structure was exposed in the previous section with various possibilities to integrate molecular probes in it and its suitability for isothermal exponential amplification with the two primers FIP and BIP [121]. The recording of fluorescence over time allows the quantification of this oligonucleotide structure in solution on broad ranges. From the theoretical description of the LAMP amplification process, many amplicons of different sizes are formed during the

amplification reaction. This section aims to propose a general framework to understand the production of amplicons and hairpins during the amplification reaction, and therefore gives a better understanding of the reaction kinetics and possible improvements.

2.4.1 Theoretical framework

The dumbbell isothermal amplification reaction as exposed in the previous section bypasses the first stages of the conventional LAMP reaction, and therefore proposes an amplification with only the primers FIP and BIP (Fig 2.13). During the amplification reaction from the dumbbell structure, hairpins of different lengths are produced. A model with the kinetics of amplification to compute the hairpin length and concentrations is derived in order to fit experimental data [125].

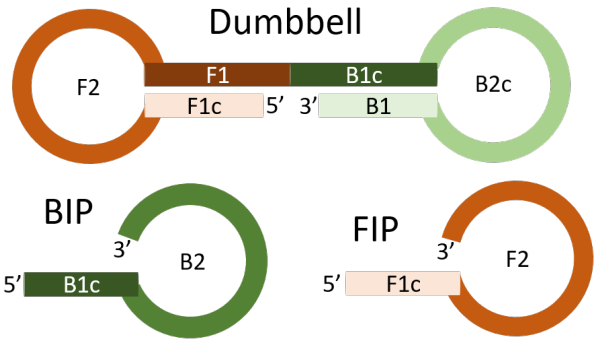

Figure 2.13: Dumbbell and primer structures with sequence names

From the dumbbell sequence, Hp1b hairpins are produced with only the help of the enzyme (Fig 2.14). In the name Hp1b, Hp stands for the hairpin, 1 for a stem containing one dumbbell sequence and b for a B2c loop compatible with BIP primer. From this hairpin Hp1b, two new hairpins are produced by the enzyme through the use of the BIP primer (Fig 2.15). The reaction showing the duplication of hairpins during the exponential amplification is therefore as follows:

$$\mathrm{Hp1b} + \mathrm{BIP} \underset{\mathrm{k_B}}{\longrightarrow} \mathrm{Hp1f} + \mathrm{Hp2f} \tag{2.1}$$

with k_B the kinetic rate constant of the reaction. In a similar fashion, Hp1f is created with the help of the enzyme, and Hp1b and Hp2b are produced with the help of the FIP primer and the Bst enzyme.

$$\mathrm{Hp1f} + \mathrm{FIP} \underset{\mathrm{k_F}}{\longrightarrow} \mathrm{Hp1b} + \mathrm{Hp2b} \tag{2.2}$$

This first duplication equation can be generalized to the creation of hairpins with various stem lengths. The equation can therefore be generalized similarly for primers FIP and BIP and for the creation of hairpins of increasing length 2^n. For simplification purposes, we considered both primer's kinetics to be equivalent and derived a general equation with primer P and creations of generic hairpins Hp with length 2^n:

$$\mathrm{Hp2}^n + \mathrm{P} \underset{k_{hyb}}{\longrightarrow} \mathrm{Hp2}^{n+1} + \mathrm{Hp2}^n. \tag{2.3}$$

To derive the evolution of hairpin concentration $c_{Hp}(t)$ and hairpin lengths $l_{Hp}(t)$ in solution, we varied the primer and dNTPs concentrations in solution. At a time n, the concentration of hairpins is expressed by $c(n,t)$ with a fixed stem length n, and the total concentration of hairpins

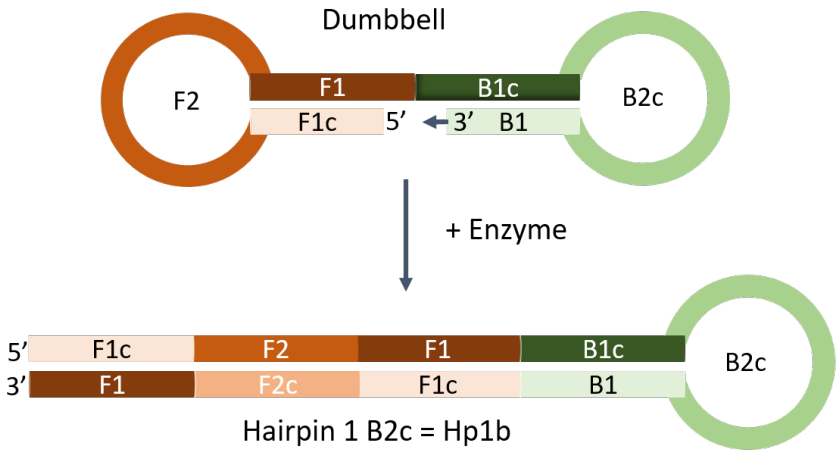

Figure 2.14: Formation of hairpin Hp1b from the dumbbell [125].

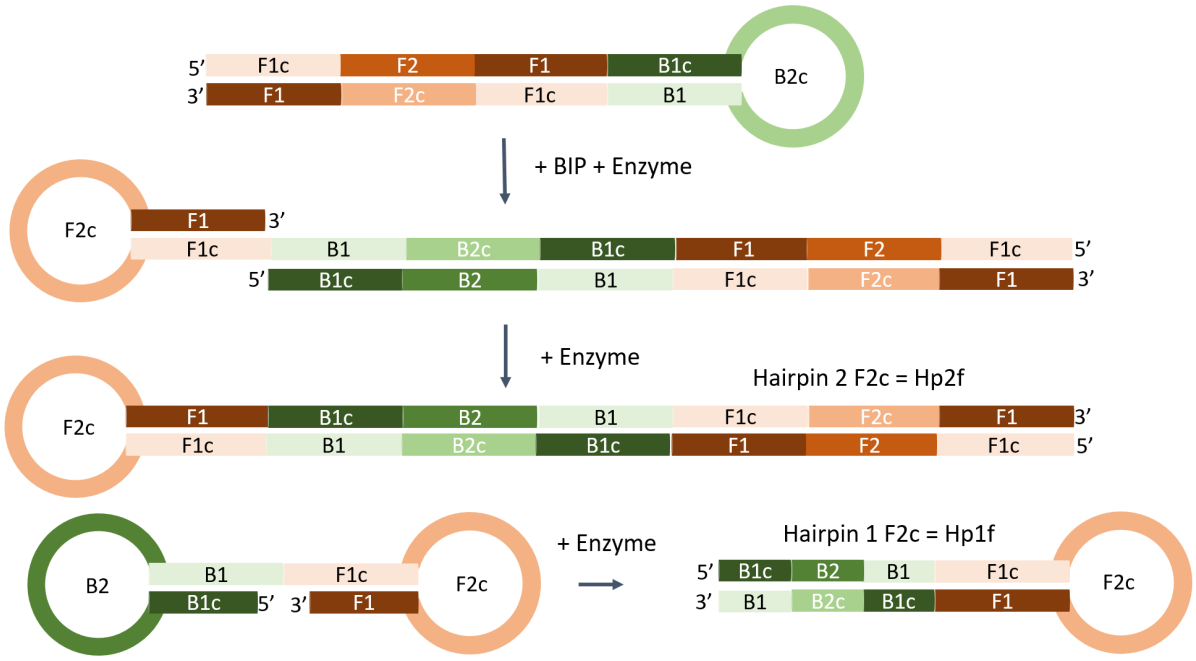

Figure 2.15: Duplication: Two hairpins Hp1f and Hp2f are created from the hairpin Hp1b [125].

is the sum of $c(n,t)$ for intermediate lengths n. l_D is the length of the dumbbell, and the length of the hairpin Hp1 is $l_{Hp1b}+l_{Hp1f}=3l_D$. Similarly, the length of a hairpin Hp2^n is $(2^n+1/2)l_D$. The concentration and length of hairpins can therefore be derived in solution with the following equations:

$$c_{Hp}(t) = \sum_{n=0}^{\infty} c(n,t) \tag{2.4}$$

$$l_{Hp}(t) = l_D \sum_{n=0}^{\infty} 2^n c(n,t) + l_D c_{Hp}(t)/2 \tag{2.5}$$

Previous work [125] pointed out two main regimes for the evolution of hairpin concentration and length: a first one limited by the hybridization of primers, and a second one limited by a finite concentration of dNTPs. The theoretical computation and hairpin length and concentration fit with experimental data from the fluorescence amplification curves. It was found that for short time the concentration of primers could be considered constant and therefore the evolution of hairpin length followed a logistic trend in the first regime such as $l_{Hp}(t) \simeq l_D c_D \exp(2k_{hyb}c_P t)$.

However, the use of intercalating dye does not allow the finite evaluation of hairpin lengths, since the dye quantity is proportional to the total length of amplicons produced, with no distinctions of various amplicon lengths. This method was used to evaluate the model for the total hairpin length over time during the amplification process. However, it was not possible to distinguish intermediate hairpin formation and their length during the amplification process. Alternative experimental techniques will be therefore used to evaluate the length of the different intermediate hairpins formed during the amplification process, and therefore try to validate the model. The theoretical values for the evolution of hairpin Hp_i lengths are exposed in table 2.2, until structure with n=2. The primary structure H corresponds to the dumbbell.

Hairpin	Theoretical length (bases)
H	≈ 150
Hp1	≈ 200
Hp2	≈ 400
Hp4	≈ 600

Table 2.2: Theoretical computations of hairpin sizes

2.4.2 Hairpin length evaluation through gel electrophoresis

The theoretical description of the hairpin evolution derives discrete hairpin length during the amplification process [125] (Table 2.2). To experimentally observe the various hairpin lengths during the LAMP reaction, gel electrophoresis method can be used. This method can evaluate the amount and length of hairpins of different stem lengths at the end of the amplification process and therefore could help to validate the theoretical model previously described that derives the hairpin length.

2.4.2.1 Experimental procedure

Isothermal dumbbell exponential amplifications are carried out at 65°C with different experimental conditions tested to observe the difference in the finally produced hairpin length on the final gel. To run this set of experiments, dumbbell D1-THR-R was chosen since it exhibits

a very fast amplification. Its total length is 152 bases (sequence in Appendix A), and it was isothermally amplified at 65°C with various conditions.

We ran a 1.5% agarose gel and used SYBR Gold stain. The total volume of sample injected on the gel was 14 μL in 0.5X Tris-borate-EDTA (TBE). The step ladder used as a molecular weight marker for base pair was comprised of between 50 and 3000 bp. Since the dumbbell LAMP hairpins are single-stranded, we denatured all the reagents prior to deposition on the gel by warming at 95°C for 5 minutes. After sample deposition, the gel undergoes migration at 150 V for two hours.

2.4.2.2 Observation of dumbbell, primers and hairpins from isothermal amplification

100 nM of dumbbell D1-THR-R was amplified with LAMP (mix 4 in appendix C). Its amplification with both primers FIP and BIP is very rapid and leads to fluorescence saturation in about 10 minutes. Two experiments were carried out with either only FIP or only BIP primers to observe the initiation steps of the LAMP reaction, and the formation of Hp1b and Hp1f structures from an individual primer only. The fluorescence observation over time led to the observation of a very late amplification, which testify of the incomplete amplification (Fig 2.16A).

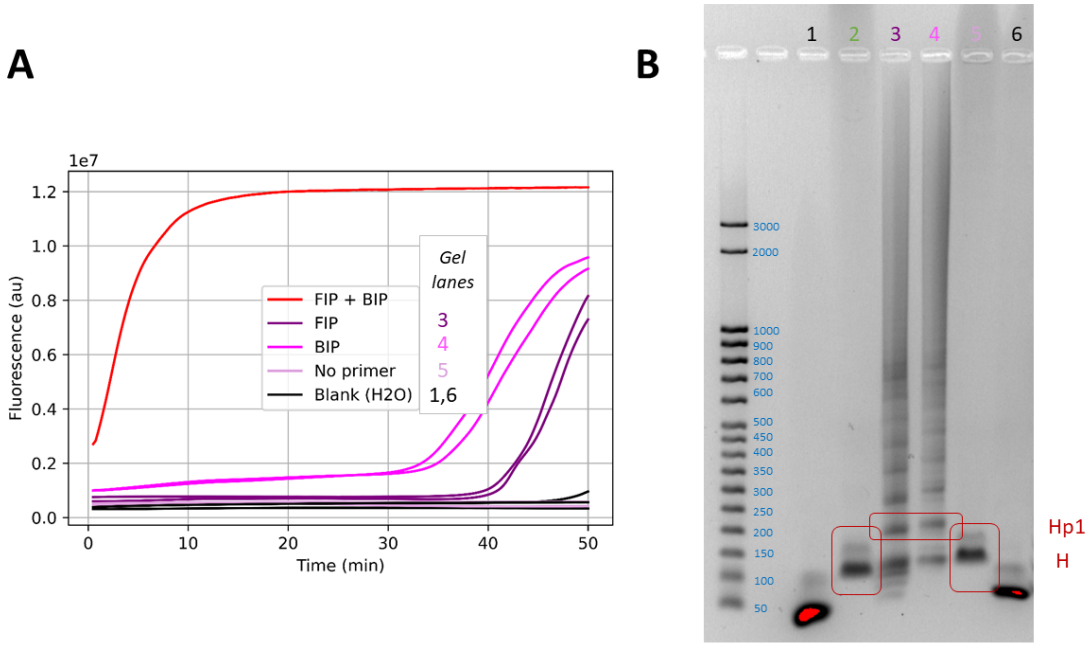

Figure 2.16: (A) Isothermal amplification of 100 nM D1-THR-R with various primer conditions. (B) Associated lanes on the gel electrophoresis. Lane 2 : 100 nM of dumbbell D1-THR-R (no amplification). Lane 3: 100 nM D1-THR-R after LAMP amplification with FIP. Lane 4: 100 nM D1-THR-R after LAMP amplification with BIP. Lane 5: 100 nM D1-THR-R after LAMP amplification without primers. Lane 1 and 6: blank samples

The associated bands in gel electrophoresis are shown in figure 2.16 B. The lane on the left corresponds to the step ladder. The first and sixth lanes correspond to blank samples, which therefore comprise the amplification mixture with both primers FIP and BIP and without D1-THR-R. The only bands present on these lanes correspond to the primers of length roughly about 50 bases. The second lane corresponds to the dumbbell oligonucleotide prior to amplification

(thus without amplification mixture). The lane presents two bands roughly around 100 and 150 bases. These two bands correspond to the single-stranded and double-stranded version of the dumbbell corresponding to the correct structure folding. Lanes 3 and 4 correspond to the amplification reaction with only FIP or only BIP. It presents the same band around 150 bases corresponding to the dumbbell, and one band around 200 bases which corresponds to the hairpin Hp1b or Hp1f. Above 300 bases, there seems to be a smear and therefore the gel resolution is not enough to assign any structure. Gel lane number 5 exhibits a band corresponding to the dumbbell only, since the lack of primers inhibited the amplification.

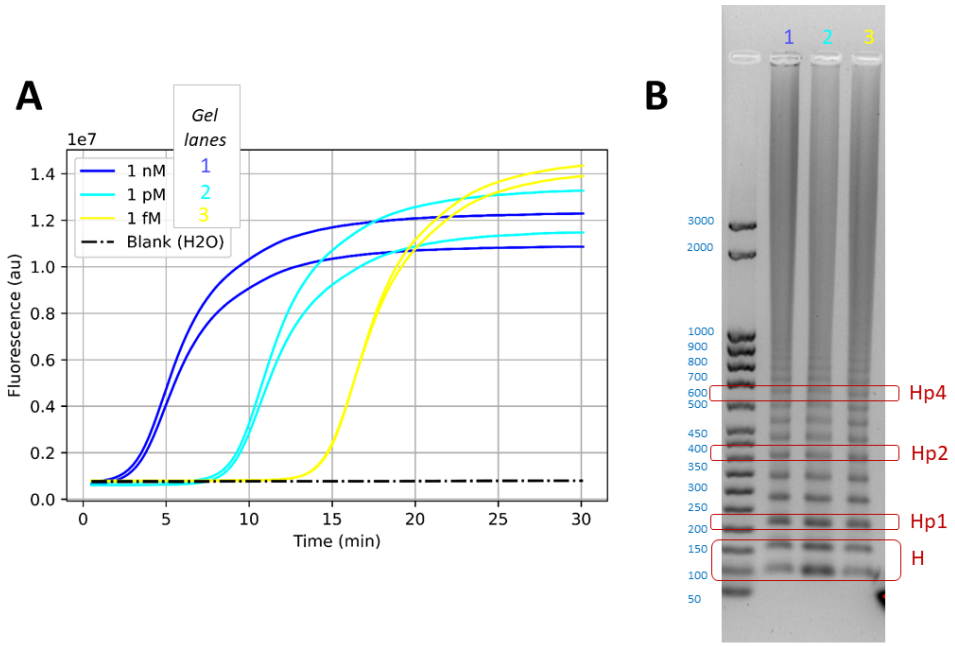

Figure 2.17: (A) Isothermal amplification of D1-THR-R in range 1 nM - 1 fM. (B) Associated lanes on the gel electrophoresis. Lane 1: D1-THR-R 1 nM. Lane 2: D1-THR-R 1 pM. Lane 3: D1-THR-R 1 fM.

Dumbbell D1-THR-R was isothermally amplified in the range 1 nM, 1 pM and 1 fM (Fig 2.17A) with mix 4 (appendix C). The three lanes correspond to the three dumbbell concentrations deposited on the gel. Interestingly, on the gel electrophoresis which is an endpoint analysis, the observed bands are very similar (Fig 2.17B). They present very distinct bands in the range 100-600 bases. From the theoretical description of dumbbell length evolution over time, we can identify the bands corresponding to the hairpin products 1, 2 and 4, with lengths respectively of around 200, 400, 600 bases. Over 600 bases, the gel presents a smear which leads to the impossibility of assigning any further longer hairpins. Between hairpin bands corresponding to Hp1 and Hp2, as well as between Hp2 and Hp4, there are many intermediate bands. These bands are not assigned or considered in the theoretical model. They could correspond to structures that were not described in the model, which would therefore mean that our model description is incomplete. However, the samples were denatured prior to deposition on the gel, but the long migration time probably led to secondary structure formation through the hybridization of similar sequences in the different hairpins produced.

The Hp1, Hp2 and Hp4 structures formed during dumbbell isothermal exponential amplification are clearly assigned in the gel electrophoresis. However, for hairpin lengths above Hp4, it is impossible to distinguish the bands. Moreover, there is an important number of intermediate

products that were not considered in the initial theoretical model for kinetic evolution [125].

As the gel electrophoresis method is an end-point analysis, it was not possible to distinguish the difference in the dumbbell concentrations after amplification. Therefore, we ran an experiment in which we stopped the amplification after 12 minutes, having an incomplete exponential amplification for dumbbell concentrations lower than 1 nM. The bands observed on the gel were similar in length, just a change in intensity was observed, testifying about the different quantity of hairpins created during the amplification, but no further information about distinct hairpin length during the different steps of the amplification was obtained.

2.4.2.3 Varying dNTPs and primers concentrations

Secondly, in order to further explore the evolution of hairpin length during isothermal LAMP amplification, the effect of primers and dNTPs concentration was studied [125]. Amplification experiments are carried out with dumbbell D1-THR-R with various primers and dNTPs concentration in the amplification mixture. The fluorescence was recorded over time during the amplification and the samples were deposited on gel electrophoresis for final endpoint analysis.

First, 100 pM of dumbbell was isothermally amplified with various dNTPs concentrations (2.8 mM, 1.4 mM, 0.7 mM and 0.35 mM) with various adaptations of mix 1 (appendix C). The fluorescence over time clearly shows faster amplification for higher dNTPs concentrations, and higher fluorescence stability value (Fig 2.18A). The associated bands on the gel are very similar for the different dNTPs concentrations (Fig 2.18B), with variation in SYBR Gold intensity coherent to the final fluorescent saturation from the amplification curves. From the lanes on the gel (Fig 2.18B), we can associate the various hairpin lengths H, Hp1, Hp2 and Hp4. Above Hp4 with length of about 600 bases, a smear in the bands makes further analysis impossible. However, below the band corresponding to original hairpin H, there are bands at length ≈ 50 bases, with increasing SYBR intensity from lane 1 to lane 4. This corresponds to the primers that were left unreacted during the amplification process. Interestingly, their quantity increases as the initial dNTPs concentration decreases, showing that the shortness in dNTPs leads to non-finite consumption of primers during the amplification process. Moreover, for bands above 600 bases, the lane fluorescence intensity decreases proportionally with the dNTPs concentration, showing that fewer amplicons of important lengths are formed due to shortness in dNTPs. This confirms the dNTPs limited regime as described earlier [125], in which the dNTPs limits the amplification reaction after a certain cross-over time. However, this dNTPs limited regime does not have an influence on the formation of the first hairpin structures Hp1 to Hp4 that we can observe clearly on the gels.

Secondly, dumbbell at concentrations of 100 pM and 1 pM was isothermally amplified with various primer concentrations (2.5, 1 and 0.4 μM) with mix 4 (appendix C). A clear reduction in amplification velocity can be observed for lower primer concentration (Fig 2.19). However, the saturation of fluorescence in intercalating dye seems to be equivalent. The associated bands on the gel are presented in figure 2.19. There is no clear difference that can be observed, and similarly to the previous experiments, we can identify bands corresponding to Hp1, Hp2 and Hp4. However, in this experiment, we can observe several bands between 600 and 1000 base pairs, but they are not described in the theoretical model for the evolution of hairpin lengths. The primer-limited regime occurs during the first half of the amplification ((Fig 2.19A), and therefore with gel electrophoresis as an endpoint analysis, it is not possible to observe clear differences during this regime.

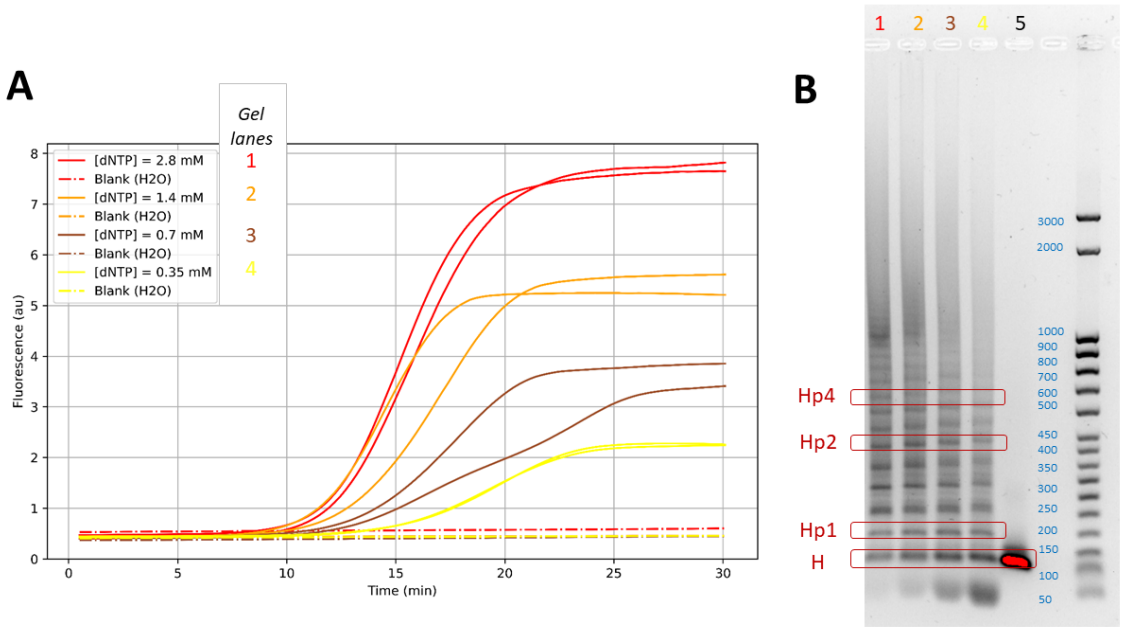

Figure 2.18: (A) Isothermal amplification of 100 pM D1-THR-R with various dNTPs concentration: 2.8 mM, 1.4 mM, 0.7 mM, 0.35 mM. (B) Associated lanes on the gel electrophoresis. Lane number 5 corresponds to the dumbbell only (no amplification)

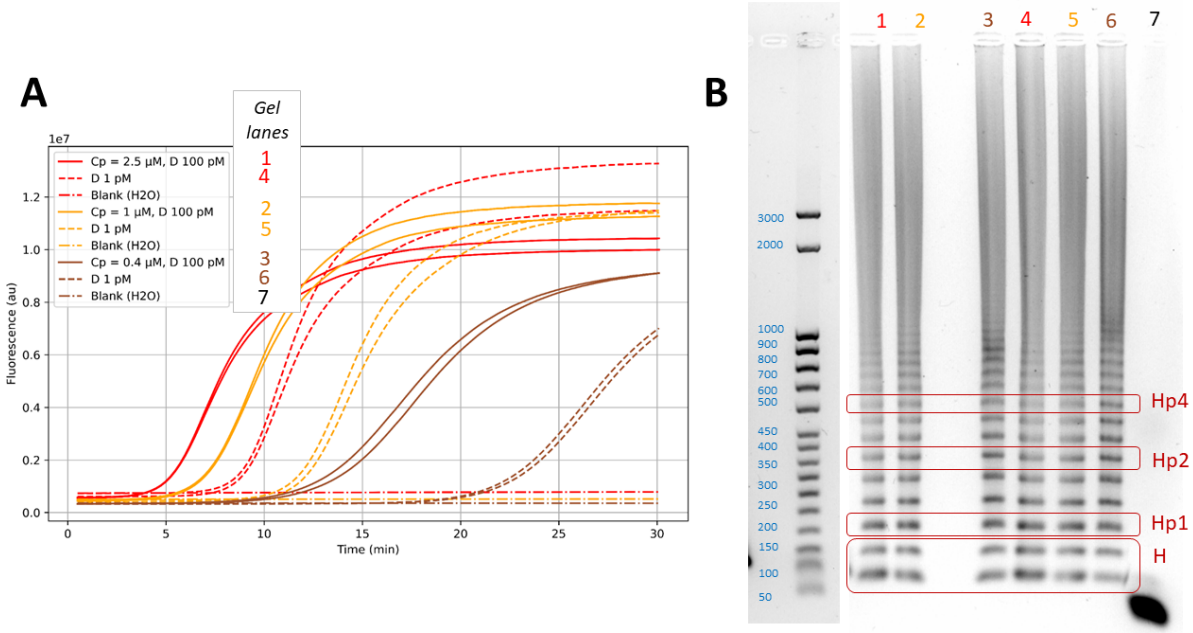

Figure 2.19: (A) Isothermal amplification of 100 pM and 1 pM D1-THR-R with various primer concentrations: 2.5 μM, 1 μM, 0.4 μM. (B) Associated lanes on the gel electrophoresis after LAMP amplification. Lanes 1-3 corresponds to the dumbbell 100 pM concentration, and lanes 4-6 corresponds to the dumbbell 1 pM concentration.

2.4.3 Conclusions

The theoretical model for the kinetics evolution during the isothermal dumbbell exponential amplification was already derived, with the formation of hairpins of increasing lengths 2^n [125]. The observation of the amplicons on gel electrophoresis was a way to investigate the correct description of the hairpins produced. On the gel, we were able to observe and identify only the shortest hairpins formed during the amplification, with increasing length matching the theoretical description for hairpins Hp1, Hp2 and Hp4. However, there are many intermediate bands that are not identified, which leads to difficulties in further analysis. These intermediate bands could represent intermediary products not comprised in the theoretical model, or secondary structures formed during the gel migration and corresponding to double-stranded DNA. The observation of amplicons with sizes larger than 500 bases was not possible since above this length the sample bands were merged, forming a smear. Lastly, there was no difference in the structures formed during the first stage of the LAMP amplification for the two main parameters under study (primers and dNTPs concentrations), but it was possible to observe the dNTPs limited regime which limits the amplification reaction after a cross-over time, but does not influence the formation of the first hairpin structures Hp1 to Hp4.

2.5 Conclusion and perspectives

The original use of LAMP amplification for genome detection was derived into a synthetic oligonucleotide template for signal amplification. From the theoretical description of the LAMP process, we derived a dumbbell structure suitable for isothermal amplification with only two primers. This generic and synthetic structure serves as a molecular biology tool that has the ability to exhibit exponential isothermal amplification. The structure isothermal amplification was experimentally validated on large DNA ranges with excellent correlation coefficient for target quantification. The dumbbell size can be reduced by removing the double stem-loops. The dumbbell can also be enhanced with the addition of synthetic nucleic acids such as aptamers in the sequence, in direct or indirect ways and various positions were studied. The addition in the 5' position seems the most favorable for the structure isothermal amplification. Lastly, in order to understand the creation of hairpins during the LAMP amplification process, LAMP products were deposited on gel electrophoresis and led to the observation of the first hairpins produced. However, due to limitations in the chosen experimental method and in the theoretical model for the evolution of hairpin length we observed additional undefined structures. The first four hairpin of increasing length 2^N were clearly observable, thus validating the first isothermal amplification steps from the initial dumbbell.

The described and engineered dumbbell structure can serve as a signal amplification template based on nucleic acids isothermal amplification. In combination with various molecular probes, such as aptamers or antibodies for example, it can become a tool for various types of assays with exponential signal amplification. The understanding of the amplification process from the dumbbell structure still remains incomplete, with intermediate structures that are not described, and we faced difficulties in finding a proper observation method.

Summary

- Description of the original and minimal dumbbell structure and suitability for isothermal exponential amplification with primers FIP and BIP
- Design of four different dumbbell designs with their associated primers
- Incorporation of aptameric sequences into the dumbbell structure and study of the most favorable position (5' dangling end)
- Generalization of the dumbbell probe incorporating generic nucleic acid sequence that serves as a binding element for various kinds of molecular probes
- Characterization of the hairpins length produced during dumbbell LAMP amplification through gel electrophoresis

Chapter 3

Application for protein detection

Objectives

- The dumbbells structures described in chapter 2 will be applied for different biosensing scenarii
- An aptameroLAMP assay will be described, with an antibody-free quantification method for the thrombin protein
- The limit of the aptameroLAMP methods will be highlighted with the example of troponin high sensitivity sensing
- The integration of the dumbbell structure in immuno-assays will be tested and different methods for coupling the dumbbell structure and antibodies will be described
- ImmunoLAMP protocols will be derived for troponin sensing, combining antibody detection and isothermal LAMP amplification

The quantification of a target present at very low concentration in a complex sample remains currently a challenge. Different techniques have been developed in the past and one of the most commonly used is the ELISA which has been developed in the early 1970s [66]. ELISA provides quantification of a target using a sandwich formed by two antibodies followed by an enzymatic amplification and is widely used for various targets (proteins, biomarkers or even viruses and cells). However, the ELISA techniques are sometimes limited or even ineffective when the target to be detected is present at very low concentrations in the sample. In order to solve this problem, more effective amplification strategies such as DNA probe amplification prove more relevant. Indeed, while enzymatic amplification is linear in time, exponential oligonucleotide amplifications are possible like in the PCR technique. Such amplification methods have been developed as alternative detection methods to ELISA.

The use of nucleic acid amplification as a signal readout is already described in the literature, and particular examples of these methods are immuno-PCR and aptamero-PCR. In immuno-PCR, [75] [126] the enzymatic amplification of the ELISA technique is replaced by DNA amplification. In this case, the secondary antibody is coupled to a nucleic acid sequence, which is then exponentially amplified by PCR. This powerful immuno-detection method combines the specificity and versatility of an ELISA with the exponential signal amplification enabled by PCR. Immuno-PCR is highly specific and quantitative [75] [126] but requires the presence of two target-specific antibodies and the development of a DNA-conjugated antibody, which makes this method complicated and expensive [127]. Aptamero-PCR is also based on the principle of

PCR amplification, but the secondary antibody is replaced by an oligonucleotide containing an aptamer sequence specific to the target to be detected and primer regions required for the PCR amplification [128]. This secondary probe is thus composed of a single oligonucleotide. While relatively uncommon, the high sensitivity of the amplification and the use of aptamers as a substitute for antibodies, make this method very interesting for detecting all types of targets, particularly in complex media [129]. Nonetheless, both immuno-PCR and aptamero-PCR have the drawbacks of PCR amplification, which are the need for temperature cycles and a high sensitivity to inhibitors that may be present in the samples. Thus, different DNA amplification methods have been developed in recent years to replace PCR [130]. Among them, the LAMP, developed in the early 2000s [106], presents the major advantage of being carried out at a constant temperature, typically around 65 °C. LAMP appears to be a promising alternative to PCR as one of the most specific and sensitive methods of all isothermal DNA amplification techniques [106] [130] and proves less sensitive to inhibitors present in biological samples. Furthermore, the isothermal nature of LAMP results in reduced power consumption, simplified temperature management and makes it easier to integrate into a portable device [64] [105].

In the scope of this project and as presented in chapter 2, a dumbbell structure was developed as a generic nucleic acid tool for isothermal amplification (LAMP) with only two primers. This chapter will therefore describe its use in different biomarker sensing scenarii. Various improvements in biological assays embedding isothermal nucleic acids amplification strategies are explored, based on this dumbbell oligonucleotide structure developed.

We will show several examples of protein quantification assays using LAMP amplification as a signal readout method to improve assay sensitivity. Firstly, an example of antibody-free quantification assay based on aptamer sandwich and LAMP amplification is described and named aptameroLAMP, and applied to the thrombin protein as a model protein. For cardiac biomarker assay development, the application of this methodology to troponin is challenging. Therefore, we derived the method with a novel quantification assay combining the dumbbell structure and the use of antibody sandwich, named immuno-LAMP, and exemplified it on complex samples (human plasma). Different methods for coupling the oligonucleotide dumbbell structure with aptamers or antibodies are described.

3.1 Antibody-free detection of thrombin as a model protein : aptamero-LAMP

Several teams have worked on the coupling of aptamer probes and isothermal DNA amplification methods [131], but only a few teams have considered LAMP. Aptamero-LAMP was first theoretically described for the detection of proteins in 2013 [78]. An aptamer (or an antibody) attached to a surface first captures the target. An oligonucleotide containing a second aptamer specific to the target and the necessary primer region for the amplification then forms a sandwich. This secondary oligonucleotide is finally amplified by the conventional LAMP method. Soon after, the team of Yuan developed a method where the aptamer used for the recognition of the mycotoxin ochratoxin A was used as a primer in the LAMP technique [132] [133]. In 2017, Cao et al [118] succeeded in the detection of the Mucin-1 protein which is a biomarker for cancer diagnosis. Magnetic beads coated with streptavidin are incubated with Mucin-1 proteins previously coupled to biotin molecules. In this study, targets are functionalized, this method does not suit for real and complex samples. Two years later, another team developed a microfluidic device enabling the detection of the H1N1 virus responsible for influenza A [134]. The sample containing the viruses is incubated with magnetic beads functionalized by specific aptamers of the virus. After rinsing, the viral RNAs are released following the lysis of the viruses and then

brought into contact with the reagents necessary for RT-LAMP amplification. In this case, the method does not rely on the aptamer probe amplification but on the viral RNA amplification, which cannot be applied to protein detection. More recently, an example of protein detection by an aptamer followed by an original but complex LAMP amplification was described [135]. The method is based on the recognition of thrombin by two aptameric sequences. However, many steps were required between the recognition of the target by the aptamers and the start of amplification. Furthermore, the aptamer probes were not directly amplified, leading to the use of several enzymes.

3.1.1 Thrombin as a model protein

In order to develop a quantification assay combining aptamer sandwich and isothermal dumbbell exponential amplification, we based our methodology on a model protein for a proof-of-concept.

In the very complex biological process of coagulation cascade, thrombin plays a particularly important role in the final stage of the cascade: it transforms fibrinogen in a fibrine network that forms the clot. The thrombin protein is a multifunctional protein with a molecular weigth of 36 kDa and has a high physiological importance. Because of its implication in the coagulation process, thrombin was the very first protein targetted for single stranded DNA aptamer selection [136]. Nowadays, it remains the gold standard protein for the validation of various biosensing strategies using aptamers. Therefore, thrombin appeared to us as a good model protein for a proof-of-concept of aptameroLAMP sensing. This protein presents two exosites I and II, one for the binding of fibrinogen and the other for heparin, which are also the binding sites of 15-mer (Thr1) and 29-mer (Thr2) aptamers, respectively. These two different aptamers binding two distinct sites of the protein have been widely described in the litterature and forms a stable sandwich [137, 63, 138]. The two aptamers have the following sequences :

- Thr1 : 5'- GGTTGGTGTGGTTGG - 3' (15 bases)
- Thr2 : 5'- AGTCCGTGGTAGGGCAGGTTGGGGTGACT - 3' (29 bases)

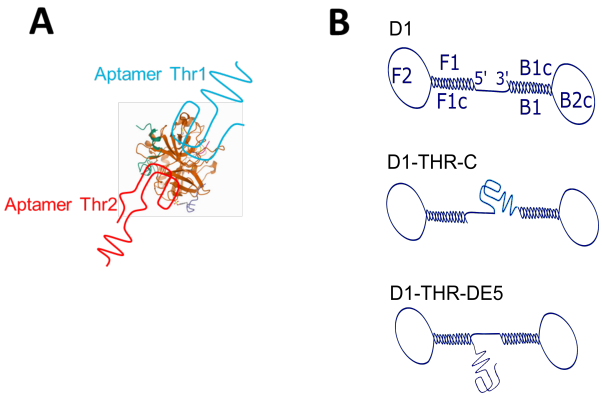

Figure 3.1: (A) Scheme of the thrombin protein and aptamer Thr1 and Thr2 binding. (B) Dumbbell designs for the proof-of-concept aptameroLAMP with thrombin protein. Original dumbbell D1 (no aptamer), dumbbell with central aptamer D1-THR-C and dumbbell with 5' dangling end aptamer D1-THR-DE5.

To develop the aptamero-LAMP method with the use of the previously described dumbbell structure for LAMP amplification, we incorporated the shortest aptamer Thr1 in the dumbbell

structure. As described in chapter 2, we have studied the incorporation of the aptamer at various locations of the dumbbell structure. Two locations appeared to us as promising in terms of aptamer optimal conformation and celerity of amplification: the central position (D1-THR-C) and the 5' dangling end position (D1-THR-DE5) (Fig 3.1). Therefore, both of these dumbbells will be used in the downstream proof-of-concept protocols. Their possible quantification through LAMP amplification has been demonstrated in chapter 2.

3.1.2 Single stranded oligonucleotide model to validate thrombin dumbbell designs

To investigate the feasibility of the developed method to detect an analyte, an oligonucleotide detection assay based on DNA hybridization was first performed. The affinity of the hybridization of a DNA duplex larger than 15 base pairs is sufficient for the sandwich formation to be complete. We thus expected the captured dumbbells will be quantitatively equivalent to the amount of oligonucleotides present in the samples, as soon as the dumbbells quantity is larger than the oligonucleotide probe.

3.1.2.1 Experimental method

The buffer used in this experimental section are the Hybridization Buffer (HB) and the Rinsing Solution (RS) described in appendix B. The detection method is based on a sandwich type detection on magnetic beads with a single-stranded oligonucleotide called Zip6Thr1c as a target (Fig 3.2A). This sequences (appendix A) contains a part Thr1c which is complementary to the Trh1 thrombin aptamer present on the dumbbell, and a Zip6 sequence that is complementary to a Zip6c sequence immobilized on the magnetic beads. All the experiments were performed in 1.5 mL LowBind Eppendord tubes with a working volume of 200 μL. The streptavidin magnetic beads (11205D, InVitrogen) are coated with the Zip6c sequence via a biotin-streptavidin bonding and are blocked with a Phosphate Buffer Saline (PBS) containing 1% BSA. These magnetic beads are used to capture the target sequence Zip6Thr1c at various concentrations from 1 nM to 1 pM for 30 minutes at 37°C with shaking (500 rpm). The concentration of Zip6c sequence grafted on magnetic beads are in excess compared to target concentration in order to have an optimal capture. The magnetic beads are washed three times with RS. Then, the dumbbell was put into contact with the magnetic beads at a concentration of 100 pM for 30 minutes at 37°C with shaking. The magnetic beads are washed again three times with RS and resuspended in HB. A negative control with no target DNA was also performed in parallel. A positive control was performed with the following configuration: the aptamer complementary sequence (Thr1c) is immobilized on the magnetic beads, and the dumbbell is added in the concentration range from 1 pM to 1 nM (Fig 3.2B). All final solution were further amplified with isothermal LAMP amplification protocols as described previously, using 2 μL of the magnetic beads solution and 18 μL of LAMP mix 2 (appendix C).

This methodology was applied to both dumbbells D1-THR-C and D1-THR-DE5 to check the ability of the method to detect oligonucleotide analytes. Both dumbbells contain the thrombin Thr1 aptamer.

3.1.2.2 Results with D1-THR-C and D1-THR-DE5

We performed the experimental procedure described above for the two dumbbells containing the Thr1 aptamer for validation: D1-THR-C and D1-THR-DE5. We analyzed the detection of this model oligonucleotide in a sandwich format along with positive control experiments to confirm the correct dumbbell grafting. Due to the strong hybridization between oligonucleotides and their high melting temperature, we expected the reaction to be complete. The positive control serves as a calibration for the oligonucleotide sandwich assay.

For the positive control, we added different concentrations of dumbbell on the magnetic beads on which the target oligonucleotide was in excess compared to the dumbbell. After 30 minutes incubation we expected the reaction to be complete and removed the unreacted dumbbells. As can be seen in figure 3.3, the T_p values present a linear behavior with respect to the initial concentration of dumbbell, as it was described in the previous chapter for the

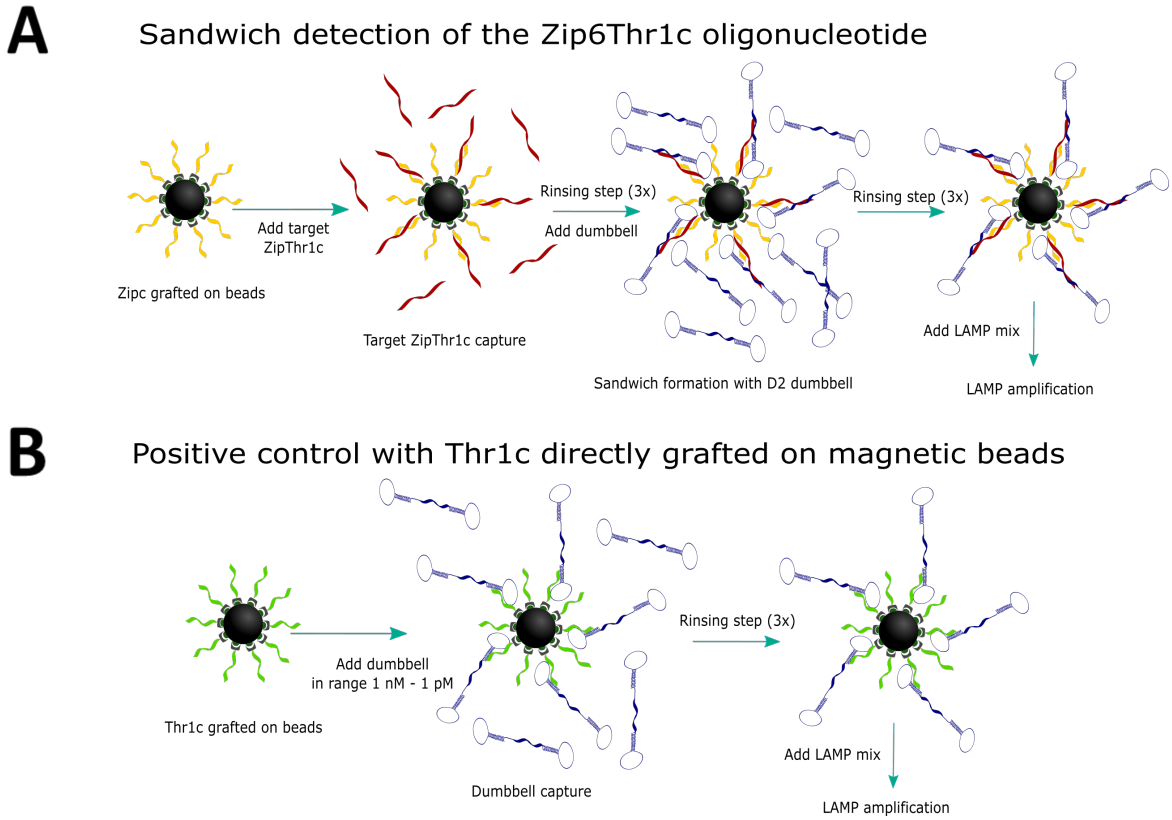

Figure 3.2: Schematic of the experimental protocol for the oligonucleotide sandwich capture and isothermal dumbbell exponential amplification

dumbbell amplification curve and dynamic range. It confirms that the dumbbells have been hybridized to the target grafted on the magnetic beads.

Figure 3.3 shows the different performances of dumbbell D1-THR-C and D1-THR-DE5. Both dumbbell shows linear range for the positive control of dumbbell hybridization on target grafted on magnetic beads (direct detection), and for the sandwich detection of oligonucleotide. Both linear coefficient are excellent (r^2¿0.99), highlighting the performance of this method to quantify the free oligonucleotide in solution. Dumbbell D1-THR-DE seems to show greater performances in terms of celerity of amplification and quantification. For dumbbell D1-THR-DE5, the isothermal amplification reaction is significantly faster, and the sandwich detection quantification range is 100 pM to 10 pM, but the sandwich assay presents an important non-specific signal at around 16 minutes of amplification, therefore limiting the assay LOD to 10 pM. However, the sandwich detection with dumbbell D1-THR-C shows a great improvement in the LOD due to lower non specific absorption of dumbbells. The sandwich assay quantification range is thus improved with D1-THR-C (100 pM - 1 pM)

The experimental procedure for oligonucleotide quantification was tested in complex medium with human plasma samples (from Etablissement Français du Sang (EFS)). The free oligonucleotide was diluted in a plasma sample and added onto the magnetic beads. Figure 3.4 linear response shows the adaptability of this method to detect free oligonucleotide in plasma samples. It is interesting to note that dumbbell D1-THR-C seems to have a higher vulnerability in plasma samples, limited by lower T_p values for the negative control, which limits the lower LOD. Dumbbell D1-THR-DE5 exhibits a quantification range of 1 nM to 10 pM with a limit of

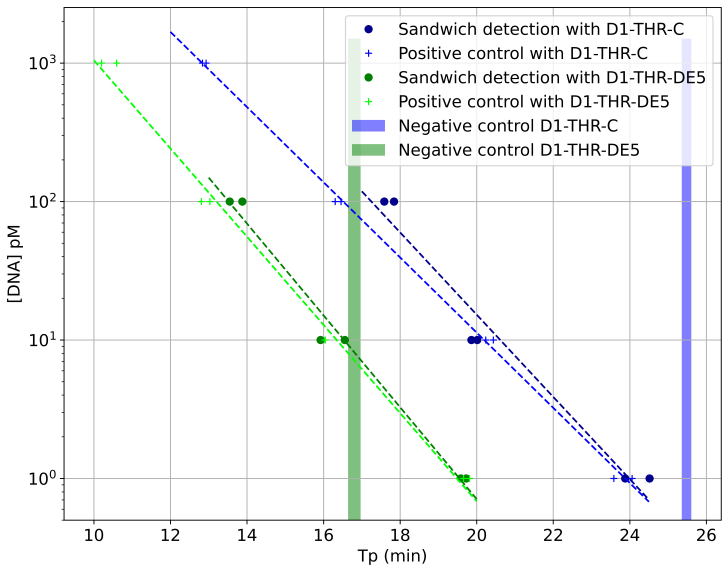

Figure 3.3: Dynamic range for the positive controls and sandwich detection of oligonucleotide Zip6Thr1c: comparison of performances between dumbbells D1-THR-C and D1-THR-DE5 in buffer solution.

detection of 10 pM in plasma. Both dumbbell exhibits longer amplification times for assays in plasma medium.

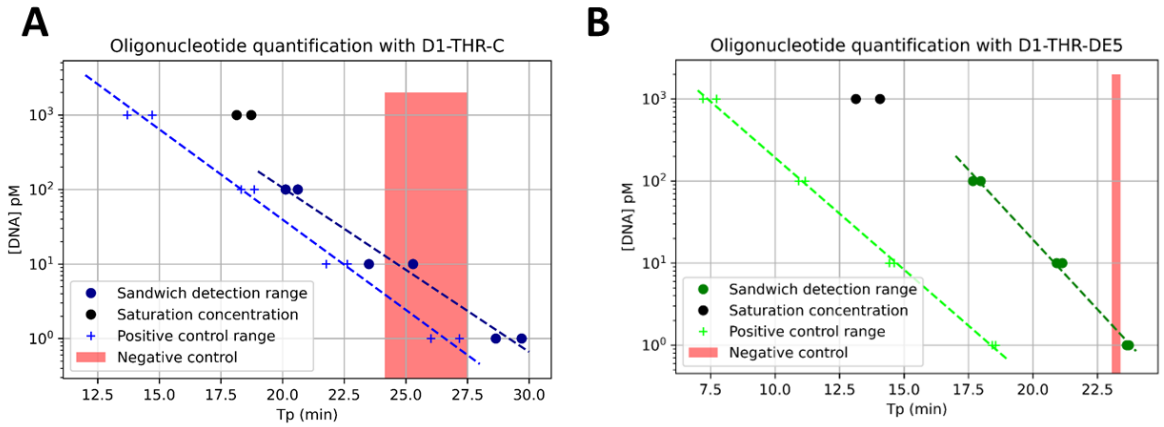

Figure 3.4: Dynamic range for the positive controls and sandwich detection of oligonucleotide Zip6Thr1c in plasma samples. (A) Detection with D1-THR-C and (B) detection with D1-THR-DE5.

This study is a proof of concept of an oligonucleotide quantification assay with our method, including double sandwich and isothermal dumbbell exponential amplification. This was a way to validate both dumbbells containing the Thr1 thrombin aptamers in sandwich assays, and their conformation did not seem to affect the hybridization of oligonucleotides. Both selected dumbbells are functional for oligonucleotide detection, and dumbbell D1-THR-DE5 seems to show greater performances it terms of amplification efficiency and functionality in plasma samples.

3.1.3 Thrombin assay with AptameroLAMP

We have seen in chapter 2 that many different dumbbells constructs containing the thrombin Thr1 aptamer are functional for isothermal exponential amplification, and the previous section validated their use for oligonucleotide detection in a sandwich format.

However, in order to be used for protein recognition, the aptamer inserted in the dumbbell structure needs to exhibit a specific conformation. More specifically, the thrombin aptamer need to adopt a G-quadruplex conformation for favorable thrombin protein recognition [138]. Many of the aptamers positions tested in chapter 2 exhibit too many sterical constraints for the aptamer G-quadruplex structure which might be affected and lead to unfavorable protein recognition. However, the two dumbbells D1-THR-C and D1-THR-DE5 should present a good affinity towards the target protein because of the central or dangling end position of the aptamer, which would allow the aptamer to adopt its G-quadruplex shape and be suitable for protein recognition. Those two dumbbell are already validated for oligonucleotide quantification, and their use for protein quantification will be further studied in this section.

3.1.3.1 Experimental method

First, in order to validate the ability of the dumbbell to properly bind to a protein, we implemented protocols for the direct detection of proteins. To this end, we grafted the thrombin protein directly on magnetic beads with covalent bonding and tested the recognition with the dumbbell. The buffer used all along this study is the Thrombin Aptamer Buffer (THAB) composed of 20 mM Tris-HCl, 120 mM NaCl, 1 mM MgCl2 and 10 mM KCl at pH 7.4 [138]. For the covalent bonding of thrombin on magnetic beads, we used Tosylactivated magnetic beads (14203, Invitrogen). We grafted 10 μg of thrombin protein on 250 μg of magnetic beads. Practically, the protocol consists in adding the protein to the magnetic beads in a coating buffer (0.1 M sodium borate, 3M amonium sulphate) overnight, rinse and block the beads with a PBS buffer containing 0.5% Bovine Serum Albumine (BSA) (step 1, Fig 3.5A). We implemented the direct detection protocols with the dumbbell in the following way: the magnetic beads coated with thrombin were diluted with streptavidin magnetic beads (11205D, InVitrogen) to obtain a ballast and to present different theoretical concentrations of thrombin on beads. The beads were blocked with a solution containing BSA. The dumbbell was diluted to 100 pM in THAB containing 20 μg/mL DNA from salmon testes. For the thrombin aptamer to adopt its G-quadruplex formation favorable for protein recognition, the dumbbell was warmed for 5 minutes at 90°C and let cool down slowly to 25°C. Then, the dumbbell was added to the magnetic beads (step2, Fig 3.5A). After 30 minutes incubation, the solution containing the dumbbell was removed and the magnetic beads were resuspended in THAB. The working volume during these experiments was 200 μL in Eppendorf LowBind tubes. The solution was further amplified with isothermal LAMP amplification protocols as described previously, using 2 μL of the magnetic beads solution with 18 μL of the LAMP mix 2 (appendix C) (step 3, Fig 3.5A). In parallel, amplification of the dumbbell in the range 10 nM to 10 pM was achieved systematically as a dumbbell amplification positive control. A negative control was achieved with only streptavidin magnetic beads presenting no thrombin target on their surface.

Secondly, the sandwich protocols to detect the thrombin protein in a sandwich manner with the aptameroLAMP protocols were tested. The protocols were achieved in microplate wells with a 40 μL working volume. Streptavidin magnetic beads were coated with the Thr2 aptamer through a biotin-streptavidin interaction (step 1, Fig 3.5B). The magnetic beads were then blocked with the buffer THAB, containing 1% BSA. These functionalized magnetic beads were used to capture the target thrombin protein with various concentrations in the range 1 μM to 100 pM, during 30 minutes at room temperature with shaking (step 2, Fig 3.5B). Unbound proteins

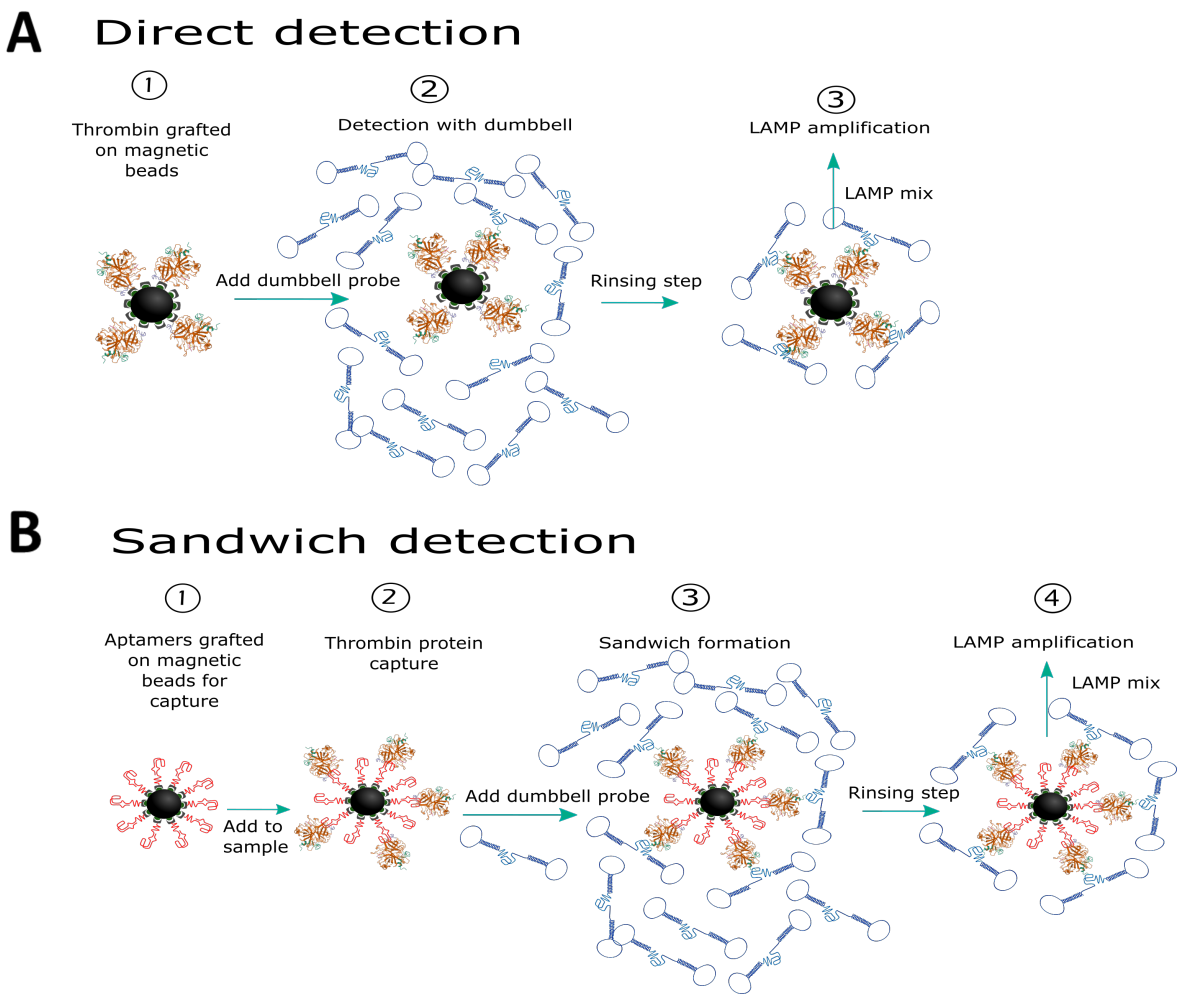

Figure 3.5: Schematic of the protocol for direct and sandwich detections of thrombin protein.

were removed using the magnet. The dumbbell was diluted at 100 pM in THAB, warmed for 5 minutes at 90°C and cooled down slowly to 25°C to adopt its G-quadruplex conformation favorable for protein recognition. This latter was added on the magnetic beads and incubated 30 minutes at room temperature (step 3, Fig 3.5B). Unbound dumbbells were removed through supernatent removal and the magnetic beads were resuspended in the THAB buffer. In parallel, amplification of the dumbbell in the range 10 nM to 10 pM was achieved systematically as a positive control. A negative control with no thrombin target (only buffer) and a specificity control with the γ-thrombin as a non specific target were also achieved systematically. The protocols were tested in buffer medium, and in human serum samples (from EFS). In those experiments with thrombin, serum samples were used instead of plasma, in order to be sure that all the proteins implicated in the coagulation cascade were removed, including thrombin. The solution was further amplified with isothermal LAMP amplification protocols as described previously, with 2 μL of the magnetic beads solution and 18 μL of the LAMP mix 2 (appendix C).

Lastly, in a similar fashion as the dumbbell amplification curve data processing, the data was processed by deriving the time-to-positive value from the QuantStudio software for each condition. Quantification curves are drawn with different analyte concentrations as a function of the time-to-positive (in logarithm scale). For the quantification assay, the highest target

concentration was used as a reference point.

3.1.3.2 Results with D1-THR-C and D1-THR-DE5

First, the dumbbell ability to detect a protein through aptamer recognition and dumbbell isothermal amplification was validated. Figure 3.6 shows the amplification curves for thrombin direct detection, and the quantification curve for different dumbbells (D1-THR-C and D1-THR-DE5). For lower concentrations of functionalized magnetic beads, thus lower concentrations of thrombin target, the amplification curve started later, suggesting that fewer dumbbells recognized the thrombin grafted on the magnetic beads. During the covalent grafting of thrombin on magnetic beads, it was not possible to evaluate experimentally the quantity of thrombin actually grafted. Therefore, only a theoretical computation could be obtained. The direct assay implementation therefore only shows the ability of the dumbbell to actually recognize the thrombin protein grafted on magnetic beads, but no actual quantification is possible. Morevoer, the two dumbbells tested for direct detection are both functional and exhibits similar behavior. With the theoretical estimation of thrombin quantity present on the surface of magnetic beads, it seems reasonable to detest the thrombin from 82 nM to 8.2 nM with such assay (Fig 3.6B).

This method requires the grafting of the target protein on magnetic beads with chemical bonding prior to the assay. Therefore, this methodology is not adapted to the detection of protein free in solution such as in a complex medium for example. However, it was a way to validate the correct thrombin aptamer conformation in the dumbbell structure and suitability to detect protein in a direct assay.

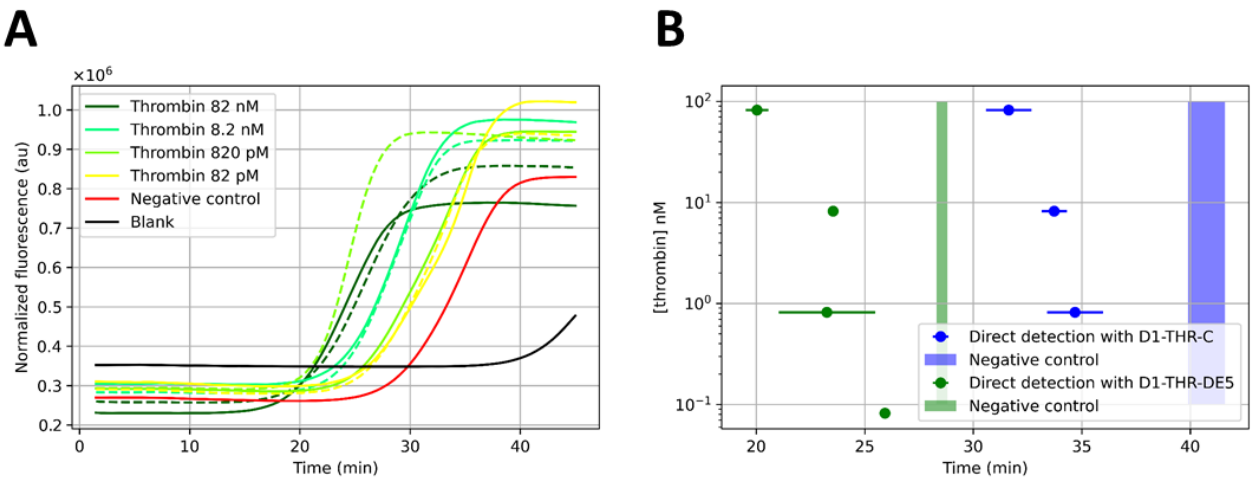

Figure 3.6: Thrombin direct capture (A) Fluorescence data over time for direct capture with dumbbell D1-THR-DE5. The thrombin quantity is estimated from theoretical computations (B). Quantification curves for both dumbbells D1-THR-C and D1-THR-DE5.

After validating the dumbbell ability to bind to a protein target through aptamer recognition, we implemented the methodology for the detection of free-proteins in solution with the sandwich detection protocols. This was a step further towards the detection in complex medium and the proof of the feasability to develop an assay based only on aptamer recognition and isothermal amplification as a detection method. This proof of concept was done mainly using the dumbbell D1-THR-C with the thrombin aptamer in the central position. The results of this study are

further detailed in [123]. This section shows supplementary results with dumbbell D1-THR-DE5 and details of the several optimizations achieved, which led to the final result of thrombin quantification with the aptameroLAMP assay.

We performed the detection of thrombin using double aptamer sandwich format (Fig 3.5B). The thrombin protein was captured on magnetic beads coated with the first aptamer Thr2, and detected with the two tested dumbbells. Many experimental parameters were tested in order to obtain the optimal quantification range. The exposed parameters are detailed in table 3.1, and the optimal parameters found are highlighted in bold.

Type of support	1.5 mL tubes, **96 microplate well**
Reaction volume	200, 50, **40** μL
Reaction medium	Buffer, blood, plasma
Magnetic beads concentration	0.1, 0.5, **1** mg/mL
Dumbbells	D1-THR-C, D1-THR-DE5
Dumbbell concentration	1 nM, **100 pM**
Number of washing steps	**0**, 1
LAMP mix	Enzyme (**mix 2, Bst 2.0**, Mix 3 Bst 3.0)

Table 3.1: Parameters optimized in the thrombin aptameroLAMP assay

As may be seen on the amplification curves in figure 3.7 A, the amplification curves for lower protein concentrations started later than for higher protein concentration. Indeed, for lower protein concentrations, fewer dumbbells forms a stable sandwich with the protein and are further amplified [123]. The quantification curve in figure 3.7 B shows the ability to quantify the free thrombin in solution on three orders of magnitude, from 1 nM to 1 μM, with the dumbbell D1-THR-C associated with the thrombin aptamer located in the central position. Similarly, we tested the detection with the dumbbell associated with the aptamer inserted in the dangling-end position (D1-THR-DE5), which showed similar performances (Fig 3.8). The quantification assay was performed on two order of magnitude from 1 nM to 100 nM. The later assay exhibits a greater difference in Tp values for the successive thrombin concentrations, yielding a finer quantification ($r^2 > 0.99$). Moreover, this dumbbell exhibits a faster amplification, being therefore more appropriate for rapid assay procedures.

In both assays, we tested the specificity of the method with γ-thrombin, the proteolized derivative of α-thrombin, which does not bind to the thrombin aptamers. The standardized Tp values for γ-thrombin are comparable to the one for the negative control with no target protein, thus showing the specificity of the method. Both negative control and γ-thrombin amplification curves show higher values than for α-thrombin 100 pM. These two quantification assays showed the ability of the developed method to quantify free-protein in buffer solutions on several orders of magnitude and with an excellent limit of detection of 100 pM. The main limitation in this assay is the dumbbell quantity binding with the target and its amplification. Indeed, the dumbbell is added in the last step of the protocol and specifically detect the captured protein. However, after this step, there is only one step in which we removed the unbound dumbbell, and there might be some left unbound dumbbells in solution afterwards that get further amplified due to the sensitivity of the LAMP amplification to detect low amoung of DNA in solution. We tried implementing additional rinsing step that did not reduced the non-specific signal, and even altered the quantification since the aptamer-target complex is weakened due to the important thrombin aptamer Dissociation constant (Kd) values. The remaining quantity of dumbbell in solution therefore prevents the method to be used to quantify lower amount of proteins.

This quantification assay was also tested on human serum samples. The serum samples were spiked with different concentrations of target thrombin, and added on the magnetic beads for

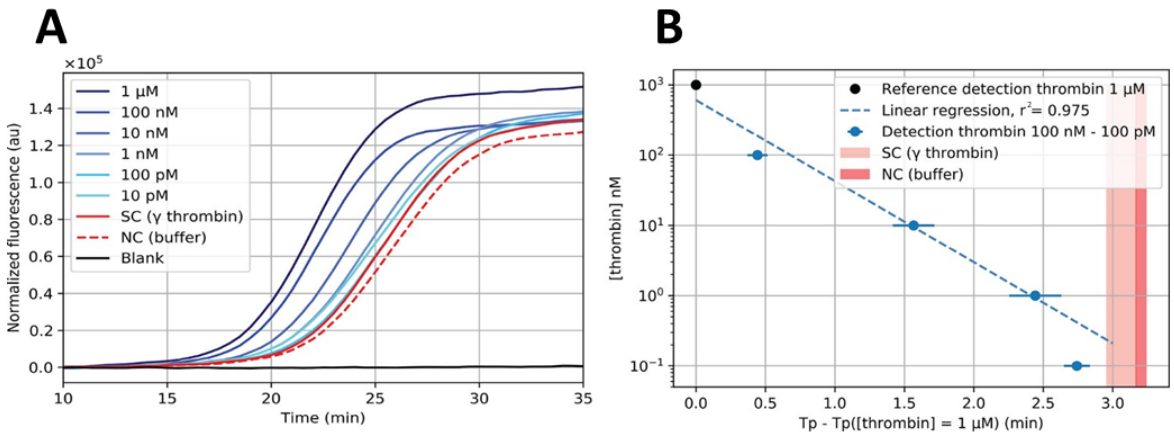

Figure 3.7: Thrombin capture through aptamer sandwich and isothermal dumbbell D1-THR-C exponential amplification [123]. (A) Fluorescence data (arbitrary unit) over time for different concentrations of thrombin targets: 1 μM, 100 nM, 10 nM, 1 nM, 100 pM, and 10 pM. Negative and specificity control are shown in dark and light red, respectively, and blank in black. (B) Dynamic range for experimental replicates standardized with reference to the detection of 1 μM thrombin (black dot). Three experimental replicates as well as two LAMP analytical replicates were achieved for each sample. Limit of detection was 100 pM, and limit of quantification was around 1 nM. Linear fit within the range 1 μM to 1 nM showed a satisfactory regression (dashed line, $r^2 = 0.975$).

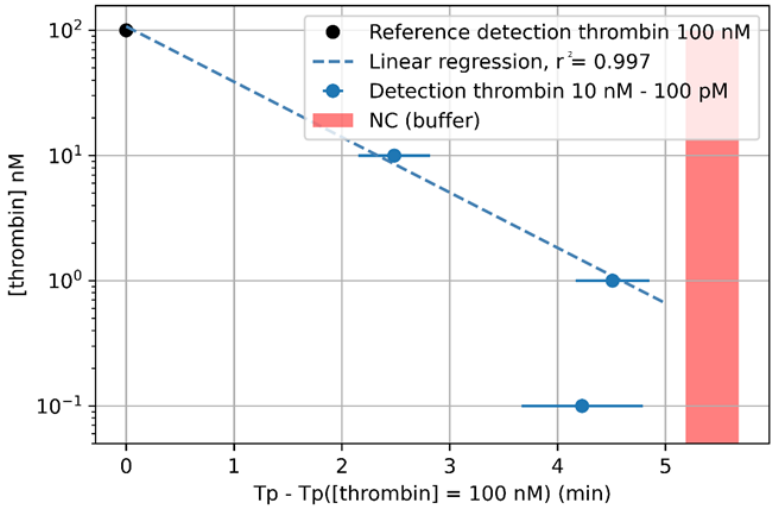

Figure 3.8: Thrombin capture through aptamer sandwich and isothermal dumbbell D1-THR-DE5 exponential amplification. Dynamic range for experimental replicates standardized with reference to the detection of 100 nM thrombin (black dot). Six experimental replicates as well as two LAMP analytical replicates were achieved for each sample. Limit of detection was 100 pM, and limit of quantification was around 1 nM. Linear fit within the range 100 nM to 1 nM showed an excellent regression (dashed line, $r^2 = 0.997$).

capture. In a similar fashion, the detection was tested with the dumbbell D1-THR-C and D1-THR-DE5. Figure 3.9 shows the amplification curves with human serum samples spiked with

thrombin protein. Amplification curves shows lower Tp values for thrombin concentrations 1 μM or 100 nM compared to lower concentrations, but the Tp values for lower concentrations of thrombin are in the same range as the one obtained for the negative control consisting in non-spiked serum. This figure highlights the main limitation of this assay, with aptamers used as capture and recognition in complex samples. Indeed, there are three main points that are limiting the use of this assay for protein quantification in complex samples: (i) the aptamer capture of the protein in the complex sample is not trivial since the complex medium does not exhibit the same conditions as the aptamer selection (pH, salinity). Therefore the capture efficiency is reduced; (ii) during the detection step, the dumbbells might bind to some unwanted molecules present in the complex medium that have previously bound to the magnetic beads, and therefore the remaining dumbbell quantity that is amplified is not specific of the thrombin protein and (iii) after incubation with the aptamer there is only one rinsing step that is performed, and therefore there might be some quantity of dumbbell left in solution, and as we use nucleic acid amplification, a single copy of dumbbell present in solution gets amplified, leading to non-specific amplification. We could not use higher numbers of rinsing steps since the aptamer-protein complex could be weakened.

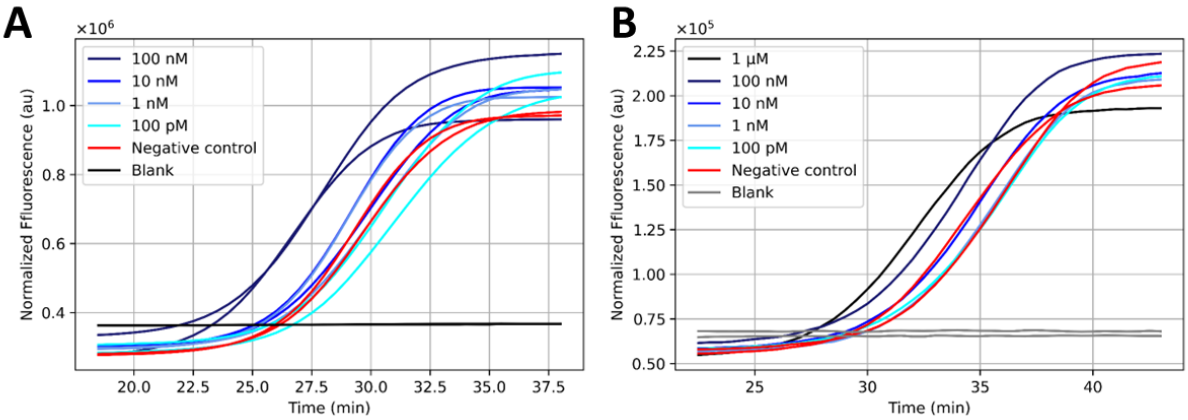

Figure 3.9: Thrombin capture in human serum samples through aptamer sandwich and isothermal dumbbell exponential amplification. Fluorescence data over time for different thrombin concentrations spiked into the serum samples, with dumbbell (A) D1-THR-DE-5 and (B) D1-THR-C. Negative control consists in serum samples.

3.1.4 Conlusions

The developped aptameroLAMP assay showed great performances for the antibody-free detection of the thrombin protein on three orders of magnitude in buffer medium, with a LOD of 100 pM, matching physiological conditions for the thrombin protein [138]. Two dumbbells presenting different aptamer positions were tested, and finer quantification was obtained with DE-THR-DE5 with the aptamer in the dangling-end position, and also shorter amplification times. Notably, both dumbbells are perfectly suitable for protein quantification with this aptameroLAMP assay. The main limitation of this assay lies in the non-specific signal, with non-specific absorption of the dumbbell on the magnetic beads surface. This non-specific absorption is reasonable in buffer medium, giving a LOD of 100 pM. It gets very important when working with complex samples (human serum) since the magnetic beads are exposed to many components presents in the serum to which the dumbbell can bind. This limits the use of the aptameroLAMP assay to medium like buffer.

AptameroLAMP is not limited to thrombin detection. Many aptamers have been described in the literature and selected for the detection of other proteins or biomarkers [139]. Aptamers present similar affinity to antibodies, and thus could be an interesting alternative to replace antibodies [123, 140]. More precisely, aptamers can be produced through chemical synthesis with high yield, whilst antibodies are biologically produced and lead to batch-to-batch variability. The described aptameroLAMP relies on DNA probes. They can be used for DNA sensing and this application is rather straightforward. For protein biomarkers, the application of this method relies on the selection of an aptamer couple binding two different epitopes of the protein target and forming a stable sandwich [141, 142, 143]. Many aptamers have been selected for various biomarkers, but only in some cases like for thrombin, two aptamers bind different epitopes and forms a stable sandwich. If only one aptamer is selected for a biomarker, this latter should be included in the dumbbell whilst another kind of probe needs to be used for capture.

We have demonstrated the proof-of-concept of the aptamero-LAMP assay for the quantification of two types of targets of different chemical nature: DNA and proteins [123]. We have developed an original LAMP amplification of an oligonucleotide dumbbell structure incorporating aptamer: the isothermal dumbbell exponential amplification with only two primers. The proof-of-concept with thrombin protein detection showed great performances with antibody-free quantification on 3 orders of magnitude and a limit of detection of 100 pM. This method is versatile and appears to be a promising method to perform various biomarkers quantification with high specificity and sensitivity [142].

3.2 Detection of troponin

In the scope of cardiac biomarkers sensor developpment, we extended the use of the aptamero-LAMP method to other biomarkers. To this end, we chose the troponin protein, the gold standard biomarker for MI diagnosis.

3.2.1 Specificities of troponin, aptamers and dumbbells

Since the beginning of the 21^{th} century, troponin has emerged as the gold standard biomarker for the diagnosis of myocardial infarction [1, 5]. Nowadays in clinical practices, troponin level measurement represents a common diagnostic procedure. Assessing its level in patient blood with short time and high sensitivity is crucial to rule-in or rule-out patients. Nowadays, most tests for cardiac troponin tests in patient blood are performed using immuno-assays, meeting the need for high sensitivity testing. Many other type of assays have been developed that meet the high sensitivity criterion [1, 144, 145]. Amongst the emerging trends in troponin biosensor developments, the detection of troponin with aptamers raised interest in the scientific community [139, 49] over the past decades and many aptamer biosensors have been described [49]. Several troponin aptamers have been reported in the literature [139]. In 2015, Jo et al [124] described a pool of aptamers against cTnI and evaluated their Kd through SPR imaging. Amongst them, the aptamer Tro4 has the highest binding capacity with a very low Kd in the picomolar range. Tro4 has become the most popular tool for the development of numerous aptasensors, since it was highly reused in other studies [146, 147, 148, 149]. Several other teams also performed various SELEX procedures to describe aptamers against troponin and their further use in biosensors [71] [96] [49]. In 2018, the 72-bases TnI2 aptamer was isolated by Sinha et al [96] with Kd values of 19 nM, and was further used in an ELONA-type assay [98]. The assay describes an integrated microfluidic platform with aptamer capture on magnetic beads and antibody detection, and achieved a limit of detection of 12 ng/L in human serum. In 2021, Cen et al [150] selected two 60 bases aptamers for cTnI named Apt3 and Apt6, with Kd in the nanomolar range. They also exemplified its use in ELONA type assays, and checked cross-reactivity with skeletal TnI, cTnT or Cardiac Troponin C (cTnC). They validated its use with clinical samples and characterized the assay with a dynamic range of 0.05-200 ng/mL. They evaluated the specificity, sensitivity and accuracy of the assay and found values to be higher than for a commercially available antibody-based detection kit [150]. The sequence and conformation of aptamers Tro4 [124], Apt3 and Apt6 [150] are exposed in figure 3.10.

In the method developed in the scope of this project, we originally used the dumbbell structure to incorporate aptamers for biosensing. To this end, we developed generic minimal dumbbells in which any aptamer can be added. As described in chapter 2, the length of the minimal dumbbell structure is roughly between 120 and 150 bases. Therefore, if the aptamer sequence to insert is longer than 30 bases, the dumbbell total length will be higher than 150 bases. As dumbbells are chemically synthesized by standard manufacturers, a maximum length of oligonucleotide is required in order to ensure good synthesis yield. Above 150 bases, standard manufacturers cannot guarantee a good yield, and therefore the dumbbell quantity available will be low.

For the developed troponin assay, we chose an aptamer available in the literature with a rather short sequence length. In the four examples of aptamers described above, Tro4 has the shortest sequence of 40 bases, the lowest dissociation coefficient and has been widely reused in research studies. Therefore, it appears to us as the optimal aptamer for our application with dumbbell isothermal exponential amplification. Moreover, this aptamer was validated in previous work in our team [17] through SPR imaging, and also widely reused in other biosensing applications [146, 147, 148, 149].

In chapter 2, we described two examples of dumbbell structure incorporating the Tro4 ap-

	Tro4	Apt3	Apt6
Conformation	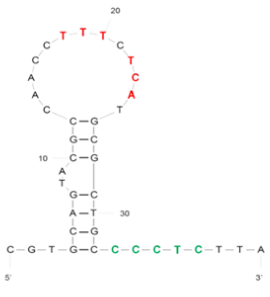	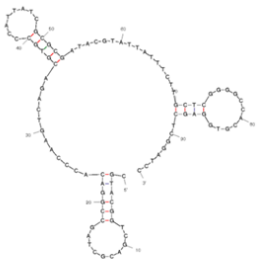	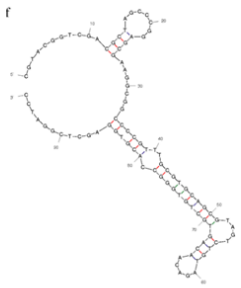
Sequence (5'-3')	CGTGCAGTACGCCAACCTTTCTC ATGCGCTGCCCCTCTTA	CGGACACCCAAGTCAGACGTGCCC ATTATCGCGCGATACGTATTATTTCT TGCTCG GGGC	CCGGAGCGAAGGCGGCCCCGT TTGCGTGCAGCGTAGTCTGTAG ACAACAGTGCTGT GGGC
Kd	270 pM	1 nM	0.68 nM
Reference	*Jo et al 2015*	*Cen et al 2021*	

Figure 3.10: Different troponin aptamers sequence and conformation: Tro4 [124], Apt3 and Apt6 [150]

tamer at various positions, namely D2-TROPO-C and D2-TROPO-DE5. However, despite the fact that we have chosen the shortest aptamer sequence, these dumbbells have a length of 159 and 172 bases respectively. We were able to validate experimentally their isothermal amplification and subsequent quantification, but in the scope of a troponin assay development, the oligonucleotide quantity obtained after chemical synthesis was not sufficient. Moreover, due to their long length, their chemical synthesis was expensive.

To overcome those drawbacks and incorporate the troponin 40-bases aptamer in the dumbbell structure, we used the generic dumbbell structure D1-Zip6-DE described in chapter 2. We designed an oligonucleotide made of the aptamer Tro4 and the complementary sequence Zip6c, in order to hybridize specifically to a part of the dumbbell D1-ZIP6-DE. In this dumbbell, we favorably placed the Zip6 sequence in the dangling-end position in order to facilitate nucleic acids hybridization. Thus, we form a complex between the dumbbell and another oligonucleotide sequence containing the aptamer Tro4. This structure will serve in the implementation of the aptamero-LAMP assay that will be described in the following paragraph.

3.2.2 Single stranded oligonucleotide model

We form a complex with the dumbbell D1-Zip6-DE and an additional oligonucleotide comprising the troponin aptamer Tro4. To investigate the feasibility of the developed complex to detect an analyte, we declined its use on an oligonucleotide model based on DNA hybridization. In the previous section, we already validated the use of the dumbbell structure for oligonucleotide detection in a sandwich format. In this section, as the aptamer is inserted in the sandwich oligonucleotide, we want to check the ability of the complex formed of the dumbbell and the oligonucleotide containing the aptamer to bind to its complementary sequence. With very strong affinity for the hybridization of a DNA duplex larger than 15 bases, we expect the binding reaction to be complete.

3.2.2.1 Experimental method

The buffer used in this experimental section are the HB and the RS described in appendix B. The dumbbell used in this section is the dumbbell D1-Zip6-DE. The linear single stranded oligonucleotide containing the Tro4 aptamer and the Zip6c strand has the following sequence (Zip6cTro4) : 5'- CGCATACCAGGTCGCATACCGGTC TTTTTTTTTT CGTGCAGTACG CCAACCTTTCTCATGCGCTGCCCCTCTTA - 3'. A spacer of 10 thymines is added between the two sequences to allow the aptamer to adopt its conformation independently from the Zip6 strand hybridization. The detection consists in preforming a so called dumbbell-aptamer complex [102], by adding the same quantity (20 nM) of dumbbell and of Zip6c-Tro4 oligonucleotide in the HB. This complex is then diluted in the range 1 nM to 10 fM in HB and the different concentrations are added on the magnetic beads. The working volume is 40 μL in microwell plate and the magnetic beads concentration is 1 mg/mL. The magnetic beads are grafted with different oligonucleotide through the biotin/streptavidin interaction: a) Tro4c oligonucleotide which is complementary to the aptamer Tro4 and should hybridize with the complex structure, and b) a random oligonucleotide (Thr1c) or c) none, for the negative control. In the negative control wells, only the highest concentration (10 nM) of complex is added. The complex and magnetic beads are incubated for 30 minutes and then the unbound complex are removed by washing the magnetic beads three time with 40 μL of RS. The final solution was further amplified with isothermal LAMP amplification protocols as described previously, with 2 μL of the magnetic beads solution and 18 μL of LAMP mix 2 (appendix C). In parallel, amplification of the dumbbell-aptamer complex in the range 10 nM-10 fM was systematically achieved as a positive control.

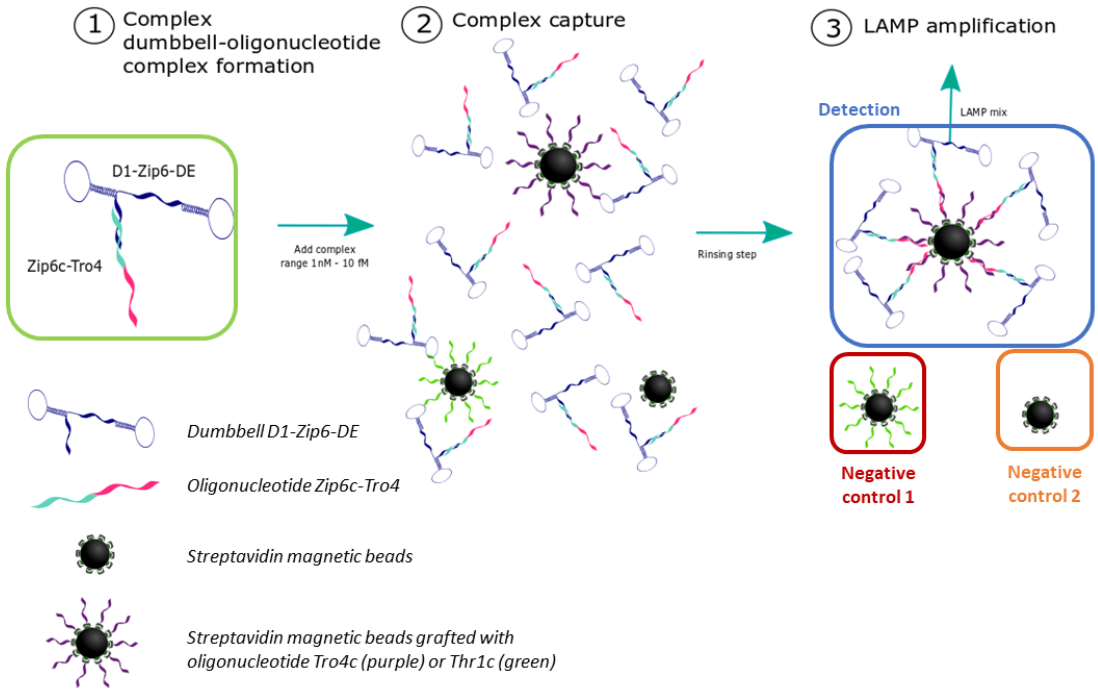

Figure 3.11: Schematic of the experimental protocol for the dumbbell-aptamer oligonucleotide complex capture on magnetic beads

3.2.2.2 Results

Due to the strong hybridization between complementary oligonucleotides and their high melting temperature, we expected the reaction to be complete. Figure 3.12 shows the dynamic range obtained with the dumbbell-aptamer complex hybridized (green curve), and with its binding on magnetic beads (blue curve). The complex formed of dumbbell D1-Zip6-DE and the oligonucleotide Zip6c-Tro4 shows excellent isothermal amplification with primers FIP and BIP, and we obtained a quantification curve in the range 10 nM - 10 pM with excellent correlation coefficient (0.995). Then, its hybridization on magnetic beads is also validated with the amplification of the structure in the range 1 nM to 10 fM with excellent correlation coefficient (0.995). The dynamic range obtained covers 5 orders of magnitude and confirms that the complex has been hybridized to the target grafted on the magnetic beads. Non specific amplification occurs after 25 minutes, limiting for now the limit of detection to 10 fM.

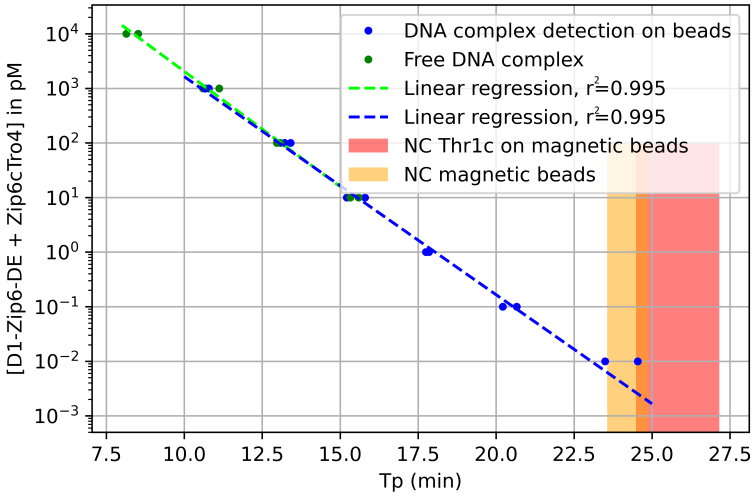

Figure 3.12: Dynamic ranges for the dumbbell-aptamer complex before reaction (green) and its binding on complementary strand on magnetic beads (blue)

This preliminary results shows the ability of the dumbbell-aptamer complex to bind to a complementary oligonucleotide strand immobilized on magnetic beads. After amplification, the comparison between the complex quantity before and after reaction shows that the hybridization reaction is complete.

This way, we validated the dumbbell-aptamer complex isothermal amplification and suitability for oligonucleotide detection. Since this complex contains an aptamer sequence, we will extend its use in protein detection assays through aptamer recognition.

3.2.3 AptameroLAMP

In the context of cardiac troponin sensing and in order to propose an innovative assay different from conventional ELISA detection methods, we tried to use aptamers as an alternative to antibodies. Therefore, we tried to decline the aptameroLAMP method described in the previous section for thrombin sensing. However, as aptamers have been developed over the last decades only, not all molecules present a double aptamer sandwich thoroughly studied and characterized. Our research group working on SPR imaging focuses on the validation of various aptamers, and worked particularly on the characterization and validation of troponin aptamers [17]. The

group tested various troponin aptamers described in the literature [124] and characterized their performances (association and dissociation constant) [17]. However, through this method it was not possible to validate a double aptamer sandwich, and we chose to first capture troponin through an antibody capture and then detect it with different aptamers [17]. The sandwich formation with troponin capture using antibodies and detection with aptamers was validated using SPR [17]. This way, the Tro4 [124] aptamer was validated in conjugation with anti-troponin antibodies (from Medix Biochemica), and showed the best performances amongst the aptamers described by Jo et al in 2015 [124].

In the perspective of testing this aptameroLAMP method on clinical samples (complex medium such as blood or plasma), the troponin capture with antibody is advantageous. Indeed, antibodies present faster association and dissociation rates, which will eventually allow the successful removal of unwanted particles in complex medium, therefore counteracting the cited drawbacks of the aptameroLAMP method. Therefore, antibodies will be used for efficient troponin capture, and aptamers for detection, included in the dumbbell complex for isothermal amplification.

3.2.3.1 Experimental protocols

The chosen troponin capture method in complex samples takes advantage of the versatility offered by magnetic beads to interact strongly with the capture antibody. Differently from the grafting of aptamers on magnetic beads exposed in the previous section, we chose a covalent link to bind capture antibodies on the magnetic beads. The chosen magnetic beads are the 1 μm size Tosylactivated magnetic beads (MyOne, InVitrogen, cat 65501) and present p-toluene-sulfonyl group (Tosyl) on their surface that will covalently bind to primary amine (NH_2) or sulphydril (SH) group. We immobilize anti-troponin capture antibody 9701 (100129 from Medix Biochehmica, lot 20000399) with the recommended coating protocol provided by the manufacturer. The immobilization protocol can be found in appendix D. The coupled magnetic beads and capture antibody was checked using a colorimetric ELISA reaction with anti-mouse HRP antibodies, and anti-rabbit HRP antibodies as a negative control. The magnetic beads are stored in the Magnetic beads storage buffer (MB) and stable for one year at +4°C.

The assay working volume was 50 μL in 96 well microplate. The troponin protein standards were obtained from HyTest (cat 8T53) and diluted in Troponin Aptamer Buffer (TAB) in the range 10 nM to 1 pM. A selectivity control is performed with Skeletal Troponin I (skTnI), a commonly used protein produced in the skeletal muscles for negative control of cardiac cTnI specific antibodies. The troponin standards (10 nM - 1 pM) are added, as well as the negative control composed of skTnI and TAB are added to the antibody-coated magnetic beads at 0.05 mg/mL. The incubation lasts 30 minutes with mixing, and the solution is washed three times with Washing Buffer (WB). The detection complex composed of an oligonucleotide strand (containing Tro4) hybridized to the D1-Zip6-DE dumbbell is achieved using the following procedure: 1 μM of each oligonucleotides (D1-Zip6-DE and Zip6c-Tro4) are added into TAB supplemented with 300 mM NaCl, and the solution is warmed at 50°C and cooled down to Room Temperature (RT). The hybridized product is subsequently diluted in TAB down to the concentration of 1 nM. This detection complex is then incubated 30 minutes with the troponin captured on the magnetic beads and after the incubation, the solution is placed above a magnet to remove unbound detection complex (Fig 3.13). Finally, the magnetic beads are resuspended in TAB and 2 μL are withdrawn and added to 18 μL of LAMP mixture containing the primers FIP and BIP for isothermal exponential amplification (mix 2 appendix C). The samples are placed for one hour on the Quant Studio device with warming at 65°C and fluorescence data is recorded every 30 seconds.

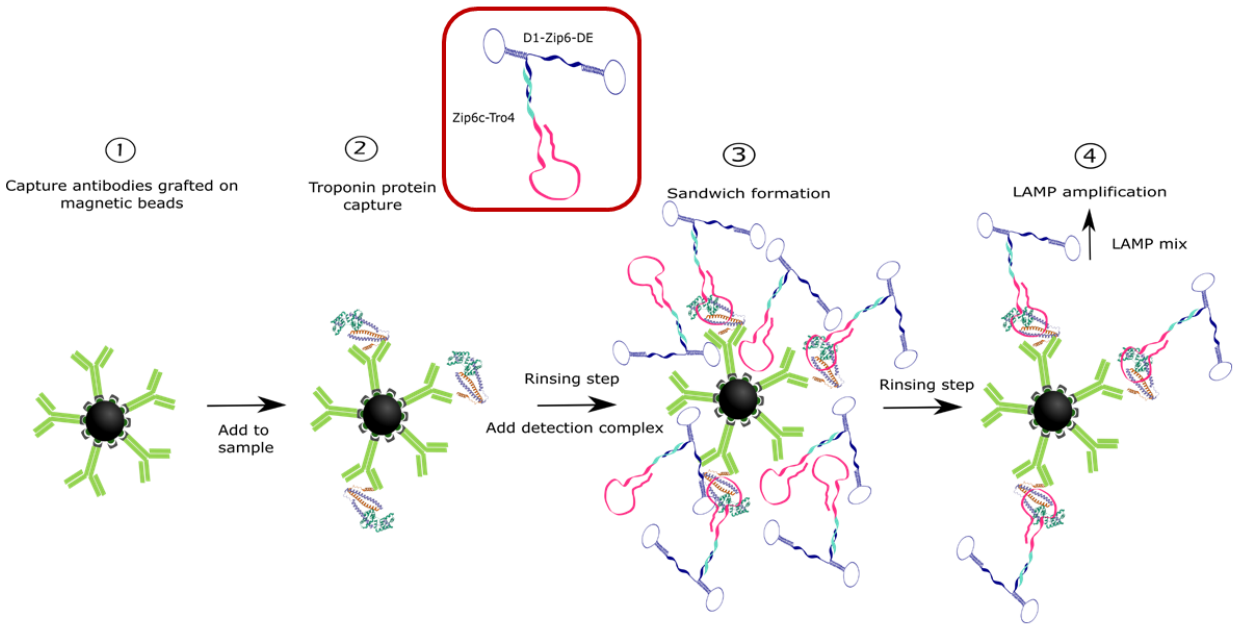

Figure 3.13: Schematic of the aptaLAMP protocol for troponin detection

3.2.3.2 Results

The antibodies grafted on the magnetic beads should ensure an efficient troponin capture. The use of antibodies allows us to carry out several washing steps after the troponin capture, in order to ensure the correct removal of non-relevant molecules present in the medium, thus reducing non-specific binding. The pre-formation of the detection complex made of the dumbbell D1-Zip6-DE and the oligonucleotide strand with the Tro4 aptamer, in a buffer containing an important concentration of salt (300 mM NaCl) with warming and slow cooling down, should ensure a correct complex formation through DNA hybridization. This complex formation, its isothermal amplification and its utility in DNA sensing protocols was already demonstrated in the previous section (3.2.2). The troponin Tro4 aptamer should also adopt its optimal hairpin conformation for protein recognition with this detection complex formation protocol (warming, salty buffer). The quantity of detection complex added on the troponin captured on the magnetic beads was 1 nM. Considering the aptamer dissociation coefficient in the nanomolar range, the absolule quantification of troponin with this protocol should be possible only above the concentration of 1 nM of troponin.

The curves of fluorescence over time presented in figure 3.14 shows that the quantification of troponin is not trivial with this modified aptameroLAMP method, and we can derive several information from these results. First, the Tp values derived from the amplification curve are very close in time from each other. Some values differ from less than 30 seconds of difference, which is below the acquisition period Tp (30 seconds) of the instrument used. Therefore, the absolute quantification seems difficult from the isothermal amplification curves. Second, in both experimental replicates achieved with this method, the quantification of troponin seems possible for the two highest concentrations of 10 nM and 1 nM. However, for lower concentrations, the amplification curves are similar to the curve corresponding to the non-specific signal. Indeed, in the last step of the protocol used, only one rinsing step is used to removed the unbound

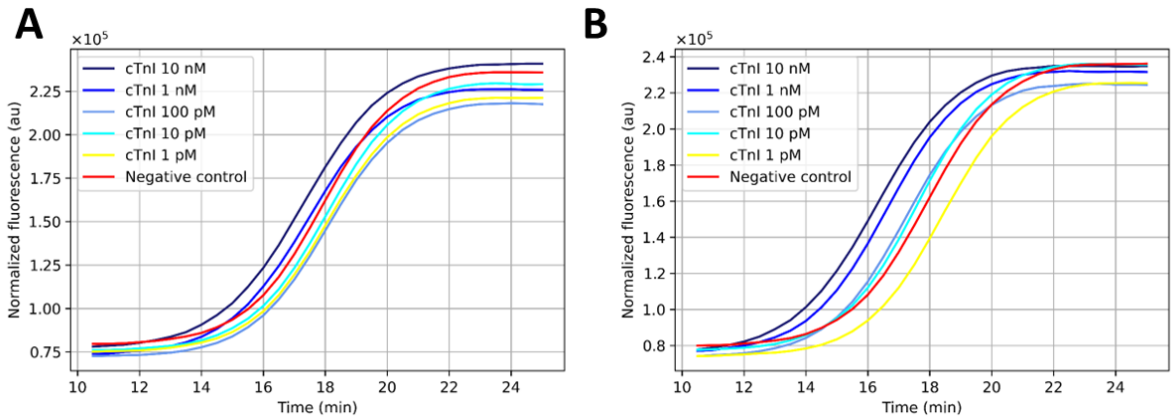

Figure 3.14: Amplification curve with fluorescence data over time for troponin aptameroLAMP sensing (A) Experimental replicate 1 and (B) Experimental replicate 2.

dumbbells from the magnetic beads, in order to limit the dissociation of the detection complex from the troponin. Therefore, there might be some dumbbells left in the solution which gets further amplified limiting the quantification of troponin for low concentrations.

3.2.4 Conclusions

The implementation of the aptameroLAMP assay on other molecules than thrombin which served as a model protein in section 3.1 is not trivial. We have implemented similar protocols as for the detection of thrombin, but since no aptamer sandwich has been thoroughly validated for the troponin protein, we used antibodies to capture troponin on magnetic beads. The troponin captured was then detected with a detection complex formed of an oligonucleotide strand containing the Tro4 aptamer in its correct conformation hybridized to the generic dumbbell structure D1-Zip6-DE. This chosen dumbbell strand is generic so it could bind to any other oligonucleotide strand containing other aptamers for example. The versatility of this new method is then improved compared to the full aptameroLAMP assay described in section 3.1, for which specific dumbbell had to be designed for the desired target. With this new generic dumbbell, only a new short linear oligonucleotide strand has to be designed for a new target. This generic dumbbell also provides us with signal exponential amplification. For the case of troponin sensing with this adapted aptameroLAMP method, it was possible to quantify troponin down to the concentration of 1 nM, as shown in figure 3.14 B. However, there are two main limitations that are hampering the use of this assay in the specific case of troponin sensing. First, the LOD achieved is in the nanomolar range, which is way higher than the troponin basal concentration in patient blood. The LOD is limited mainly by the use of the aptamer Tro4 which has a Kd value in the nanomolar range. Moreover, the implementation of this assay was only achieved in a buffer medium, and the negative signal is already quite important. Therefore, we can think that its implementation in complex medium such as blood or plasma will be difficult, since many other molecules present in those medium could lead to even higher non-specific signals. The results of the implementation of the aptameroLAMP method with thrombin exposed in section 3.1 shows that the quantification of thrombin is difficult in plasma samples, and restricted to the nanomolar range. Therefore, this comforts us in the fact that this method is limited to buffer or rather simple medium, and also mainly restrained by the aptamer-target dissociation constant Kd often in the nanomolar range, thus limiting the use of the assay for high sensitivity sensing.

The use of aptamers is limited with this method in complex medium (blood, plasma), and the high sensitivity required in troponin sensing assays requires to lower the LOD compared to what was already obtained with the aptameroLAMP examples exposed since the beginging of this chapter. Therefore, the next section will expose an innovative detection methodology that stills takes advantage of the signal exponential amplification given by the dumbbell LAMP amplification, but also takes advantage of specificities offered by antibodies to reach high sensitivity sensing.

3.3 Detection of troponin combining antibodies and isothermal dumbbell exponential amplification: ImmunoLAMP

The use of aptamers combined with nucleic acids amplification have been described as an innovative antibody-free detection method, but presents several limitations, mainly in terms of biosensors limit of detection. In order to keep the sensitivity given by the nucleic acid amplification, we design innovative protocols based on antibody sandwich, for their specificity and high affinity.

3.3.1 State of the Art

Very few examples of assays combining antibodies and LAMP amplification have been described in the literature. ImmunoPCR and ImmunoLAMP are ultrasensitive methods combining the versatility of ELISA with the exponential amplification capacity of nucleic acids amplification [72]. The coupling of the detection antibody and the reporter DNA is a critical step of these assays, and will be thoroughly detailed in this section.

3.3.1.1 Detection protocols including antibody and oligonucleotide for nucleic acid amplification

A search in Scopus in April 2023 with the term 'Immuno LAMP' gave only 78 results. On the contrary, a search in Scopus with the term 'Immuno PCR' gave 3021 results.

Immuno-PCR was first described in 1992 [126]: in this approach the second antibody is coupled with an oligonucleotide which is exponentially amplified by PCR. This powerful method combines the specificity of ELISA tests with the exponential signal amplification offered by the PCR. It shows a greater sensitivity than conventional immunoassays (approximately 10^5 times lower). It is applicable to the detection of various biomarkers, and several examples can be shown in the literature. In 2014, Sadhasivam et al [76] showed an example of ImmunoPCR method on carbon nanotubes and applied on breast cancer marker, with an achieved sensitivity of 0.01 U/mL (Fig 3.15A). In 2015, Yang et al [74] implemented a competitive immune reaction directly on the PCR tube walls to detect polychlorinated biphenyls. Gold nanopoarticles are modified with detection antibody, capture and signal DNA, and are fixed to the PCR tube walls through a competitive immuno-reaction (Fig 3.15B). The signal DNA is released from the nanoparticles and used as a template for real-time PCR. A detection limit of a few pg/mL was obtained showing the potential of this method for sensitive detection. In 2018, Singh et al [73] described a magnetic bead-coupled gold nanoparticle-based immunoPCR assay for the detection of Myobacterium tuberculosis (Fig 3.15C). The detection methodology is similar to Yang et al. in 2015, and takes advantage of nanoparticles and capture and signal DNA, and the detection limit achieved was of a few fg/mL, 10^5 times lower than analogous ELISA. Lastly, in 2022, a magneto-fluidic immunoPCR for COVID-19 detection was described [75] for serological testing (Fig 3.15D). They propose a fully integrated and portable platform for magnetofluidic

immunoPCR giving results in 30 minutes. Their LOD was 21 pg/mL and they achieved very good sensitivity and specificity with a rapid point of care testing method.

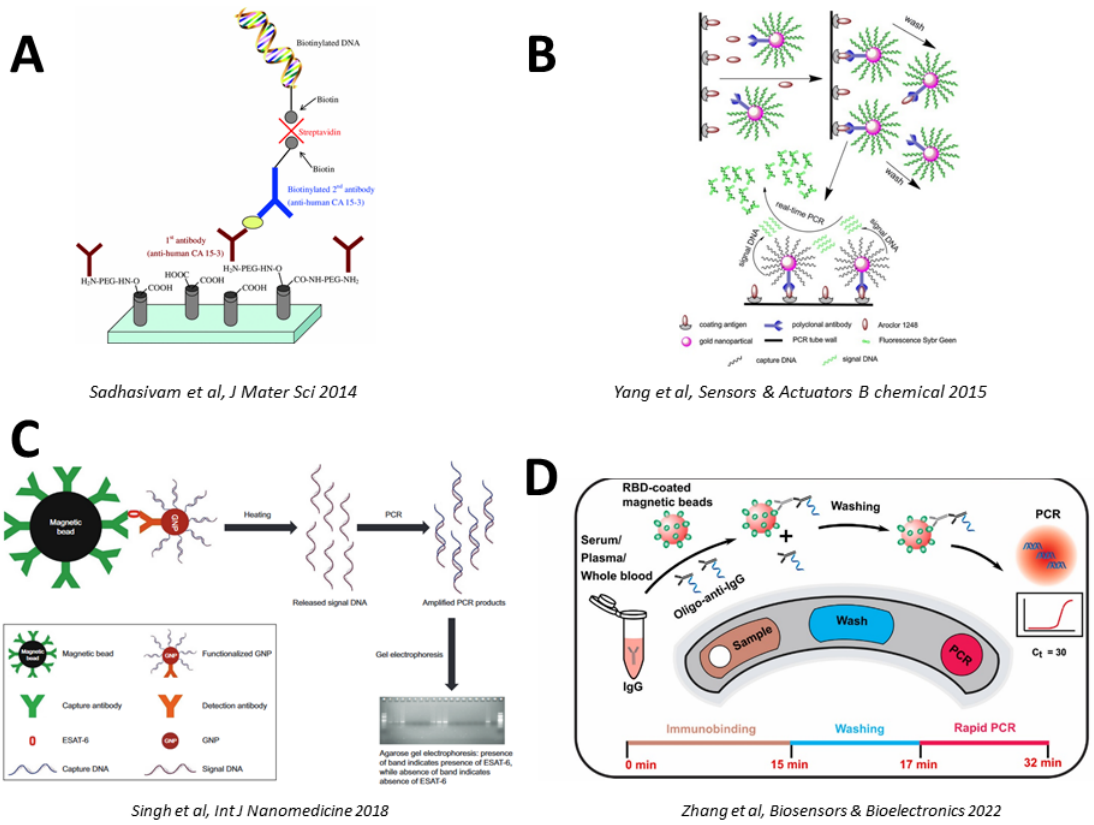

Figure 3.15: Examples of ImmunoPCR biosensors: (A). Detection of breast cancer market [76]. (B) Detection of polychlorinated biphenyls [74]. (C) Detection of myobacterium tuberculosis [73]. (D) Detection of COVID-19 antibodies [75].

ThermoFischer commercializes an immunoassay combining antibody capture and PCR amplification [69]. It uses proximity ligation assay (PLA) technology to combine antigen-antibody recognition with qPCR signal amplification. When the two antibody conjugates binds to the protein target, the 3' and 5' oligonucleotides of those conjugates come into proximity, bind to the complementary oligonucletoide and subsequently join each other with DNA ligase. After that, 95°C heat inactivation denatures the ligase antibodies and release a 100 base strands that serves as a template for subsequent PCR amplification (Fig 3.16). This strand quantity is proportionnal to the level of analyte originally bound by the antibodies. ThermoFischer developped a Human Troponin Immunoassay kit based on this technology with an analytical sensitivity below 0.3 pg/mL, a very wide dynamic range (0.32 - 25 000 pg/mL), and low sample consumption (few µL).

In a similar fashion as immunoPCR detection methods, immunoLAMP methods can similarly be developped. In 2013, the first iLAMP techniques were theoretically described [78] in regards to product analysis with different nanoprobes (Fig 3.17A). The potential of combining immunorecognition and LAMP amplification in an iLAMP assay was highlighted for different application cases such as low concentration proteins, non-immunogenic proteins, rare cells or non protein small molecules.

In 2016, an immunoassay based on the RT-LAMP technique was described for the detection

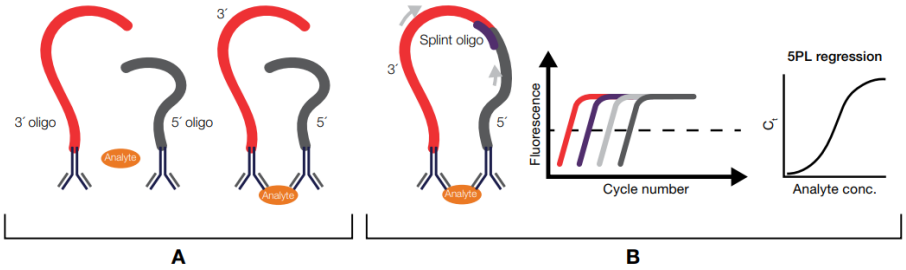

Figure 3.16: Principle of the ProQuantum Assay (ThermoFischer) [69]

of Influenza A virus subtype H5N1 (H5N1) viremia in blood samples with one pot detection [90]. The method uses virus capture with antibody coated directly on PCR tubes, followed by virus thermal lysis and RNA release for LAMP amplification of the genome (Fig 3.17C). In 2017, Cao et al described a magnetic Immuno-Loop Mediated Isothermal Amplification [118] called Im-LAMP for the ultrasensitive detection of P-glycoprotein. In this assay, the target is capture on antibody coated magnetic beads and detected with antibody DNA liposome. After sandwich formation, DNA template is released from liposomes and initiate the ImLAMP reaction, generating rapidly a fluorescence signal ((Fig 3.17N). They achieved a very low detection limit of 5 fg/mL which is substantially better than conventional ELISA assays.

It is important to note that in both of these assays, there is a step preceding the LAMP amplification to release DNA template, either through lysis of the catched virus, or through released in liposomes.

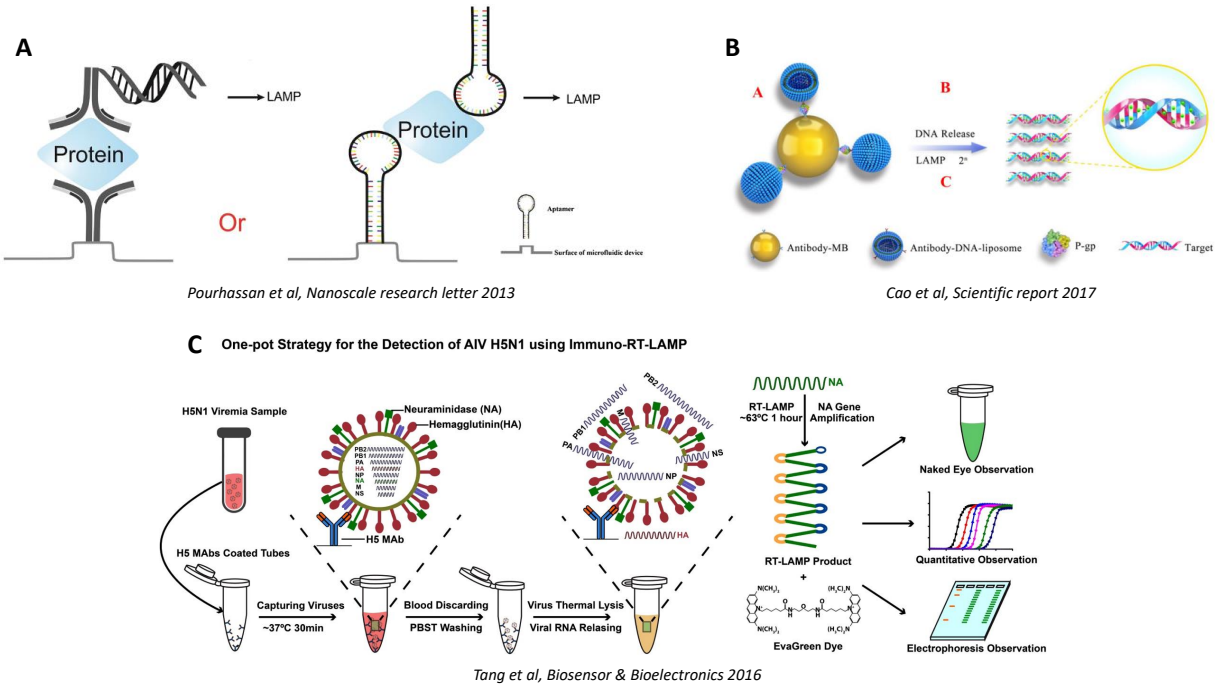

Figure 3.17: Examples of ImmunoLAMP biosensors: (A). Theoretical description of iLAMP and aptamer-iLAMP sensing [78]. (B) Detection of P-glycoprotein through magnetic Immuno-Loop Mediated Isothermal Amplification [118] (C) Detection of H5N1 virus [90].

There are numerous examples of immunoPCR detection methods for various biological analytes detection. However, immunoLAMP detection examples are fewer in the scientific literature. Only a few teams have successfully described and combined antibodies with LAMP amplification [118, 90], and in most cases, there is a step preceding the LAMP amplification to release DNA template, either through lysis of the catched virus, or through release in liposomes. LAMP is a powerful nucleic acid amplification technique that shows great promises in the diagnostic fields, mainly with its low non specific amplification and its reduced sensitivity to inhibitors in the sample, and its isothermal characteristics. Due to its recent discovery only few examples of integration of LAMP nucleic acids amplification technique as a signal amplification in immunoassays have been described [72]. The few examples of biosensors combining immuno-recognition and PCR amplification shows great performances [76, 74, 73, 75]for various biological species, and we have reasons to think that similar biosensors using LAMP amplification for signal readout would also give very good performances. Therefore, we would like to develop an innovative immuno-LAMP detection method, and we challenge ourselves with the example of troponin sensing. Troponin appears as a key molecule in the scope of this PhD project in general, but also as a challenging biomarker since high sensitivity sensing down to the picomolar level is required to get clinical valuable information. For troponin detection, there is no immunoLAMP assays described to date.

3.3.1.2 Different methods for coupling antibody and oligonucleotide

In order to use nucleic acid amplifications techniques for signal readout in immunoassays, a DNA strand needs to be introduced in the assay biological reagents. More precisely, the DNA strand that will serve as a template DNA for the amplification needs to be linked to the detection antibody. Producing antibody-DNA conjugates is a biochemistry labor, and there are many research going on in this field, but many are focused on protein-DNA conjugation strategies for therapeutic purposes [127]. Fewer scientific literature is available for coupling proteins and oligonucleotides for diagnostic purposes [127]. In the review written by Dugal-Tessier in 2021 [127], a summary of the key technological advancements in the preparation of antibody-oligonucleotide conjugates (AOCs) is given, with advantages and disadvantages of each method. Conjugation of antibodies to various other molecules is commonly achieved in different therapeutic projects. In most cases, the binding is direct (chemical bonding), but with oligonucleotides, more conjugation methods are available compared to typical small molecules. There are four main ways to link antibody and oligonucleotides: ionic interactions (figure 3.18A), affinity binding (figure 3.18B), direct conjugation (figure 3.18C) and utilization of the double-strand as a conjugation moiety (figure 3.18D). Examples of use of these conjugation strategies in biosensors will be detailed in this paragraph, along with the advantages and disadvantages of each method.

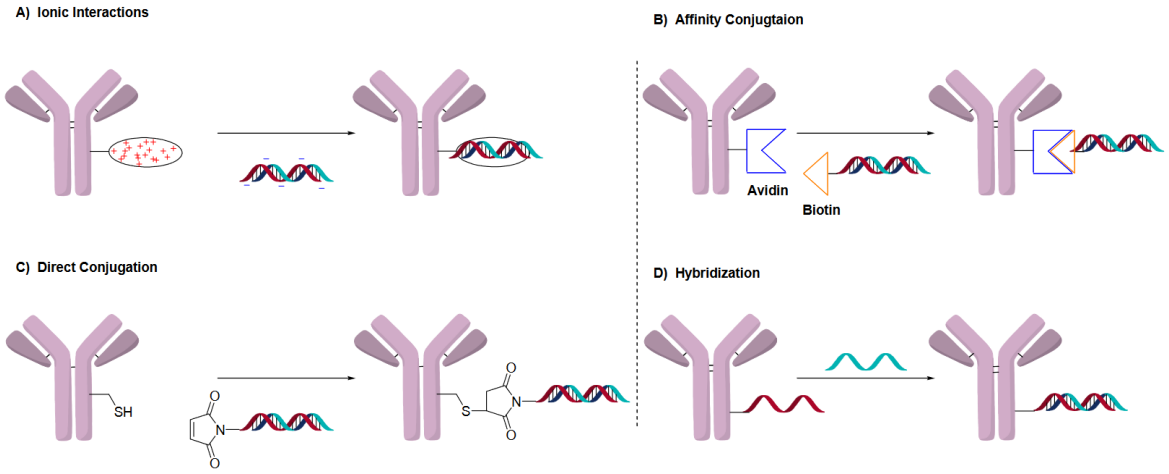

Figure 3.18: General methods to conjugate oligonucleotides and antibodies by (A) electrostatic interaction, (B) affinity between biotin and avidin, (C) directly to antibody and (D) using double strand hybridization [127]

Preparing antibody-oligonucleotide conjugate (AOC) presents several challenges, specially in comparison with more common antibody-drug conjugates used in therapeutics. The Molecular Weigth (MW) of oligonucleotide strands can be greater than 10 kDa, therefore influencing the physical and chemical properties of the conjugated antibody. Oligonucleotides are negatively charged, and their conjugation to antibodies changes the overall charge of the antibody, leading to difficulties in their analysis and characterization. The AOC conjugate behaves both like an antibody and an oligonucleotide, leading to challenges in its purification and analytics [127]. There is a need for novel approaches for the purification and characterization of AOCs. Several examples of the use of these conjugation strategies and their use in biosensors already exists and are summarized in table 3.2.

The different AOC strategies present various interests and application cases. Ionic interaction is simple and flexible, but is a reversible interaction unstable over changes in pH or

Conjugation method	Example of biosensor	Target and LOD	Advantages	Disadvantages
Ionic	Gene silencing		Simplicity, flexibility	Reversible interaction, unstable conjugate (salt, pH), determination of OAR
Affinity	[76]	Breast cancer markers 0.001 U/mL	In vivo stability, resistance, strong bonding	Antibody and DNA chemical modification, hybrid method (not general)
Direct	[75]	Covid-19 serological test 1 ng/mL	Linker versatility, linker size (less impact, on the conjugate), various conjugation chemistry	Purification and characterization steps, determination of OAR
Hybridization conjugation	[74]	polychlorinated biphenyls pg/mL	Versatility, rate and specificity of the hybridization	Length of the DNA (stability, secondary structures), linker payload cost

Table 3.2: The four main antibody-oligonucleotide conjugation strategies, with examples of biosensors if so, and pros and cons

temperature. This conjugation strategy is mainly used in gene silencing protocols, but its reversibility aspect makes it less attractive for use in diagnostic. The affinity conjugation method exhibits a great stability with a strong binding, but requires the chemical modification of both antibody and oligonucleotide with either biotin or streptavidin. Lastly, the direct and indirect conjugation strategies using chemical linkers are versatile, and there are many choices of linker in the literature [127]. The addition of the small linker show less impact on the conjugate than for example conjugation through the streptavidin molecule. However, both of these methods require purification and characterization steps that are not always easy to implement, as well as the determination of the oligonucleotide to antibody ratio (OAR) which is not trivial. The following paragraph will exemplify the use of direct conjugation strategies in biosensors and analyze their methods and final results.

As AOC have gained importance in diagnostic procedures, many conjugation strategies have been presented in the literature and used in biosensors. The main challenges remaining in this field to transfer the signal readout from the protein to the DNA level are the improvement of the low coupling yield, and the setup of efficient purification methods. In 2012, Bombera et al. [151] proposed a DNA-based biochip for cell-type analysis in a label-free manner. The DNA-array is converted into antibody-array using antibody-DNA conjugates. The protein-DNA hybrid molecules are chemically synthesized with maleimide activation and covalent coupling of short oligonucleotides to antibodies directed against cell-type specific markers. In 2019, Li and Moellering [152] described a "plug-and-play" antibody conjugation method with succinimidyl functionalized oligonucleotides Disuccinimidyl suberate (DSS). The oligonucleotides can be prepared under a large scale format and long-term stored for high quantity coupling. Wiener et al. described in 2020 [153] a preparation method for single and double oligonucleotide conjugates using a non-site directed antibody conjugation technique relying on copper-free click chemistry. They combined it with ion-exchange chromatography to obtain purified single and double coupled antibodies with oligonucleotides. They reached a total conjugation yield of 30 %, and evaluated the influence of several experimental parameters such as the crosslinker, reaction temperature, duration, oligonucleotide length and secondary structures. In 2022, Baranda Pelle-

joro et al [154] described a DNA-template chemical reaction by employing two DNA-antibody conjugates that represents two individual systems responsive to human serum albumin and human IgG. To synthesized the DNA-antibody conjugate, they used a low-density lipoprotein receptor (LDLR) reagent for site-directed labeling reaction that preferentially target the hinge region of the antibody to insert an azide handle [154]. The azide-labeled antibody is then added to dibenzocyclooctyne (DBCO)-modifiedDNA sequence. The AOC construct is obtained after strain-promoted azide-alkyne cycloaddition (SPAAC) reaction, and the mono-labelled conjugate was isolated via purification through anion exchange chromatography using salt gradient, which allow the purification of mono-labelled conjugate.

With the various examples of AOC synthesis presented above for diagnostic procedures, direct conjugation methods seems the most robust ways to produce AOC products. These conjugations rely on the use of a chemical linker and purification of the product using conventional techniques. There are various types of linkers available for click chemistry implementation. Chromatography methods seem the most reliable methods to characterize the conjugate product, but they present low yield after characterization.

3.3.2 Conjugation of troponin detection antibody and oligonucleotide

In iLAMP protocols, coupling of the detection antibody with the reporter DNA is the critical step. In this chapter, the reporter DNA will be the dumbbell oligonucleotide, described in the previous chapter. We take advantage of the previous development on the dumbbell structure and its use in isothermal amplification protocols. We implemented and tested different strategies to obtain the hybrid product composed of the antibody and reporter dumbbell DNA. The first one consisted in a coupling procedure involving the biotin-streptavidin interaction, by adding a biotin function to both the antibody and the oligonucleotide (affinity conjugation). The second one consisted in using a covalent bonding using chemical reaction between the antibody and thiolated oligonucleotide using a cross-linking agent (direct conjugation). Both of these procedures are detailed in this section and represented in figure 3.19. Structure A describes the streptavidin interaction, and structures B and C describe the covalent bonding, either directly between the antibody and the dumbbell or indirectly through the grafting of a short oligonucleotide.

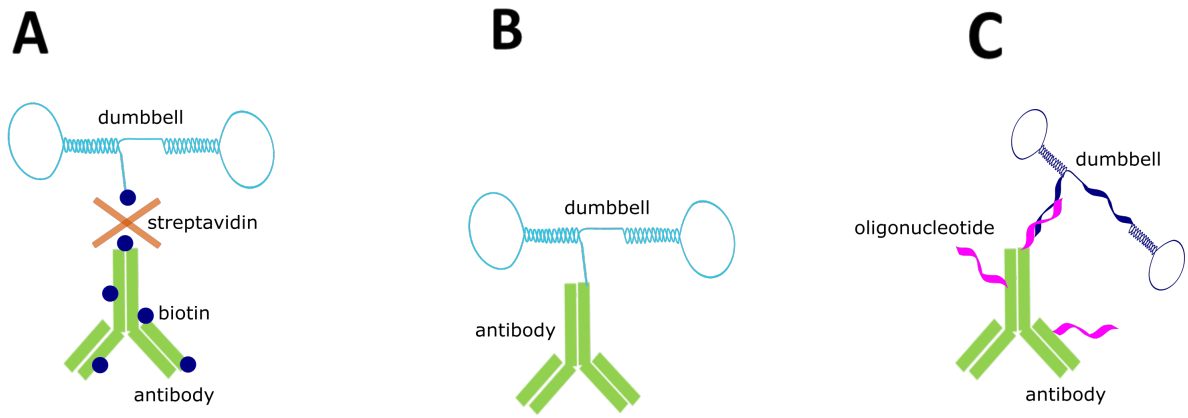

Figure 3.19: Schematic of the antibody-DNA detection complex with different strategies. (A) Affinity conjugation with streptavidin interaction. (B) Direct conjugation with dumbbell directly grafted on the antibody and (C) Indirect conjugation with short oligonucleotide grafted on the antibody.

3.3.2.1 Streptavidin methodology

This methodology to produce the antibody-DNA conjugate takes advantage of the strong interaction provided by the streptavidin-biotin complex, which is the strongest known non-covalent interaction ($K_d = 10^{-15}M$). The bond formation between biotin and streptavidin is very rapid, and once formed, it is unaffected by changes in pH, temperature, solvents or denaturing agents. Streptavidin, a biotin-binding protein derived from Avidin, has the ability to bind to up to four biotin molecules, making this interaction ideal for use in detection strategies.

The detection complex takes advantage of this strong interaction and uses biotin-modified antibody and oligonucleotide that binds to a streptavidin molecule. The detection complex is formed of the detection antibody 9703 (100181 from Medix Biochemica, lot 0047672) and the dumbbell D1 modified with a 5 thymine spacer at the 5' end with a biotin function. The detection antibody is functionalized with NHS-biotin. To do so, the antibody is first washed on a 30 kDa Vivaspin membrane to remove the conservative (sodium azide). A 10 molar excess of NHS-biotin compound is added to the purified antibody, and the solution is incubated at 4°C overnight. After the incubation, the product is washed twice again on a 30 kDa Vivaspin membrane to remove the unbound biotin. The final concentration of antibody is assessed using a spectrophotometric assay (complete protocol in appendix D). The oligonucleotide D1 is ordered from Eurogentec with a 5T thymine and a biotin modification at the 5' end (sequence in appendix A)

The detection complex is produced by mixing the same quantity of streptavidin (Sigma S4732) and biotinylated antibody, and a 3 fold excess of biotinylated oligonucleotide in the Incubation Buffer (IB) (description in appendix B). The biotinylated antibody at a concentration of 0,5 μg/mL and oligonucleotide (final concentration 10 nM) are first added in the solution, and the streptavidin is added after, following by rapid vortexing for 1 minute, and a 10 minutes incubation at 500 rpm rotation.

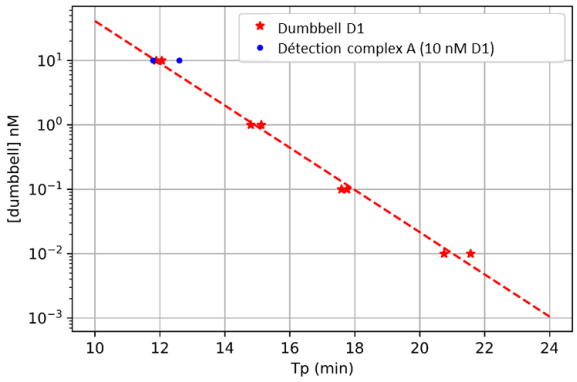

Figure 3.20: Calibration curve for isothermal amplification of dumbbell D1 (10 nM - 1 pM) and detection complex A (containing dumbbell D1 at 10 nM).

Figure 3.20 shows the suitability of the detection complex A for isothermal amplification. 10 nM of pure oligonucleotide D1 are amplified and compared with the complex A, also containing 10 nM of oligonucleotide D1 bound to the antibody through streptavidin. Both Tp values found after amplification are similar (blue and red dots at 10 nM on fig 3.20), and the complex can be quantified for subsequent lower concentration values down to 10 pM. Therefore, the formation of the complex A with dumbbell D1 and antibody is suitable for isothermal amplification and quantification on large dynamic ranges (10 nM - 10 pM).

3.3.2.2 Covalent coupling

We also studied another form of antibody-DNA conjugate to be used in a similar detection strategy. We chose to synthesized the complex using covalent bonding, and we will detail in this section its synthesis and purification steps. To do so, we chose to use a cross linker on the antibody to covalently bind the oligonucleotide. Amongst the examples described in the previous paragraph, we chose the methodology described by Bombera et al in 2012 [151] since its implementation was facilitated thanks to the knowledge already in place in our research team. The paper describes several stochioemetric coefficient for OAR that will be interesting in our further detection protocols. This work was achieved with great help from Christine Saint-Pierre, research engineer at Systèmes Moléculaires et nanoMatériaux pour l'Énergie et la Santé (SyMMES).

The preparation of the antibody-DNA conjugate is inspired from protocols described in [151], using covalent coupling with hetero-bifunctional cross-linker $SM(PEG)_{12}$. The detection antibody is anti-troponin 9703 (100181 Medix Biochemica, lot 0047672). We implemented several coupling strategies using different antibodies, oligonucleotides type and quantities. The coupling protocols are composed of the following steps.

The antibody was washed on a 30 kDa Molecular Weigth Cut Off (MWCO) membrane, and resuspended at a concentration of 5 μM in PBS buffer, and allowed to react with a 100 molar excess of the $SM(PEG)_{12}$ coupling agent, for one hour at room temperature. A large excess of reactant was used to ensure proper conjugation of the N-Hydroxysuccinimide (NHS) to the primary amines on the antibody. The reactive sample was purified on a 30 kDa MWCO spin filter membrane (15 minutes, 15,000g) and resuspended in PBE (PBS, 5 mM EDTA). The activated antibody concentration was determined by 280 nm absorbance measurement. In parallel, oligonucleotide suspended in deionized water at 50 μM were mixed with 5 mM tris(2-carboxyethyl)phosphine (TCEP) in order to reduce potential disulfide bonds formed between thiolated DNA oligomers. The reduction was carried out during 30 minutes at room temperature under mixing, followed by a purification on NAP-5 column, and concentrated using 3 kDa MWCO membrane. The reduced oligonucleotide was resuspended in Phosphate Buffer EDTA (PBE) and the final concentration was assessed using 260 nm absorbance measurement.

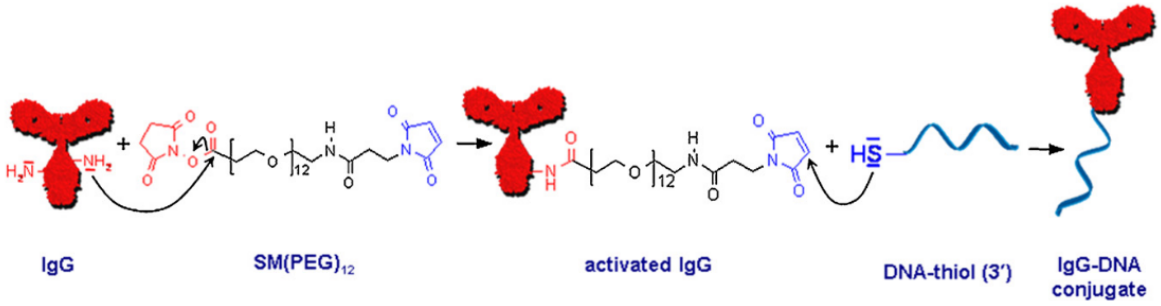

Figure 3.21: Antibody-DNA cross link reaction scheme. First, the antibody undergoes covalent coupling with heterobifunctional maleimide cross linker $SM(PEG)_12$, and is subsequently coupled to (5') thiol modified DNA strand to produce the hybrid molecule [151]

The solutions of reduced oligonucleotide and maleimide activated antibody were used for the final coupling reaction (Fig 3.21). Several antibody-DNA ratios were tested, and both modified products were combined and allowed to react overnight at room temperature with mixing. In some cases, an anion exchange column HiTrap Q FF 1 mL (GE Healthcare) was used to separate unreacted proteins as well as fractionning the conjugation products. The samples were eluted from the column with a starting buffer containing 20 mM Tris-HCl with NaCl grandient flow

starting from 137 mM up to 3 M. Collected fractions were concentrated on 50kDa MWCO membrane (15 minutes, 15,000g) and the buffer exchanged to PBS. The final concentration of the antibody after coupling was estimated using Quick Start Bradford Protein Assay (BioRad).

First, we used a model antibody (mouse CD63, 49.129.15 SCBT) and the dumbbell D1 described in the previous paragraph. Since dumbbell D1 has a length of 134 bases (over 100 bases) the oligonucleotide quantities obtained by a standard manufacturer are indeed rather low. We were able to couple 0.26 nmol of antibody with 0.52 nmol of oligonucleotide D1, and used the anion exchange column in the final step of the protocol to try to separate unbound compound. However, the High Performance Liquid Chromatography (HPLC) procedure gave very low yield, and starting from very low quantities of samples, the obtained quantities of the coupled product are too low to be used in subsequent detection protocols.

Therefore, we changed the oligonucleotide that is grafted on the antibody for a shorter oligonucleotide strand, inspired from the hybridization methodology described in the patent FR2109667 [102] and in the section 3.2.2. This short oligonucleotide is complementary to a specific part of a larger dumbbell sequence and will bind to it through strong DNA hybridization. The 34-mer short oligonucleotide grafted on the antibody is called Zip6c and is complementary to the Zip6 dangling-end part on the D1-Zip6-DE dumbbell. It has the following sequence 5' – TTT TTT TTT TCG CAT ACC AGG TCG CAT ACC GGT C – 3' and is synthesized with a 10 thymine spacer and a thiol modification at its 5' end.

We tested the grafting of this short oligonucleotide on the model antibody mouse CD63. We coupled 1.38 nmol of antibody with 2.91 nmol of oligonucleotide Zip6c, and used the anion exchange column in the final step of the protocol to try to separate unbound compounds.

Lastly, we implemented the protocols on the anti-cTnI detection antibody 9703 (100181 Medix Biochemica, lot 0047672). We tested several antibody-DNA ratios, 1:2 and 1:10. In these coupling campaigns, we removed the HPLC purification step in order to keep a reasonable coupling yield for the product to be used in subsequent detection protocols. Actually, the model CD63 antibody HPLC graphs indicated two main things: (i) there were very few unreacted antibodies and (ii) with this anion exchange column, it was impossible to separate mono- and poly-coupled antibodies. Therefore, it appears reasonable to remove this purification step, but keep a purification on a MWCO membrane to remove unreacted oligonucleotides. In the subsequent detection protocols, the unreacted antibodies should not alter the detection performance since they will not bind to the dumbbell and therefore not get amplified and detected.

A summary of the different coupling campaigns is exposed in figure 3.22. The product highlighted in green on the figure corresponds to the optimal product obtained and will be used subsequently in the main troponin detection protocols that are detailed in the following result section (3.3.3).

We tested the three complexes exposed in figure 3.19 for antibody-DNA coupling. Their synthesis varies with both advantages and drawbacks. The structure A with the biotin-streptavidin interaction has the main advantage of being easy to implement, having high synthesis yield (biotinylation), and providing a very strong interaction between the antibody and DNA through the streptavidin bonding. However, the obtained hybrid product is limited by the stoichiometric control, given by the streptavidin interaction, which is that one streptavidin binds to four biotin molecules. Moreover, once formed, it is difficult to characterize the hybrid product. On the contrary, it is possible to characterize the covalent structures B and C with for example HPLC or Bradford protein assay. However, with the covalent bonding and the different purification steps, the synthesis yield is reduced to 50 % maximum. Structure B presents the advantage to directly link the dumbbell structure used in subsequent isothermal amplification protocols, but

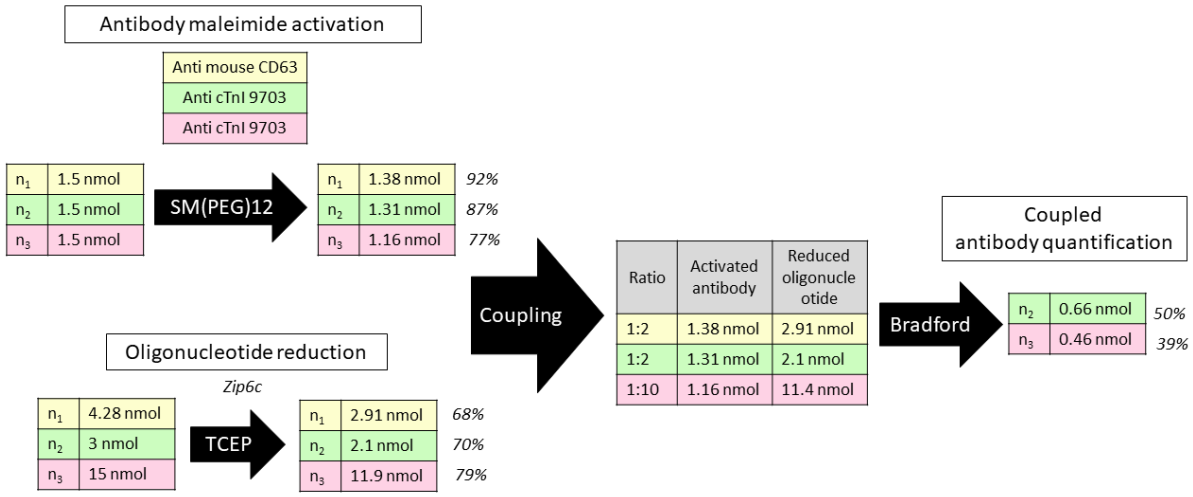

Figure 3.22: Summary of the 3 main antibody-DNA conjugate synthesis and purification steps. Two different antibodies were tested : anti-mouse CD63 (yellow) and anti-cTnI 9703 (green and pink) with different antibody-DNA ratios.

has a very low yield due to the large dumbbell size, limiting its chemical synthesis by a standard manufacturer. With structure C, it is possible to synthesize important quantities and characterize them, but the use of the short oligonucleotide leads to indirect detection methodology and therefore longer assay times in detection protocols. The main characteristics of the three products synthesis and purification are exposed in table 3.3

	Structure A	Structure B	Structure C
Type of synthesis	Biotinylation of antibody and oligonucleotide	Covalent and direct	Covalent and indirect
Typical yield	80 %	20 %	50 %
Advantages	Ease of implementation Ease of use Biotin-streptavidin very strong interaction	Direct coupling of antibody and dumbbell Possibility to characterize the hybrid product	Satisfactory yield (50 %) Large scale synthesis Possibility to characterize the hybrid product
Disadvantages	Stoichiometric control given by the streptavidin bonding Difficulty to characterize the hybrid product	Very low yield Impossible to synthesize important quantities	Indirect detection methodology (longer incubation times)

Table 3.3: Main characteristics of the three antibody-DNA conjugate synthesis strategies (figure 3.19)

The structures A and C will be used in detection assay as a detection antibody-DNA hybrid product. The next section will detail the protocol implementation in the case of cardiac troponin sensing.

3.3.3 Troponin detection with iLAMP protocols

When designing a cardiac troponin assay, the sensitivity is a major challenge. In the first two sections of this chapter, we implemented detection assay with the use of aptamers as an

alternative to antibodies and designed a complete assay type called aptameroLAMP. However, as we have observed, aptameroLAMP efficiency is limited to simple medium like PBS buffer, and the sensitivity is limited. For cardiac troponin assays, the desired limit of detection is in the picomolar range, and for clinical use, the medium is the complex human blood or plasma. Therefore, we change the detection methodology and use a sandwich antibody for troponin capture, with the detection antibody conjugated with an olignucleotide for isothermal amplification which should provide a good sensitivity through the exponential amplification. This method is derived for troponin sensing, a cardiac biomarker of great interest in the scope of this project.

3.3.3.1 Experimental method

In our developed assay, we took advantage of the versatility offered by magnetic beads to link to capture antibodies. We chose a covalent link between the magnetic beads and the capture antibody, and therefore used the 1 μm size Tosylactivated magnetic beads (MyOne, InVitrogen, cat 65501). We immobilize troponin capture antibody 9701 (100129 from Medix Biochehmica, lot 20000399). The immobilization protocols can be found in appendix D. The coupled magnetic beads and capture antibody was checked using a colorimetric ELISA reaction with anti-mouse HRP antibodies, and anti-rabbit HRP antibodies as a negative control. The magnetic beads are stored in the MB and stable for one year at +4°C.

The assay working volume was 50 μL in 96 wells microplate. The troponin protein standards were obtained from HyTest (cat 8T53) and diluted in an IB composed of PBS and 1% BSA (Sigma Aldrich). A selectivity control is performed with skTnI, a commonly used protein produced in the skeletal muscles for negative control of cardiac cTnI specific antibodies. Two experimental procedures are designed for the use of both detection complexes A and C from figure 3.19.

For detection with complex A, consisting in a mixture of biotinylated anti-cTnI detection antibody, biotinylated dumbbell D1 and streptavidin, the detection protocols are the following (Fig 3.23). Cardiac troponin is diluted in the range 10 nM to 1 pM, and added to the magnetic beads concentrated to 0.5 mg/mL for 30 minutes incubation with mixing, and then washed three times with 300 μL WB. The complex A was preformed and several concentrations of dumbbell D1 were tested: 10 nM and 1 nM. The preformed detection complex A was added on the magnetic beads and incubated for 30 minutes at RT with mixing, followed by 3 washes with 300 μL WB, and the magnetic beads are resuspended in the IB. Lastly, 2 μL of the magnetic beads solution are withdrawn and added onto 18 μL of LAMP mix 5 (appendix C), containing the primers FIP and BIP. The samples are then heated at 65°C for one hour on a Quant Studio device and fluorescence is recorded every 30 seconds.

For detection with complex C, consisting in the anti-cTnI detection antibody covalently linked to the short oligonucleotide Zip6c, two types of assay are designed. The first one consists in the sequential incubation of each reagent. The magnetic beads at 0.5 mg/mL are first incubated with troponin target in concentration range 100 ng/mL to 10 pg/mL for 15 minutes and washed three times with WB. Then, the detection antibody conjugated with Zip6c oligonucleotide is added into the magnetic beads at a concentration of 1 μg/mL, incubated for 15 minutes and washed three times with WB. Last but not least, the dumbbell D1-Zip6DE was incubated for 30 minutes at a concentration of 100 pM in a buffer containing PBS 1X, 1 % BSA, 5 mM $MgCl_2$ and 20 μg/mL DNA from salmon sperm (Dumbbell Buffer (DB)). The solution is finally washed three times with WB and resuspended in the dumbbell buffer DB. An alternative protocol consisted in a "one pot" detection, consisting in the direct incubation of the magnetic beads with the troponin target and the detection antibody (total volume 100 μL), for 30 minutes followed by three washes with the washing buffer (Fig 3.24). Lastly, the dumbbell is added in the solution at 100 pM, incubated 30 minutes with mixing, and the magnetic beads are washed three times

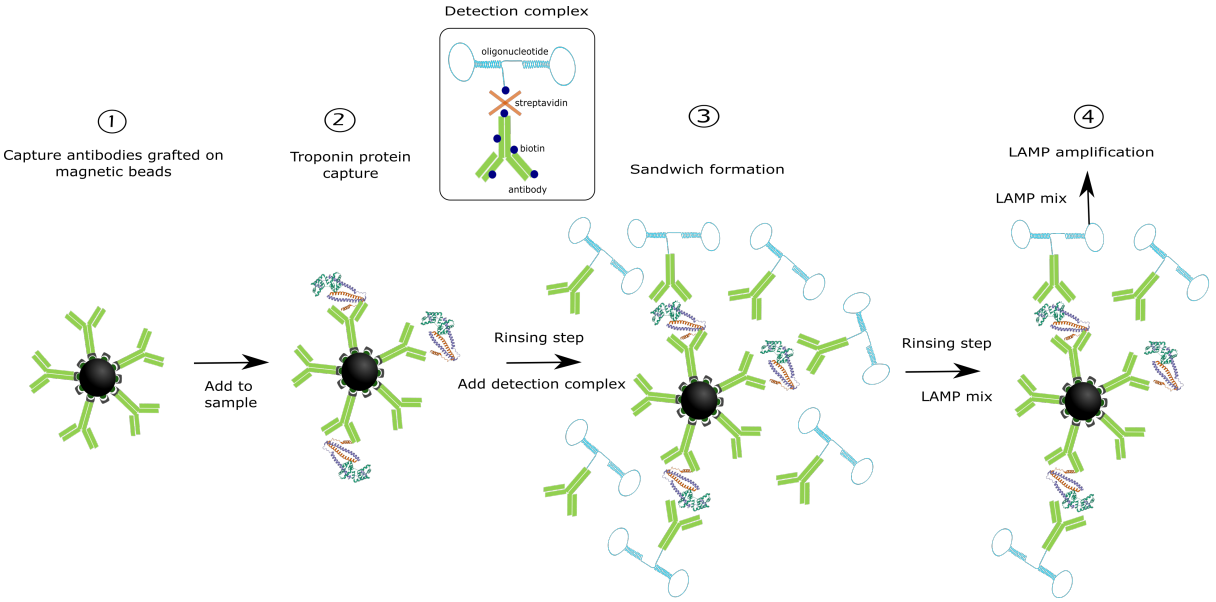

Figure 3.23: Principle schematic of the iLAMP troponin detection protocol with detection complex A.

with WB and resuspended in the dumbbell buffer DB. Lastly, in both protocol types 2 μL of the magnetic beads solution are withdrawn and added into 18 μL of LAMP mix 5 (appendix C) for isothermal exponential amplification. The solution was incubated in the commercial Quant Studio device at 65°C for one hour with fluorescence recorded every 15 seconds. The data is processed by deriving the time-to-positive value for each condition, and calibration curves are drawn for different analyte concentrations.

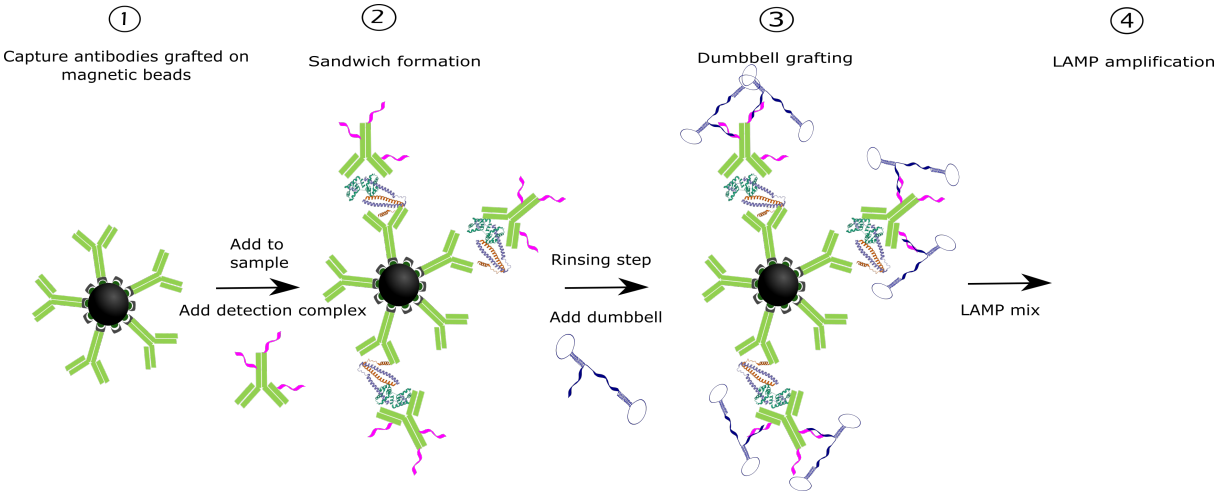

Figure 3.24: Principle schematic of the iLAMP troponin detection protocol with detection complex C with "one pot" detection method.

3.3.3.2 Results with antibody and oligonucleotide through streptavidin bonding

The troponin capture through sandwich antibodies (anti-cTnI 9701 and 9703 from Medix Biochemica) was first validated using colorimetric ELISA. To do so, we used a similar sandwich

procedure as described in the previous paragraph, but we used the biotinylated 9703 antibody as a detection antibody, and revealed the sandwich formation with strepta-HRP (Thermo N100, lot UG287 194A), Tetramethylbenzidine (TMB) substrate (Thermo 34028), and stop solution (2M Sulfuric Acid). Absorbance was measured at 450 and 620 nm and both results were subtracted.

In parallel, the iLAMP protocol with detection complex A was tested in the exact same conditions as ELISA. Troponin was first diluted in the range 10 nM, 1 nM and 100 pM, and the solution detected with detection complex A was finally amplified through LAMP amplification.

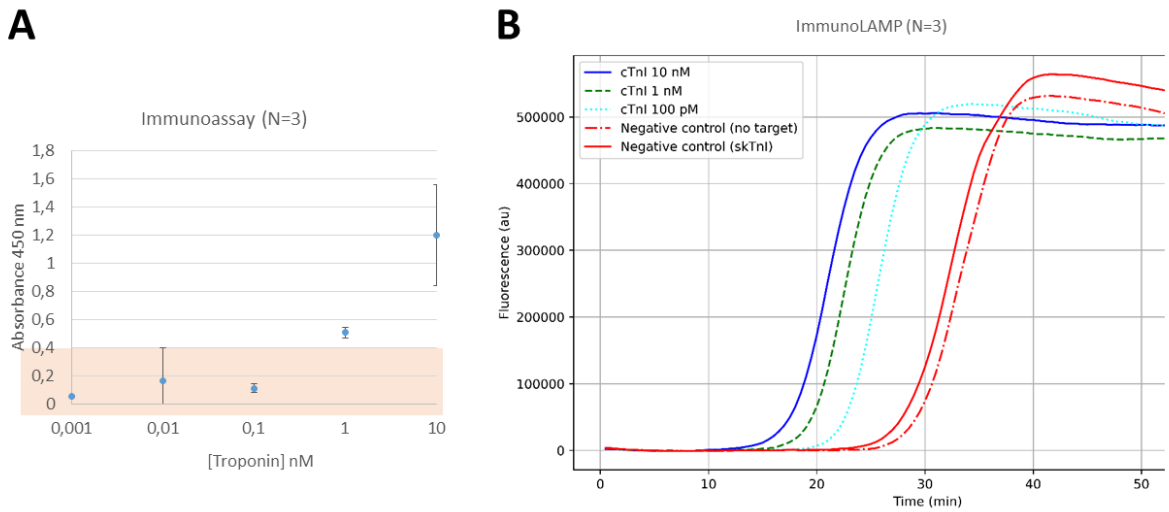

Figure 3.25: Troponin sensing using in-house developped ELISA and iLAMP detection. (A) Absorbance (450-620 nm) as a function of troponin concentation in ELISA Immunoassay with troponin sandwich antibodies 9701 (capture) and 9703 (detection). Blue curve corresponds to troponin standards (1 pM - 10 nM) and the orange line to the background signal (no troponin) (B) Fluorescence data over time for immunoLAMP sandwich protocols using antibody 9701 (for capture on magnetic beads) and antibody 9703 (in the detection complex A) after LAMP amplification

The immunoassay implementation showed greater absorbance for troponin concentration above 1 nM (Fig 3.25A). For lower troponin concentrations, the absorbance value was found to be similar to the negative control values, with no target or skTnI as a non-specific target. In parallel, the immunoLAMP assay was carried out, and the fluorescence over time after LAMP amplification can be plotted (Fig 3.25B). The amplification for troponin concentrations 100 pM, 1 nM and 10 nM appears faster than for the negative control (no target and skTnI as a non-specific target). These results showed two things: (i) the antibody sandwich is validated through colorimetric ELISA and (ii) the immunoLAMP protocol showed greater performances in similar conditions (buffer, incubation times, rinsing steps), with troponin detection down to 100 pM.

The immunoLAMP protocols were therefore tested on a larger troponin concentration range, from 10 nM to 1 pM, and with buffer medium or human plasma samples (EFS). Figure 3.26 shows the quantification curve in buffer and plasma samples. Note that the important difference in amplification times between the two assay is only due to a change of LAMP mixture (mix 2 and 5, appendix C). The upper blue point corresponds to the injected quantity of dumbbell D1 in the preformed detection complex A. For the assay in buffer medium, a quantity of 1 nM dumbbell D1 was added onto the magnetic beads, and it led to the quantification of troponin on 3 orders of magnitude from 10 nM to 10 pM (Fig 3.26A). For the assay in plasma samples, several optimization led to the addition of a larger quantity of dumbbell (10 nM) onto the magnetic

beads. Despite several tests, the non-specific signal remained very high and thus limited the LOD of the assay in plasma samples to 1 nM (Fig 3.26B).

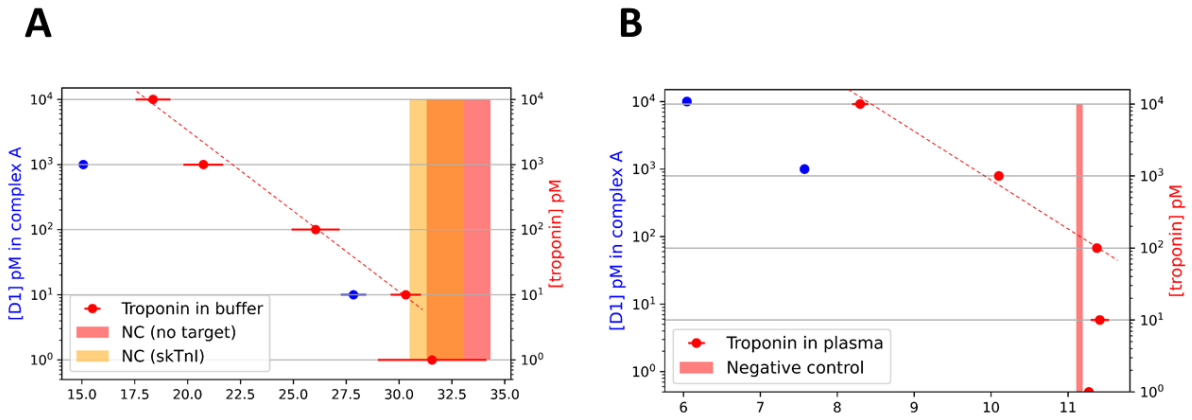

Figure 3.26: Quantification curves for iLAMP troponin detection protocols with streptavidin detection complex A. (A) Buffer medium (N=6) and (B) plasma medium (N=2).

The limit of detection in the pM range obtained with this iLAMP protocols is significantly lower than the previously described aptameroLAMP method. The very low dissociation kinetic constant Kd given by antibodies allow the efficient removal of unbound detection complex and therefore unreacted dumbbell. The performances obtained in complex medium are also enhanced compared to the aptameroLAMP protocols due to the possibility to remove the unbound detection complex through several washing steps.

This method is versatile since it is applicable to the detection of a protein with a pair of antibodies forming a stable sandwich. The detection complex formed through the biotin-streptavidin interaction lead to two main limitations. First, the complex medium (plasma) contains some free biotin that might bind to some free streptavidin sites in the detection complex, altering the performance of the assay [155]. In figure 3.26 B, we observe a non specific signal after about 11 minutes amplification, limiting the quantification of troponin to the subnanomolar range with this method. Secondly, to respect the stoichiometric coefficient in the biotin streptavidin interaction (1 streptavidin binds 4 biotin sites), the oligonucleotide quantity added in the detection complex is dependant on the detection antibody quantity added in the assay. This leads to an important quantity of dumbbell added in the detection complex (in the nanomolar range), which might affect the detection antibody sterical constraints, since the dumbbell chosen for this assay has a molecular weight of about 42 kDa. Statistically, as three oligonucleotide binds to 1 antibody on the detection complex, then the total molecular weight added on the oligonucleotides is similar to the molecular weight of the detection antibody, probably giving important sterical constraints for the detection.

In this section, we successfully validated the cTnI antibody sandwich (Medix Biochemica) through colorimetric ELISA. We successfully implemented the iLAMP detection protocols and obtained the quantification of cardiac troponin with this assay on 3 orders of magnitude from the nanomolar to the picomolar range. We obtained linear quantification with N=6 experimental replicates in buffer medium. We faced some difficulties validating the assay in complex medium such as human plasma samples, but we obtained the quantification of cardiac troponin in the nanomolar range with two experimental replicates. However, clinical values of cardiac troponin are in the picomolar range. Therefore, this developed assay is not sensitive enough to be used

for clinical diagnostic. Its main limitation lies in the non-specific signal very likely due to the nature of the detection complex A used.

The challenges faced in the development of the iLAMP assay with detection complex A using streptavidin bonding lead us to consider the second type of detection complex for isothermal amplification that could possibly counteract the drawbacks presented here.

3.3.3.3 Results with antibody and oligonucleotide through covalent bonding

The troponin antibody sandwich formation was validated in the previous section through the in-house developed ELISA and iLAMP assays with detection complex A. In order to take advantage of the exponential amplification given by the dumbbell probe, we will try another detection complex consisting in the covalent bonding of the detection antibody and small oligonucleotide (complex C). This detection complex should not present the limitations encountered with the streptavidin detection complex A, mainly in terms of sensitivity and troponin quantification range in complex samples. This assay development is the result of many optimizations that were carried out with the great help from Patricia Laurent, molecular biology technician in the LSMB laboratory.

We implemented the troponin detection protocols with detection complex C. Cardiac troponin I was diluted in the clinically relevant range from 100 ng/mL to 10 pg/mL. This range corresponds to troponin concentrations from 4.2 nM down to 0.42 pM. We tested two main strategies for the assay, sequential and "one pot" incubation of antibodies. We compared both strategies with assay performances. Several experimental parameters were tested and optimized to obtain optimal troponin quantification assay with this method. The different optimized parameters are presented in table 3.4 and the results with the optimal value are described hereafter. The iLAMP protocols with detection complex C are tested on buffer and human plasma samples from EFS.

Antibody incubation	Sequential, **One-pot**
Incubation times	Sequential : **15**, 30 minutes One-pot : **30** minutes
Number of washing steps after antibody sandwich	**3**, 6
Number of washing steps after dumbbell addition	3, **6**
Volume of washing steps	150 μL, **300 μL**
Dumbbell incubation buffer	PBS with **150**, 300, 600, 900 mM NaCl
LAMP mix	Final concentration 1X (mix 4), **0.75X (mix 5)**

Table 3.4: Parameter optimized in the troponin iLAMP assay with detection complex C. The optimal parameters found are in bold.

The dumbbell D1-Zip6-DE is added on the assay at a concentration of 100 pM. Along with the assay, its LAMP quantification curve in the range 100 pM to 100 fM is systematically drawn as a positive control and as a reference point for the dumbbell quantity added in the assay, to compare with the obtained Tp values after grafting on detection complex C in the assay. The Tp values for different troponin concentrations are also plotted and compared with the initial dumbbell quantity added on the assay. In figures 3.27 and 3.28, the dumbbell Tp values are plotted in blue with the quantification line (blue), and the Tp values corresponding to different troponin concentration are plotted in red, with a guide-to-the-eye as a quantification line (red).

For the sequential protocols implementation, the quantification of cardiac troponin was ob-

tained on two orders of magnitude down to 50 pM (Fig 3.27A). Similar performances are obtained for the same assay procedure in plasma samples (Fig 3.27B). Compared to the assay developed with detection complex A in the previous section (Fig 3.26), the assay performance in buffer medium are similar (LOD $\approx$ 50 pM), but the performances are greatly improved in plasma samples, by a factor 10 in LOD.

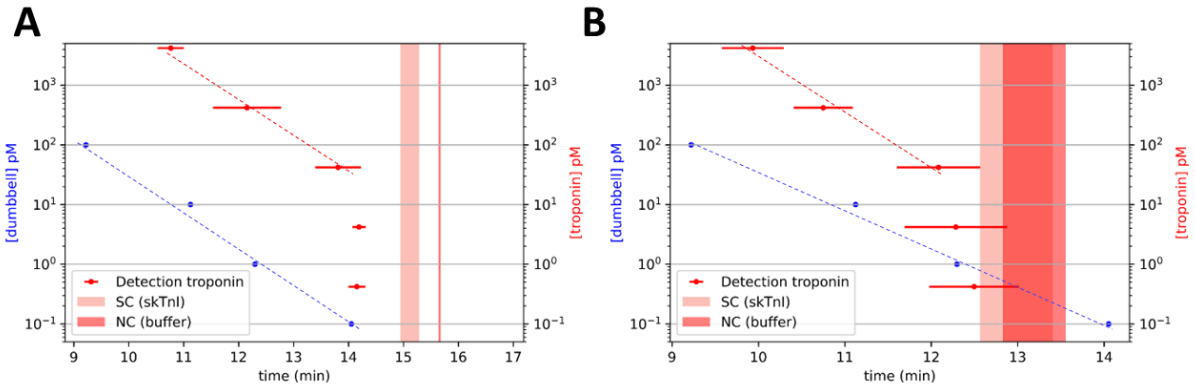

Figure 3.27: Quantification curves for iLAMP sequential protocols with detection complex C. (A) Buffer medium (N=2) and (B) plasma samples (N=4). The blue line corresponds to the dumbbel D1-Zip6-DE quantification curve (100 pM - 100 fM) and the red line is a guide to the eye for the troponin quantification.

We compared the performance with the "one-pot" antibody incubation strategy, and we found that in buffer, the quantification range was enhanced down to 5 pM (Fig 3.28A). In plasma samples, the performances are similar with a quantification range from 5 nM to 50 pM (Fig 3.28B), and limited in lower LOD by the non-specific amplification. However, the "one pot" antibody incubation significantly reduces the incubation times and therefore the total assay time, which is a major advantage of the developed assay.

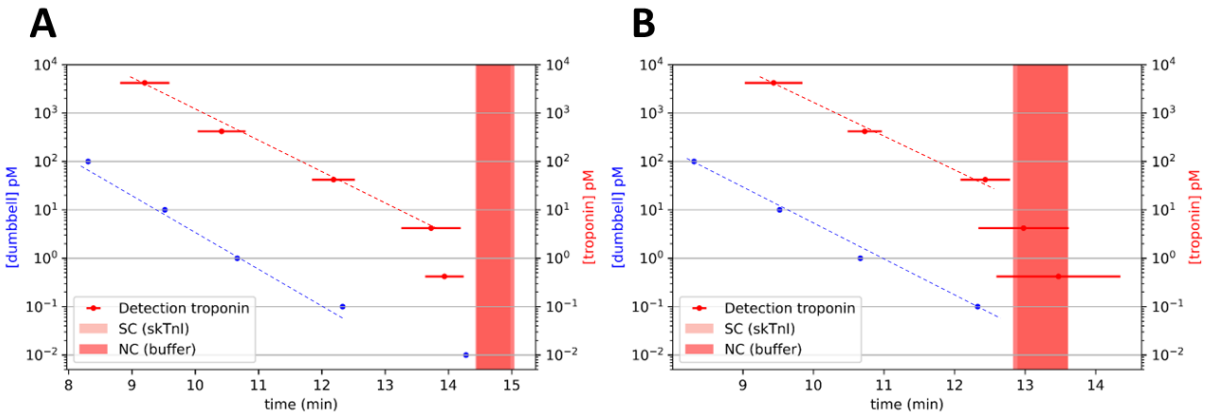

Figure 3.28: Quantification curves for iLAMP "one pot" protocols with detection complex C. (A) Buffer medium (N=8) and (B) plasma samples (N=5)

The implementation of cardiac troponin sensing protocols with detection complex C allowed the quantification of troponin on 3 orders of magnitude in buffer medium, with LOD of a few pM, and 2 orders of magnitude in human plasma samples, with LOD at $\approx$ 50 pM. The "one pot" incubation shows the best performance with reduced time and lower LOD in buffer samples. The

quantification of cardiac troponin in human plasma samples is improved compared to detection complex A. In addition, these results match the cardiac troponin I physiological concentrations, a rise of troponin levels in the range (100 - 1 ng/mL) in case of myocardial infarction.

3.3.4 Conclusion

To date, there were very few examples in the literature of protein detection through Immunocapture and nucleic acid amplification as a detection method. We chose the example of troponin sensing for the development of an innovative iLAMP assay. To design our iLAMP protocols, we implemented several antibody-DNA conjugation strategies and characterized the hybrid product suitability for isothermal amplification. We compared the obtained detection complexes in various iLAMP assays (Table 3.5). We obtained a large quantification range (10 nM - 10 pM) of cardiac troponin in buffer medium with both detection complexes. The detection complex C showed the best performances for troponin detection in complex medium (human plasma samples), and we highlighted one type of protocols to achieve the quantification of troponin down to 50 pM. High-sensitivity assays for troponin sensing propose quantification down to the picomolar range [5]. Therefore, there are still some room for improvements in the developed iLAMP assay. The main limitations lies in the non-specific amplification reducing the use of the method for quantification down to the picomolar range. This non specific amplification is very likely due to non-specific absorption of the dumbbell on the magnetic beads. Some strategies could be implemented to reduce this non specific absorption, such as a chemical modification of the magnetic beads, with for example linear polymer such as Polyethylene glycol (PEG). Random short oligonucleotides could also be grafted on the magnetic beads and prevent the dumbbell binding through electrostatic repulsion. However, special care should be given so that they do not interfere with the dumbbell hybridization on the detection complex. Moreover, the isothermal amplification as the final step of the assay is carried out directly on the magnetic beads with the troponin sandwich captured. Prior to the isothermal amplification step, we could implement an additional step which would consist in the release of the dumbbell oligonucleotide from the magnetic beads, and carry out the amplification on this product. Several methods could be used such as the use of a salty buffer, warming, or the use of a complementary DNA strand.

Detection complex	**Antibody incubation**	**Medium**	**Quantification range**	**LOD**	Assay time
A	Sequential	Buffer	10 nM - 100 pM	10 pM	1h30
A	Sequential	Plasma	10 nM - 1 nM	500 pM	1h30
C	Sequential	Buffer	5 nM - 50 pM	50 pM	2h
C	Sequential	Plasma	5 nM - 50 pM	50 pM	2h
C	One-pot	Buffer	5 nM - 5 pM	5 pM	1h30
C	One-pot	Plasma	5 nM - 50 pM	50 pM	1h30

Table 3.5: Summary of the different iLAMP implementation strategies with detection complex, reaction medium, assay type and achieved troponin quantification range and LOD

This iLAMP method is versatile and can be applied to other biomolecules presenting an antibody sandwich for target capture in a sample. In the case of cardiac biomarkers sensing which is the topic of this thesis, most of the biomarkers presented in the first chapter and used to diagnose cardiovascular diseases have been widely employed in various biosensing applications and usually present validated antibody sandwich. Therefore, the translation of the iLAMP method should be trivial with the adequate experimental parameters determined above.

3.4 Conclusion and perspective

In this chapter, we studied nucleic acids amplification techniques in two different types of assays. First, aptamers were considered to capture an analyte of interest, and we took advantage of the aptamer nucleotide sequence to provide signal exponential amplification through LAMP amplification. This lead to the successful quantification of thrombin as a model protein after double aptamer sandwich and isothermal amplification [123] from 1 μM to 1 nM, and with a LOD of 100 pM.

However, for the case of cardiovascular biomarkers sensing, higher sensitivity is required, and the aptameroLAMP assay did not exhibit enough sensitivity to be implemented as a clinically relevant troponin test. Therefore, we took advantage of the versatility of the developed dumbbell structure and combined it with an immunoassay for troponin capture. Several detection complexes formed with the detection antibodies and the dumbbell sequence for isothermal exponential amplification were described, and tested in subsequent troponin detection protocols in human plasma samples. The iLAMP troponin assay shows a LOD of 5 pM in buffer medium and 50 pM in plasma samples, and quantification ranges on 3 orders of magnitude. There are still some room for improvement of the assay, particularly in complex samples to achieve a LOD in the picomolar range in order to propose a clinically relevant troponin test. The main limitation of this assay is the non-specific signal, and several strategies can be considered to counteract this, such as magnetic beads chemical modification to reduce oligonucleotide binding or DNA release.

The aptameroLAMP and ImmunoLAMP methods show various performances for the quantification of free molecules in a sample on broad concentration ranges. Both methods are generic and applicable for the detection of other analytes such as other proteins, free oligonucleotides, toxins, peptides etc... AptameroLAMP has the main advantage to be antibody-free, therefore relying only on synthetic and relatively cheap biological reagents. Therefore, this method shows great interest for the developments of antibody-free assays with required sensitivity in the nanomolar range. ImmunoLAMP takes advantage of the exponential amplification provided by the dumbbell structure linked to the detection antibody, and therefore shows great interest to combine the specificity of immunoassays and the sensitivity of nucleic acids amplification mainly for the detection of proteins.

Both methods are not limited to the detection of proteins in sample. In the context of cardiovascular diseases testing, the patient blood sample contains other types of molecules, such as NTproBNP [21, 5] or miRNA [14], whose concentrations increase, and that could be tested similarly with the developed assay. The versatility of the developed aptameroLAMP and ImmunoLAMP methods paves the way for applications to other types of biomarkers, to propose multiplexed detection.

Lastly, in order to increase the sensitivity and the rapidity of aptamero or immunoLAMP assays, microfluidic technologies can present a great interest. Indeed, microfluidic cartridges propose the automation of many assay steps, thus reducing the time and biological reagent consumption, and improving the robustness [156]. In combination with actuation and detection platform, it can provide a quick and reliable biological test result from sample-in-to-result. Such developments are very important for the development of POC diagnostic devices, and will be presented in the next chapters, in order to propose an automated platform to integrate such assays in a portable device.

Summary

- Two types of biological assays taking advantage of the isothermal amplification given by the dumbbell structure were described: aptameroLAMP and ImmunoLAMP
- AptameroLAMP was exemplified with the thrombin protein and the achieved quantification range is 1 μM to 1 nM, with a LOD of 100 pM.
- For the case of troponin sensing, the implementation of the aptameroLAMP method does not allow the detection of troponin in physiologically relevant concentrations (pM)
- To improve the sensitivity of the aptameroLAMP assay, we proposed an immunoLAMP assay and exemplified its implementation with troponin sensing
- We described several detection structures combining antibodies and dumbbell oligonucleotides to be used in the ImmunoLAMP assay
- Several optimizations yielded the following iLAMP performances for troponin sensing: a LOD of 5 pM in buffer medium and 50 pM in plasma samples.
- The developed aptameroLAMP and ImmunoLAMP methods exemplified on proteins are versatile and easily transferable to other molecules (DNA, RNA, peptides...)

Chapter 4

Development of a portable instrument for Point-of-Care detection

Objectives

- An overview of POC devices for cardiac biomarker detection using various microfluidic technologies is given
- A generic instrument for microfluidic integration and automation of various protocols will be described
- This instrument is adapted with appropriate modules for the integration of protocoles described in the previous chapter in the scope of this PhD (thermal, optics, magnet)
- Several microfluidic cartridges are designed to integrate all the steps of the assay
- A final microfluidic cartridge is proposed for complete protocol integration and automation on the portable platform

In order to meet the REASSURED criteria for biological testing devices developments [25], POC devices show great potential. In the context of cardiovascular diseases testing in particular, sensitivity and rapidity are crucial criteria for cardiac POC development. In this project, we have developed innovative sensitive protocols for the detection of various bioligical analytes [123]. We applied the methodology for protein detection, and particularly for cardiac troponin sensing through the iLAMP method. The sensitivity and specificity of the developed troponin assay were described in chapter 3, and are matching current physiological and pathological concentrations. The iLAMP protocols are versatile and transferable to other analytes, such as other cardiac biomarkers. The total assay lasts between one and two hours, and embed many steps from sample recovery to results. Microfluidic technologies have the potential to integrate many biological assay operations in an automated way and should reduce the total assay time. To improve the iLAMP assay time and portability, we propose its integration into a portable platform and microfluidic cartridges. To do so, we combine a digital microfluidic technology with its associated instrumentation and declined its use for the specific case of iLAMP protocols. The general aim is to propose a portable platform and associated microfluidic cartridges to carry out the iLAMP protocols and apply it to cardiac biomarkers sensing. This development was made

possible based on the expertise in the LSMB at the CEA-Leti, and with the great help of Yves Fouillet and Charlotte Parent.

4.1 State of the art: microfluidic and instrumentation for Point-of-Care testing

4.1.1 Point-of-Care testing

In current medical laboratories, most of the biological tests are performed using heavy machinery for sample collection and automated analysis. Most of this machinery is bulky, costly, uses important volumes of biological reagents which can be expensive, and require trained staff to carry out long and complex protocols. Figure 4.1 shows different tools use in medical laboratories such as a microplate to process blood sample, an operator pipetting and a Roche Cobas 6000 instrument [157] to perform various blood analysis.

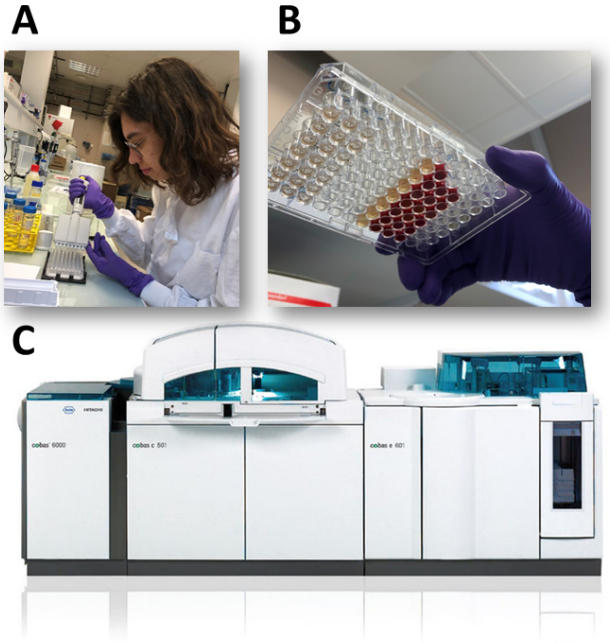

Figure 4.1: Different tools used in medical laboratories (A) Pipetting operator, (B) 96-wells microplate with plasma and blood samples and (C) Roche Cobas 6000 instrument [157]

It is interesting to look at how medical tests are carried out in central laboratories in order to point out the potential improvements. In a lot of cases, to perform a medical test, the current practice is the following (Fig 4.2): from patient symptoms, patient sample is collected and sent to a medical analysis laboratory, in which the sample is analyzed to test for various molecules that witnesses a certain disease. The chain presented in figure 4.2 does not take into account the transport time between the sample recovery and its arrival in the laboratory. In a central hospital, this time is reduced since the hospital has its own core laboratory, but in remote hospitals without central laboratories, the sample needs to be transported to a laboratory, and this could dramatically delay the result. In the case of cardiovascular diseases, if the patient with symptoms presents himself in a central hospital with central medical laboratory, then the shortest time between sample to results is 45 minutes, and it can take up to 8 hours in many other cases. The average time from sample to result is about 2 hours [28, 156].

Figure 4.2: Main steps in a medical test, from patient symptoms, sample recovery, analysis to results

Over the past decades, a category of devices called POC have been developed to perform portable medical analysis. Such instruments propose a portable and automated diagnostic with low sample and reagent consumption. The development of POC devices can reduce significantly the time-to-result in scenario where it is crucial (ED, remote areas...) [156]. There are many developments going on in this field with various POC devices already commercialized, for various biomolecules, and with different sensing method and sensitivity. Some of the POC devices take advantage of microfluidic technologies that allow the automation of all fluidic operations from sample collection with reduced reagent consumption [158, 159, 160]. The recent developments over the past decades of various microfluidic technologies allowed many improvements in the POC medical diagnostic field, and there is currently a high market demand highlighted by the Covid-19 pandemic in 2020 [75, 161].

Besides their fast turnaround time, POC devices have many other benefits for patient and healthcare systems. Several studies have been conducted in different countries pointing out their potential to improve healthcare [26]. For the case of cardiovascular diseases, POC device allow a better patient care reducing the time-to-result, and therefore the time a patient spends in the ED.

POC devices have the huge potential to improve healthcare practices, but as pointed out in the first chapter, there is a great need for engineers to develop systems that give a biological result equivalent to the one obtained by conventional methods in central laboratories. There are many R&D efforts going on in this direction, and this chapter will detail the development in the scope of this PhD to develop a portable platform for cardiac biomarker sensing. During this development, particular attention is given to the different parameters defined in the REASSURED acronym [25].

4.1.2 Microfluidic technologies for cardiovascular diseases testing

The development of POC devices must ensure that it integrates all the necessary functions to carry on all the operations from sample recovery to results delivery, respecting the characteristics presented in the REASSURED acronym (Real-time connectivity, Ease of sample collection, Affordable, Sensitive, Specific, User-friendly, Rapid and robust, Equipment-free and Deliverable to end-users) [25].

The combination of microfluidic technologies and their associated instrumentation is promising for the development of POC devices. Microfluidic technology is a category of science that manipulates fluids in a device with dimensions ranging from few micrometers to few millimeters. It allows fluid handling, and when combined with adequate instrumentation, it can do it autonomously, therefore proposing autonomous and portable platform for sample analysis. The

Massachusetts Institute of Technology (MIT) Technology Review in 2001 defined microfluidics amongst the 10 major breakthroughs in technological research [162]. This paragraph will expose several example of microfluidic technologies used for cardiac biomarker sensing, their fabrication, functions and potential to improve the field of cardiac POC.

The company Triage commercializes a one step immunoassay that only requires sample addition on the autonomous microfluidic chip [86]. The microchannel based microfluidic device (Fig 4.3A) contains dried reagents spotted along the flow path, incorporates a blood filter to separate blood cells from plasma, and a hydrophobic barrier to control sample incubation time and a waste reservoir for excess liquid. With three different assay and control zones, it allows the quantitative readout with high sensitivity and include a hand held reader. In 2021, Jing et al [68] propose a very simple microfluidic cartridge that uses only 1 μL of plasma for the detection of cTnT (Fig 4.3B). The chip is made of PDMS placed on a glass substrate coated with antibodies. It is a multizone microfluidic channel with functionnalized troponin capture antibodies and it creates a troponin concentration gradient along the channel because of binding induced depletion. The number of bound antibodies are counted with optical imaging using differential counting. The total assay time is about 30 minutes and the LOD is 6.2 pg/mL. In 2014, Mohammed et al [88] exposed an autonomous capillary microfluidic system for the detection of cTnI. They present a new CO_2 laser engraving technique for the rapid prototyping of polymeric capillary systems with embedded optics (planar lenses) and biosensing elements. The chip was made of PMMA and its surface was functionnalized using APTES chemistry for the antibody coating. It uses capillary action to actuates, stop and trigger delay valves and the capillary pumps to provide chip automation (Fig 4.3C). The systems reaches a LOD of 24 pg/mL in less than 10 minutes. Its portability, low power consumption and sensitivity is promising for the development of future cardiac POC devices.

In 2019, Sinha et al [96] described an original device combining a microfluidic chip and a FET for the rapid detection of four different cardiac biomarkers (CRP, NTproBNP, cTnI and fibrinogen). The device is an integrated microfluidic platform with immobilized aptamer probes and FET based sensor array and is made of several PDMS layers for pneumatic control, liquid flow, tape and FET substrate (Fig 4.3D). The fully automated and portable device uses very low amount of sample (4 μL) and is an interesting device for the next generation of POC devices analyzing multiple CVD markers on the same platform. Also in 2019, Gopinathan et al [98] described an original assay for the detection of cTnI on an integrated microfluidic platform. The microfluidic chip (Fig 4.3E) is composed of an air control layer placed above a liquid channel layer on a glass substrate. The operation principle of the pneumatically controlled chip is the following: the thin PDMS barrier at the top of the fluid layer forms the barrier between liquid and air channels. Compressed air or vacuum is allowed to flow in the air control layer and leads to fluid flow accross the microfluidic chip. The devices reaches a limit of detection of 12 ng/L in 30 minutes with 5 μL sample consumption, which shows that the device could be use for a reliable diagnosis of AMI. In 2023, Zhu et al [163] described an integrated microfluidic electrolumuinescence device for POC testing of AMI (Fig 4.3F). It targets the heart-type fatty acid binding protein (H-FABP), a biomarker for early AMI. The microfluidic channels are used for fluid handling and transport from inlets to different reaction zones, and the electronic system as well as electrodes are integrated below the chip. The dynamic range achieved in human serum is 1-100 ng/mL and the LOD 0.72 ng/mL with this sandwich-type ECL embedded immunoassay strategy.

In the field of cardiac POC, there are many interesting devices already existing, some commercialized, others still in the research field. The combination of various microfluidic technologies and their associated instrumentation benchtops for signal transduction gives completely autonomous devices from sample collection to result delivery. When combined with powerful

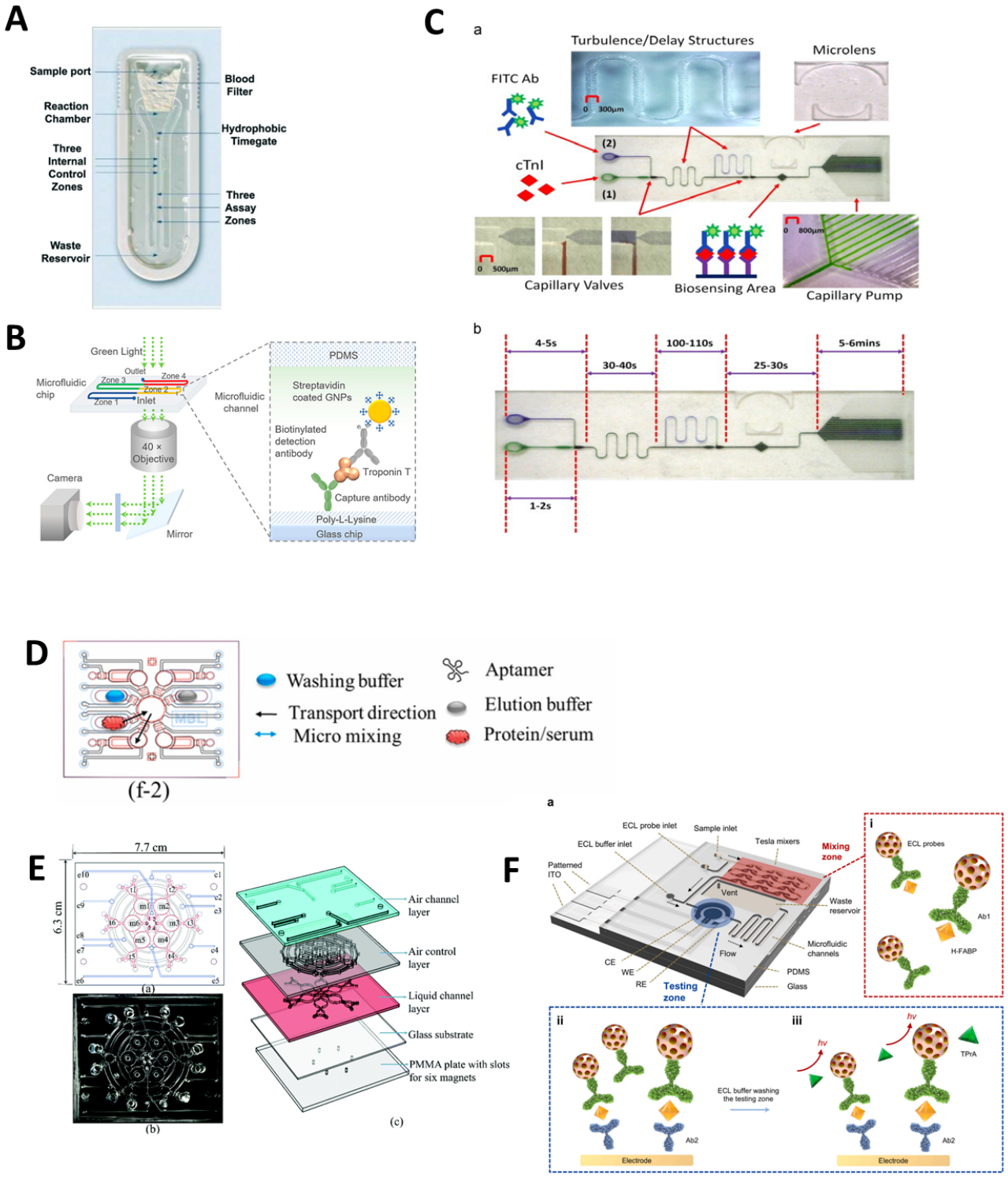

Figure 4.3: Five examples of microfluidic devices for cardiac POC sensing. (A) Triage microfluidic chip for one step immunoassay [86]. (B) Gradient-based rapid digital immunoassay for hs-cTnI detection [68]. (C) Autonomous capillary microfluidic chip for cTnI detection [88]. (D) Integrated microfluidic system with FET for the detection of multiple cardiac markers [96]. (E) Microfluidic chip assembly for multiple sample analysis cTnI detection with enzyme linked aptamer assay [98]. (F) Microfluidic ECL device for POC testing of AMI [163].

biosensing methods, these devices can reach very interesting sensitivity that is required in many cardiac sensing applications.

4.1.3 Ongoing developments in microfluidics

There are many ongoing developments in the field of microfluidics over the past decades. Those developments lead to great innovations in the field and contributed to the emergence of very powerful POC devices. In a lot of cases, POC devices are the combination of a microfluidic chip and its associated instrument for chip actuation and automation that can be of different nature and of different size. This section focuses on the microfluidic chip and its global developments, as well as the need for standardization of developments.

There is a wide variety of microfluidic applications, ranging from micro Total Analysis System (microTAS) to lab-on-chip and organ-on-chip up to POC devices. It is a growing field of research and development, and there is a need for homogeneity in the developments. To facilitate this, a consortium of European organizations (researchers and industries) gathered over the past years to create guidelines for the microfluidic developments, leading ultimately to the birth of the Microfluidic Association [164] Their goal is to initiate and follow up on actions to advance the microfluidics industry by publishing guidelines for microfluidics design and fabrication for example. A specific International Organization for Standardization (ISO) working group (ISO/TC48/WG3) [165] was also installed, which published an ISO standard on microfluidic devices in 2022 (ISO 22916:2022) [166], a worldwide premier. Some key elements of this standard and main recommendations will be exposed in this paragraph.

The basic principle behind this work is to facilitate intercompatibility between microfluidic chips. Since there are some elementary elements of a microfluidic cartridge that are known from microfluidic researchers and developers, there are some recurrent basic elements in a microfluidic devices that one could integrate as different parts into or onto a cartridge. Any of these parts can be different materials, differently fabricated and thus differently assembled.

First of all, the material used to fabricate chips can be of different nature. Historically, polymers were mostly solicited for their easiness in molding and their low price [167]. PDMS and PMMA were therefore highly used in most of the first microfluidic chip developments [168]. Since a few years, COC has become increasingly popular in microfluidics for its compatibility with various microfluidic requirements (porosity, strength, thermal conduction, optical properties, chemical inertness, etc...), but also for its medical compliance [169]. At CEA-Leti in Grenoble, the developments in microfluidics followed the semi-conductor industry principles, and therefore started with semi-conductor type materials such as silicon or glass [170]. Those two materials are also very commonly used in microfluidics to conduct fluids electrically, or are very interesting surfaces for the grafting of various molecules [171].

Secondly, after a material choice for a microfluidic device, the associated prototyping and fabrication method can vary [159], from micro-machining to laser engraving, polymerization or soft-lithography techniques. Then, the chip can be assembled through different procedures such as thermal bonding, adhesives, wax, magnets, screwing, chemical bonding etc... The main challenge in the assembly process is to ensure the impermeability between various layers. Then, the fluid can be actuated with various techniques: capillary flow, electrical, piezoelectric, mechanical, pneumatic etc... The chip connections are ensured through various inlets, tubes, reservoirs, vents etc... Lastly, if the microfluidic chip is not passive, then it is installed into a device for connection and actuation that can contain a case, a chip holder etc... [86].

This paragraph shows only some of the possibilities offered by the microfluidic components to actuate fluids at microscale. These possibilities are summarized in table 4.1.

The various possibilities shown in table 4.1 allow for the creation of a plethora of different microfluidic chips. To fasten development, facilitate interoperability and collaboration, the

Feature	Possibilities
Materials	PDMS, PMMA, COC, glass, silicium...
Patterning process	Micro-machining, laser, polymerization, soft lithography, injection moulding...
Assembly	Thermal, adhesives, wax, magnets, screws, chemical bonding...
Fluid actuation	Capillary, electrical, piezoelectric, mechanical, pneumatic...
Connections	Inlets, tubes, reservoirs, vents...
Device packaging	Case, holders...

Table 4.1: Microfluidic chips basic elements

ISO/TC48/WG3 puts in place standardization guidelines. Firstly, they defined a vocabulary (standard ISO/DIS 10991) with the general terms relevant to microfluidics, and the flow, interfacing and modularity related terms. Then the working group described the microfluidic devices (standard ISO 22916:2022) with their interoperability requirements for dimensions, connections and initial device classification. The microfluidic chip "credit card" format used in the LSMB laboratory is compliant with this ISO norm (Fig 4.4A). Lastly and currently, they are working on a catalogue of components and datasheets (ISO/AWI TS 6417). The example of microfluidic pumps is exposed in figure 4.4, with the catalogue of various pumps in panel B, and the datasheet of a specific pump in panel C.

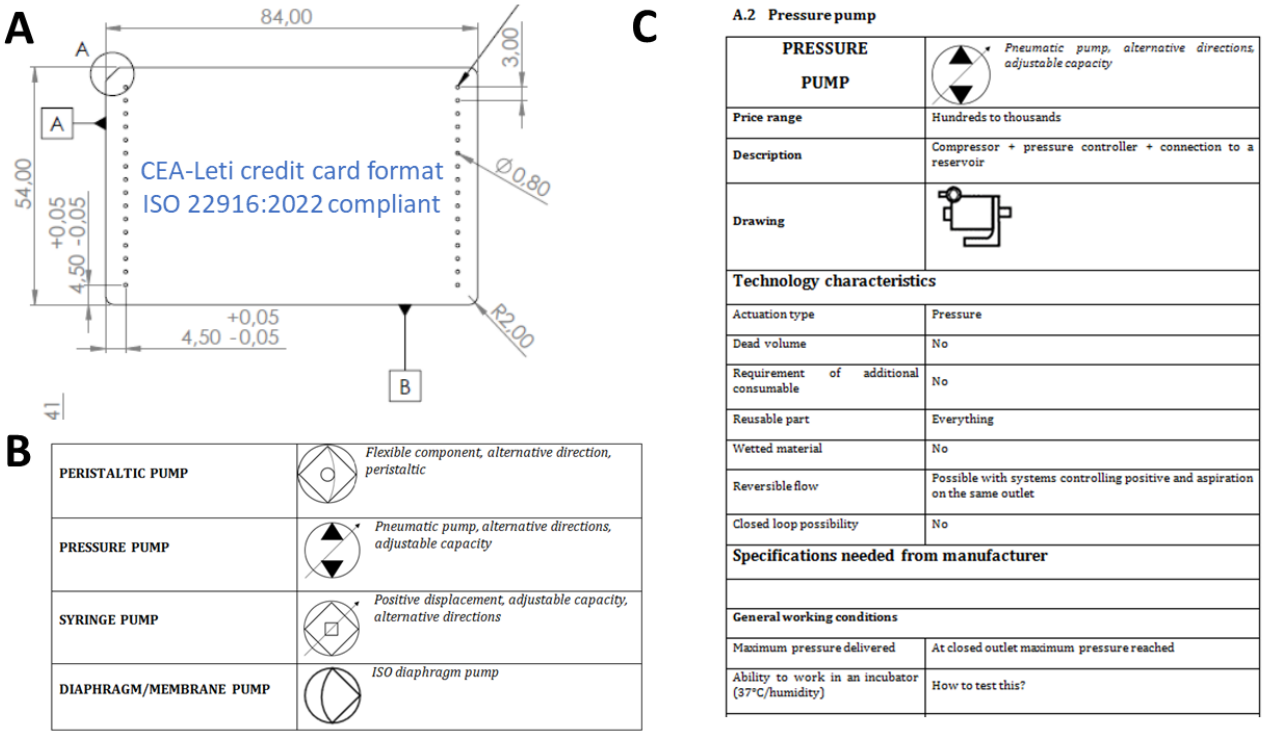

Figure 4.4: Examples from ISO standards in microfluidics. (A) ISO 22916:2022 Microfluidic devices: interoperability requirements for dimensions, connections and initial device classification. Microfluidic chip dimensions. (B) and (C) ISO AWI TS 6417 (currently under development) Microfluidic pumps: symbols and performance communication

Currently there are great efforts going on in the standardization of microfluidic components and developments. This is necessary to speed up the development of microfluidic devices for

example in the medical industry. At the beginning of the 21^{st} century, microfluidics was described as a potential major breakthrough and there have been decades of lab-on-chip research to develop various types of devices [156]. Yet thus far we only see the emergence of successful commercialized devices in the medical diagnostic field. There is a great potential for new innovative equipment to reach the market. To stimulate this, worldwide standards for microfluidics are a powerful tool. Homogeneity in design rules and fabrication can speed up the development of microfluidic technologies.

4.2 Description of the automated platform and microfluidic technology

The recent developments in microfluidic technologies and associated instruments shows very interesting portable and automated systems. In the medical field, these autonomous and rapid devices can become very competitive to central laboratories and are very promising for the POC devices market.

To translate biological assays carried out in 96-well microplates, we chose the FlowStretch microfluidic technology and associated FlowPad instrumentation benchtop developed in the LSMB laboratory. This microfluidic technology relying on digital microfluidics allows the manipulation of small and large volumes of fluid in a controlled and automated way. It has already been exemplified to integrate ELISA assays [169], and is therefore adapted to the translation of similar assays. The association with the instrumentation benchtop leads to the complete integration of the sample preparation in the cartridge to the final detection result.

This section will describe the working principle of this microfluidic technology, and the inhouse developed portable platform to integrate the required functions of the biological assay for troponin detection developed in the scope of this PhD project.

4.2.1 FlowStretch technology for digital microfluidics

The FlowStretch technology proposes digital microfluidics cartridges for the integration of various assays. It proposes a network of collapsible chambers and valves that allows to perform elementary fluidic functions in an automated way, such as fluid transfer, volume calibration, mixing etc... The fluid actuation is made possible by the two main elements, chambers and microvalves, that are engineered on the surfaces of double layers polymeric (COC) cartridges. A stretchable membrane (EcoFlex) is placed between the two layers and pneumatic actuation allows the fluid movement (Fig 4.5A) [56]. The chip elementary components (valves and chambers) are switched from open (1) to close state (0) for fluid actuation. In open state (1), negative pressure is applied on the membrane to push it downwards and let the liquid flow, and in closed state (0), positive pressure is applied on the membrane to block the liquid. Chambers are switched from opened to closed state to get filled with liquid, and valves stop the fluid movement at a precise location. Typical actuation pressures are -150 mbar for the negative pressure (open state) and +150 mbar for the positive pressure on chambers (closed state) and a higher pressure of +500 mbar to close the valves and ensure their impermeability.

The pneumatically actuated multiple microfluidic chambers and valves are arranged in a XY architecture to form a 2D network of chambers and microvalves and therefore allows the discrete fluid manipulation in two directions on the cartridge [56].

In order to get a clearer idea of how this microfluidic technology works and is implemented, an example of a generic microfluidic architecture is presented in figure 4.5 B, with reagent inlets and outlets, a microfluidic chamber, channels, and a system for pumping the fluid to a waste. The samples are added into the microfluidic cartridge in the inlets i_1 and i_2. Figure 4.5 C

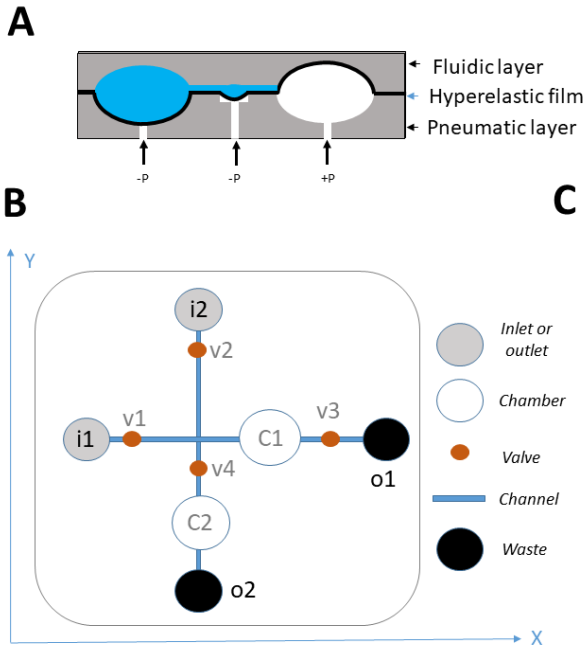

C

Component	P+ (mbar)	P- (mbar)	Fluid transfer in the X direction			Flui transfer in the Y direction		
V1	500	-150	1	0	0	0	0	0
C1	150	-150	1	1	0	0	0	0
V2	500	-150	0	0	0	1	0	0
V4	500	-150	0	0	0	1	0	0
C2	150	-150	0	0	0	1	1	0
V3	500	-150	0	1	1	0	0	0

Figure 4.5: Principles of FlowStretch technology and XY architecture. (A) Examples of two spherical chambers and an intermediate valve. Fluid (in blue) displacement from right to left chamber. (B) Example of a typical microfluidic XY architecture using FlowStretch technology. Inlets are used for sample and reagent injection. The liquid can be actuated either in X or Y direction depending on the chamber and valve position. (C) Typical chambers and valve actuation pressures and state for fluid transfer in X or Y direction on chip. 1 indicates an open state (negative pressure) and 0 a closed state (positive pressure)

depicts the typical valve and chambers states during fluid transfer in the X or Y direction. To calibrate a volume of sample from inlet i_1 to chamber C1, therefore in the X direction, valve v1 and chamber C1 are opened. Similarly, to transfer this liquid to the outlet o1, valve v1 is closed, valve v3 is opened and chamber C1 is closed. All along the transfer in the X direction, valves v2 and v4 are kept closed to prevent the fluid actuation in the Y direction. Similarly, to calibrate a volume of sample from inlet i_2 to chamber C2, therefore in the Y direction, valves v2 and v4 and chamber C2 are opened, whilst the others remain closed, therefore transferring the liquid to C2 in the Y direction.

From the basic pneumatic actuation and XY architecture principles exposed above, one can design complete microfluidic cartrdiges for a desired application. The complete microfluidic cartridges are designed with CAD on the SolidWorks software (Dassault system). The LSMB laboratory has built its own library of generic microfluidic elements that can be machined on the polymeric layers to form complete microfluidic cartridges. Typical microfluidic elements used with the FlowStretch technology are channels, valves, chambers and inlets or outlets (Fig 4.6A). Basic microfluidic elements are placed on the fluidic and pneumatic layers to form the complete cartridge. Design rules have been implemented for successful actuation and precise fluid control using FlowStretch technology [169]. The chambers are composed of two spherical caps, one half machined in the pneumatic COC layer, the other half in the fluidic layer. The chamber volume can be tuned by an adequate choice of spherical radius and heigth [169]. Groove-shape microchannels are patterned in the top of the chamber to avoid bubble trapping and incomplete

fluid filling or draining [169]. The microfluidic channels typical width and heigth are 300 μm. Valves are composed of a spherical cap in the fluidic layer, and a cylinder shape in the pneumatic layer connecting with the pneumatic connections on the bottom layer.

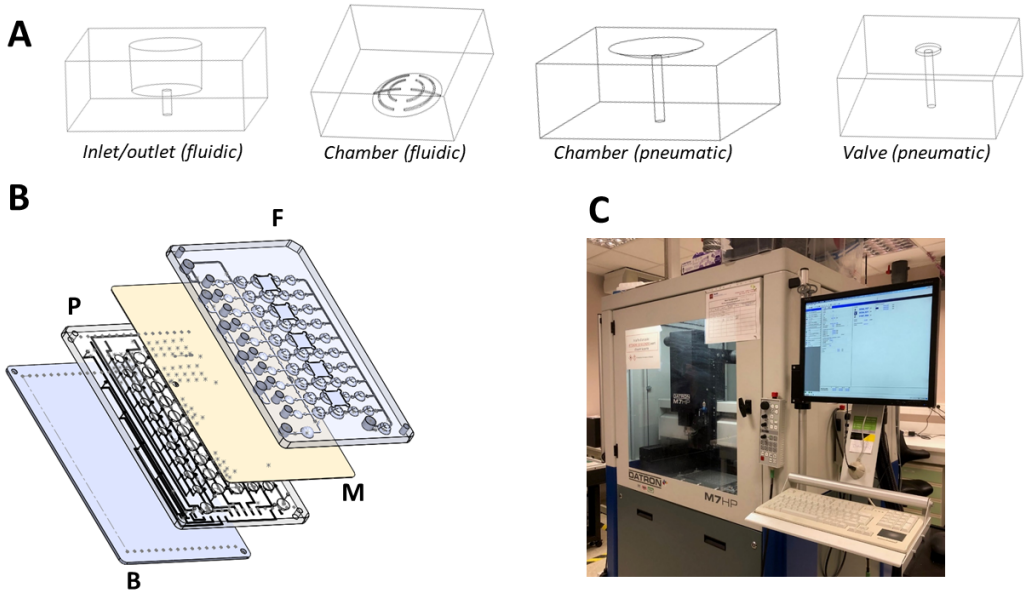

Figure 4.6: Elements for microfluidic cartridges design, engineering and fabrication. (A) Typical elements from the LSMB microfluidic library. (B) CAD view of microfluidic chip assembly with bottom (B), pneumatic (P) and fluidic (F) layers, stretchable membrane (M). (C) DATRON M7HP equipment to micromachine patterns on COC sheets.

The complete cartridge design is credit card format (ISO 22916:2022) and made of three polymer layers with the 200 μm stretchable membrane (EcoFlex, Smooth) inserted between upper and lower COC layers (Fig 4.6 B). The microfluidic patterns (chambers, channels, valves) are directly machined from the COC sheets, using DATRON M7HP equipment [169] (Fig 4.6C). The cartridge assembly is done as follow. The pneumatic (P) and bottom (B) layers and thermally bonded. The stretchable membrane is positioned between the fluidic and pneumatic layers and plasma bonded. To do so, the pneumatic (P) and fluidic (F) surfaces are activated by oxygen plasma, followed by a silanization with 30 minutes immersion in a 2% APTES solution. The layers are rinsed with water and dried, and then the plasma activated EcoFlex membrane is laminated on the pneumatic layer and then covered with the fluidic layer. Finally, the full assembly is sealed by pressing for 15 minutes [169].

Microfluidic cartridges dedicated to the biological protocols developed in the scope of this PhD are engineered based on the expertise and design rules described in this paragraph. We designed several cartridges and reasoned with blocks for different main steps of the protocols.

4.2.2 FlowPad as a generic platform

The FlowStretch microfluidic cartridges are placed on an associated instrument called FlowPad that allows the cartridge actuation. Figure 4.7 shows a picture of the generic instrument (A) and the instrument used with microfluidic FlowStretch cartridges (B) [169]. This instrument is developed in LSMB laboratory at the CEA and is generic and common to several projects.

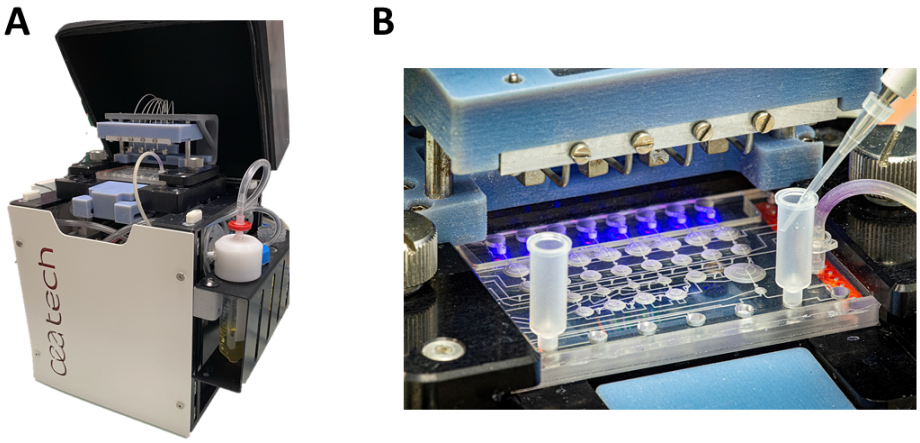

Figure 4.7: FlowPad platform developed at CEA-Leti: (A) picture of the generic FlowPad instrument and (B) picture of a microfluidic cartridge for ELISA protocols placed on the instrument [169]

4.2.2.1 Basic modules

The FlowPad platforms already contains some basic modules that fit the actuation requirements for the FlowStretch technology.

Three pressure controllers (Fluigent) allows the pressure regulation from compressed air and vacuum, down to the desired values for FlowStrech actuation (-150 mbar, +150 and +500 mbar). 32 solenoid valves are used to spread the regulated pressure on the microfluidic chip (Fig 4.8A). A chip holder allows the connection between the pneumatic lines and the access ports on the microfluidic chip. A motorized arm with 4 or 5 magnets allows the magnetic beads manipulation through its vertical control with an actuator [169]. When the magnets are pushed down onto the cartridge, the magnetic beads are attracted to the top side of the chamber and the fluid can be withdrawn to perform washing (Fig 4.8B).

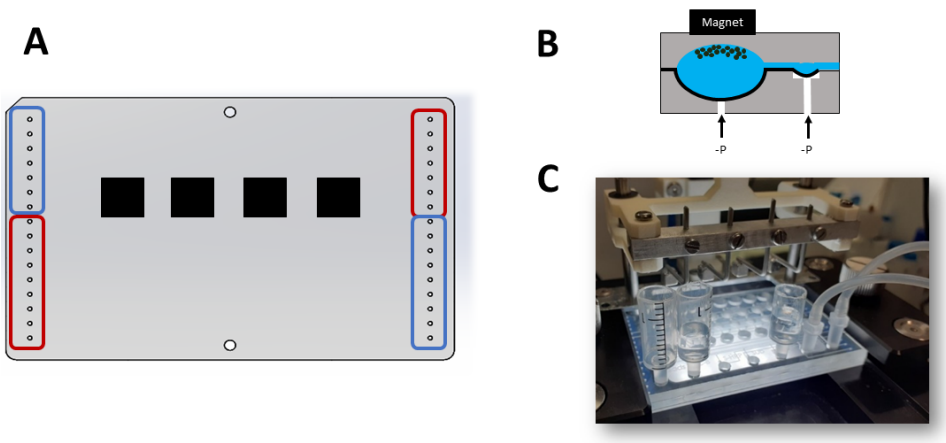

Figure 4.8: Basic modules in the FlowPad platform. (A) Microfluidic cartridge view with the 32 solenoid valves entries (blue for valve pressure entry and red for chamber pressure entry) and the 4 magnets positions (black). (B) Principle of magnetic beads capture in FlowStretch chambers. (C) Picture of a microfluidic chip on the FlowPad instrument

The basic FlowPad platform was developed for the integration of biological quantitative immunoassay [169], but does not include components for other types of protocols such as nucleic acid amplification which requires thermal heating and optical detection. Therefore, in order to propose a platform that could integrate microfluidic cartridges designed for the developed immunoLAMP protocols, the instrumentation needs to be enhanced with the required hardware components. A thermal and an optical module designed for on-chip isothermal nucleic acids amplification will therefore be added on the platform and characterized. This modification was achieved with the participation of Hélène Jousset, Charles Raymond, Xavier Mermet, Yves Fouillet and Charlotte Parent.

4.2.2.2 Thermal module

The final stage of the iLAMP protocol is a nucleic acids isothermal amplification (LAMP), which requires to maintain the solution at a constant temperature of 65°C for one hour. Therefore, the FlowPad platform must contain a thermal modul for on-chip heat activation. This module is composed of two Peltiers of size 25x25 mm, with an aluminium block placed above to allow good thermal conduction. Below them, ventilators and heat dissipators are placed for thermal dissipation. The Peltiers are regulated thanks to a thermoelectric controller working with a temperature probe and a feedback loop. The position of the heating modules below the microfluidic cartridge placed on the instrument is detailed in figure 4.9.

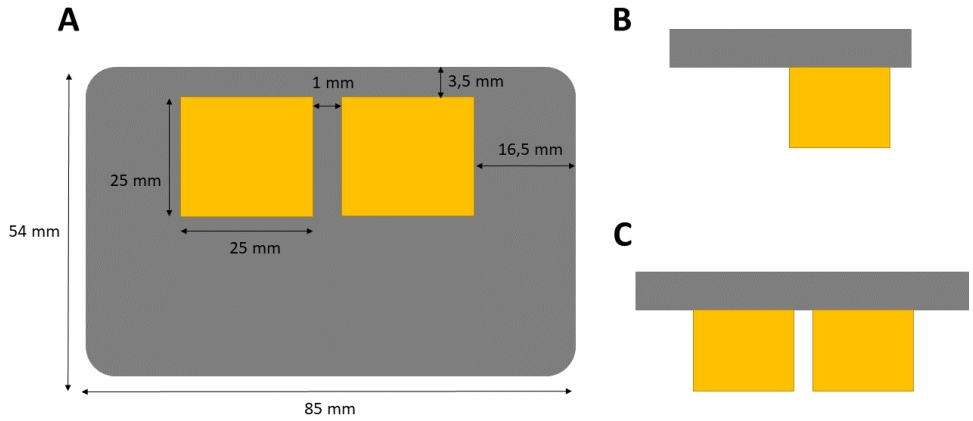

Figure 4.9: Peltier positions on the microfluidic chip (A) top view, (B) side view and (C) front view

The thermoelectric controler is directly linked to the two Peltier modules and their own temperature probes, and the control is achieved with a proportional–integral–derivative (PID) corrector. This corrector is provided with the controler and its associated software, and is necessary to tune each Peltier with its controler for the desired temperature. This tuning is done manually initially and allows the Peltier to use minimal energy and time to reach the desired temperature.

The thermal module once set up is used to carry out isothermal amplification protocols on chip. For the developed protocols, the amplification temperature is 65°C (typical LAMP temperature). The microfluidic cartridge will contain dedicated chambers containing the solution

to be amplified. The temperature inside these chambers needs to be determined precisely. Indeed, the microfluidic chips are thick (7 mm) and made of a succession of polymer layers that are not ideal for heat transfer. The combination of the polymer layers, channels and chambers either filled with air or with different kind of fluid influences greatly the heat transfer on chip and must therefore be characterized. This study will be presented in section 4.3.2.2 with a combination of theoretical studies and numerical simulation to evaluate the heat transfer on the designed microfluidic chip.

4.2.2.3 Optical module

During the LAMP amplification, the fluorescence increase in the solution is recorded over time to plot fluorescence amplification curve and eventually quantify the amount of analyte in solution. For the protocol integration, an optical module is added to the instrumentation benchtop (Fig 4.10). This module is composed of a mounted LED (Thorlabs, M490L) with an excitation wavelength of 490 nm (blue). The fluorescent dye placed in the solution on chip has an excitation wavelength of 490 nm and an emission spectrum starting at 500 nm. A camera (IDS Eye) with an adequate filter (500 nm) is placed above the chip to collect images. The LED power, lightning duration and camera acquisition period can be tuned. The typical parameters values used can be found in table 4.2.

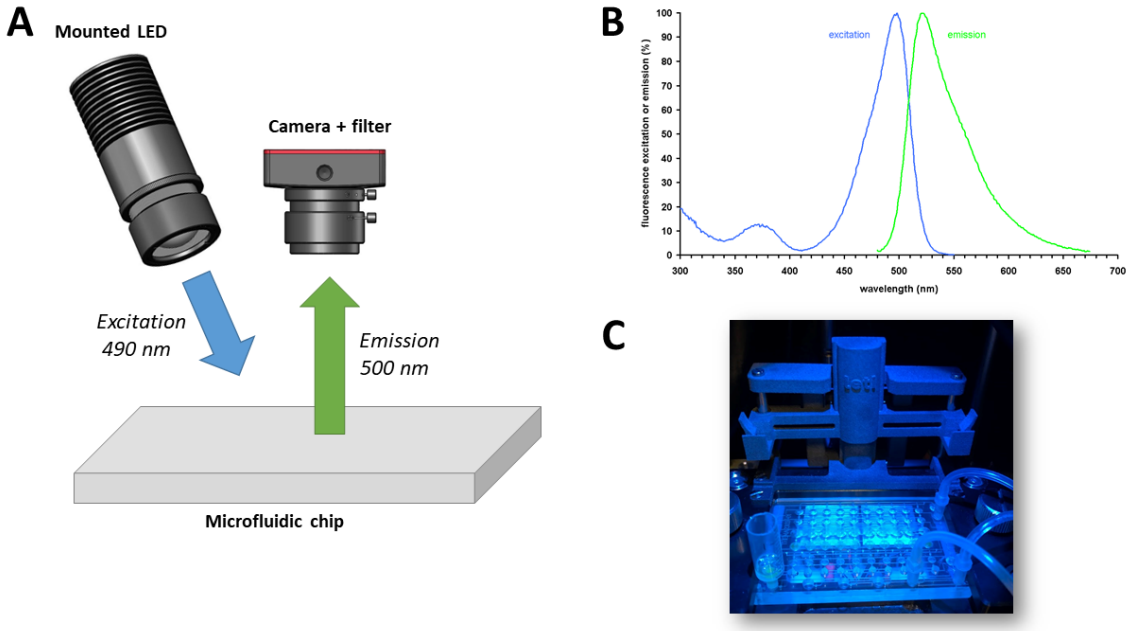

Figure 4.10: Optical set up (A) Schema of the mounted led, camera and chip, (B) SYBR Green excitation and emission spectra and (C) Picture of the set up with LED lightning

LED	Power	1000 mA
	Lightning duration	2 sec
Camera	Acquisition period	150 ms
	Gamma	0.8
	Gain	0%

Table 4.2: Optical module parameters

One of the main challenges with this optical set up is the lightning homogeneity given by the LED. The microfluidic cartridges have a fixed size of 54×84 mm, and the microfluidic chambers are placed on a horizontal line that covers about 60 mm length. In order to get accurate fluorescent data, optical homogeneity needs to be achieved over the different chambers and therefore along this horizontal line. We therefore implemented a mounted LED inspired from epifluorescence microscopy set ups in order to improve the homogeneity on the microfluidic cartridge.

4.2.2.4 Uflu Software as a control interface

The platform is controlled in real-time with an in-house developed software named Uflu factory and programmed in C++. The development of this software is achieved by Jean Porcherot and Lucas Audebert. The software presents an easy-to-use interface that gives access to the different hardware components (Fig 4.11A). The connections with the previously described hardware module required in the scope of this project are presented in figure 4.11B. Instructions on each hardware component are written by users in Python scripts to automate the different steps in a chronological order. Examples of a script for pressure actuation can be found in appendix G.

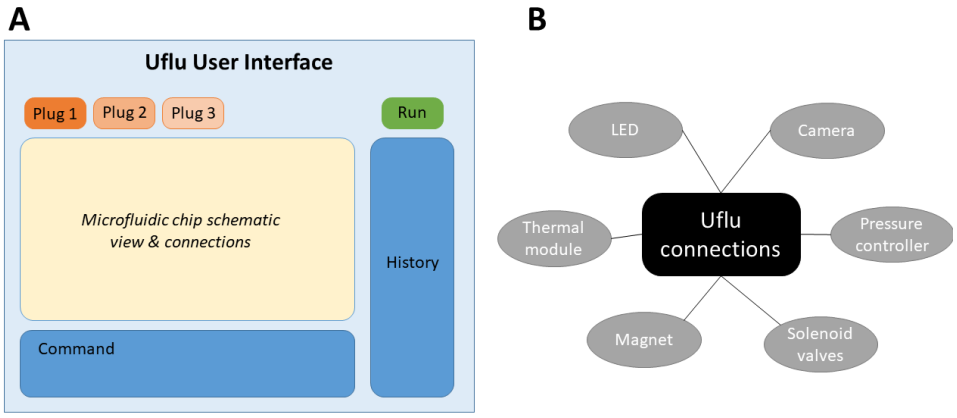

Figure 4.11: Uflu Software. (A) User interface and (B) Hardware modules used in this PhD project

4.2.2.5 Complete instrumentation

Overall, the complete instrumentation was enhanced with thermal and optical module to perform nucleic acids isothermal amplification on chip. The system total size is 30 × 25 × 75 cm, and contains the basic components for fluid actuation, magnetic beads handling, heating and optical detection. The complete instrumentation schematic and pictures are presented in figure 4.12. The motorized magnetic arm is adaptable so that it can comprise a row of 4 or 5 magnets (appendix H).

From the FlowPad generic platform available in the LSMB laboratory, we implemented several additional hardware modules required for the integration of the protocols developed in the scope of this PhD. The thermal module provides the chip with the required thermal activation to carry out nucleic acids amplification. With the optical module, the solution is excited and fluorescence emission is recorded over time, to draw amplification curves. The newly designed magnetic arm with flexible magnet position will allow the versatility of the microfluidic cartridges that will be designed in the next section.

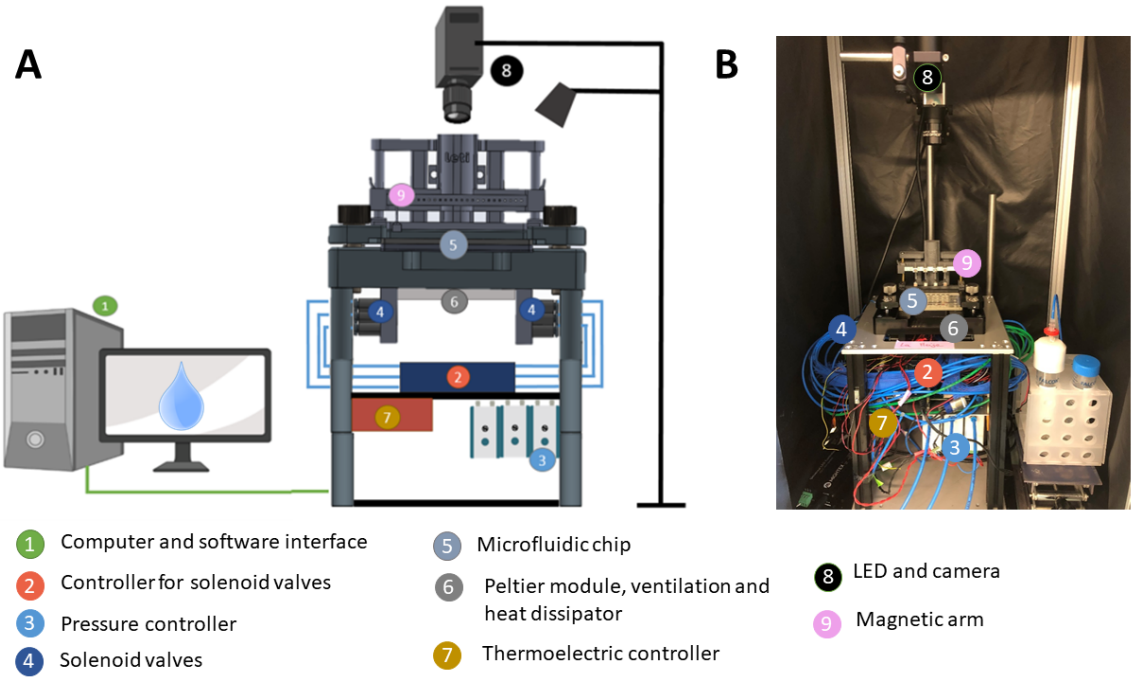

Figure 4.12: Schematic (A) and picture (B) of the instrumentation benchtop with the different modules

With a functional microfluidic instrumentation benchtop and appropriate hardware modules, we can now design credit card format microfluidic cartridges with dedicated architecture for complete protocol integration. The next section will describe these cartridges.

4.3 Design and engineering of microfluidic cartridges for different biological assays

Based on expertise developed over the past decades in the LSMB laboratory, and with great help of Nicolas Verplanck, Joris Kaal, Charlotte Parent and Yves Fouillet, we took advantage of a specific microfluidic technology developed in the laboratory and designed several microfluidic cartridges adapted to the developed instrumentation benchtop and to the biological protocols developed in the scope of this PhD. The chips are in-house designed, fabricated and tested with the great help of a dedicated microfabrication and packaging team, especially with the work of François Boizot and Romain Nony.

The protocols for troponin sensing developed in the scope of this PhD and described in the previous chapter process the patient blood or plasma to find its troponin level (Fig 4.13). A calibration curve is spiked using fixed troponin concentrations, and the unknown sample from the patient is analyzed in parallel. The troponin protein is captured on magnetic beads, that are then rinsed after incubation. The captured troponin is detected with the detection complex made of the detection antibody linked to the dumbbell. The solution is rinsed again, and the detection complex is amplified isothermally (LAMP). The goal of this section is to describe the microfluidic cartridge development to integrate each step of this troponin assay. Three cartridges are presented with increasing order of complexity. First a magnetic beads sample preparation module (cartridge SP) is described. Secondly a cartridge dedicated to isothermal amplification (cartridge L), and lastly a final cartridge that integrates both modules for the complete protocol integration (cartridge C) will be described. The cartridges presented here are the results of

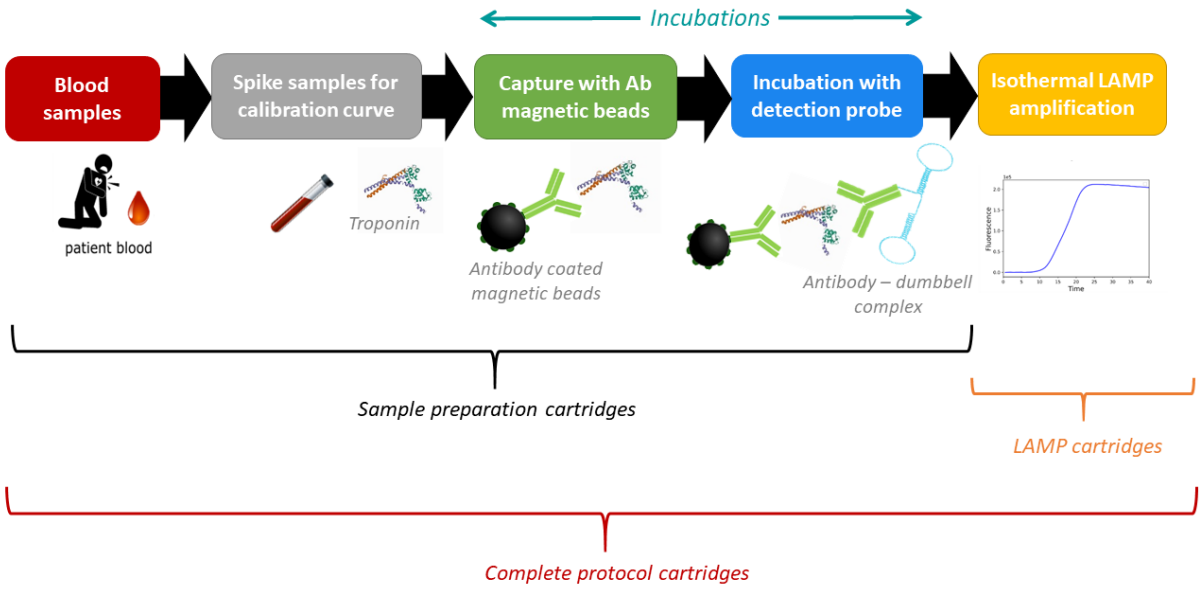

Figure 4.13: Streamline of troponin detection protocols developed in the scope of this PhD: blood sample recovery, troponin standard addition, capture on antibody-coated magnetic beads, incubation with the detection probe (antibody and dumbbell complex) and LAMP isothermal amplification. The three associated cartridges are (i) the sample preparation (SP), (ii) LAMP (L) and (iii) complete protocol (C) cartridges.

several design optimizations. All design iterations can be found in appendix F.

4.3.1 Microfluidic sample preparation cartridges

The first microfluidic chip design is dedicated to the sample preparation module. Its design is based on the architecture of a microfluidic chip used to integrate ELISA protocols for gluten detection [169]. The versatile architecture presented in the article employs a magnetic-bead-based protocol, similar to the protocols developed in the scope of this PhD. The designed microfluidic chip should integrate each step of the protocol. This consists of the troponin capture by magnetic beads, the drawing of a calibration curve with different troponin standards and samples, followed by several rinsing steps. Then, the captured troponin is detected with the detection complex formed of the detection antibody linked to the dumbbell oligonucleotide for isothermal amplification. The solution is again rinsed several times, and the magnetic beads are re-suspended in a buffer for further analysis with LAMP. A generic architecture is developed comprising each step of this protocol, and we used the 2 dimensions XY architecture [56] for quantitative biological assays. We parallelized the reaction in rows in order to be able to obtain a calibration curve with spiked samples and analyze an unknown sample. This generic architecture can contain either 8 or 10 rows depending on the target and application case. The unitary module of this architecture with only one row with its valves and chambers connections is presented in figure 4.14 A, and picture from the design are presented in 4.14 B and C.

The architecture presented in figure 4.14 is named **cartridge SP** and functions as follows. The reagent inlets are used to add different solutions into the microfluidic chambers in the vertical direction, by first draining the liquid into the central channel with the help of the pumping chamber C4. The fluids are then scattered in the calibration chambers C2 (40 μL) and

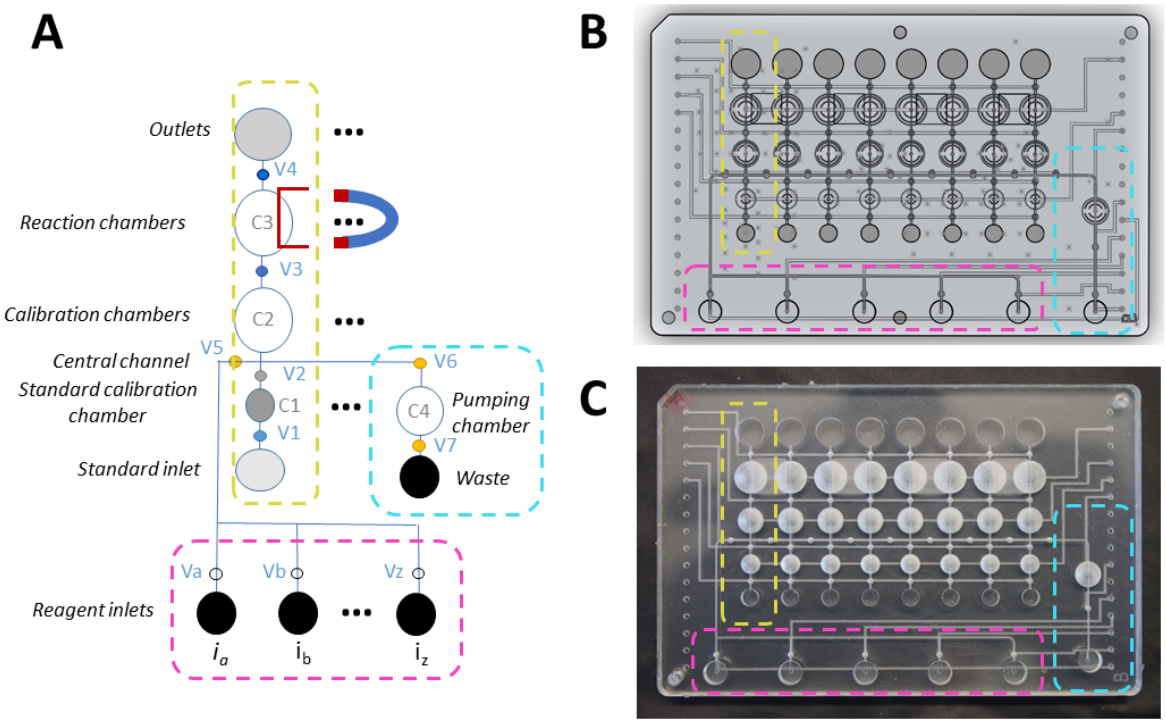

Figure 4.14: Microfluidic **cartridge SP** for magnetic beads sample preparation protocols (A) Schematic view of the unitary module. Rows of valves (V1 to V4) and chambers (C1, C2, C3) are connected pneumatically and actuated simultaneously. Each reagent inlet is controlled independently (Va to Vz, depending on the number of inlets). A system with a central channel at the exit and a pumping chamber is used to drain fluids to waste. The red half square corresponds to the position of the external magnet. (B) CAD of the microfluidic cartridge. (C) Picture of the cartridge after fabrication

can be transferred into the reaction chambers C3 (50 μL). Between each inlet activation, the central channel is washed by passing a washing solution in it. The standard solutions are added in the standard inlets from which 10 μL of fluid are calibrated in chamber C1. The solution can then be transferred in the reaction chamber C3. A location site for magnets is localized above the chamber C3, which can be activated with the motorized arm on the instrument. This latter helps to perform the various magnetic beads manipulation: magnetic beads injection, washing and resuspension. Pressure ramps with 15 mbar steps are used to ensure correct draining of fluids. Sample mixing can be achieved on chip by transferring way and back the solution from chamber C2 to C3. Finally, the fluid can be transferred to the outlet and withdrawn for further analysis.

The sample preparation cartridge is designed specifically for the troponin iLAMP protocols described in chapter 3. The fluidic basic functions to perform this type of protocol are detailed in figure 4.15 and functions as follow:

- Step 1: Magnetic beads are injected in reagent inlet i_a and transferred into the calibration chamber C2 (40 μL) and the reaction chamber C3 (50 μL). The magnet is pushed down onto the microfluidic cartridge and attracts the magnetic beads [169]. A pressure ramp (15 mbar) is used to withdraw slowly the fluid from the reaction chambers to the waste.

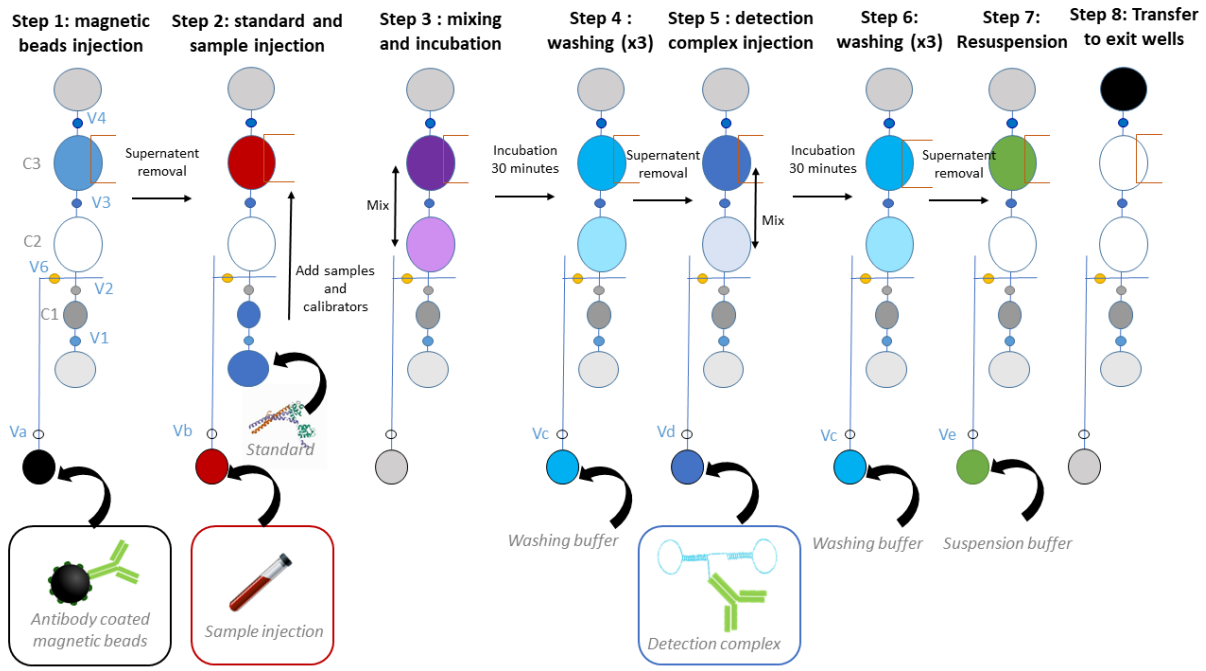

Figure 4.15: Working principle of the troponin assay in cartridge SP. The figures shows a schematic top view of the unitary module for each step of the protocol: magnetic beads injection (step 1), standards and sample injection (step 2), mixing and incubation (step 3), washing (step 4), detection complex injection (step 5), washing (step 6), resuspension (step 7) and transfer to outlets (step 8).

- Step 2: The reaction medium (buffer, plasma, blood sample), is added in reagent inlet i_b and passed into the calibration chambers C2, and then into the reaction chambers C3 to resuspend the magnetic beads into the sample. Troponin standards concentrations are added in the standard inlets, and 10 10 μL of standards are calibrated through C1. The standards are transferred from C1 to C2 and then reaction chamber C3 with the magnetic beads and sample. The full resuspension of magnetic beads is achieved by moving way and back the solution between chamber C2 and C3.
- Step 3: The solution in C3 is incubated for 30 minutes with mixing (transfer between C3 and C2) every 15 seconds.
- Step 4: The magnetic arm is pushed down, and a pressure ramp (15 mbar) is used to withdraw the liquid after incubation from chamber C3 to the waste. Then, reagent inlet i_c is used to add WB in the chamber C2, which is transferred to the reaction chamber to resuspend the magnetic beads. The magnetic arm is then again pushed down and this same procedure is applied thrice for a total of three washes.
- Step 5: The detection complex made of the detection antibody coupled to the dumbbell oligonucleotide is added in reagent inlet i_d and passed into chamber C2 and then C3. The magnetic beads with troponin captured are resuspended in this solution by mixing (transfer between C2 and C3), and incubated for 30 minutes.
- Step 6: Washing (3x), similar procedure to step 4.
- Step 7: The reagent inlet i_e is used to calibrate 40 μL of buffer in C2, which is transfered in C3 and resuspend the magnetic beads.

- Step 8: the magnetic beads solution is passed slowly from the reaction chambers C3 into the oulets with a pressure ramp (15 mbar), and the solution is withdrawn by pipetting for further LAMP analysis (in tubes using commercial instruments).

Prior to the first use, the cartridge is incubated at least one hour with PBS and 1 % BSA to prevent the binding of proteins on the cartridge surfaces. After use, washing of the cartridge is achieved with the following procedure: (i) washing all chambers with WB, (ii) incubation of all chambers with decontaminant (RNAse AWAY)for 30 minutes, (iii) washing of the complete cartridge with WB again, and finally (iv) washing of the complete cartridge with water. The cartridge is dried with compressed air and stored for further use.

This cartridge gathers all the necessary microfluidic functions for the magnetic beads sample preparation module of the developed protocols. From the functional protocols described in figure 4.15, two versions containing 8 or 10 rows are designed and used to integrate the troponin sample preparation module. Several parameters can be tuned with this cartridge, such as the incubation times, number of washing steps, WB composition, and reagent concentrations. Indeed, translating a biological protocol from a microplate to a microfluidic cartridges changes the assay conditions and therefore many parameters need to be adapated. This will be explored in chapter 5.

4.3.2 Microfluidic cartridge for isothermal amplification

In the developed troponin iLAMP assay, the final step consists in the isothermal amplification of the solution (Fig 4.13). The previous paragraph deals with the integration of the sample preparation on magnetic beads into the microfluidic chip, but does not include the amplification reaction. The goal of this paragraph is to present the design and development of the microfluidic cartridge for the isothermal amplification. This work was part of a six-month master internship of Hélène Jousset in the LSMB laboratory in 2022. One of the project goals was to integrate the isothermal amplification protocols in the microfluidic cartridges using the FlowStretch technology. The mechanical and fluidic effects are therefore characterized, and several cartridge designs were proposed. One of the propositions deals with 10 rows of amplification chambers and places them adequately on the chip. Only the most optimal design is exposed in this paragraph together with its thermal characterization. The cartridge is experimentally validated to prove the feasibility of such protocols with this microfluidic technology.

4.3.2.1 Cartridge L architecture

The architecture presented in figure 4.16A shows the unitary module (one row) of an architecture for on-chip LAMP amplification. This latter can be declined by replicating this functional row 10 times, thus creating 2×10 amplification chambers C1 and C2. With that configuration, the cartridge amplification zone only occupies half of the chip, and therefore the cartridge can be used two times when flipped 180°.

Figure 4.17 shows the succession of steps from the reagent injection to washing to perform isothermal amplification on chip. The fluidic basic functions to perform this type of protocols are as follow:

- Step 1: The solution containing the LAMP mixture mixed with the DNA template at various concentration is added into the reagent inlets (50 μL wells).
- Step 2: Valve V1 is opened, and then chamber C1 is opened to be filled with 20 μL of liquid. This latter is then transferred into chamber C2, and 20 μL of solution is transferred again from inlet to chamber C1.

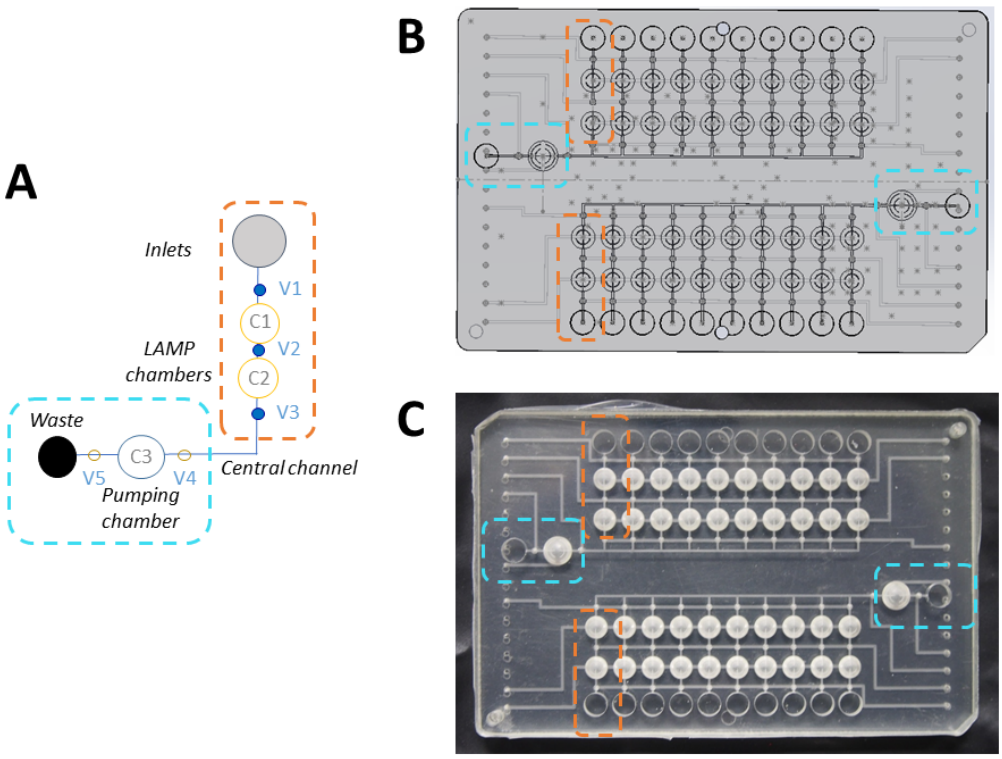

Figure 4.16: Microfluidic **cartridge L** for LAMP amplification protocols (A) Schematic view of the top unitary module. Rows of valves (V1 to V3) and chambers (C1 and C2) are connected pneumatically and actuated simultaneously. Reagent inlets are used to add the LAMP mixture and DNA template independently for each row. A system with a central channel at the exit and a pumping chamber (C3) is used to throw the liquid away after amplification. (B) CAD of the microfluidic cartridge. (C) Picture of the cartridge after fabrication

- Step 3: A liquid that stops the amplification (RNAse AWAY decontaminant) is added into the inlet to inhibit the reaction with the remaining reagent in the inlets.
- Step 4: Isothermal amplification (65°C). During this step, the inlets are isolated from the outside by adding a MicroAmp film.
- Step 5: After the amplification, the solutions are thrown away in the waste. Pumping chambers C2 and associated valves (V4 and V5) are opened, and the LAMP chambers are successively closed (in the order C2, V2, C2 and V1).
- Step 6: Washing procedure by passing decontaminant (RNAse AWAY) through the chambers to wash away the amplified DNA.

During step 4, LAMP isothermal amplification requires a precise thermal management of the fluid on chip. Indeed, the reaction mixture inside the chambers needs to be maintained at 65°C for the DNA amplification. Therefore, the temperature inside the chambers needs to be precisely controlled. Hence, we performed a theoretical thermal characterization of the heat conduction on chip.

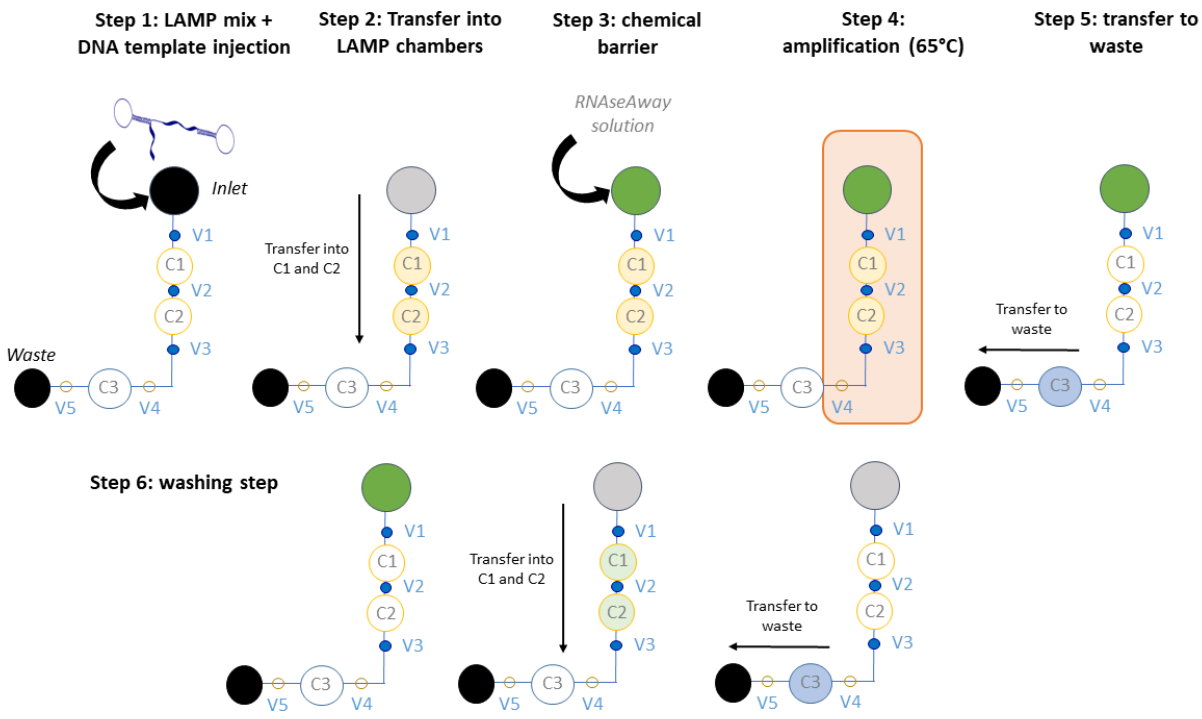

Figure 4.17: Schematic top view of the unitary module for each step of the amplification protocol in cartridge L: DNA and LAMP mix injection (step 1), transfer into reaction chambers (step 2), Decontaminant (RNAse AWAY) injection (step 3), amplification at 65°C (step 4), transfer into waste (step 5), and finally washing procedure using RNAse AWAY decontaminant (step 6).

4.3.2.2 Thermal characterization

A first way to evaluate the heat transfer on chip is to use a simplified 1D model consisting of the different microfluidic layers placed above each other. This helps to get an overview of the temperature distribution vertically across the system and thus characterize the heat losses. The system is represented vertically in 1D with the different subunits (heating source, microfluidic layers etc...), and we use the electrical analogy to compute the thermal resistance of the different subunits. Figure 4.18 shows the electrical-thermal analogy and the 1D representation of the microfluidic assembly and the heating module. Figure 4.19 shows the temperature variation across the different layers after the computation with the electrical analogy. This model was tuned to determine which input temperature the Peltier should input in order to get about 65°C at the chamber location (across the membrane). The temperature drops linearly in the polymeric layers, and the Peltier input temperature was found to be about 75°C in order to get 65°C in the microfluidic chambers (between the fluidic and pneumatic layer). We also found that the temperature drop across the membrane is rather low due to its small thickness, thus this component can be removed in further models. This first model only allowed to compute the thermal variation accross the microfluidic chip assembly, but without any microfluidic chambers and channels. We therefore implemented another model with a layer that would mimic a microfluidic chamber. This was done by adding a 2 mm layer of water between the pneumatic and fluidic layers (appendix E). This way, we evaluated a temperature drop of about 1°C across a microfluidic chamber placed on the cartridge. Thus, the microfluidic chambers reduce the heat losses in the cartridge, and should therefore improve the chip thermal conduction.

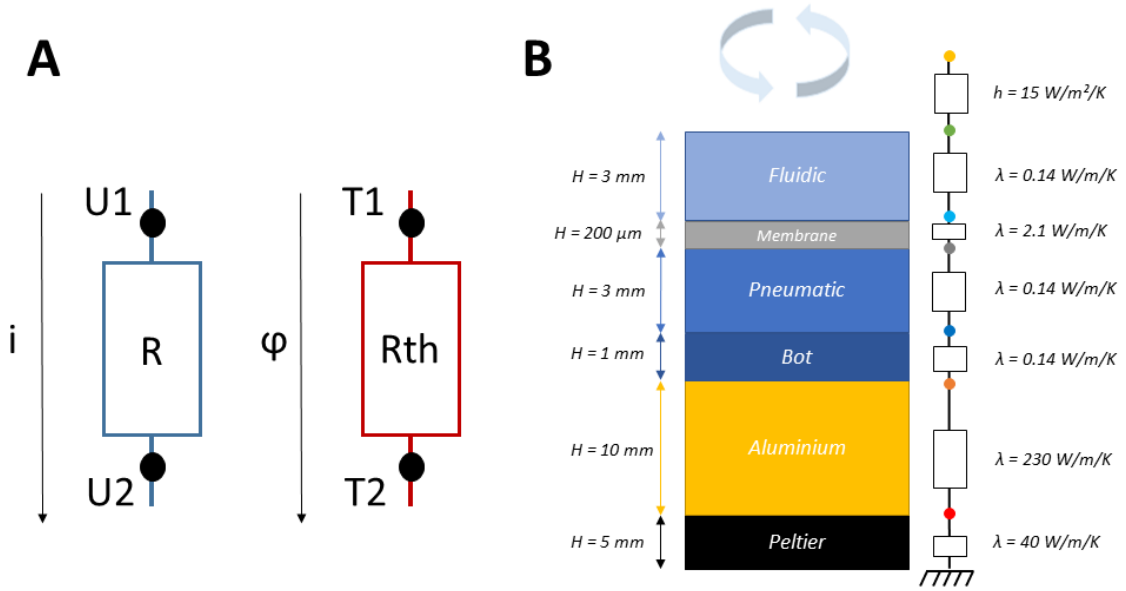

Figure 4.18: (A) Thermal-electrical resistance analogy and (B) 1D representation of the microfluidic chip layers and thermal module with their resistance and intermediate temperature

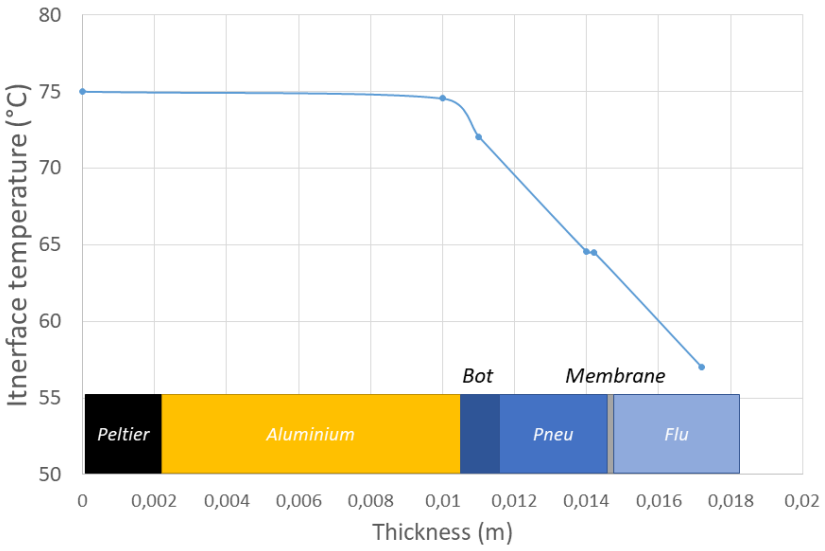

Figure 4.19: Temperature variation across the different system assembly layers (Peltier, aluminium block and microfluidic cartridge layers)

This study of the chip thermal response allows the theoretical characterization of the temperature inside the microfluidic cartridge layers. It highlights important temperature losses across the COC pneumatic and fluidic layers (above 5°C) as well as the reduction in heat losses with the presence of liquid in microfluidic chambers. However, this model does not account for the temperature distribution on a horizontal plane with various chambers as described in

the cartridge designs. Moreover, this model highlighted the importance of microfluidic chambers for heat transfer, and should be characterized with correct location on a horizontal plane. Therefore, we implemented a 2D model of the heat transfer on chip with the simulation software COMSOL Multiphysics®on a vertical plane across the microfluidic chip assembly. This was a way to cross-validate both the 1D analogy and the correct physics implementation of the heat transfer in the system with the COMSOL®software.

We also implemented a 3D model of the system with the complete cartridge and microfluidic chamber locations. This helps us to obtain the temperature variation across a horizontal axis on chip. This information is crucial to help determine the optimal chamber location for isothermal amplification. The cartridge material parameters and geometry can be found in table 4.3.

Layer	Surface (m^2)	Thickness (mm)	ρ (kg/m^3)	λ (W/m/K)	C_p (J/kg/K)
Aluminium	0.0045	10	2700	238	900
Bot COC	0.0045	1	1200	0.14	1470
Pneu COC	0.0045	1	1200	0.14	1470
Silicone EcoFlex	0.0045	0.2	250	2.1	1460
Fluidic COC	0.0045	1	1200	0.14	1470

Table 4.3: System parameters for implementation in COMSOL Multiphysics ®

A stationary study was performed and we plot the temperature across a horizontal layer placed in between the pneumatic and fluidic layers (Fig 4.20A), and across a vertical layer (Fig 4.20B). The simulation of 10 microfluidic chambers with water inside is added to make the model more realistic and characterize the exact temperature inside the chambers. An input temperature of 75°C on the Peltier was given based on 1D simulation results.

Figure 4.20A highlights clearly a square area where the temperature is the closest to the desired value of 65°C. In figure 4.20B, we can see that the areas where the temperature is comprised between 60°C and 65°C corresponds greatly with the microfluidic chambers' location. Differently from the simplified 1D model of heat transfer, the temperature drop in the chambers is about 2°C. This can be explain by the more realistic cartridge geometry representation in the COMSOL Multiphysics ®software, and the inclusion of the pneumatic channels filled with air below the chambers.

The mean temperature inside each chamber is computed and plotted (Fig 4.21B). Except for the two extreme chambers of each rows which temperature varies around 60°C, each other chamber has a temperature that varies around 64°C with less than 1°C variation between chambers.

Secondly, a temporal study of the chip heat distribution was conducted. We ran other simulations with time dependence, and characterized the time to reach the desired stabilization temperature inside the chamber. This serves as a way to evaluate the transition time and to cross-validate the COMSOL ®model implementation by comparing the model results with experimental data. To do so, we drilled a hole in the upper COC (fluidic) layer in the microfluidic cartridge, in order to insert a thermocouple into a microfluidic chamber. This way, we measured the increase in temperature with water inside the chamber, straight after an instruction of 75°C given on the Peltier module. The temperature curve over time (20 minutes) are exposed in figure 4.22.

The temporal temperature curves shown in figure 4.22 confirm the correct implementation of the system geometry and physics in COMSOL ®. It takes between 5 and 10 minutes to reach a stable temperature inside a microfluidic chamber. This stabilization time needs to be included during the isothermal amplification protocols, as a delay time. Either the chip needs to be warmed 10 minutes beforehand, or this delay time needs to be substracted in the obtained

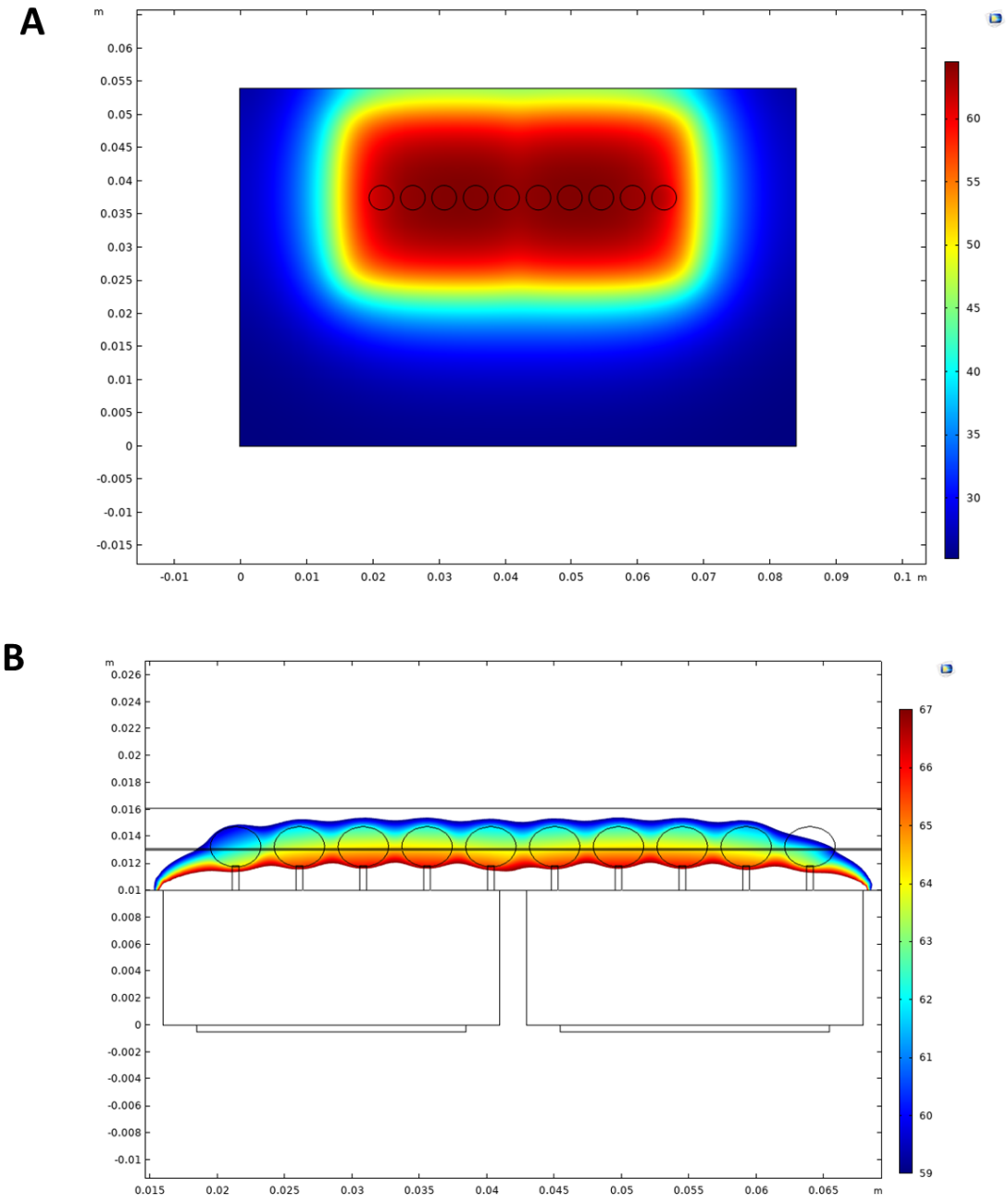

Figure 4.20: Cartridge L temperature profile in celcius (A) on a horizontal plane placed between the fluidic and pneumatic layers and (B) on a vertical plane located at X = 38 mm.

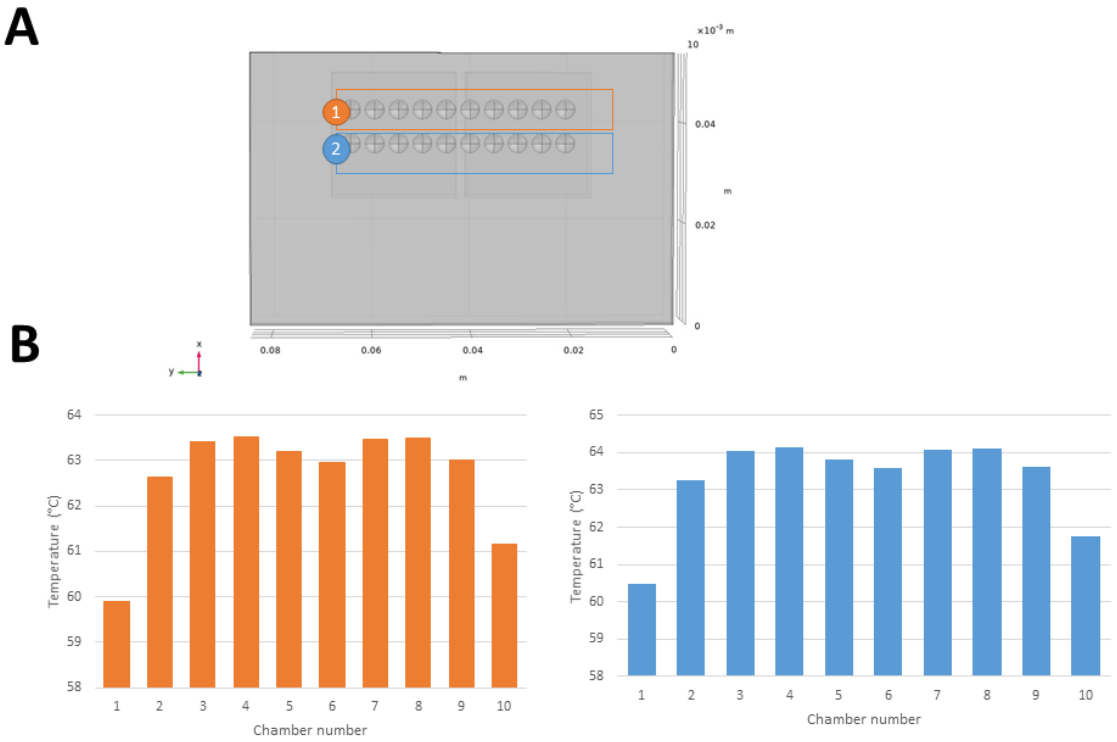

Figure 4.21: Thermal characterization of the microfluidic cartridge for LAMP amplification. (A) Schematic of the chip in the COMSOL® software. (B) Mean temperature inside each chambers. Chambers are numbered from 1 to 10 from left to right.

amplification times Tp.

Interestingly, there is a difference of roughly 5°C between the COMSOL ®simulation results and the experimental data. During the experimental data acquisition, a hole was drilled into the top fluidic layer of the microfluidic chip to insert the thermocouple. This led to a different physical system since there was an air channel above the microfluidic chamber. Therefore, the drilled hole might have induced more heat dissipation with the air contact, which led to an underestimation of the experimental temperature. However, both theoretical and experimental curves have a similar shape and this still confirms the validity of the model. The COMSOL ®simulation is however simplified, the chip is not placed on the instrument which might change the system boundary conditions and the convection that can occur. Elementary microfluidic components such as pneumatic and fluidic channels, microvalves were also not considered in the model because their size and impact were small.

From the simulation of heat distribution in cartridge L, we characterized the temperature inside the microfluidic chambers dedicated to LAMP amplification protocols, and we obtained a temperature of 64°C in most of the chambers (16/20). This cartridge should therefore be functional for isothermal amplification protocols and will be experimentally validated in chapter 5.

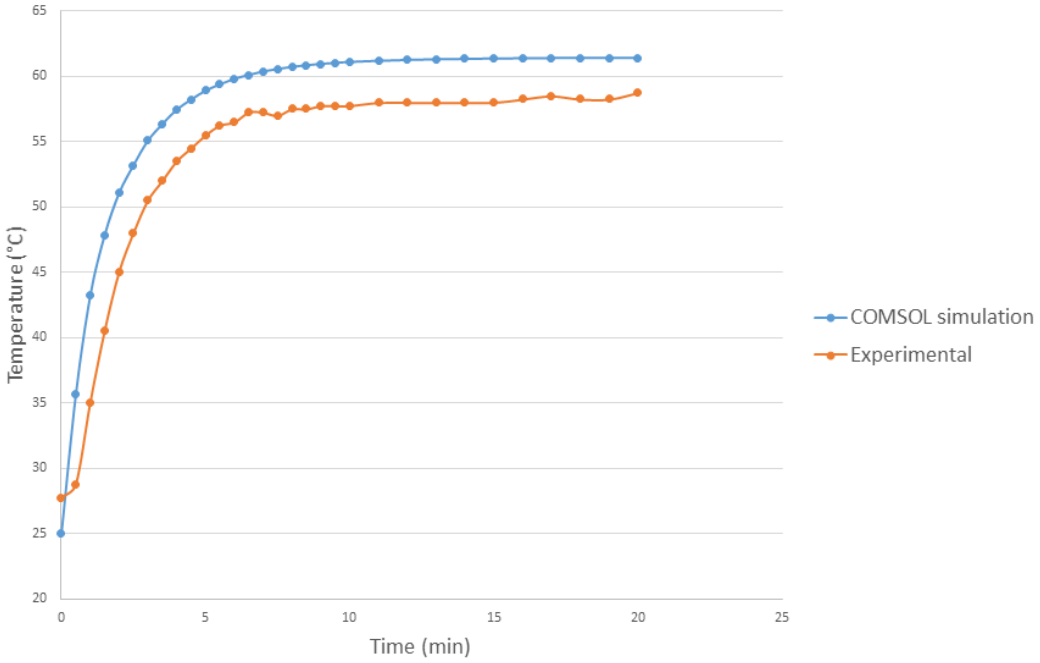

Figure 4.22: Temperature over time inside a microfluidic chamber for the theoretical COMSOL ®time-dependant study (blue) and experimental data with a thermocouple inserted in the chamber (orange)

4.3.3 Microfluidic cartridges for complete protocol automation

Two cartridges have been designed and exposed, to integrate (i) the magnetic beads sample preparation protocols (**cartridge SP**), and (ii) the isothermal amplification protocols (**cartridge L**) independently. We finally combine those two cartridges and expose an ultimate microfluidic chip for complete protocol integration, from sample preparation to final isothermal amplification, named **cartridge C**.

4.3.3.1 Cartridge C architecture

The unitary module of the complete microfluidic cartridge is presented in figure 4.24. This latter is similar to the sample preparation cartridge SP but comprises two last rows for the amplification reaction, and an additional waste system. Therefore, this cartridge is designed by replacing the outlet of the sample preparation cartridge by the two amplification chambers of the isothermal amplification cartridge. The inlet from the amplification cartridge becomes the reaction chamber from the sample preparation cartridge. This procedure to design the complete protocol cartridge is exposed in figure 4.23.

Before its use for complete protocol integration, the cartridge was tested and optimized for functional isothermal amplification (LAMP¨). This was done using the following procedure (Fig 4.25):

- Step 1: The LAMP mix reagents are added on reagent inlet i_a, and drained to calibration chamber C2 (40 μL).
- Step 2: DNA templates (dumbbells) at various concentrations are added in the sample

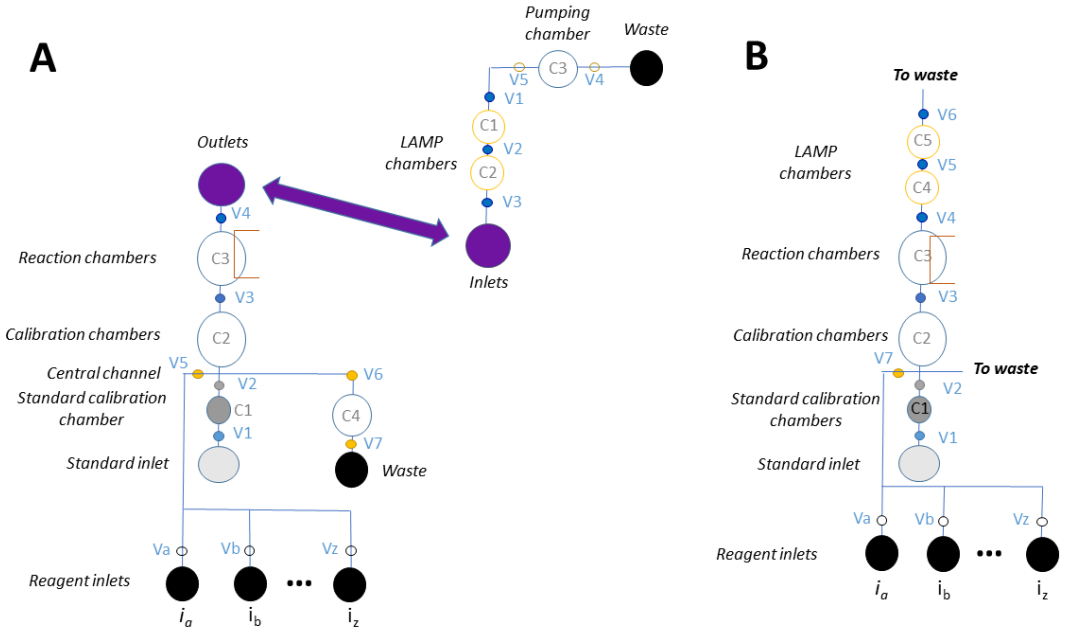

Figure 4.23: Complete microfluidic cartridge C architecture (A) Functional schematic of the unitary modules of sample preparation and isothermal amplification cartridges. The sample preparation cartridge outlet is removed, and the isothermal amplification cartridge inlet is also removed (the link between the two architectures is achieved through the reaction chamber) (B) Functional schematic of the unitary unit of the complete protocol cartridge C.

inlets, and calibrated in the sample calibration chambers C1 (10 μL).

- Step 3: Chambers C1 and C2 contents are slowly transferred into the reaction chamber C3 (50 μL) with a pressure ramp (25 mbar). Then, the solution is mixed by transferring the liquid back and forth between chambers C2 and C3. Pressure ramps (25 mbar) are also used to limit the bubble formation during the mixing.

- Step 4: From chamber C3, the amplification solution is transferred in the LAMP chambers C4 and C5 (20 μL each), with a pressure ramp (25 mbar) to limit the air injection and bubble formation. Once the amplification solution is filled in the chambers C4 and C5, the intermediate valve V5 is kept opened (-150 mbar).

- Step 5: Before the start of the amplification, the reagent inlet i_a is used to inject decontaminant RNAse AWAY solution into chamber C2. This decontaminating solution is mixed in chamber C3 to remove the excess amplification mixture and inhibit a potential amplification. The RNAse AWAY solution is stored in chamber C2 to form a chemical barrier in order to avoid any contamination in the microfluidic cartridges with the amplification reaction taking place in the chambers C4 and C5.

- Step 6: Isothermal amplification reaction (65°C)

- Step 7: After the amplification reaction, the solution in chambers C4 and C5 is evacuated to the waste dedicated to the LAMP amplification at the top of the cartridge. The RNAse AWAY solution stored in chamber C2 is transferred into chambers C3, C4 and C5, with mixing and then transferred to the waste.

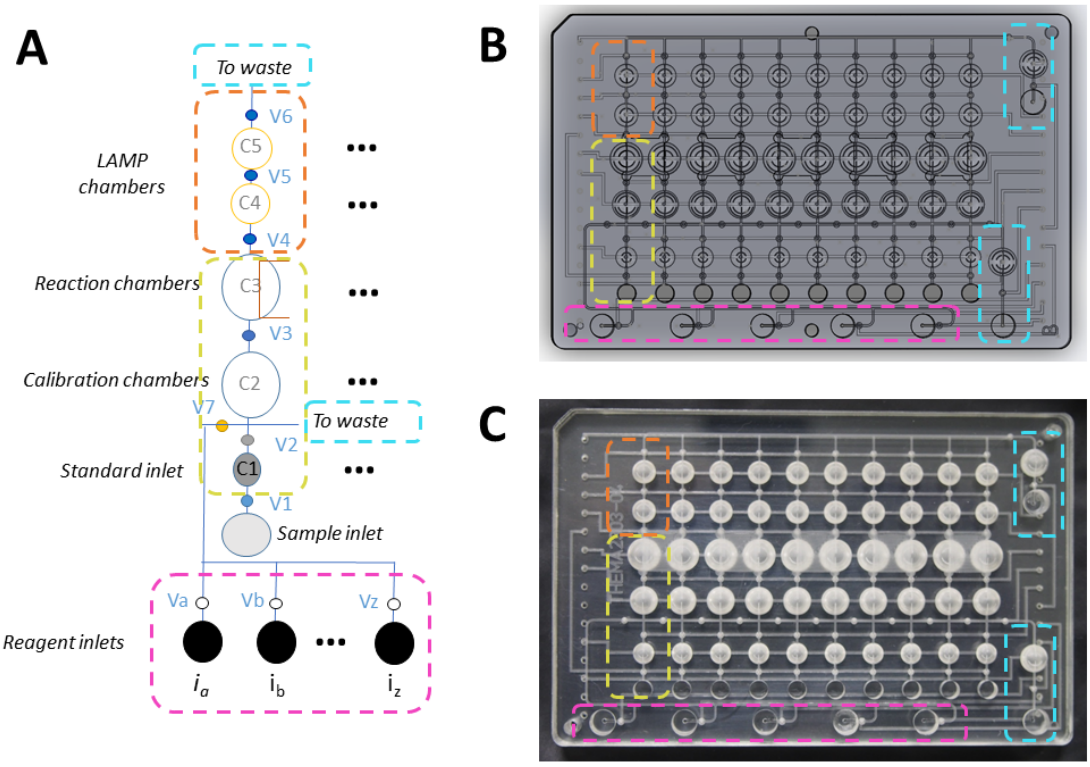

Figure 4.24: Microfluidic **cartridge C** for complete troponin detection protocol automation (A) Schematic view of the unitary module. Rows of valves (V1 to V6) and chambers (C1 to C5) are connected pneumatically and actuated simultaneously. Each reagent inlet is controlled independently (Va to Vz). Waste systems with a central channel at the exit of (i) the reagent inlet and (ii) the amplification chambers are used to drain dead volume and liquid to waste. The red half square corresponds to the position of the external magnet. (B) CAD of the microfluidic cartridge. (C) Picture of the cartridge after fabrication

- 8 : Lastly, RNAse AWAY solution is spread in all the cartridge chambers and incubated for 30 minutes. The solution is then removed to the waste, and the cartridge is fully rinsed with a PBS Tween solution (5 times) and with water (5 times).

This microfluidic cartridge C architecture and function for isothermal amplification protocols are described in figure 4.25. In a similar way than for the cartridge L dedicated only to LAMP protocols, a thermal characterization of the chip temperature is achieved in order to obtain the suitable temperature for isothermal amplification on chip.

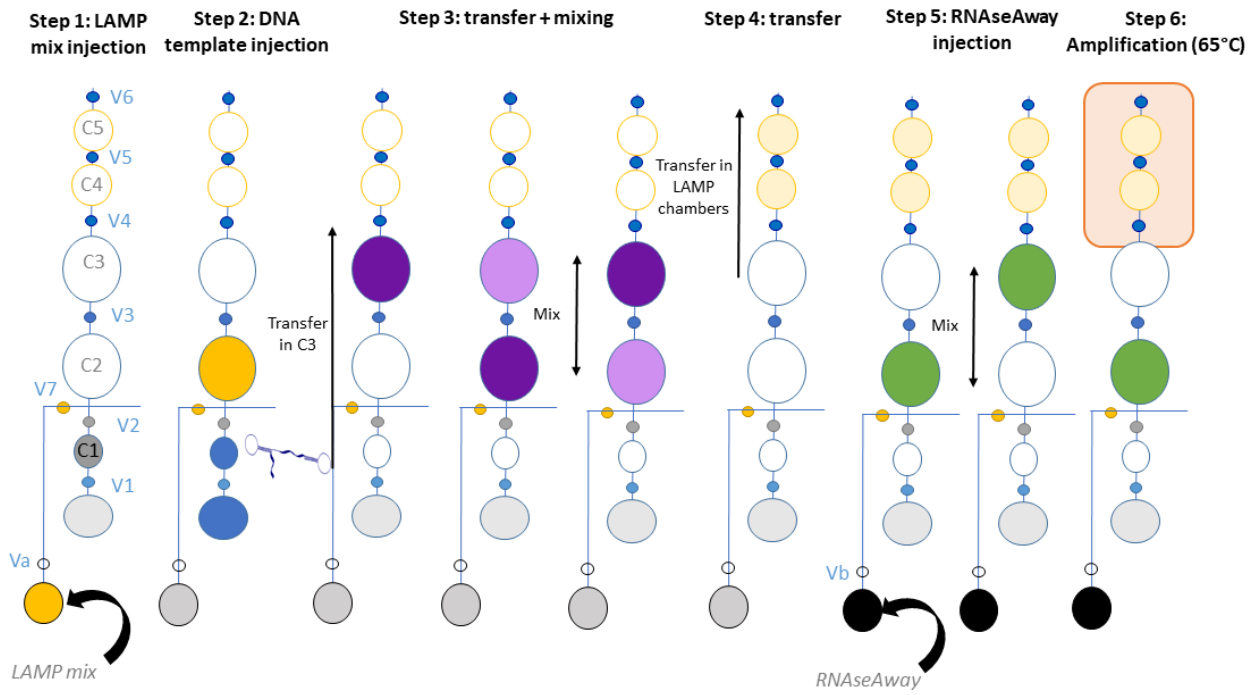

Figure 4.25: Schematic view of the unitary module for each step of the amplification protocol carried out in the complete protocol cartridge C. LAMP mix injection (step 1), DNA template injection in standard inlet (step 2), transfer in chambers C2 and C3 and mixing (step 4), transfer into amplification chambers C4 and C5 (step 4), RNAse AWAY injection and transfer into chamber C2 (step 5) and finally amplification at 65°C (step 6)

4.3.3.2 Thermal characterization

In the design of cartridge C, we kept the same double row of 10 microfluidic chambers as was described in cartridge L. However, due to constraints in the geometry for the combination of the magnetic beads sample preparation module, the exact positions of the LAMP chambers on the cartridge was changed. Therefore, based on the simulation results exposed for the cartridge L and in a similar way, we simulated the temperature distribution in the cartridge with this new architecture and LAMP chambers positions.

An horizontal cut was drawn between the cartridge fluidic and pneumatic layer, and the thermal profile was plotted (Fig 4.26A). This vertical layer seems to exhibits homogeneous temperature of about 64°C from chambers 3 to 9 (yellow area). These results are confirmed with the plot of the mean temperature inside each chambers (Fig 4.26B), with a computed average temperature of 63 ± 1°C.

Cartridge C architecture is suitable for isothermal amplification protocols in the chambers C4 and C5, which temperature was theoretically evaluated to be about 63°C in most of the chambers (14/20). This cartridge should therefore be functional for isothermal amplification protocols and will be tested experimentally in chapter 5.

The cartridge C design was inspired from the sample preparation and LAMP amplification modules. We will first validate cartridge C suitability for isothermal amplification, but since

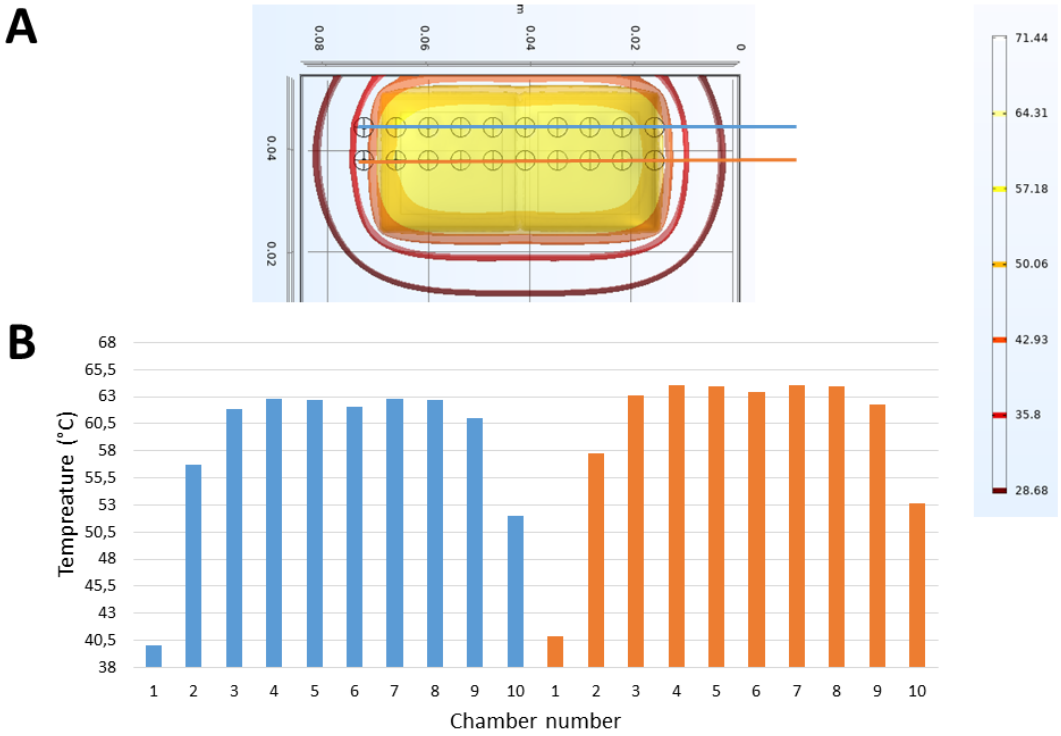

Figure 4.26: Thermal characterization of the microfluidic cartridge C for LAMP amplification. (A) Heat distribution in Celsius on an horizontal line on chip with the COMSOL ®software. (B) Mean temperature inside each chambers. Chambers are numbered from 1 to 10 from left to right.

the cartridge also include the functions for the initial sample preparation parts of the iLAMP protocols, the cartridge could further be used for the full iLAMP protocol automation. This will be considered in chapter 5.

4.4 Conclusion and perspectives

This chapter presented the latest developments of POC devices for cardiovascular diseases diagnosis. The important developments of microfluidic technologies over the last decades enabled the development of new POC devices with interesting performances (portability, time, sensitivity, sample consumption...). This lead to very promising applications of microfluidic in the field of POC equipments for portable and fast diagnostic devices. There is a joint development of various microfluidic technologies and their instrumentation to design powerful POC devices.

In the context of cardiac biomarkers, we aimed to integrate the iLAMP assay described in chapter 3 with the example of troponin tests, that could alternatively be applied to other cardiac biomarkers. This assay combines immunocapture on magnetic beads and nucleic acids amplification. As observed previously in the literature, the manipulation of magnetic beads in microfluidic devices is already described in several ways [169], as well as carrying nucleic acids isothermal amplification protocols on chip [172, 173, 174], but new challenge arise to combine both steps in a single cartridge and device.

We based our engineering and developments on the expertise and skills at the LSMB laboratory. The FlowPad platform proposes a compact device with required hardware components for pneumatically actuated FlowStretch microfluidic cartridges [56]. Those cartridges take advantage of digital microfluidic technology to handle broad range of volumes in an automated way. This technology was already validated for ELISA immunoassays and its versatility ensured a good compatibility with other types of assays [169].

To integrate the iLAMP protocols, we included several additional hardware components on the FlowPad platform: a thermal module to provide the microfluidic chip with an homogeneous temperature in the reaction chambers, and an optical module to stimulates the fluorescence in the solution and record it over time during the amplification reaction. Cartridges architectures were proposed to integrate each assay steps using digital microfluidic and taking advantage of the possible full automation of basic operations such as volume calibration, mixing, washing etc... Three main cartridge architectures were proposed, for the magnetic beads sample preparation (cartridge SP), for the isothermal amplification (cartridge L) and for the complete protocole integration (cartridge C). We described the fluidic functions and operations of each cartridge for each step of the generic iLAMP protocol. The combination of the enhanced FlowPad platform and the microfluidic cartridges architecture should ensure the complete integration and automation of the iLAMP assay.

There are still some challenges to tackle for the development of a portable instrument for cardiac POC detection. The chosen microfluidic actuation principle relies on pressure controllers that needs to be connected to a vacuum and compressed air source. This makes the pneumatic system quite bulky, but considering the low actuation pressure used in the technology, portable pumps could be considered and thus reduce the system size. Additionally, the optical system to record the fluorescence is the most bulky and fragile part of the system, since it requires careful alignment due to the large field to image on the credit size microfluidic cartridge, and therefore the need for broad optical path lengths with the camera and LED. Lately in the field of microfluidics for POC diagnostic, alternative optical portable detection method emerged with for example the use of smartphone imaging [134, 175]. Despite its important portability and ease-of-use, this imaging technique is often limited to colorimetric detection [134] or requires the addition of several components on the smartphone to allow a quantitative image analysis [175]. Lastly, sustainable developments is an important matter for the design of POC diagnsotic devices, and several improvements could be implemented on the developed platform [159]. The important number of hardware connections on the instrument requires many electronic connections, which

are all limited to 24V and 3A, but this power consumption could be reduced with adequate engineering for each hardware module added on the system. Moreover, the designed cartridge are quite long and complex to manufacture, therefore a special attention should be given to their re-usability for successive assays.

The versatility of the chosen microfluidic technology and cartridge architecture opens several ways for future developments and applications. First, the cartridges are generic enough so that it could be used with similar detection protocols for other targets. Lastly, the number of rows presented in the cartridge is rather important (8-10) and therefore can lead the way to the multiplex target detection in a single cartridge, by partionning the detection rows to different targets. Lastly, the LAMP amplification protocols are generic and common to many other type of targets, which therefore shows the promises of this cartridge use for various types of assays [173].

Summary

- A generic instrument for microfluidic cartridge pneumatic actuation, magnetic beads manipulation, thermal heating, and fluorescence detection was described for the integration of iLAMP protocol
- Three different microfluidic cartridges for the integration of the differents steps in the iLAMP protocols are described, with their operating way.
- Cartridge SP is dedicated to magnetic beads preparation module for troponin capture.
- Cartridge L is dedicated to LAMP isothermal amplification protocols validation and thermal chararcterization implementation.
- Cartridge C is proposed for the complete iLAMP protocol integration, from sample preparation for troponin capture to LAMP isothermal amplification. This cartridge is characterized thermally and its operating way for isothermal amplification protocols is described.

Chapter 5

Detection of cardiac biomarkers on an automated and portable platform

Objectives

- A summary of microfluidic technologies for isothermal amplification will be given
- The use of the platform described in chapter 4 is exemplified with the various developed microfluidic cartridges and their associated biological protocols
- The sample preparation cartridge SP is first validated with a simplified magnetic beads based protocol for sandwich oligonucleotide detection
- Troponin capture is achieved on-chip in the sample preparation cartridge SP in both buffer and plasma samples
- On-chip isothermal amplification is studied and tested with the two cartridge architectures (cartridge L and C)
- Complete cartridge C is considered for full iLAMP protocol automation

For the development of POC diagnostic devices, microfluidic technologies and their associated instrumentation benchtops are very powerful tools, allowing the development of rapid, simple, automated and easy to use platforms. The various technologies allow the integration of a broad range of biological assays. We have described in chapter 4 a portable instrument and its associated cartridges to integrate biological protocols in an automated way. This instrument should allow the equipment-free and delivered implementation of biological protocols in a rapid and user-friendly way. This portable and generic platform will now serve as a tool for the portable detection of cardiac biomarkers, specially with the example of troponin detection.

The iLAMP assay developed and described in chapter 3 for the troponin detection are integrated on the designed microfluidic cartridges. This assay includes magnetic beads based sample preparation and signal readout with fluorescence recording during dumbbell isothermal amplification. The several steps employed in the troponin iLAMP assay highlight the use of the complete microfluidic cartridge embedding many steps such as sample injection, magnetic beads based capture, washing, incubation, mixing etc... Therefore, the microfluidic cartridge developments, tests and validations will be implemented by order of complexity to validate the different modules. First, the microfluidic cartridge sample preparation module based on magnetic beads will be validated. Secondly, the on-chip isothermal amplification will be tested with a dedicated module, and finally, the isothermal amplification will be tested on a complete

cartridge including both sample preparation and isothermal amplification module.

The combination of the fully-integrated microfluidic chip and the innovative iLAMP troponin assay should ensure a sensitive troponin detection on a portable and automated platform.

5.1 State of the Art: isothermal amplification on microfluidic chip

Several POC platforms integrating microfluidic technologies for the detection of cardiac biomarkers have already been described [1]. We designed microfluidic cartridges for the integration of the sample preparation module to capture cardiac biomarkers. In our developed assay, the final step of the protocol is the isothermal amplification (LAMP). This section will focus and present some microfluidic technologies implemented and dedicated for LAMP isothermal amplification on-chip, and discuss their technological choices and implementations, as well as their analytical performances and assay time.

Nucleic acids amplification techniques have played an important role in POC diagnostic, by delivering detection from biological samples at a relatively low concentration [176]. Amongst nucleic acids amplification techniques, the LAMP developed since the beginning of the 21^{st} century and greatly used over the past two decades has emerged as a powerful molecular diagnostic tool [173] [111]. Its rapidity, specificity, sensitivity and robustness make it very advantageous to use in various detections such as medical diagnosis, environment, agriculture etc... This nucleic acids amplification technique is particularly interesting over PCR for its integration into a POC device due to its isothermal characteristics, removing the need for bulky thermal control equipment [176] [172] [173]. To develop POC systems for nucleic acids amplification, microfluidic technologies and devices have enable the possibility to develop a system that provides with a "sample-in-result-out" that enhances the analysis and delivers rapid detection with high sensitivity [173]. Therefore, LAMP-on-a-chip systems represent advanced solutions for POC diagnostic. Particularly in recent years it has become an important source of various microfluidic developments with the spread of the Covid-19 virus and the need for powerful, rapid and robust diagnostic tools [176].

This section will review different types of implementation of LAMP-on-chip protocols. Since the biological assay developed during this project includes a final step of isothermal amplification that will be integrated on-chip, it was interesting to review the different possible integration. Two main aspects will be considered: (i) systems with real-time fluorescence detection for quantitative analysis and (ii) systems with integrated sample preparation based on magnetic beads for similarity with the troponin iLAMP protocol.

5.1.1 LAMP-on-chip with real-time fluorescence detection

In order to propose a LAMP-on-chip system giving quantitative results for precise diagnosis, real-time signal readout is often a key parameter compared to end-point analysis [174] [176]. Indeed, the quantification of troponin with the proposed iLAMP assay occurs after real-time fluorescence detection in solution. Several examples of LAMP-on-chip systems including real-time fluorescence detection have been described and combinated with various microfluidic chip technologies.

In 2021, Nguyen et al. described a centrifugation-chip-based, fully integrated portable genetic analyzer for multiplex RT-LAMP detection of Sars-Cov2 [161]. The centrifugal chip (Fig 5.1A) allows the simultaneous detection of 10 samples with the integration of the multiple steps including RNA purification, multiplex RT-LAMP and real-time fluorescence detection. The structure of the disc is shown in figure 5.1A and it contains chambers connected with zigzag

channels and a glass filter column for RNA extraction. The chip uses passive valves and capillary pressure to enable the automatic sample distribution in chambers, and centrifugal force is used to perform the washing and elution steps. The system has a detection limit of 20 copies/μL in about 1.5 hours.

With a similar centrifugation force principle, Loo et al. described in 2017 a sample-to-answer molecular diagnostic tool for bacterial infection on a lab-on-a-disc [177]. Their platform includes a circular microfluidic chip that allows the automation of sequential analytical steps in bacterial detection (Fig 5.1C). The platform relies on the centrifugation force for the actuation of sample reagents, and performs the three major functions: DNA extraction, isothermal amplification and real-time detection. The disc contains chemical lysis buffer and silica microbeads for DNA extraction. The system was applied to detect *Mycobacterium tuberculosis* and *Acinetobacter baumanii* within 2h after sample loading and with a detection limit of 10^3 cfu/mL in sputum and 10^2 cfu/mL in blood.

Lastly, a fully integrated rotary-valve assisted microfluidic device was described in 2021 [178] for fully integrated nucleic acids detection coupled with CRISPR/Cas12a method. In this PMMA chip, the liquid flow and stirring was achieved with the rotary valve, and all biological reagents were pre-stored on-chip (Fig 5.1B). The full detection was completed in 80 minutes and the achieved LOD was 31 copies/reaction for the detection of *V.parahaemolyticus*.

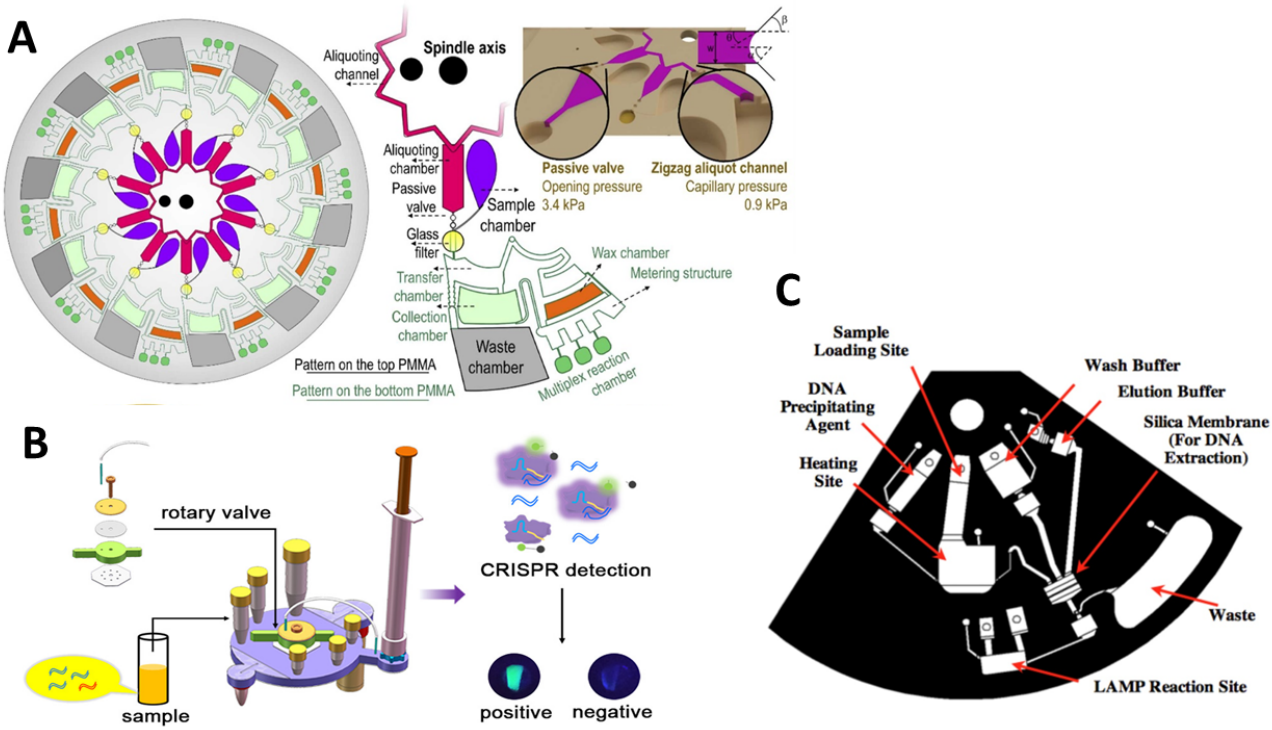

Figure 5.1: Example in the literature of LAMP on-chip with real-time fluorescence detection. (A) Layout of the microfluidic cartrdige of the centrifugal genetic analyzer for Covid-19 testing [161]. (B) Rotary valve assisted fluidic system for fully integrated nucleic acids detection [178]. (C) Lab-on-a-disc layout for sample-to-answer diagnosis of bacterial infection with isothermal amplification [177].

More complex microfluidic chips, using for example centrifugal forces or rotary valves combined with real-time detection, allow the fully integrated detection with isothermal amplification. With complete sample preparation modules, they also allow multiple sample analysis associated

with a visual detection system.

5.1.2 Fully integrated LAMP-on-chip

To perform molecular diagnosis with nucleic acids amplification, several sample preparation steps are often needed [176]. There are many types of sample preparation steps that comes prior to the amplification, for example, blood fractionation, lysis, nucleic acids extraction, and isolation etc... In this section, we review different types of fully integrated devices performing LAMP-on-a-chip for viruses and pathogens detection. We focus on devices with DNA extraction using beads (silica, magnetic), that can easily be integrated into versatile microfluidic chips, with similarities to the magnetic beads sample preparation module developed in the scope of this project. Complete microfluidic cartridges integrating the sample preparation module and the on-chip LAMP amplification have been described by several teams in the literature.

In 2011, Wang et al. [179] described a magnetic bead-based assay integrated in a microfluidic system with LAMP amplification for the detection of methicillin-resistant *Staphylococcus aureus*. The detection protocol relies on specific probe-conjugated magnetic beads to recognize specifically the target DNA from the sample. The clinical sample lysates are then mixed, purified and concentrated by applying a magnetic field. The nucleic acids amplification of the target genes is achieved on-chip through LAMP via the incorporation of a micro temperature controller. The chip layout is exposed in figure 5.2 A and is made of a glass substrate with metal electrodes, and two PDMS layers for chambers and thin membrane. The achieved LOD is found to be 10 fg/μL within 60 minutes of total reaction time.

A simple integrated microfluidic chip for the detection of bacteria with nucleic acids amplification was described in 2015 [180]. This chip contains a double layer of PDMS with silica beads for bacterial extraction, separate channels and multiple LAMP chambers. One channel is used for sample loading, and the other for washing step, and there were separated using a micro-valve to control the fluid flow (Fig 5.2B). The chip is used for the detection of 3 bacteria (*E.coli* 0157:H7, Methicillin-resistant *Staphylococcus aureus* (MRSA) and Methicillin-sensitive *Staphylococcus aureus* (MSSA)), and the detection limit was found to be 10^2 CFU/100μL with a turnaround time of about 2h.

In 2019, Ma et al. [181] described an integrated, self driven microfluidic chip for the rapid detection of influenza A virus through RT-LAMP. It is an autonomous microfluidic chip able to perform the virus isolation with aptamer conjugated magnetic beads, virus lysis, isothermal nucleic acids amplification and colorimetric detection. The chip is made of PDMS layers on a glass substrate and relies on capillary forces and hydrophobic soft valves to passively manipulates fluids (Fig 5.2D). The entire test on the system lasts 40 minutes and the LOD was found to be 3x10^{-4} hemagglutinating units (HAU)/reaction.

In 2022, Tsai et al. [182] described an electrochemically-driven integrated microfluidic platform using RT-LAMP for the detection of Sars-Cov2. The electrochemically-driven microfluidic chip (EMC) contains all the features to perform the lysis of the virus, RNA extraction, and multiple RT-LAMP analysis. The EMC is composed of a magnetic control layer, a double side tape layer, a liquid channel layer, and a glass substrate (Fig 5.2C). A succession of microvalves and micropumps allows the fluid flow control. Several areas are controlled at different temperatures for the different protocol steps: lysis (95°C), RNA capture (45°C), and RT-LAMP (60°C). The assay total time was 82 minutes for a LOD of 5000 copies/reaction.

There are various examples of fully integrated microfluidic chips performing isothermal amplifications (LAMP, RT-LAMP). Bead-based methods for sample preparation, such as DNA extraction, are often advantageous in terms of versatility and ease of integration in complete microfluidic cartridges. The isothermal amplification steps and lysis steps require a precise ther-

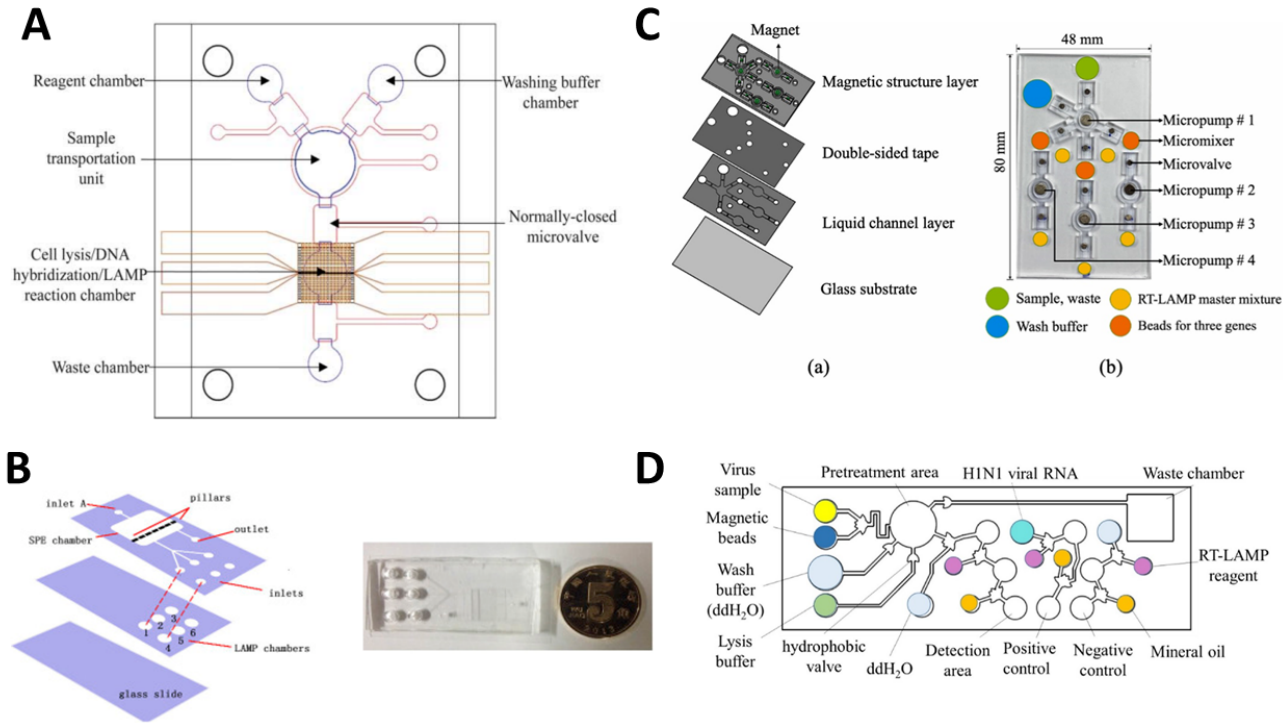

Figure 5.2: Example in the literature of LAMP on-chip including bead-based DNA extraction. (A) Layout of the microfluidic chip for magnetic bead-based assay for the detection of *Staphylococcus aureus* [179]. (B) Microfluidic device design for the detection of bacteria [180] (C) View of the electromagnetically-driven microfluidic chip for the detection of Sars-Cov2 [182]. (D) Individual components of the microfluidic chip for rapid detection of Influenza A virus by RT-LAMP [181]

mal control made possible with temperature micro controllers integrated the systems. However, the temperature required for the lysis and amplification steps is often different and therefore the chip and instrument design must be adequate to include both areas. From the sample deposition to the signal readout, there are many steps integrated within the microfluidic device which are bulky and often restrict the detection to single gene in single amplification chambers, thus limiting the wide used for multiplex detection.

A summary of the main features of the microfluidic systems for LAMP on-chip described in this section is presented in table 5.1.

Microfluidic technology appears as a very powerful tool to integrate nucleic acids amplification in POC [176]. It has a high potential for rapid, simple, high-throughput, automatic, and accurate detection. However, fully automated platforms including sample preparation, amplification, and visual detection using clinical samples are often limited [174]. These platforms often yield quantitative results, which are sufficient for virus and bacterial detection, but quantitative results are needed for other types of POC diagnostic devices, such as for the monitoring of diseases and treatments. There is a need to design fully integrated, sample-in-answer-out with quantitative result readout for the future developments of nucleic acids amplification microfluidic systems [176].

Target	**Microfluidic technology**	**Signal readout**	**Assay time LOD**	**Reference**
Sars-Cov2	Centrifugal PMMA chip	Real-time fluorescence	1.5 hours 20 copies/μL	[161]
V.parahaemolyticus	Rotary valve PMMA chip	Real-time fluorescence	80 minutes 31 copies/reaction	[178]
Bacteria *E. coli* O157:H7, MRSA, MSSA	Silica-beads PMMA	Real-time fluorescence	2h 10^2 CFU/100μL	[180]
Sars-Cov2	EMC driven mirofluidic chip	Real-time fluorescence	82 minutes 5000 copies/reaction	[182]
Staphylococcus aureus	PDMS multilayer microfluidic chip	Optical density	60 minutes 10 fg/μL	[179]
Mycobacterium tuberculosis, Acinetobacter baumanii	Centrifugal microfluidic chip	Real-time fluorescence	2h 103 cfu/mL	[177]
Influenza A	PDMS capillary microfluidic chip	Colorimetry	40 minutes 3.10^{-4} (HAU)/reaction	[181]

Table 5.1: Main features of LAMP-based microfluidic platforms

5.1.3 Objectives

Most of the LAMP-on-chip technologies presented here are used for the direct detection of viruses and pathogens. To date and to our knowledge, there are no examples of on-chip isothermal amplifications for the detection of proteins. With the detection of such analytes, new challenges arise to combine sensitive and quantitative tests to propose a precise diagnostic. In our proposed iLAMP assay for the detection of troponin, the dumbbell isothermal exponential amplifications allows to reach a high sensitivity assay and leads to possible quantification. Therefore, the on-chip integration of the dumbbell exponential amplification should allow to reach a good sensitivity and affer a fully integrated on-chip quantitative detection method.

This chapter will present some key results for the integration of a fully integrated microfluidic platform for the detection of troponin I, through the iLAMP method from the troponin capture on magnetic beads to the dumbbell isothermal amplification. The developed troponin sensing method includes a sample preparation module for troponin capture on magnetic beads and a final stage with nucleic acids isothermal amplification (LAMP). The complete instrumentation benchtop and associated cartridges functions were described in chapter 4. Each cartridge module will be validated individually in this chapter with their associated biological protocols, as exposed in figure 5.3.

First, the microfluidic cartridge sample preparation module (SP) based on magnetic beads is validated with a single stranded oligonucleotide model assay. Secondly, the on-chip troponin capture on magnetic beads is validated on the same cartridge (SP), and several sample media are tested (buffer, plasma). Lastly, two microfluidic cartridges to conduct isothermal LAMP amplification on-chip are proposed, tested and validated. The first LAMP cartridge L is used for a proof-of-concept of on-chip isothermal amplification with such technology and comprises only isothermal amplification reaction chambers. The second one (cartridge C) consists in the complete protocol integration from sample preparation to amplification reaction, and was

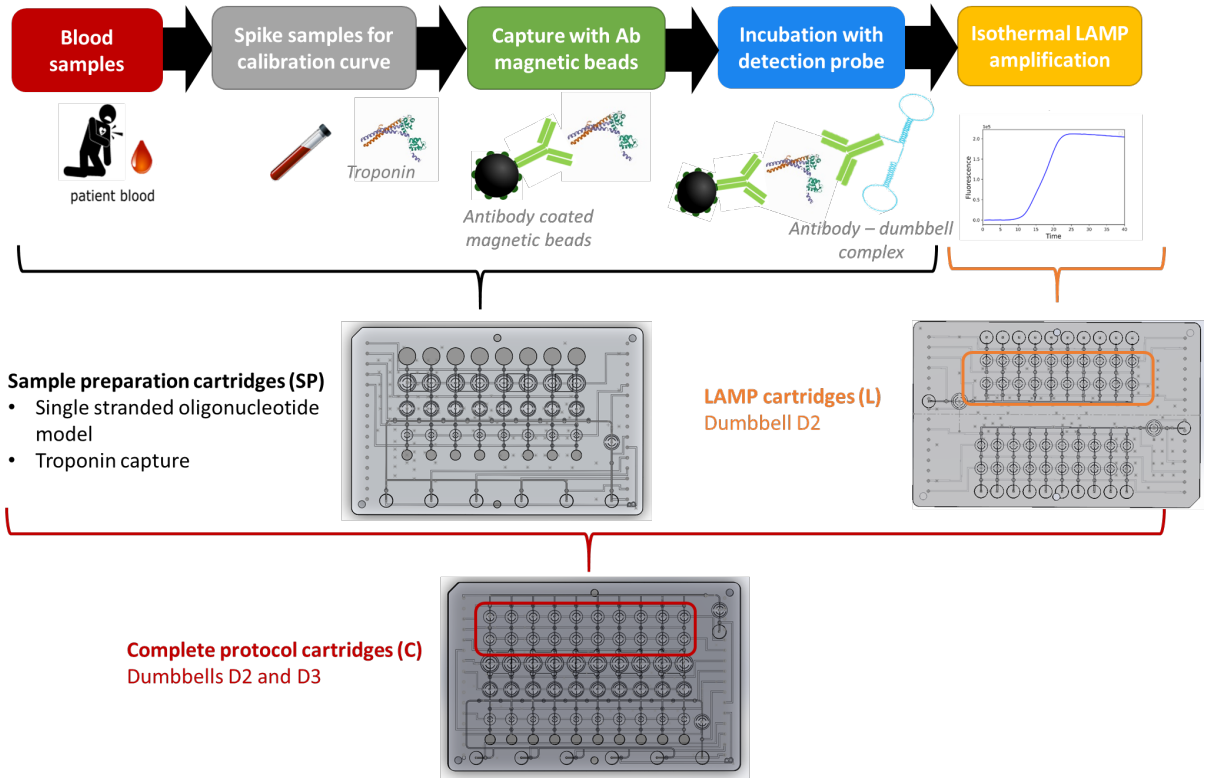

Figure 5.3: Streamline of troponin I iLAMP detection protocols and developed microfluidic cartridges with their respective validations.

validated for isothermal amplification.

5.2 On-chip sample preparation with magnetic beads

In chapter 3, we described an innovative iLAMP assay for the detection of troponin. This assay includes two main steps: (i) the troponin sandwich capture on magnetic beads with the dumbbell structure and (ii) dumbbell isothermal exponential amplification. This section presents the validation of step (i) on-chip and the evaluation of the assay performances in comparison to the one obtained in microplate. On the contrary of the previous microplate procotols where all steps are perfomed manually, all the assay operations are carried out automatically on-chip, only the samples and reagents needs to be inserted manually in the inlets. This automation is based on the adequate cartridge design and on the Uflu script that automates every action.

The microfluidic cartridge sample preparation module SP is first validated with a cartridge dedicated only to the sandwich formation on magnetic beads. At the end of the protocol, the solution is withdrawn from the outlets and placed on a commercial instrument for LAMP amplification.

5.2.1 Preliminary results: on-chip single stranded oligonucleotide model detection on magnetic beads

To investigate the feasibility of the developed biosensing method to be embedded in the designed microfluidic cartridge, an oligonucleotide detection assay based on DNA hybridization was first performed. This single stranded oligonucleotide model was already used as a dumbbell validation model in chapter 3, and we use it now for microfluidic validations. This simplified

assay also helps to check the compatibility of each assay reagent with the developed microfluidic technology. Indeed, the FlowStretch technology was validated with ELISA protocols for gluten quantification [169], but never with aptamers or DNA strands. Therefore, the compatibility of the magnetic beads (Streptavidin or Tosylactivated), DNA strands, dumbbells, and various assay buffers is checked with this model.

Experimental method The single stranded oligonucleotide sandwich detection protocols are inspired from the protocols described in chapter 3. The protocols are achieved in parallel in a microplate and in the microfluidic chip for comparison of performances. The buffers used in this experimental section are the HB and the RS described in appendix B. The detection method is based on a sandwich type detection on magnetic beads with a single-stranded oligonucleotide called Zip6Thr1c as a target. This sequence contains a part Thr1c which is complementary to the Thr1 thrombin aptamer present on the dumbbell, and a Zip6 sequence that is complementary to a Zip6c sequence immobilized on the magnetic beads (Fig 5.4A).

Prior to first use, the microfluidic cartridges are incubated in a buffer made of PBS with 1% BSA for at least one hour, in order to coat the surface with the BSA protein and therefore limit the binding of other proteins or molecules during the assay procedure.

The assay working volume in both microplate and chip procedures is 50 μL. The magnetic beads are previously grafted with the Zip6c sequence via a biotin-streptavidin bonding and are blocked with a solution containing 1% BSA. These magnetic beads are used to capture the target sequence Zip6Thr1c at various concentrations from 1 nM to 1 pM for 30 minutes with shaking. On-chip, shaking is achieved through transferring way and back the solution between two chambers of similar size. The magnetic beads are washed three times with 40 μL RS. Then, the dumbbell was put into contact with the magnetic beads at a concentration of 100 pM for 30 minutes with shaking. The magnetic beads are washed again three times with RS and resuspended in HB. A negative control with no target DNA was also achieved in parallel. The final solution of resuspended magnetic beads was further amplified with isothermal LAMP amplification protocols as described previously, using 2 μL of the magnetic beads solution with 18 μL of LAMP mix 2 (appendix C). The amplification was run on a commercial instrument with warming at 65°C for one hour and recording of fluorescence every 30 seconds.

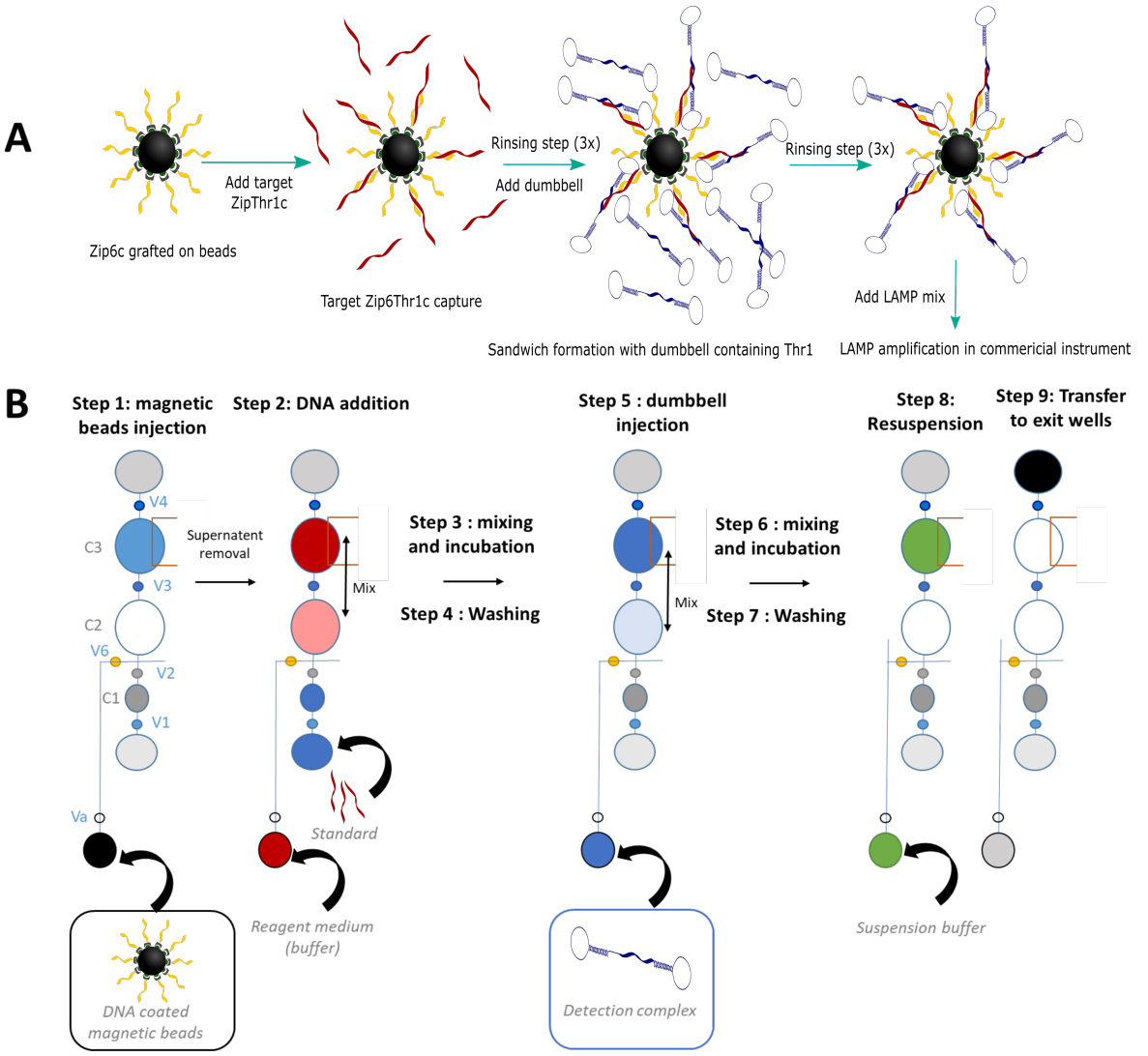

Figure 5.4: Protocols for single stranded oligonucleotide detection (A) Schematic of the experimental protocol for the oligonucleotide sandwich capture on magnetic beads and (B) Schematic top view of one row of the sample preparation microfluidic cartridge for each step of the oligonucleotide detection.

This methodology was applied to both dumbbells D1-THR-C and D1-THR-DE5 to check the ability of the method to detect oligonucleotide analytes. Both dumbbells contain the thrombin Thr1 aptamer that binds to the Tr1c strand in the free oligonucleotide.

Figure 5.4.B shows the succession of the assay steps in the microfluidic cartridge with the protocol described above. Every operation achieved manually in the microplate single stranded oligonucleotide assay is performed automatically on-chip by adding each reagent on the appropriate inlet. The washing procedure is also achieved automatically through the magnetic arm activation. The Uflu software with specific scripts written for this protocol automatizes every operation chronologically. The solution is withdrawn in the outlets after resuspension in HB, for further LAMP analysis on a commercial instrument (QuantStudio, Applied Biosystems).

Results The results of the oligonucleotide quantification on-chip and on microplate are presented in figure 5.5. The amplification times confirm the trend already observed in chapters 2 and 3: dumbbell D1-THR-DE5 is faster for isothermal amplification than D1-THR-C, even after hybridization with a free oligonucleotide in a sandwich format. This is valid for both microplate and on-chip protocols. Moreover, the free oligonucleotide quantification is similar for both types of protocols, except that the amplification appears about one minute slower on-chip. With this method embedded on-chip, it is possible to quantify oligonucleotide strand in a sandwich format down to 10 pM, with a LOD of $\approx$ 5 pM. The deviation between two experimental replicates is larger on-chip than on microplate. This deviation would need to be studied and characterized more thoroughly, but was beyond the scope of our study.

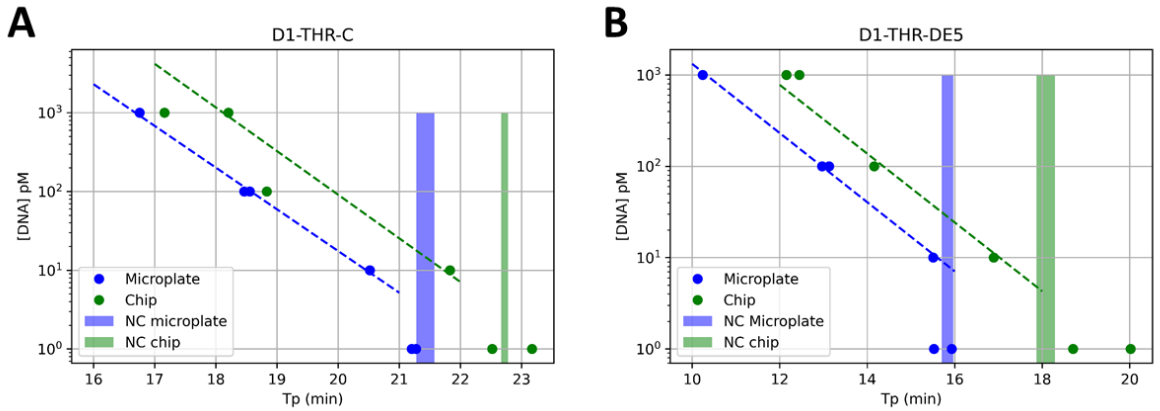

Figure 5.5: Dynamic ranges for the sandwich oligonucleotide detection. Comparison of performances for protocols achieved in microplate and on-chip with (A) D1-THR-C dumbbell and (B) D1-THR-DE5 dumbbell. The straight lines are a guide to the eye for the quantification of free oligonucleotide.

Through this single stranded oligonucleotide model on-chip, we validated the use of the assay reagents (DNA coated magnetic beads, free oligonucleotides, dumbbells...) with the developed microfluidic cartridge and instrumentation benchtop. For two different dumbbells, we have reached similar assay performances on microplates and on-chip, with a quantification range from 1 nM to 10 pM and a LOD of 5 pM. This study would require more detail on the chip experimental repeatability between rows for a similar target DNA concentration, in order to know exactly the chip rows variability. Indeed, it would be interesting to quantify which variability is induced intrinsically by the cartridge through the statistical evaluation of the variability between different rows for a similar target concentration. In the experiments conducted here, only two target concentrations were added in duplicate and the variation after amplification have reached 1 minute difference in Tp value. As we see in figure 5.5 A, this variability alters the quantification straight line plotted on the points from 1 nM to 10 pM as a guide to the eye. Therefore, it seems that the cartridge variability between rows could alter the quantification assay. However, no further study were conducted with this model oligonucleotide quantification assay since it was used in this section as a cartridge and assay reagent proof-of-concept model.

5.2.2 On-chip capture of troponin I on magnetic beads

The sample preparation cartridge SP is tested for troponin capture on magnetic beads, to integrate the first step (sandwich capture) of the previously developed troponin iLAMP protocols (Fig 5.6A).

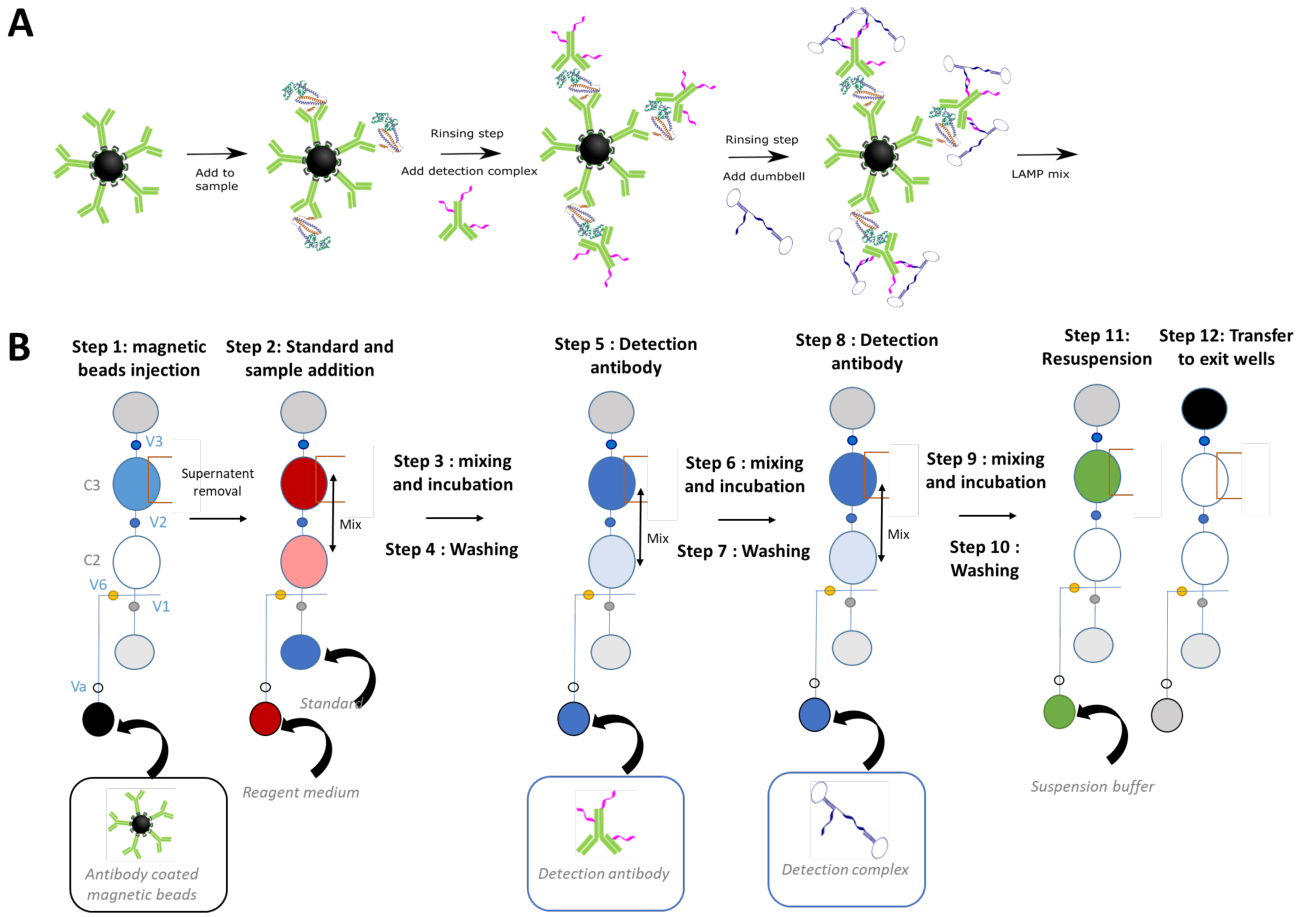

Figure 5.6: Protocols for troponin iLAMP detection on-chip (A) Schematic of the experimental protocol for the troponin sandwich capture (B) Schematic top view of one row of the sample preparation microfluidic cartridge for each step of the troponin sandwich capture. The final LAMP amplification step is achieved off chip with a commercial instrument.

Experimental method The troponin iLAMP assay was described in chapter 3 (Fig 5.6A), and the reagents used are similar. The assay working volume is 50 μL, the IB is composed of PBS (pH = 7.4) with 1% BSA, and the WB is composed of PBS (pH = 7.4), 1% BSA, 0.3% Tween 20 and 20 µg/mL DNA from salmon sperm. The sample preparation microfluidic cartridge SP is previously incubated with PBS containing 1% BSA for at least one hour to prevent the binding of proteins to the cartridge surfaces.

The troponin sandwich capture on-chip is achieved with the following procedure ((Fig 5.6B):

- Step 1 : Magnetic beads injection. 600 μL of the anti-troponin coated magnetic beads (MyOne Tosylactivated, InVitrogen, in-house functionalization) at 0.5 mg/mL are injected in the first reagent inlet, and transferred into the reaction chambers. The supernatent is withdrawn with the magnet and pressure ramps.

- Step 2 : Sample and standard injection. 600 μL of the reaction medium (buffer, plasma, blood) is injected in the second reagent inlet. In parallel, 14 μL of the troponin standards are added in the standard inlets (100, 10 and 1 ng/mL, and negative controls with buffer). The sample and standards are transferred into the reaction chamber to resuspend the magnetic beads.

- Step 3-4 : Incubation and mixing for 30 minutes in the reaction chamber, followed by 3 washing steps.
- Step 5: Detection antibody injection. 600 μL of the detection antibody at 1 µg/mL is added into the third reagent inlet, and transferred into the reaction chamber to resuspend the magnetic beads.
- Step 6-7 : Incubation and mixing for 30 minutes in the reaction chamber, followed by 3 washing steps.
- Step 8 : Dumbbell addition. 600 µL of dumbbell D1-Zip6DE at 100 pM (in DB) is added in the inlet and transferred into the reaction chamber to resuspend the magnetic beads.
- Step 9-10 : Incubation and mixing for 30 minutes in the reaction chamber, followed by 3 washing steps.
- Step 11-12 : Resuspension. 600 μL of the suspension buffer (IB) is added into the fourth reagent inlet, and then transferred into the calibration chamber and into the reaction chamber to resuspend the magnetic beads. After several mixing, the solution is transferred into the exit wells and withdrawn for further analysis with LAMP amplification on a commercial instrument.

The same procedure is achieved in parallel on a microplate with manual operations for each step of the protocol. The washing of the magnetic beads is achieved with an microplate washer (HydroFlex, Tecan). In both procedures (on-chip and on microplate), the LAMP amplification (final step of the assay) is achieved on a commercial instrument (QuantStudio, Applied Biosystems), by adding 2 μL of magnetic beads solution to 18 μL of LAMP mix 5 (appendix C).

Results Figure 5.7 A shows two pictures of the microfluidic cartridge placed on the instrument. The top picture corresponds to the beginning of step 2 in the experimental procedure, the magnetic beads are positioned in the reaction chamber, and the plasma samples is injected in the calibration chambers (yellow zone). The bottom picture corresponds to end of the step 2 with the beads after resuspension and mixing with the sample.

Different concentrations of standard troponin are added in the standard inlets: 100, 10 and 1 ng/mL in duplicates (6 inlets), and 2 inlets were used for negative control (buffer containing no troponin standard). The fluorescence data over time (Fig 5.7B) after LAMP amplification on a commercial instrument shows clearly faster amplification for higher concentrations of troponin. From the fluorescence curves, the troponin assay calibration curves can be plotted (Fig 5.8). The dumbbelll calibration curve is also systematically achieved and drawn to get the reference point of the dumbbell grafting on the magnetic beads, and evaluate the detection efficiency.

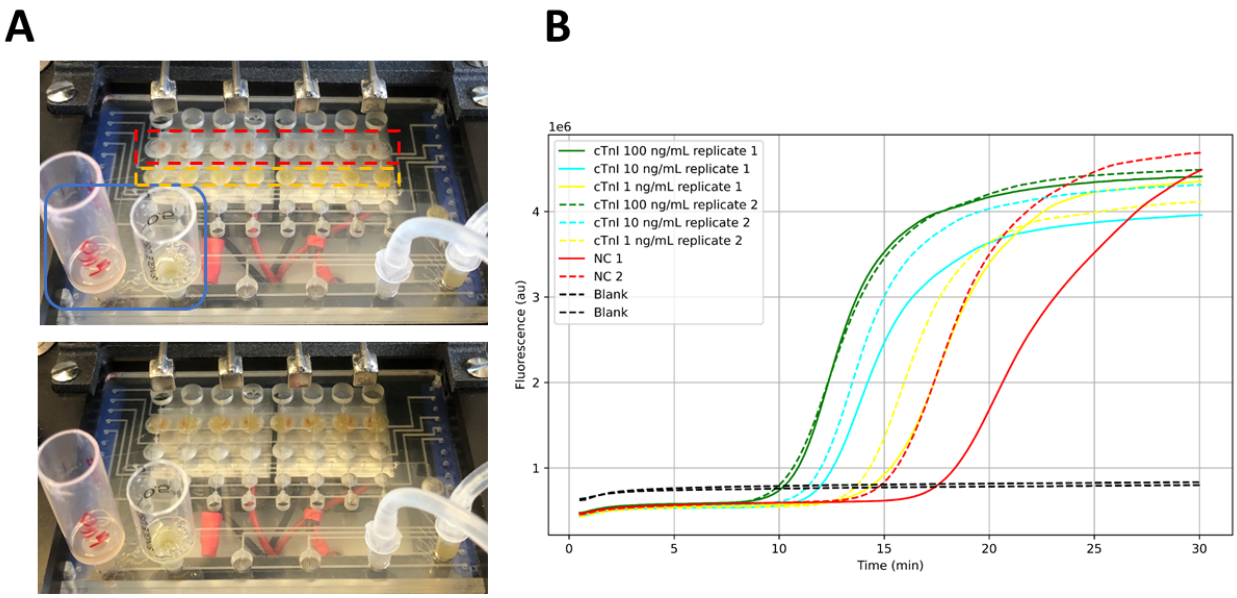

Figure 5.7: on-chip troponin capture. (A) Pictures of the microfluidic chip under operation. Top picture represents the magnetic beads positionned in the reaction chamber (red), sample (yellow) and the reagent inlets (blue), and the bottom picture represents the magnetic beads during resuspension in the sample. (B) Fluorescence over time after isothermal LAMP amplification for on-chip various troponin concentrations replicates, with negative control and blank.

Figure 5.8 A shows the troponin quantification range for 4 experimental replicates (achieved over two different days of experiments) for detection in buffer sample (IB). The three different troponin concentration (100 ng/mL - 1 ng/mL) are clearly distinguished in terms of Tp values. The signal corresponding to the negative control appears after 16 minutes, therefore after the lowest troponin point to detect at 1 ng/mL. This result is very encouraging for the detection of troponin on a large dynamic range, and the late non specific signal suggests that we could lower the LOD to reach a better sensitivity, probably down to 0.1 ng/mL. On figure 5.8 B a similar troponin quantification curve is drawn for the protocols achieved in plasma sample (from EFS). The quantification of troponin is also successfully validated in the range 100 ng/mL - 1 ng/mL.

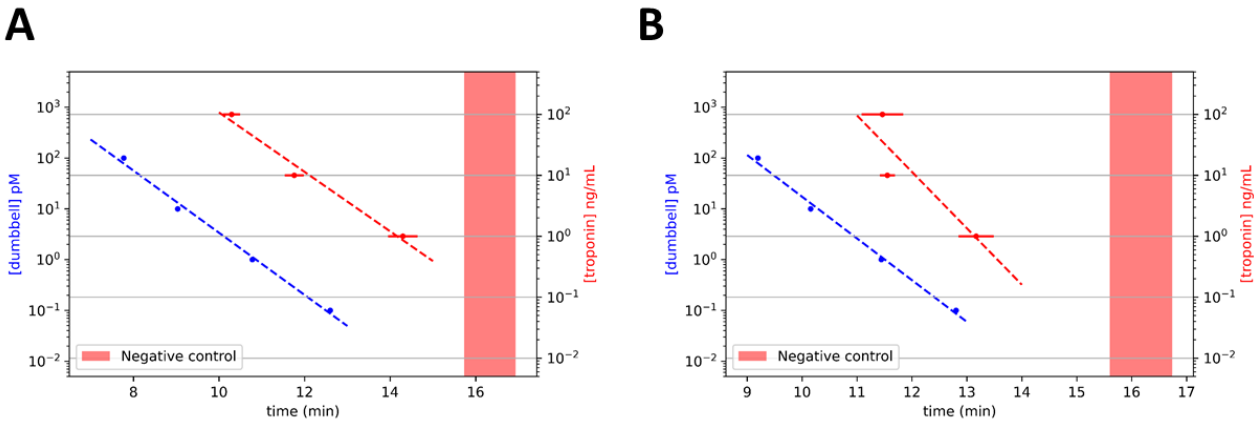

Figure 5.8: Quantification ranges for on-chip troponin capture in (A) buffer medium (N=4) and (B) plasma medium (N=2). The blue dots and line corresponds to the dumbbell quantification range (100 pM - 100 fM), and the red dots corresponds to the troponin standards (100 - 1 ng/mL), with the red straight line as a guide to the eye for the troponin quantification. The red bar corresponds to the negative control with no troponin standard addded.

With the proposed sample preparation microfluidic cartridge outlined in chapter 4, we have validated its compatibility with two different types of protocols: first the free oligonucleotide detection in sandwich format, and secondly, the troponin capture on magnetic beads and sandwich formation with the dumbbell structure. Both protocols are functional on-chip. We have reach a quantification range from 1 nM to 10 pM for free oligonucleotide detection, and from 100 to 1 ng/mL for troponin detection in buffer.

For both protocols, the final step of the assay, the isothermal amplification (LAMP), was achieved off chip on a commercial instrument. The next step in the microfluidic developments is the integration on-chip of the isothermal amplification. Thus, the next section exposes the validation of a specific module for isothermal amplification, that can later be combined with the sample preparation module.

5.3 On-chip isothermal amplification

To integrate the last step in the iLAMP assay, isothermal amplification, specific cartridges were designed. The instrument described in chapter 4 comprises a heating module and an optical system to recover the data from the amplification reaction. Two specific cartridges were designed with increasing order of complexity. This section sums up the experimental validation of the cartridges and the several optimizations brought to achieve the isothermal amplification protocols on-chip.

5.3.1 Preliminary results with cartridge L

A cartridge dedicated only to the isothermal amplification protocols was first designed. It contains 2 × 10 rows of chambers located favorably for heating homogeneously at 65°C. 10 sample inlets allow the fluid deposition and transfer into the LAMP reaction chambers, and a waste system pumps the liquid to waste after amplification.

5.3.1.1 Experimental protocol

The chip experimental validation was achieved using a dumbbell and its associated primers set, with the isothermal amplification mixture (enzyme, dNTPs, appropriate buffers..). During the experimental validation, a different dumbbell than the one used during all the protocols described in chapter 3 (aptaLAMP and iLAMP) was used in order to prevent cross-contamination between amplification reagents. Therefore, the dumbbell design 2 presented in chapter 2 was used, extended with a thrombin aptamer at its dengling end. This dumbbell is called D2-THR-DE5 (sequence and primers in appendix A). The dumbbell quantity used in the final iLAMP protocols is 100 pM. The aim is to be able to quantify the dumbbell down to a concentration in the picomolar range on-chip. As this first chip serves as proof-of-concept, we chose to validate the chip with dumbbell concentrations in the range 10 nM to 100 pM, and we will refine this concentration range later.

The on-chip isothermal amplification procedure is carried out as follow :

- The chip is pre-incubated with PBS containing 1% BSA for 30 minutes. After the chip incubation, all the chambers are rinsed with water.
- The dumbbell template at different concentration (10 nM, 1 nM, 10 pM) is prepared by diluting the oligonucleotide in water. The mixing of the LAMP mix and dumbbell is done off chip by adding 5 μL of DNA (10 nM, 1 nM, 100 pM and blank) with 45 μL of LAMP mix 5 (appendix C).
- The LAMP amplification mixture is deposited in the chip inlets (figure 5.9 for on-chip deposition)
- The LAMP chambers are filled, and decontaminant RNAse AWAY is added in the inlets to inhibit amplification of the remaining liquid.
- The camera parameters are set up (details in chapter 4)
- The temperature controllers are set up to 75°C.
- The data acquisition Python script is launched. The LED is turned on every 30 seconds, and a picture is taken by the camera at the same time. The recording lasts for one hour.

- After amplification, the liquid is pumped into the waste and discarded in a specific waste tube contaning decontaminant RNAse AWAY.
- The LAMP chambers are incubated for 30 minutes with RNAse AWAY, and then the full chip is rinsed with water five times.

The dumbbell sample distribution on-chip is shown in figure 5.9. The chip design allows to have experimental duplicates for each reagent inlets, with the two distinct chambers.

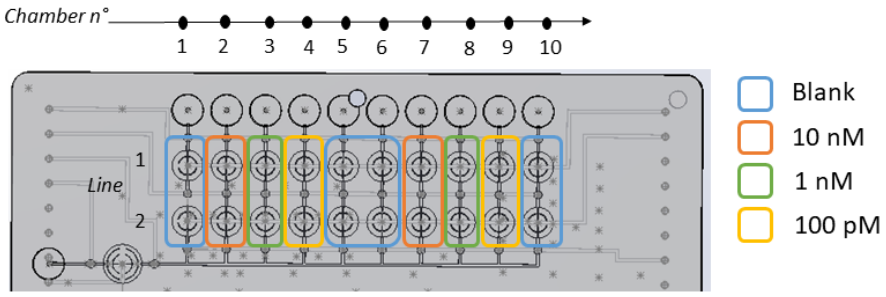

Figure 5.9: Schematic of the upper part of the microfluidic cartridge L with sample deposition in the chambers for isothermal amplification.

5.3.1.2 Results

The fluorescence over time is plotted in the different chambers (Fig 5.10). We can observe faster amplification times for higher dumbbell concentration. The orange curves (10 nM) are clearly distinguishable from other concentrations. However, for lower concentrations, 1 nM and 100 pM (in green and yellow), the amplification curves over time are closer to each others, therefore the estimated Tp values would be similar. Moreover, the LOD is limited by the high non specific signal given by the amplification of blank samples (water, no target DNA, blue curve). This is the main limitation for the sensitivity of the on-chip LAMP amplification.

The amplification curves given in figure 5.10 gives a proof of the compatibility of the chosen microfluidic cartridge and technology with nucleic acids amplification protocols. We achieved a functionnal amplification in about 30 minutes and recorded the fluorescence over time with a dedicated optical set up. The chosen design with two rows of 20 μL microfluidic chambers is rather simple and brings homogeneous temperature for amplification in most of the chambers.

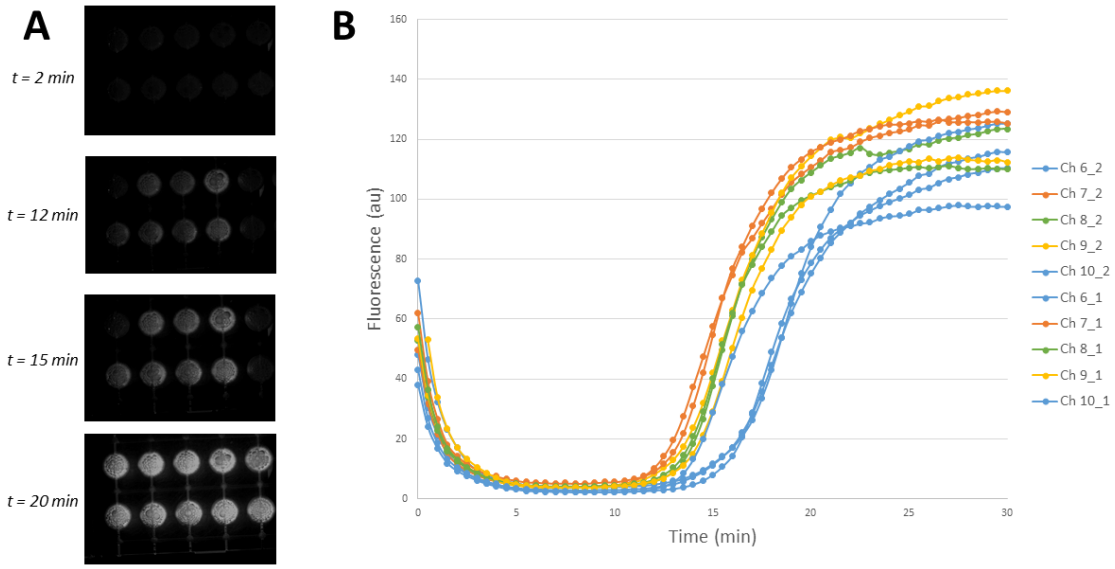

Figure 5.10: (A) Pictures of the microfluidic chambers (6-10) at different time points during the amplification. (B) Fluorescence over time for LAMP reaction in microfluidic chambers 6-10.

5.3.1.3 Discussion

From the fluorescence curves, several algorithms can be used to compute the Tp values for each target DNA, to be able to draw calibration curves from on-chip amplification. However, with the results presented here, it was not possible to quantify lower amount of dumbbell than 10 nM, due to high non specific amplification. This latter is due to different reasons. First, during the LAMP chambers filling through hyper-elastic membrane deformation, there can be important and random bubble formation in the chambers due to the membrane trapping bubbles, and to the inherent property of the LAMP mixture to foam. With such filling protocols, the random bubble formation during filling is not controllable and alters the fluorescence reading in the chamber (Fig 5.11A), as well as a the repeatability between chambers. There are some improvements to bring to achieve a correct and repeatable chamber filling with the LAMP solution and through membrane activation. Moreover, during the amplification, we observe the apparition of many small bubbles in the chambers (Fig 5.11B). The valves across the chambers are closed with a pressure ranging from 450 to 600 mbar, and we therefore assign this important pressure to the apparition of bubbles in the chamber. Lastly, despite the important pressure used to close the valves, their impermeability to fluids is incomplete, which therefore leads to liquid waste and to cross contamination between chambers through the central exit channel. There is probably a trade-off to find between valve permeability and air injection in the chambers.

This LAMP microfluidic cartridge was used to check the functionality of the chosen microfluidic technology with LAMP amplification protocols, in order to integrate the iLAMP troponin detection protocols in a complete FlowStretch microfluidic cartridge. We implemented some cartridge designs and architectures and tested them experimentally. The thermal characterization of the designed chambers was achieved, and showed an homogeneous temperature around 64°C in most of the chambers. We validated the on-chip dumbbell isothermal exponential amplification with a concentration in the nanomolar range, limited mainly to non-specific amplification

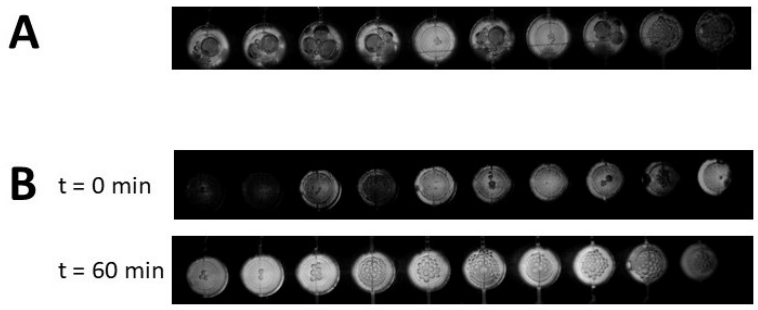

Figure 5.11: Examples of fluorescence data acquired. (A) Bubbles formation just after filling the chambers with biological reagents. (B) Microfluidic chambers before and after amplification. Many bubbles have appeared in the central chambers for example due to the valves permeability to air.

and bubbles apparition limiting the optical reading. This first cartridge was rather elementary, since the sample mixing (LAMP mix and target DNA) was achieved off chip. Only the functionality of the amplification was tested in the microfluidic chambers. Several technical issues appeared, limiting the sensitivity of a LAMP assay with this cartridge. With this cartridge and method, it appears difficult to quantify the dumbbell below the nanomoral range, thus limiting the use of this architecture for sensitive dumbbell detection through LAMP. In the next section, we demonstrate another cartridge with a different architecture that should help to counteract the technical issues encountered, and which should therefore help to lower the LOD. This new cartridge shows an increased complexity since it also integrates the sample preparation module. Experimental tests are carried out to focus on solving the two major technical issues, mainly the bubble formation (during filling and from the valves permeability), and the cross contamination between chambers, in order to lower the quantification range achieved with this on-chip LAMP assay.

5.3.2 LAMP-on-chip with cartridge C

We propose here another microfluidic cartridge named C inspired from the one described and used in the previous section (5.3.1), specific to the LAMP amplification protocols, and from the sample preparation cartridge described and use in sections 5.2.1 and 5.2.2. This complete cartridge therefore integrates (i) the sample preparation module (various reagent inlets, volume calibration, waste system, standard inlets...), and (ii) two rows of 20 μL chambers to perform the isothermal amplification. This new cartridge architecture has many advantages. First, it contains many reagent inlets and a central channel with a waste system for volume calibration. With the standard inlets, it becomes possible to mix various dumbbell concentrations with the LAMP amplification mixture on-chip. It also contains a specific post-amplification waste system to remove the excess liquid, and also to facilitates the washing procedure after amplification.

This cartridge will be validated for isothermal amplification. Figure 5.13 A shows the chip architecture, with the sample preparation module highlighted in purple, and the LAMP module in yellow.

5.3.2.1 Fluidic optimizations to limit the bubble formation

The cartridge C functions for isothermal amplification was described in chapter 4 (section 4.3.3.1). The complete cartridge presents two rows of 20 μL chambers dedicated to LAMP amplification protocols, connected with a sample preparation module. The LAMP chamber architecture and geometry is similar to the one presented and validated in section 5.3.1 with the initial LAMP cartridge. Therefore, similar limitations with the use of this architecture should appear. However, we implemented several strategies, taking advantage of the sample preparation module of the cartridge, to overcome these limitations.

The first limitation was the random bubbles formation during chamber filling. With this new architecture design, the succession of chambers from sample preparation module to the LAMP chambers induces several fluid transfers which inherently creates bubbles. The reaction chamber C3 total volume (50 μL) was designed to be superior to the total volume of the LAMP chambers. To fill the LAMP chambers, we implemented a pressure ramp to limit the transfer of bubbles and keep them in the reaction chamber. The pressure ramp principle is exposed in figure 5.12 A. Pressure steps of 25 mbar are used to shift the input chamber pressure value from -150 to +150 mbar, and to shift the output chamber pressure from +150 to -150 mbar. This way, the random formation of bubbles during LAMP chambers filling was greatly reduced (Fig 5.12B and C).

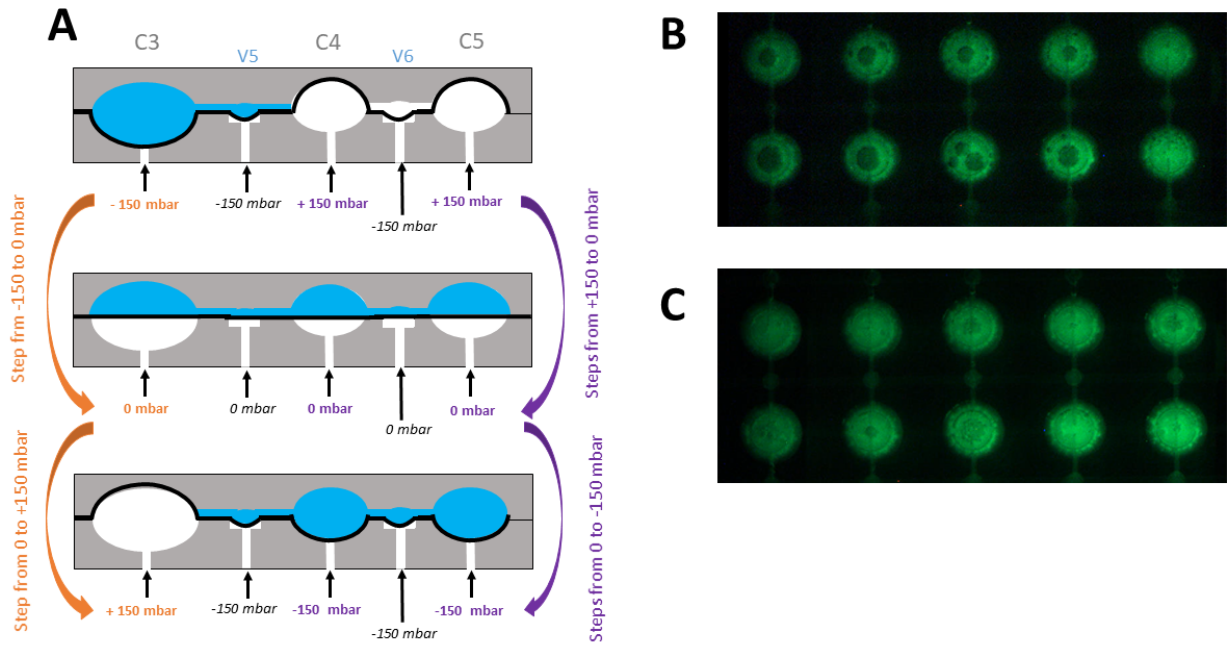

Figure 5.12: Implementation of pressure steps for chamber filling. (A) Pressure ramp process to fill two output chambers (C4 and C5) from a single input chamber C3 (vertical sectionnal view). The input chamber C3 volume must be larger than the two output chambers volume. (B) Visualisation of 10 microfluidic chambers with a liquid containing fluorescein with a filling process without a pressure ramp and (C) Visualisation of 10 microfluidic chambers with a liquid containing fluorescein with a pressure ramp as exposed in A.

The second challenge was the formation of bubbles during the amplification reaction. Previous observations lead to the conclusion that the valves are the major input of bubble during

the reaction. The important pressure applied on the valves to maintain them closed (500 mbar) inherently inject air in the fluidic layer due to the air permeability of the stretchable membrane. In terms of microfluidic, other types of valves could be considered without pneumatic actuation for example (mechanic, capillary...), but their implementation in the designed cartridge would be too complex in terms of packaging. We studied a valve actuation pressure range (300 - 600 mbar) to find a balance between their air permeability and the air injection, but we found that in all cases it lead to important air injection in the chamber from the valves. Therefore, we describe specific chambers and valves positions in the architecture design that limit the air injection in the reaction chamber during the amplification reaction. The table in figure 5.13 B shows the chambers and valve positions during the different LAMP protocol steps.

A

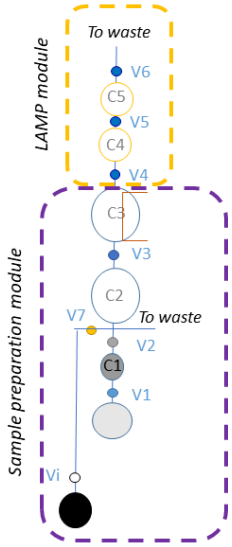

B

			Protocol steps											
Elements	P+ (mbar)	P- (mbar)	Step 1 : LAMP mix injection	Step 2 : DNA template injection		Step 3 : Transfer into reaction chamber		Mixing	Step 4 : transfer into LAMP chambers		Step 5 : RNAse Away injection			Step 6 : LAMP
Vi, V7	500	-150	1	0	0	0	0	0	0	0	1	0	0	0
V1	500	-150	0	1	0	0	0	0	0	0	0	0	0	0
C1	150	-150	0	1	1	1	0	0	0	0	0	0	0	0
V2	500	-150	0	0	0	1	0	0	0	0	0	0	0	0
C2	150	-150	1	1	1	1	0	1	0	0	1	0	1	1
V3	500	-150	0	0	0	1	0	1	0	0	0	1	0	0
C3	150	-150	0	0	0	1	1	1	1	0	0	1	0	0
V4	500	-150	0	0	0	0	0	0	1	1	0	0	0	1
C4	150	-150	0	0	0	0	0	0	1	1	1	1	1	1
V5	500	-150	0	0	0	0	0	0	1	1	1	1	1	1
C5	150	-150	0	0	0	0	0	0	1	1	1	1	1	1
V6	500	-150	0	0	0	0	0	0	0	0	0	0	0	0

Figure 5.13: Schematic of microfluidic cartridges chambers and valves state during LAMP amplification protocols. (A) Schematic view of the complete microfluidic cartridge, with sample preparation module (purple) and LAMP module (yellow). (B) Table of the chambers and valves state during the LAMP protocol steps implementation in the cartridge. State 1 corresponds to an open state (negative pressure, filled with liquid), and state 0 to a closed state (positive pressure, empty). The different elements actuation pressures are indicated, and each element state at various steps of the protocols is depicted in the table.

The key steps of the on-chip isothermal amplification are:

- Step 1 and 2: LAMP mix injection in chamber C2, and DNA templates injection in chamber C1.
- Step 3 : Transfer of C1+C2 in reaction chamber C3 using pressure steps (25 mbar). Soft mixing between chambers C2 and C3.
- Step 4 : Transfer of C3 into LAMP chambers C4 and C5 with the filling process with pressure steps described in figure 5.12.
- Step 5 : RNAse AWAY injection in chamber C2.

- Step 6 : Amplification reaction at 65°C.

Importantly, during step 6 corresponding to the amplification reaction, the valves and chambers positions are the following. LAMP chambers C4 and C5 are opened with the LAMP mixture and template DNA. The intermediate valve V5 is opened. Valve V4 is also kept opened, and the isolation of the LAMP reaction chambers from the sample preparation module of the cartridge is achieved by keeping the chamber C3 closed at +150 mbar. This way, this C3 chamber acts as a valve, but since its actuation pressure is lower than a valve, the injection of air is greatly reduced. For the isolation of the LAMP chambers to the waste system, valve V6 must be kept closed, and is therefore the main source of air injection in the LAMP chambers. In addition, for further isolation of the LAMP chambers to the remaining part of the cartridge (sample preparation module), RNAse AWAY solution is stored in chamber C2 and acts as a chemical barrier. Lastly, valve V4 is not closed to limit the bubble formation, but the reaction chamber isolation is ensured with both chamber C3 kept closed and chamber C2 filled with a fluid acting as a chemical barrier.

In order to limit the air injection prior and during the isothermal amplification protocols in cartridge C, we implemented several strategies. The first one consisted in using pressure steps to limit the air injection during the LAMP reaction chambers filling. However, despite correct reaction chamber filling, air was injected in the reaction chamber during the amplification reaction due to the membrane permeability to air, the inherent foam property of the LAMP solution and to the warming of the chamber. We proposed specific chamber and valve positions during the amplification reaction to limit the air injection, mainly using chamber C3 and C2 to ensure impermeability from the LAMP module and sample preparation module on cartridge C, and limiting the number of closed valves.

5.3.2.2 Experimental results

The functionality of the microfluidic cartridge for LAMP amplification with the previous fluidic optimizations was achieved using different dumbbell designs. To do so, we used dumbbell D2-THR-DE5 and dumbbell D3 described in chapter 3 (sequences in appendix A). Their quantification curves after LAMP amplification on a commercial instrument are plotted in figure 5.14, and serves as reference data for the implementation of the on-chip amplification.

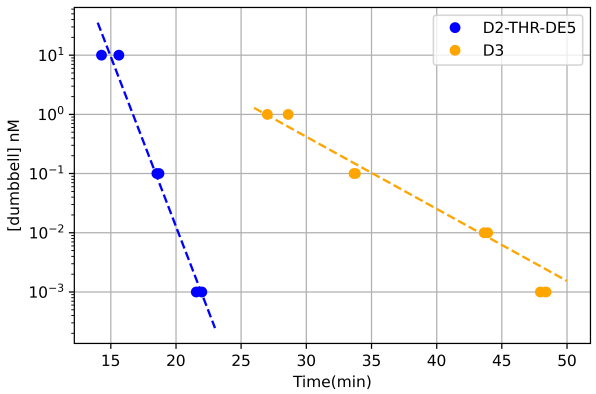

Figure 5.14: Dumbbells quantification curve (dumbbell concentration over Tp values) for LAMP amplification of dumbbell D2-THR-DE5 and D3 on a commercial instrument (Quand Studio).

Dumbbell D2-THR-DE5 has a short amplification time, and is used for the first implementation of the on-chip complete protocols, and to evaluate the performances of the on-chip amplification on a broad concentration range. To refine the quantification range, dumbbell D3 with a slower amplification time (twice as long) is used, which should allow the differentiation of closer concentrations. Those two dumbbells will therefore be used for complementary chip performance evaluation of the on-chip isothermal amplification reaction.

Cartridge reuse The cartridge C architecture containing the sample preparation modules with various inlets, calibration, reaction chambers, and waste system can be advantageously used to perform a full washing procedure to allow cartridge reuse after amplification. Therefore, we implemented a specific cartridge full washing procedure and validated the cartridge reuse after successive implementation of LAMP amplification in the same cartridge.

For the full cartridge washing procedure, at the end of the amplification reaction, the decontaminant RNAse AWAY solution stored in chamber C2 is transferred into chamber C3, C4 and C5 with mixing, keeping the valve V7 closed to prevent cross-contamination with the remaining part of the cartridge. Then, reagents inlets are used to add RNAse AWAY solution in every chamber of the cartridge, and the solution is incubated for 30 minutes. After that, the solution is withdrawn to the waste system, and the complete cartridge is rinsed with PBS/Tween (5 times) and then with water (5 times).

We validated this washing process and carried out successive amplification on a single cartridge. Half of the chambers were filled with dumbbell D3 at a concentration of 10 nM, and the other half with blank sample. After the first use of the cartridge, one of the chamber was switched from dumbbell template to blank sample to evaluate cross contamination and the efficiency of the washing procedure. Figure 5.15 shows the amplification curve during the first (A) and second (B) experimentation with the same cartridge. Chamber 5 contains first dumbbell sample, and then a blank sample to evaluate the cross contamination. The late non specific amplification of the blank sample in chamber 5 during the second experimentation validates the washing procedure and reuse for isothermal amplification.

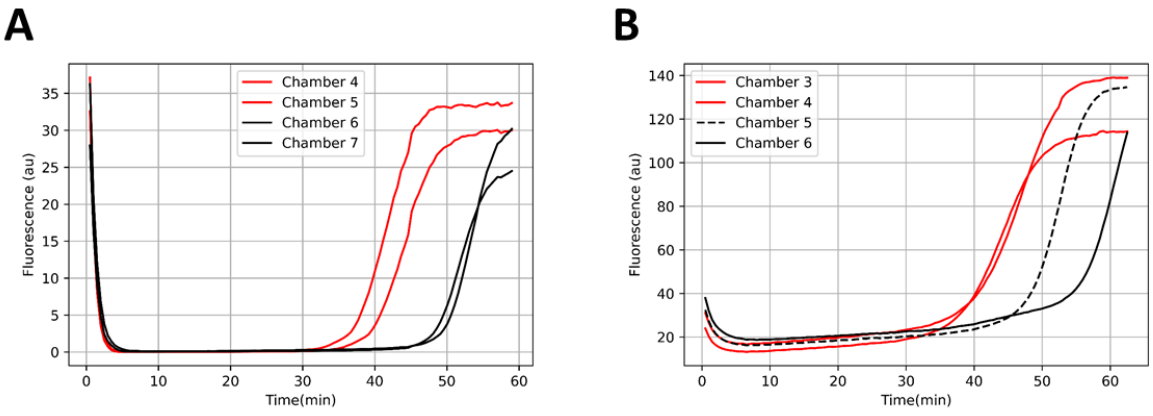

Figure 5.15: Fluorescence over time in different microfluidic chambers to evaluate cross-contamination. (A) First experimentation, chamber 4-5 contains 10 nM dumbbell template, and chambers 6-7 contains blank samples. (B) Second experimentation, chambers 5 (dashed line) now contains a blank sample.

This way, the cartridge C architecture and washing process allows it re-usability for successive LAMP amplification protocols.

Dumbbell D2-THR-DE5 The chip was characterized using the dumbbell D2-THR-DE5 with its associated set of primers (appendix A). The dumbbell at concentrations of 10 nM, 100 pM and 1 pM was deposited on-chip with experimental duplicates, and 4 blank samples (Fig 5.16A). The fluorescence in each microfluidic chamber can be plotted (Fig 5.16B). First, an important fluorescence drop can be observed during the first minutes of amplification. The complete system is placed in the dark only at the beginning of the amplification. There can be optical bleaching of the intercalating dye appearing when the system and LAMP solutions are placed under darkness. This drop may also be due to the thermal bleaching of the intercalating dye in the reaction mixture during the system increase in temperature.

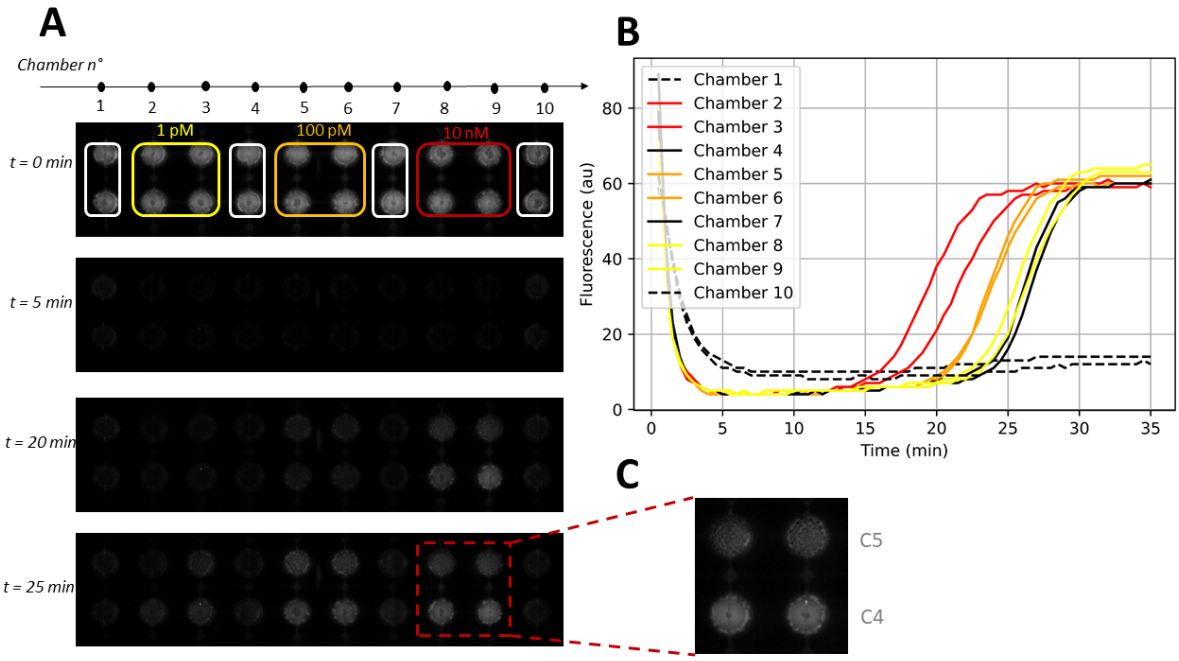

Figure 5.16: LAMP-on-chip with dumbbell D2-THR-DE5 (A) Images of the microfluidic chambers at different times of the amplification reaction. (B) Plot of the fluorescence over time in the chamber: zoom until 35min is shown to visualise easily the time shift due to various dumbbell concentrations. Each curve corresponds to the fluorescence data of C4 chamber. (C) Final image of the amplification reaction in chambers 8-9. Bubbles are trapped in chamber C5 and chamber C4 is free of bubble for optimal optical reading.

First, the final image (Fig 5.16C) of the microfluidic chamber shows that the LAMP chamber C5 gathers the air bubbles that infiltrates through valve V6 while the reaction chamber C4 is preserved from the air injection during the reaction. Therefore, based on these results, we considered only the fluorescence data in chambers C4 to plot the fluorescence curve (Fig 5.16B).

Secondly, the fluorescence curves clearly shows a shift for different DNA template concentration. Higher dumbbell concentrations lead to faster amplification curves. Dumbbell concentrations at 10 nM and 100 pM can clearly be distinguished from blank samples, whilst the concentration of 1 pM has a similar amplification to the blank samples located in chambers 4 and 7. Four different blank samples were deposited on-chip, and interestingly their amplification curve differs. For the blank samples deposited on chambers 1 and 10, there is no visible amplification. If we relate the chamber 1 and 10 locations to the thermal study presented in chapter 4, those two chambers have a significantly lower temperature than the other chambers. Therefore, the amplification reaction in those two chambers is impaired and therefore should

not be considered in this study.

Dumbbell D2-THR-DE5 validated the chip functionality for isothermal amplification on two orders of magnitude, from 10 nM to 100 pM, in less than 30 minutes.

Dumbbell D3 In order to refine the quantification range, we chose a different dumbbell with a slower amplification time (Fig 5.14B).

Figure 5.17A shows an image of the microfluidic chip with various dumbbell concentrations deposition. The chambers are numbered from 1 to 10 and their associated fluorescence increase over time is plotted in figure 5.17B. Figure 5.17C shows the normalized fluorescence over time and we removed the first 4 minutes on which there was an important decrease of fluorescence (optical and thermal bleaching). The normalized fluorescence is computed using the general formula :

$$F_N(i) = \frac{F(i) - F_{min}}{F_{max} - F_{min}} \tag{5.1}$$

with F(i) the fluorescence value at time i, F_N the normalized fluorescence value, and F_{min} and F_{max} the maximum and minimum fluorescence values.

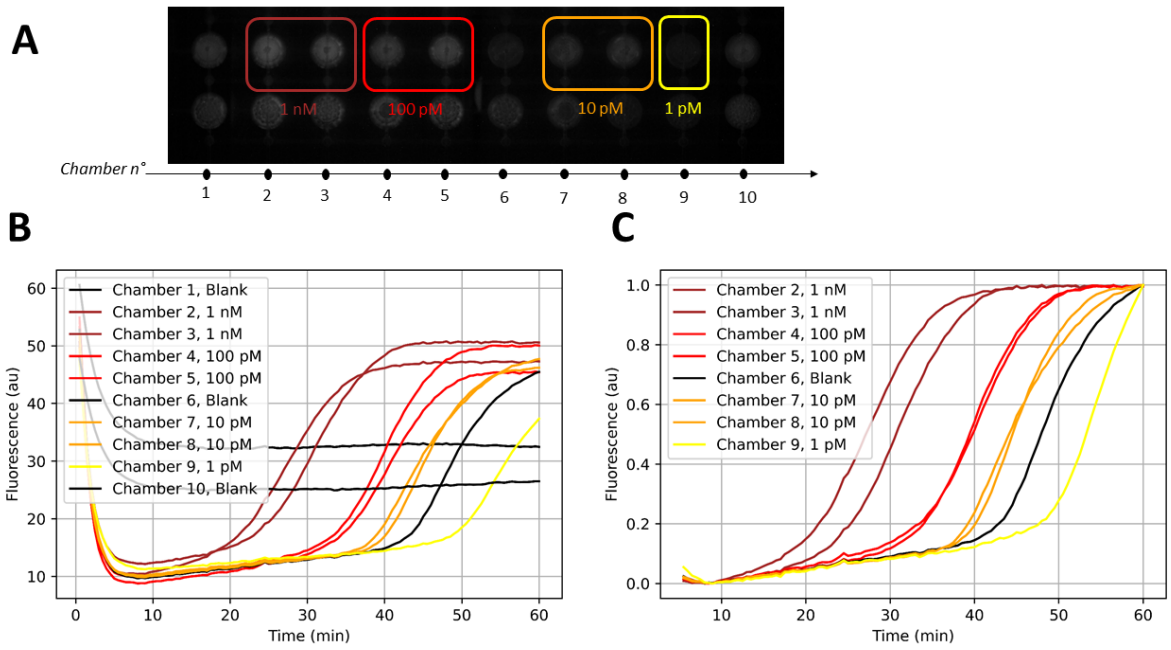

Figure 5.17: on-chip amplification of dumbbell D3 at 1nM, 100pM, 10pM and 1pM (A) Images of the microfluidic chambers during the amplification reaction and the dumbbell concentrations deposition along the chambers. (B) Plot of the raw fluorescence over time in the different chambers and (C) Plot of the normalized fluorescence over time.

The microfluidic filling process described above, associated with specific chamber and valve states during the amplification also lead to the successful removal of air bubble in the reaction chambers. With dumbbell D3, the plot of fluorescence over time (Fig 5.17B and C) clearly shows an important shift for different dumbbell concentrations. The dumbbell concentrations from 1 nM down to 10 pM present a reasonable shift in amplification times, and are clearly distinguishable from the blank sample. From this plot of fluorescence data over time, it seems possible to quantify the dumbbell amount in the range 1 nM to 10 pM, but more investigation needs to

be done to derive Tp values from the amplification curve and actually obtain a quantification range.

5.3.2.3 Data analysis and quantification

From the fluorescence curve, the Tp value can be computed for a possible DNA quantification from amplification data. Before this chapter, the Tp was computed automatically with the QuantStudio software. With the on-chip isothermal amplification, the Tp value needs to be defined from the fluorescence curves. Therefore, several methods and associated algorithms to compute the Tp values are implemented (Fig 5.18).

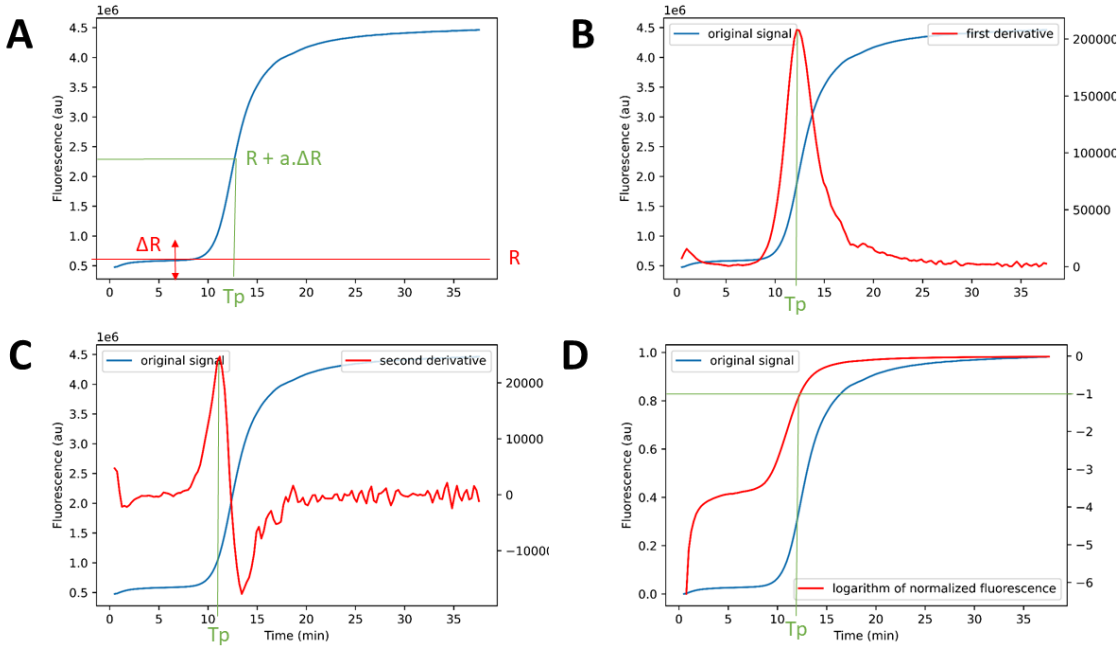

Figure 5.18: Different methods to compute the Tp from normalized fluorescence data. (A) Threshold method, (B) First derivative method, (C) Second derivative method and (D) Threshold method with the logarithm of the normalized fluorescence.

The first algorithm implemented works similarly to the one used in the QuantStudio software (Fig 5.18A). It defines a threshold value by deriving the mean fluorescence value R in the baseline. The baseline length is manually defined (usually tens of cycles). Then, the typical signal variation ΔR is defined as the fluorescence variation between the maximum and minimum value along this baseline. The Tp value is defined as the time when the fluorescence value reaches the value of $R + a\Delta R$, where a is a user-defined coefficient. Typically, $a \in [2, 10]$. The second algorithm implemented uses the first derivative of the fluorescence signal to compute the time when the fluorescence derivative is the highest, therefore corresponding to the inflexion point of the exponential amplification (Fig 5.18B). Similarly, the third algorithm uses the maximum of the second derivative (Fig 5.18C). Lastly, the last algorithm uses the logarithm of the normalized fluorescence (Fig 5.18D) curve to compute the time when it reaches the value of -1. Compared to the three other algorithms, this one is the only one to use the upper part of the exponential amplification curve, therefore towards the end of the amplification.

These four algorithms were tested on the on-chip amplification data set obtained with dumbbells D2-THR-DE5 and D3 to show the possibilities to quantify the amount of dumbbell.

From the amplification curve obtained with dumbbell D2-THR-DE5 in figure 5.16 B, we can derive Tp values with the different algorithms. We removed the initial fluorescence drop in the first 4 minutes of the amplification. For the threshold algorithm, the baseline was set as 7.5 minutes, and the coefficient $a = 5$.

Algorithm	Tp (10 nM)	Tp (100 pM)	Tp (1 pM)	Tp (neg)
Threshold	16.75 (1)	20.75 (0.35)	22.5 (0.7)	22.8 (0.7)
1^{st} derivative	20.5 (1.4)	23.25 (0.35)	25.5 (0)	26 (0.7)
2^{nd} derivative	17 (0.7)	22.25 (0.35)	24.5 (0.7)	24.75 (0.35)
Logarithm	19.5 (1.4)	23.25 (0.35)	25.5 (0.35)	26 (0.7)
QS	15.0	18.6	21.8	ND

Table 5.2: Mean Tp values (N=2) computed with the four algorithms from fluorescence data in figure 5.16 and comparison with QuantStudio Tp values. Standard deviation is shown in parenthesis.

All algorithms output Tp values with at least 1 minute difference between the concentration, which is reasonable considering an acquisition period of 30 seconds. All algorithms distinguish reasonably the dumbbell concentrations of 10 nM and 100 pM, but the 1 pM concentration is often mistaken with the blank sample.

The on-chip amplification curves obtained in figure 5.16B and the Tp values derived with the different algorithms show that the dumbbell quantification after LAMP amplification on-chip is possible in the range 10 nM to 100 pM. Below 10 pM, the amplification times are equivalent to the non specific signal, therefore limiting the LOD.

Similarly, from the amplification curve obtained with dumbbell D3 in figure 5.17, we derived Tp values with the different algorithms. We removed the initial fluorescence drop in the first 4 minutes of the amplification. For the threshold algorithm, the baseline was set as 7.5 minutes, and the coefficient $a = 5$. With dumbbell D3, the amplification curve is slower, and therefore the exponential increase is less important than for other dumbbell amplification curve, specially at the beginning and towards the end of the amplification. Therefore, with this type of curve, the algorithm using the 2^{nd} derivative is not adapted since it is too noisy and does not exhibit a maximum value to be used for quantification. Therefore the computed Tp values with this method are not displayed.

Figure 5.19 shows the computed Tp values with the different methods, as long as the one obtained with the amplification on the commercial instrument. This latter serves as a reference. From the four Tp values computation algorithms, the algorithm using threshold conditions gives the closest linear regression to the commercial instrument values. This seems reasonable since the commercial instrument software uses a similar method to compute the Tp values. The algorithm using a threshold with the logarithm of the normalized value also exhibits similar performances as the commercial instrument, with a different interception coefficient b. The 1^{st} derivative algorithm has a low correlation coefficient, showing the limitations of this computation methods. From this study, the most optimal Tp computation method seem to use a threshold, either directly with the raw fluorescence data, or with the logarithm of the normalized data.

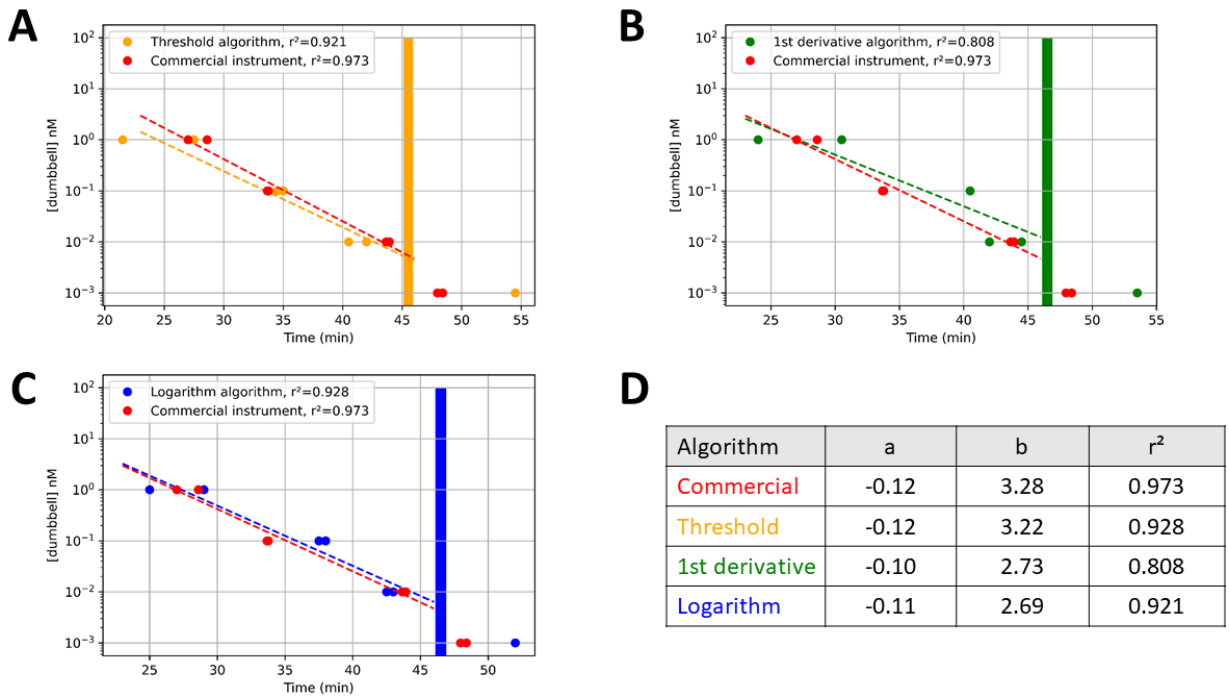

Algorithm	a	b	r^2
Commercial	-0.12	3.28	0.973
Threshold	-0.12	3.22	0.928
1st derivative	-0.10	2.73	0.808
Logarithm	-0.11	2.69	0.921

Figure 5.19: On-chip quantification of dumbbell D3 compared to in tube commercial amplification. Dumbbell concentration (nM) as a function of the computed Tp values for the different methods (data from figure 5.17B). (A) Threshold algorithm, (B) First derivative algorithm, (C) Logarithm algorithm and (D)Evaluation of the linear regression performance of the different algorithm used. a is the slope, b the interception value and r^2 the correlation coefficient.

5.3.2.4 Discussion

It is possible to quantify dumbbell D3 with on-chip isothermal amplification. There is a clear shift in the fluorescence data over time for different dumbbell concentrations, and the implementation of Tp values computation methods lead to the successful quantification in the range 1 nM to 10 pM. The performances are similar to the ones obtained on a commercial thermocycler instrument, which therefore is encouraging for the integration of amplification protocols on-chip with the automated instrument. The architecture with chambers and valves allow the fine manipulation of fluids in a parallelized manner, and an optimal process was found to take advantage of this architecture. The quantification range achieved is coherent with the dumbbell quantity added in the troponin iLAMP protocols (100 pM), and should allow the full protocol automation.

However, the LOD is limited by the non specific amplification signal. We assign this non specific amplification to the permeability of the valves which inherently creates air filtration in the system and alters the permeability of the microfluidic rows. This represents the main limitation of this microfluidic chip architecture for isothermal amplification. A way to counteract this would be to use valves that have a better impermeability to ensure no cross-contamination between the chambers, or to form a chemical barrier with RNAse AWAY for example at the exit of the LAMP reaction chambers. Valve impermeability could be improved by using a higher actuation pressure, but this would be incompatible with the chosen digital microfluidic technology with stretchable membrane, and would also inject more air in the system. An additional chemical barrier at the exit of the amplification chamber would be bulky to implement

on the credit-size format cartridge. There are also many parameters that can be tuned to optimize the on-chip isothermal amplification, such as the dumbbell choice (with its amplification celerity), or various LAMP mixture optimizations (choice of enzyme, buffers, concentrations etc...) that affects the fluid properties and therefore the microfluidic cartridge filling process and fluid behavior during warming. Lastly, the inhomogeneity in chambers temperature needs to be taken into account for inter-rows repeatability. Interestingly, the two extreme chambers (1 and 10) with the lowest estimated temperature showed very few non specific amplification. This paves the way to a method to reduce the non specific amplification which currently limits the on-chip LAMP assay LOD by reducing the overall system temperature (down to 60-50°C). Moreover, due to the multi-layer microfluidic cartridge, there is a transition time to reach the desired temperature in the chambers, that could be reduced by implementing first a higher input temperature on the heating system, and then reducing it to the desired value. This could reduce the transition time and therefore improve the on-chip LAMP amplification velocity. Lastly, several algorithms were tested to quantify the amount of dumbbell from fluorescent amplification curves. It seems that the threshold method yields the best quantification results, but more statistics need to be obtained to conclude on the method.

The designed microfluidic cartridge and the implementation of on-chip isothermal amplification protocols led to the successful recording of fluorescence increase in dedicated microfluidic chambers, and the possible quantification with data processing methods. The microfluidic cartridge design with rows allows the implementation of 10 amplification reactions in parallel. From the cartridge design and using synthetic dumbbells, it was possible to draw dumbbell quantification curves in the subnanomolar range. The dumbbell is used in subsequent iLAMP assay with a concentration of 100 pM. Therefore, its on-chip quantification when being used as the detection complex should be possible. In combination to the sample preparation module already present in the cartridge design, these results open the way for various opportunities for POC device development integrating isothermal amplification protocols.

5.4 Conclusion and perspectives

In the context of portable medical diagnostic with POC systems, the development of microfluidic technologies appears as a very powerful tool for the integration of various biological assays. There are already many cardiac POC systems relying on the use of microfluidic technology [163, 68, 88, 98], some of them even led to commercialized devices [86].

For the detection of cardiac biomarkers, we propose an innovative and original assay called iLAMP combining immunoassay formation and nucleic acids isothermal amplification. The scientific literature already highlights a broad variety of microfluidic tools for immunoassays [160] and nucleic acids isothermal amplification [176, 172]. We proposed a single microfluidic chip for the integration of the two main steps of this iLAMP assay. To do so, we took advantage of polymer pneumatically actuated microfluidic cartridges [169] and an associated instrumentation with all the required hardware (pneumatic control, heating and optical system, magnetic arm...). We based our reasoning on building blocks to validate each module individually and therefore validate sequentially each step of the iLAMP protocol on-chip.

First, the troponin was successfully captured with magnetic beads on the cartridge sample preparation module. The chip architecture is versatile and allows to carry out each step in the sandwich formation, from reagent injection and calibration, to incubation, mixing, and washing. With this on-chip sandwich formation, troponin was quantified in the range 100 ng/mL to 1 ng/mL, in buffer and in plasma medium. In order to reduce the assay total time, an additional module could be added on the cartridge in order to separate plasma from blood [183], and

therefore proposing a cartridge functioning directly with full blood samples, without previous plasma preparation. However, such a blood preparation modules could be bulky to implement directly inside the chosen microfluidic cartridge, but it could be interesting to add it above the reagent inlets.

Secondly, the dumbbell isothermal amplification (LAMP) was validated on-chip with real-time fluorescence detection in dedicated chambers. This specific LAMP module on the cartridge was validated individually for two different dumbbells (D2-THR-DE5 and D3). Several optimizations (LED lightning, heating module, fluidic actuation, architecture...) led to the successful quantification of dumbbell in the range 10 nM to 10 pM. The on-chip dumbbell isothermal amplification quantification range is consistent with the dumbbell quantity added in the final step of the iLAMP assay (100 pM). Several fluidic optimizations were conducted to take advantage of the chambers and valves architecture on the cartridge and limit the air injection in the LAMP reaction chambers that alters the fluorescence detection. This way, we proposed 10 rows of double amplification chambers after the sample preparation module. However, the important number of chambers rows and their link through the central channel is the main limitation of the implementation of the on-chip amplification, which led to important non specific amplification. In order to lower the LAMP assay sensitivity, the impermeability of microfluidic chambers needs to be enhanced to limit the non specific amplification emerging from cross-contamination between chambers. Perspectives to solve this issue are the use of non porous membrane, but the elasticity of such membranes is reduced, or the removal of hyperelastic membrane in the LAMP reaction chambers. The optical and thermal system implemented to perform on-chip amplification represents the most bulky part of the system. They were necessary to achieve large thermally and optically homogeneous areas on-chip for quantification, but some improvements can be made to reduce their size, and therefore propose a small portable device. Lastly, we implemented a specific cartridge washing procedure and validated the cartridge reuse for successive LAMP amplifications, therefore proposing a cartridge with multi-usage meeting sustainable developments strategies and the reduction of waste associated to research and medical devices [159].

The combination of the sample preparation module for troponin capture, and the isothermal amplification module should lead to the full on-chip protocol integration for troponin sensing through the iLAMP method (Fig 5.20 B and C). The two modules for sample preparation and isothermal amplification (Fig 5.20A) were already validated individually and their performances evaluated. The troponin was successfully captured in the sample preparation module, and the dumbbell isothermal amplification was conducted on the LAMP module, with quantification possible down to 10 pM. The next challenge that arises is the succession of the magnetic beads sample preparation and subsequent dumbbell isothermal amplification in the complete cartridge. The complete iLAMP protocols steps implementation in cartridge design C is represented in figure 5.21.

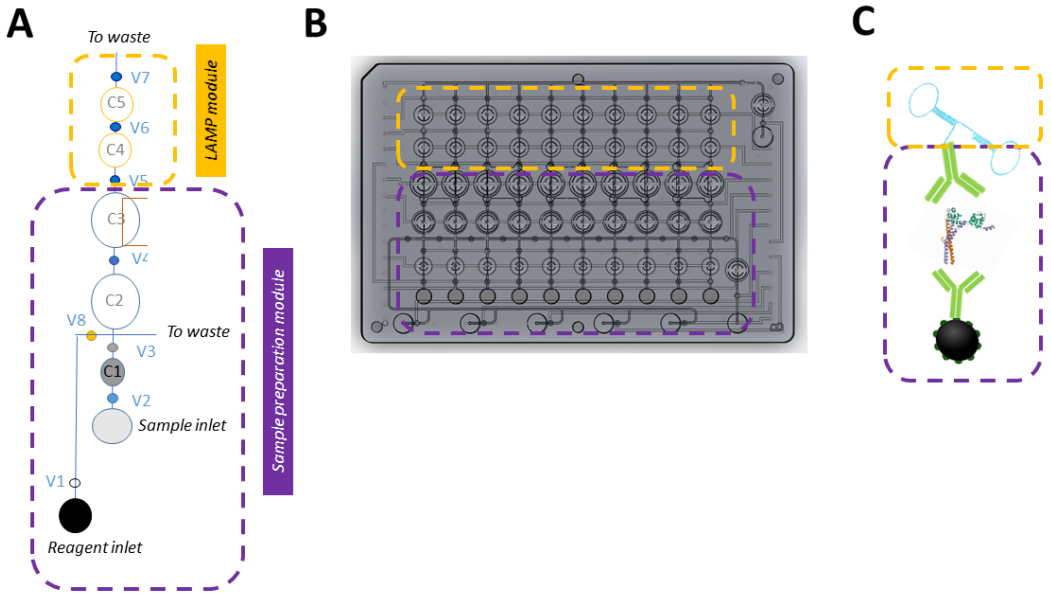

Figure 5.20: Complete iLAMP protocol integration with sample preparation (purple) and LAMP (yellow) module (A) Cartridge architecture for one row, (B) Complete cartridge architecture with 10 rows and (C) iLAMP detection principle

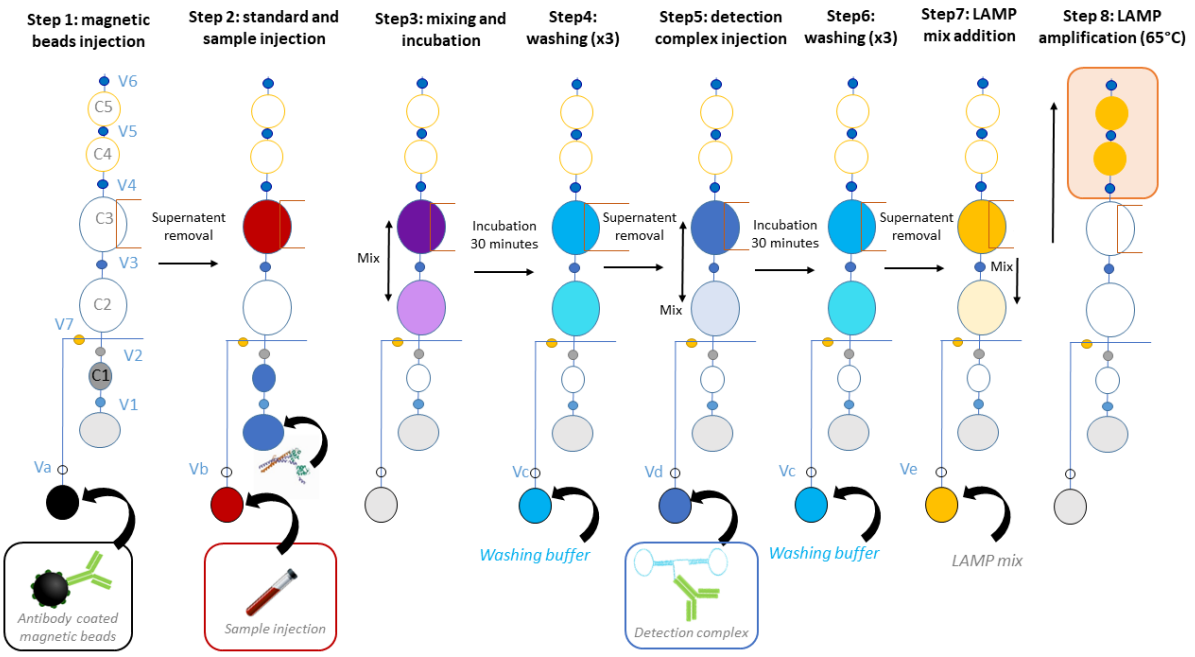

Figure 5.21: Schematic top view of the unitary module for each step of the complete troponin detection protocol in the microfluidic cartridge. Magnetic beads injection (step 1), standard and sample injection (step 2), mixing and incubation (step 3), washing (step 4), detection complex injection (step 5), washing (step 6), LAMP mix addition and mixing (step 7) and finally LAMP amplification.

With promising results on the troponin capture and the dumbbell isothermal amplification on-chip, the combination of the two developed modules should lead to the complete integration of the iLAMP troponin assay. This way, a portable platform can be proposed for a full troponin test from sample deposition on-chip to the quantification of troponin from the fluorescence curves. The protocols, the platform and cartridges developed are versatile and can therefore be applied to other types of biomarkers in the context of cardiovascular diseases testing, and also in other contexts (environmental, agricultural...). For example, the methodology developed for troponin iLAMP protocols can be declined for the peptide NTproBNP, another important cardiac biomarker. Moreover, an emerging category of cardiac biomarkers, miRNA can be detected with various isothermal amplification methods [120], which can therefore be integrated on-chip. This opens the way to the development of a cartridge for the multiplex detection of different cardiac biomarkers on a single microfluidic cartridge, comprising dedicated isothermal amplification rows for each target. This multiplexing could also be achieved using a single microfluidic row but using different dyes for the target-specific amplification signal readout [114].

Summary

- Cartridge SP validation for free oligonucleotide capture on magnetic beads with quantification range from 1 nM to 10 pM
- Cartridge SP validation for troponin sandwich capture on magnetic beads with quantification range 100 - 1 ng/mL in buffer and plasma samples
- Fluidic optimizations to limit the air injection in the LAMP reaction chambers
- Quantification of dumbbell D3 from 10 nM to 10 pM in cartridge C
- Implementation of washing strategy to ensure cartridge reusability for successive protocols
- With the validation of troponin capture and LAMP amplification on-chip, cartridge C is proposed for a full automation of troponin iLAMP protocols

Chapter 6

Conclusions and perspectives

Cardiovascular diseases represent the major cause of death worldwide and several biomarkers are released in the patient blood prior to an accident and used clinically to diagnose patients [21]. Cardiac troponin I is the gold standard for the diagnostic of myocardial infarction, and natriuretic peptides such as NTproBNP are appropriate biomarkers for the diagnostic of heart failure and myocardial infarction [5]. Other types of biomarkers such as miRNA have emerged over the past years in the scientific literature and have a high potential in the field of cardiovascular diseases testing [14]. In hospital emergency departments, testing patient blood for cardiac biomarkers is crucial to rule-in or rule-out patients, and current methods use central laboratory equipment to perform ELISA tests, which are costly and time-consuming tests [1]. In the context of cardiovascular diseases testing, Point-of-Care devices propose on-site and rapid testing, and appear as promising tools to propose a better patient care and facilitate hospital workflows [101].

The literature review highlighted the latest advances in terms of cardiovascular POC testing devices, and pointed out the very competitive devices and methods already existing to propose portable detection of cardiac biomarkers. However, they are usually limited in sensitivity and to single target detection, with reduced options for the simultaneous detection of several cardiac biomarkers on a single platform. Several strategies and trends were highlighted in the literature to design high sensitivity assays for cardiac biomarkers. They consist mostly in using innovative signal amplification methods and in integrating the tests on portable platforms, relying on the use of microfluidic technologies. Based on these inputs, designing a POC device for the high sensitivity and multiplexed detection of cardiac biomarkers in blood was the main objective of this PhD.

To improve the sensitivity of bioassays, we developed a synthetic nucleic acid sequence called dumbbell that serves as a nucleic acid template for isothermal exponential amplification (LAMP) in various types of assays. We combined it with different types of molecular probes, such as aptamers or antibodies, to design a complete biological assay with exponential signal amplification. We used this structure in two different types of assays for the detection of proteins. We integrated a thrombin aptamer sequence in the dumbbell structure and proposed a complete antibody-free assay for the thrombin detection, called aptameroLAMP. In addition, we combined this dumbbell structure with antibodies to provide exponential amplification for immunoassays, and proposed an immunoLAMP assay for the quantification of troponin, reaching physio-pathological concentration range in human plasma samples.

The dumbbell structure opens many perspectives for its integration into quantitative assays for the detection of various targets. The dumbbell structure can be directly used for the direct dosage of free nucleic acids sequences, through the specific design of the dumbbell sequence

to particularly hybridize to a target. This was implemented in chapter 3, for the quantitative detection of free short oligonucleotide strands in a sandwich format, but could also be implemented for the detection of miRNA, an emerging category of cardiac biomarkers [14]. This quantification with the dumbbell could be applied in a sandwich manner as already described or by splitting the dumbbell into two loops, each containing a portion that will bind to half of the target, which will form the complete dumbbell structure when hybridized to the target of interest. Moreover, this structure was validated for isothermal amplification with intercalating dye, but could also be associated with quenchers, in order to proposed multiplexed detection of targets in solution, through multi-fluorescence [114]. Furthermore, the application of the aptameroLAMP or immunoLAMP method is not limited to the detection of proteins, and can be adapted to any other target presenting a validated aptamer or antibody sandwich [142]. It would be particularly interesting to design a similar assay for NTproBNP, biomarker of heart failure, that could be integrated with the same detection methodology as troponin [49]. The developed biological assay method relying on the use of the dumbbell structure, as a template for exponential amplification, is versatile and presents many opportunities to be used for other types of markers than the one exposed in this project. This is encouraging for the development of cardiac biomarker multiplexed assays, but also for other types of high sensitivity assay developments.

Secondly, in order to offer portable, rapid and sensitive biological assays, we propose a complete portable instrument for protocol integration into microfluidic cartridges. We designed microfluidic cartridges relying on the use of digital microfluidic technology, for the integration of each steps of the biological assay. This was made possible by pneumatically actuated multi-layer polymeric microfluidic cartridges, with a network of valves and chambers in a XY architecture for discrete volume manipulation. First, we validated the on-chip troponin capture on magnetic beads with a specific sample preparation module handling magnetic beads. Then, we validated the on-chip dumbbell isothermal amplification with the microfluidic cartridge placed on the thermal actuation system, associated with an optical module to record the real-time fluorescence. The combination of the instrument and the microfluidic cartridges allows the complete automation of the two main biological assay steps: sample preparation and isothermal amplification. The next challenge in this development would be to use the final designed complete cartridge C for the full iLAMP protocol integration, including these two main steps. This way, a portable platform could be proposed for a complete iLAMP troponin test, from sample deposition on chip, to the quantification of troponin.

One of the great advantage and innovation of the proposed microfluidic cartridge and its inclusion into a cardiac POC device is that it includes an on-chip calibration curve for each performed assay. Indeed, the patient sample is spiked with the analyte of interest for each test, and a calibration curve is drawn each time, thus reducing the sample dependance test result. Thus, this assay and its integration into a complete POC device could propose a patient dependant blood test result, counteracting the lack of standardization in current cardiac POC devices [5]. Moreover, this portable platform and associated cartridges is generic and not limited to troponin detection. With the developed assay and microfluidic cartridges, there are several ways to propose multiplexed detection on the platform. We could propose a cartridge architecture with a common sample preparation module with dumbbell-design specific detection complexes, each associated with a specific set of primer, for different analytes. After the common sample preparation module with various dumbbells recognition, two main on-chip multiplexing strategies could be implemented. First, the use of quenchers and multi-fluorescent recording could be considered, and we could propose multiplexing in single amplification chamber, with each dumbbell amplification associated to a fluorescent wavelength (Fig. 6.1A). Secondly, the digital

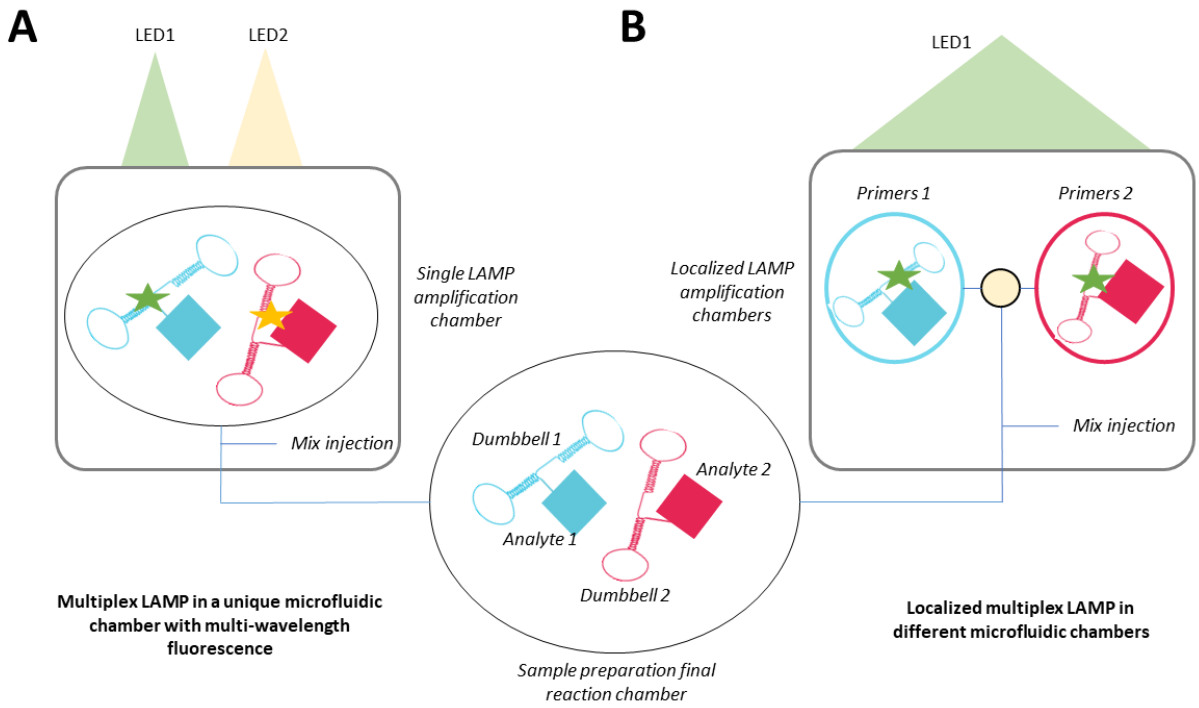

Figure 6.1: Schematic representation of the considered multiplexing options for LAMP amplification as the final stage of the multiplexed on-chip immunoLAMP protocols. In both cases, the multi-target sandwich is achieved in the sample preparation module in a single chamber, with two different dumbbells targeting different targets. In the final stage of the protocol, two multiplexed scenarii are possible: (A) Use of multi-wavelength fluorescence in a single microfluidic chamber for fluorescence-specific amplification with several dedicated wavelengths and (B) Localized multiplex LAMP in different microfluidic chambers, with dedicated primer set associated to each dumbbell

microfluidic with the discretization of volumes on chip allows the confinement of reactions in different chambers. By taking advantage of the volume partitioning and the use of different dumbbell designs and associated sets of primers, we could design specific LAMP amplification chambers depending on the target of interest, with dedicated dumbbell and primers (Fig. 6.1B).

Lastly, it appeared that the on-chip dumbbell amplification is limited in sensitivity (10 pM), which could be a limit for the complete integration of the proposed iLAMP troponin assay, due to non-specific amplification, which would restrained the achieved embedded assay sensitivity. A way to counteract this limitation would be to partition the samples into digital droplets, after the on-chip sample preparation module [184, 185, 175]. Indeed, as it is the case for ddPCR [186], the partitioning of sample into thousands of small droplets for individual isothermal amplification and statistical analysis should lower the limit of detection achieved with the LAMP amplification. This integration could be achieved on the developed microfluidic cartridge by replacing the FlowStretch LAMP module by a specific fluidic structure with a channel for oil injection, that would partition the sample into thousands of droplets (Fig. 6.2). These will then be transferred into a microfluidic cell (Hele-Shaw type) for isothermal amplification. The partitioning of the sample into thousands of droplets and the combination with statistical analysis after amplification, should help to lower the limit of detection achieved on-chip with this digital droplet LAMP (ddLAMP) method, following the sample preparation module. However, this

requires several microfluidic developments to bridge together the two microfluidic technologies and demonstrate the sensitivity improvement of such a ddLAMP amplification device. This investigation will be carried out in a subsequent PhD project.

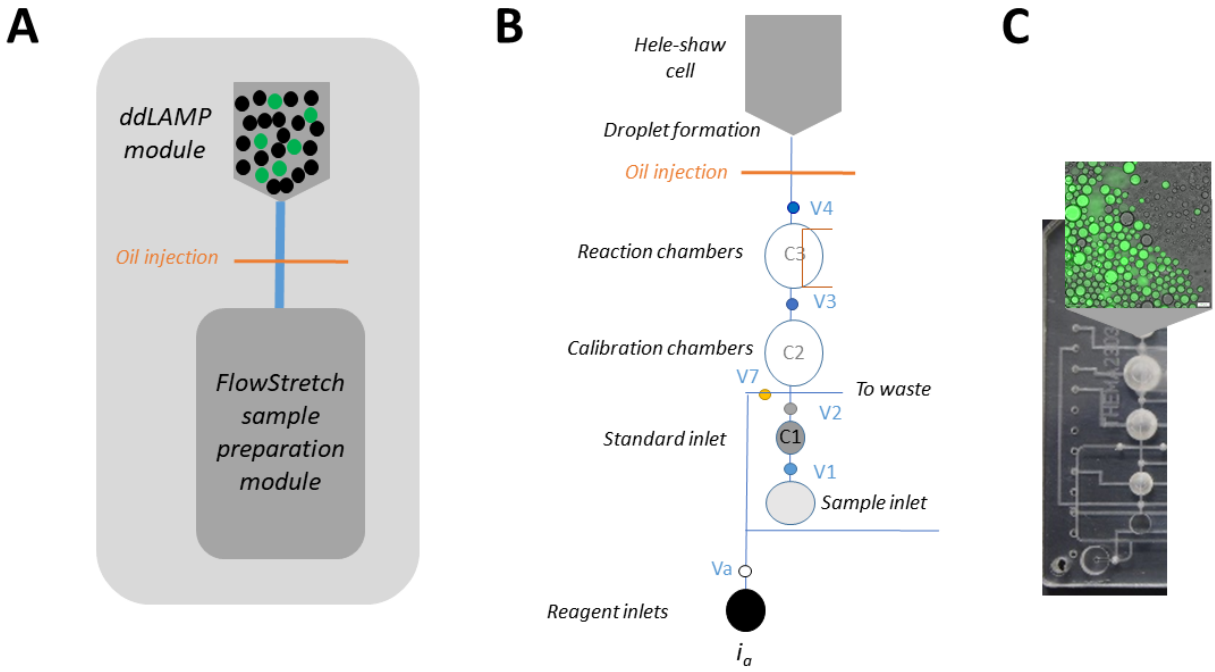

Figure 6.2: Coupling of the sample preparation microfluidic cartridge and the ddLAMP module. (A) Schematic representation of the two modules on a single chip. (B) Schematic view of the unitary module for the sample preparation module with an oil injection channel for droplet formation and Hele Shaw cell type chip for isothermal amplification. (C) Pictures of the sample preparation module and on-chip droplets formation (separate chips).

A summary of the main results obtained during this PhD project can be found in figure 6.3, as well as the associated perspectives.

During this PhD project, we explored several pathways to propose sensitive detection assays, portable instrument and we opened many perspectives for the application of the method for multiplex detection of several cardiac biomarkers on a single platform. In particular, it leads to the automated quantification of troponin I in blood samples on the portable platform, and even though there are many improvements to bring in order to achieve high sensitivity sensing, the development could lead to a complete medical device for the multiplex detection of cardiac biomarkers on a single platform [144]. There is currently no commercialized cardiac POC device for the multiplex detection of cardiac biomarkers. Additionally, current cardiac POC devices currently lack standardization [5] for the cut-off value definition. The proposed platform should propose patient-dependant blood test result, counteracting the difficulty to find a universal cut-off value in cardiac POC devices. One of the main perspective of this project is the *in situ* testing of the developed device on clinical samples. During this project, we collaborated with the Saint-Etienne Centre Hospitalier Universitaire (CHU), particularly with an ICU practitioner who guided us on the use of cardiac POC in various hospital settings. In the hospital ICU,

troponin tests are run daily in a very short time-frame due to the proximity with the central medical laboratory, but in ambulances or in remote small country-side hospitals, the time to get the blood test results can be long, while facing critical medical situations. Therefore, in such contexts, the proposed medical device could greatly improve the time-to-result by delivering a quantitative blood test result directly at the patient site. Such clinical *in situ* tests could be implemented in collaboration with the Saint-Etienne CHU in order to evaluate the performance and improvements brought by the complete device, for the portable, patient-dependant and multiplex detection of cardiac biomarkers.

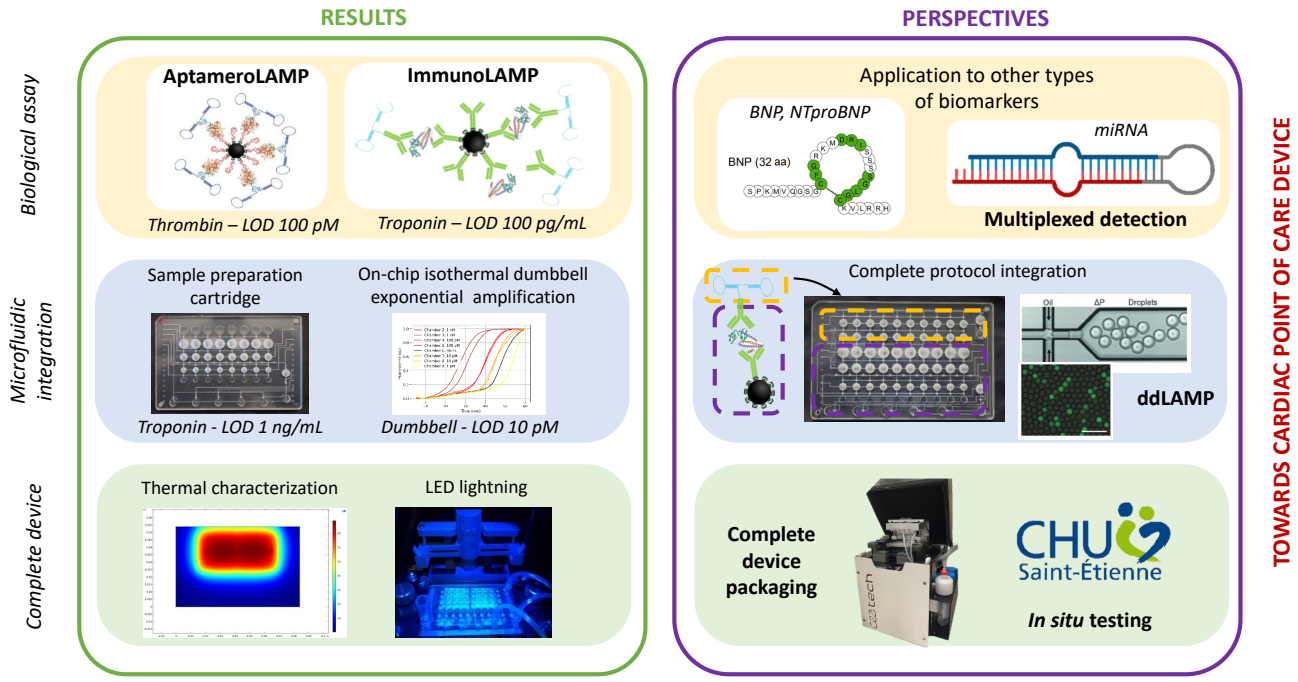

Figure 6.3: Synthesis of PhD main results and perspectives

Bibliography

[1] Maud Savonnet et al. "Recent advances in cardiac biomarkers detection: From commercial devices to emerging technologies". In: *Journal of Pharmaceutical and Biomedical Analysis* 194 (2021), p. 113777. DOI: 10.1016/j.jpba.2020.113777. (Visited on 09/06/2022).

[2] United Nations. *Health - United Nations Sustainable Development*. URL: https://www.un.org/sustainabledevelopment/health/ (visited on 09/06/2022).

[3] WHO. *Cardiovascular diseases*. URL: https://www.who.int/health-topics/cardiovascular-diseases (visited on 09/06/2022).

[4] W. Huo et al. "A Novel High-Sensitivity Cardiac Multibiomarker Detection System Based on Microfluidic Chip and GMR Sensors". In: *IEEE Transactions on Magnetics* 51.11 (2015). DOI: 10.1109/TMAG.2015.2457513.

[5] Holger Thiele et al. "2020 ESC Guidelines for the management of acute coronary syndromes in patients presenting without persistent ST-segment elevation: The Task Force for the management of acute coronary syndromes in patients presenting without persistent ST-segment elevation of the European Society of Cardiology (ESC)". In: *European Heart Journal* 42.14 (Aug. 2020), pp. 1289–1367. DOI: 10.1093/eurheartj/ehaa575.

[6] Li Yang et al. "Economic burden of cardiovascular diseases in China". In: *Expert Review of Pharmacoeconomics & Outcomes Research* 8.4 (2008-08), pp. 349–356. DOI: 10.1586/14737167.8.4.349.

[7] Sabine Szunerits et al. "Electrochemical cardiovascular platforms: Current state of the art and beyond". In: *Biosensors and Bioelectronics* 131 (Apr. 15, 2019), pp. 287–298. DOI: 10.1016/j.bios.2019.02.010.

[8] C. Navarro et al. "A point-of-care measurement of NT-proBNP for heart failure patients". In: *IEEE Access* 8 (2020), pp. 138973–138983. DOI: 10.1109/ACCESS.2020.3007988.

[9] Kristian Thygesen et al. "Recommendations for the use of natriuretic peptides in acute cardiac care†: A position statement from the Study Group on Biomarkers in Cardiology of the ESC Working Group on Acute Cardiac Care". In: *European Heart Journal* 33.16 (2012-08-01), pp. 2001–2006. DOI: 10.1093/eurheartj/ehq509.

[10] Meysam Gachpazan et al. "A review of biosensors for the detection of B-type natriuretic peptide as an important cardiovascular biomarker". In: *Analytical and Bioanalytical Chemistry* 413.24 (2021), pp. 5949–5967. DOI: 10.1007/s00216-021-03490-6.

[11] C. Sinning et al. "Up-and-coming markers: Myeloperoxidase, a novel biomarker test for heart failure and acute coronary syndrome application?" In: *Congestive Heart Failure* 14.4 (2008), pp. 46–48. DOI: 10.1111/j.1751-7133.2008.08334.x.

[12] Michael Sarhene et al. "Biomarkers in heart failure: the past, current and future". In: *Heart Failure Reviews* 24.6 (2019), pp. 867–903. DOI: 10.1007/s10741-019-09807-z.

[13] Abdelmonaim Azzouz et al. "Nanomaterial-based aptasensors as an efficient substitute for cardiovascular disease diagnosis: Future of smart biosensors". In: *Biosensors and Bioelectronics* 193 (2021-12-01), p. 113617. DOI: 10.1016/j.bios.2021.113617.

[14] Perry V. Halushka, Andrew J. Goodwin, and Marc K. Halushka. "Opportunities for microRNAs in the Crowded Field of Cardiovascular Biomarkers". In: *Annual Review of Pathology: Mechanisms of Disease* 14.1 (2019), pp. 211–238. DOI: 10.1146/annurev-pathmechdis-012418-012827.

[15] Kyriacos Felekkis and Christos Papaneophytou. "Challenges in Using Circulating MicroRNAs as Biomarkers for Cardiovascular Diseases". In: *International Journal of Molecular Sciences* 21.2 (2020), p. 561. DOI: 10.3390/ijms21020561.

[16] Andreea Campu et al. "Cardiac Troponin Biosensor Designs: Current Developments and Remaining Challenges". In: *International Journal of Molecular Sciences* 23.14 (2022), p. 7728. DOI: 10.3390/ijms23147728.

[17] Maud Savonnet. "Développement d'une méthode de détection innovante appliquée au diagnostic terrain des pathologies cardiaques". 2020GRALY061. PhD thesis. 2020. URL: http://www.theses.fr/2020GRALY061.

[18] Bernadette Cummins, Margaret Lucy Auckland, and Peter Cummins. "Cardiac-specific troponin-l radioimmunoassay in the diagnosis of acute myocardial infarction". In: *American Heart Journal* 113.6 (1987-06-01), pp. 1333–1344. DOI: 10.1016/0002-8703(87)90645-4.

[19] James L. Januzzi et al. "Recommendations for Institutions Transitioning to High-Sensitivity Troponin Testing: JACC Scientific Expert Panel". In: *Journal of the American College of Cardiology* 73.9 (2019-03-12), pp. 1059–1077. DOI: 10.1016/j.jacc.2018.12.046.

[20] Akshay Bagai et al. "Use of Troponin Assay 99th Percentile as the Decision Level for Myocardial Infarction Diagnosis". In: *American heart journal* 190 (2017), pp. 135–139. DOI: 10.1016/j.ahj.2017.04.016.

[21] Xi-Ying Wang et al. "The Biomarkers for Acute Myocardial Infarction and Heart Failure". In: *BioMed Research International* 2020 (2020-01-17), e2018035. DOI: 10.1155/2020/2018035.

[22] David P Bartel. "MicroRNAs: Genomics, Biogenesis, Mechanism, and Function". In: *Cell* 116.2 (2004), pp. 281–297. DOI: 10.1016/S0092-8674(04)00045-5.

[23] Laura Anfossi et al. "Multiplex Lateral Flow Immunoassay: An Overview of Strategies towards High-throughput Point-of-Need Testing". In: *Biosensors* 9.1 (2019), p. 2. DOI: 10.3390/bios9010002.

[24] Xin Zhao, Yao Wang, and Xianglan Sun. "The functions of microRNA-208 in the heart". In: *Diabetes Research and Clinical Practice* 160 (2020-02-01), p. 108004. DOI: 10.1016/j.diabres.2020.108004.

[25] Kevin J. Land et al. "REASSURED diagnostics to inform disease control strategies, strengthen health systems and improve patient outcomes". In: *Nature Microbiology* 4.1 (2019), pp. 46–54. DOI: 10.1038/s41564-018-0295-3.

[26] Samiksha Nayak et al. "Point-of-Care Diagnostics: Recent Developments in a Connected Age". In: *Analytical Chemistry* 89.1 (2017), pp. 102–123. DOI: 10.1021/acs.analchem.6b04630.

[27] P. O. Collinson et al. "A prospective randomized controlled trial of point-of-care testing on the coronary care unit". In: *Annals of Clinical Biochemistry* 41 (Pt 5 Sept. 2004), pp. 397–404. DOI: 10.1258/0004563041731547.

[28] Pierre Hausfater et al. "Impact of Point-of-care Testing on Length of Stay of Patients in the Emergency Department: A Cluster-randomized Controlled Study". In: *Academic Emergency Medicine* 27.10 (2020), pp. 974–983. DOI: 10.1111/acem.14072. URL: https://onlinelibrary.wiley.com/doi/abs/10.1111/acem.14072.

[29] Assurance maladie. *Actes de biologie médicale - Biol'AM - en 2020 — L'Assurance Maladie*. 2020. URL: https://assurance-maladie.ameli.fr/etudes-et-donnees/actes-biologie-medicale-biolam-2020 (visited on 09/08/2022).

[30] Masataka Nishiga et al. "COVID-19 and cardiovascular disease: from basic mechanisms to clinical perspectives". In: *Nature Reviews Cardiology* 17.9 (2020-09), pp. 543–558. DOI: 10.1038/s41569-020-0413-9.

[31] Roche. *Cobas h 232 POC system*. URL: https://diagnostics.roche.com/global/en/products/instruments/cobas-h-232-ins-653.html#productSpecs (visited on 10/13/2022).

[32] Nikhil Bhalla et al. "Introduction to biosensors". In: *Essays in Biochemistry* 60.1 (2016-06-30), pp. 1–8. DOI: 10.1042/EBC20150001.

[33] Giuseppe Pantaleo et al. "Antibodies to combat viral infections: development strategies and progress". In: *Nature Reviews Drug Discovery* 21.9 (2022), pp. 676–696. DOI: 10.1038/s41573-022-00495-3.

[34] Carl A Ascoli and Birte Aggeler. "Overlooked benefits of using polyclonal antibodies". In: *BioTechniques* 65.3 (2018-09), pp. 127–136. DOI: 10.2144/btn-2018-0065.

[35] Ph.D Tyasning Kroemer. *An Overview of Polyclonal and Monoclonal Antibodies: Their Differences and How to Choose*. GoldBio. 2023. URL: https://goldbio.com/articles/article/an-overview-of-polyclonal-and-monoclonal-antibodies-their-differences-and-how-to-choose.

[36] Amado J. Pesce and J. Gabriel Michael. "Artifacts and limitations of enzyme immunoassay". In: *Journal of Immunological Methods* 150.1 (1992), pp. 111–119. DOI: 10.1016/0022-1759(92)90070-A.

[37] Paul J. Conroy et al. "Antibody production, design and use for biosensor-based applications". In: *Seminars in Cell & Developmental Biology*. A Special Edition on Biosensors and Development of Pigment Cells and Pigment Patterns 20.1 (2009), pp. 10–26. DOI: 10.1016/j.semcdb.2009.01.010.

[38] Craig Tuerk and Larry Gold. "Systematic Evolution of Ligands by Exponential Enrichment: RNA Ligands to Bacteriophage T4 DNA Polymerase". In: *Science* 249.4968 (1990), pp. 505–510. DOI: 10.1126/science.2200121.

[39] Jon Jyoti Kalita, Pragya Sharma, and Utpal Bora. "Recent developments in application of nucleic acid aptamer in food safety". In: *Food Control* 145 (2023-03-01), p. 109406. DOI: 10.1016/j.foodcont.2022.109406.

[40] S. D. Jayasena. "Aptamers: an emerging class of molecules that rival antibodies in diagnostics". In: *Clinical Chemistry* 45.9 (1999), pp. 1628–1650.

[41] Zhenjian Zhuo et al. "Recent Advances in SELEX Technology and Aptamer Applications in Biomedicine". In: *International Journal of Molecular Sciences* 18 (2017), p. 2142. DOI: 10.3390/ijms18102142.

[42] Andrew D. Ellington and Jack W. Szostak. "Selection in vitro of single-stranded DNA molecules that fold into specific ligand-binding structures". In: *Nature* 355.6363 (1992), pp. 850–852. DOI: 10.1038/355850a0.

[43] Nasim Shahidi Hamedani and Jens Müller. "Capillary Electrophoresis for the Selection of DNA Aptamers Recognizing Activated Protein C". In: *Nucleic Acid Aptamers: Selection, Characterization, and Application*. Ed. by Günter Mayer. Methods in Molecular Biology. New York, NY, 2016, pp. 61–75. ISBN: 978-1-4939-3197-2. DOI: 10.1007/978-1-4939-3197-2_5. URL: https://doi.org/10.1007/978-1-4939-3197-2_5.

[44] Hao Jiang, Xue-Fei Lv, and Ke-Xin Zhao. "Progress of Aptamer Screening Techniques Based on Microfluidic Chips". In: *Chinese Journal of Analytical Chemistry* 48.5 (2020), pp. 590–600. DOI: 10.1016/S1872-2040(20)60015-9.

[45] Glen Hybarger et al. "A microfluidic SELEX prototype". In: *Analytical and Bioanalytical Chemistry* 384.1 (2006), pp. 191–198. DOI: 10.1007/s00216-005-0089-3.

[46] Seung-min Park et al. "Selection and elution of aptamers using nanoporous sol-gel arrays with integrated microheaters". In: *Lab on a Chip* 9.9 (2009), pp. 1206–1212. DOI: 10.1039/B814993C.

[47] Saw Yi Toh et al. "Aptamers as a replacement for antibodies in enzyme-linked immunosorbent assay". In: *Biosensors & Bioelectronics* 64 (2015), pp. 392–403. DOI: 10.1016/j.bios.2014.09.026.

[48] Diana A. Sousa et al. "Recent Advances in the Selection of Cancer-Specific Aptamers for the Development of Biosensors". In: *Current Medicinal Chemistry* 29.37 (2022), pp. 5850–5880. DOI: 10.2174/0929867329666220224155037.

[49] Natalia Komarova et al. "Aptamers Targeting Cardiac Biomarkers as an Analytical Tool for the Diagnostics of Cardiovascular Diseases: A Review". In: *Biomedicines* 10.5 (2022), p. 1085. DOI: 10.3390/biomedicines10051085.

[50] Emre Ozan Polat et al. "Transducer Technologies for Biosensors and Their Wearable Applications". In: *Biosensors* 12.6 (2022-06), p. 385. DOI: 10.3390/bios12060385.

[51] Berta Esteban-Fernández de Ávila et al. "Multiplexed Determination of Amino-Terminal Pro-B-Type Natriuretic Peptide and C-Reactive Protein Cardiac Biomarkers in Human Serum at a Disposable Electrochemical Magnetoimmunosensor". In: *Electroanalysis* 26.2 (2014), pp. 254–261. DOI: 10.1002/elan.201300479.

[52] Fereshteh Chekin et al. "Sensitive electrochemical detection of cardiac troponin I in serum and saliva by nitrogen-doped porous reduced graphene oxide electrode". In: *Sensors and Actuators B: Chemical* 262 (June 1, 2018), pp. 180–187. DOI: 10.1016/j.snb.2018.01.215.

[53] Nandhinee Radha Shanmugam, Sriram Muthukumar, and Shalini Prasad. "Ultrasensitive and low-volume point-of-care diagnostics on flexible strips – a study with cardiac troponin biomarkers". In: *Scientific Reports* 6.1 (2016), p. 33423. DOI: 10.1038/srep33423.

[54] Iwona Grabowska et al. "Electrochemical Aptamer-Based Biosensors for the Detection of Cardiac Biomarkers". In: *ACS Omega* 3.9 (2018), pp. 12010–12018. DOI: 10.1021/acsomega.8b01558.

[55] Francesca Torrini et al. "Characterization of troponin T binding aptamers for an innovative enzyme-linked oligonucleotide assay (ELONA)". In: *Analytical and Bioanalytical Chemistry* 411.29 (2019). Number: 29, pp. 7709–7716. DOI: 10.1007/s00216-019-02014-7.

[56] C. Parent et al. "Quantitative biological assays with on-chip calibration using versatile architecture and collapsible chambers". In: *Sensors and Actuators B: Chemical* 261 (2018), pp. 106–114. DOI: 10.1016/j.snb.2018.01.111.

[57] Piyush Kar et al. "Ultrahigh sensitivity assays for human cardiac troponin I using TiO2 nanotube arrays". In: *Lab on a Chip* 12.4 (2012-01-23), pp. 821–828. DOI: 10.1039/C2LC20892J.

[58] Dongkui Liu et al. "A novel fluorescent aptasensor for the highly sensitive and selective detection of cardiac troponin I based on a graphene oxide platform". In: *Analytical and Bioanalytical Chemistry* 410.18 (2018). Number: 18, pp. 4285–4291. DOI: 10.1007/s00216-018-1076-9.

[59] Kangning Cheng et al. "Automated and rapid chemiluminescence immunoassay for cardiac troponin I based on digital microfluidics". In: *Microfluidics and Nanofluidics* 27.6 (2023), p. 39. DOI: 10.1007/s10404-023-02652-5.

[60] Wendy U. Dittmer et al. "Rapid, high sensitivity, point-of-care test for cardiac troponin based on optomagnetic biosensor". In: *Clinica Chimica Acta*. This Issue Includes Abstracts from the Asian Pacific Conference of Chromatography and Mass Spectrometry 411.11 (2010), pp. 868–873. DOI: 10.1016/j.cca.2010.03.001.

[61] Danielle WM Kemper et al. "Analytical evaluation of a new point of care system for measuring cardiac Troponin I". In: *Clinical Biochemistry* 50.4 (2017), pp. 174–180. DOI: 10.1016/j.clinbiochem.2016.11.011.

[62] Maria Pawula, Zeynep Altintas, and Ibtisam E. Tothill. "SPR detection of cardiac troponin T for acute myocardial infarction". In: *Talanta* 146 (2016), pp. 823–830. DOI: 10.1016/j.talanta.2015.06.006.

[63] Camille Daniel et al. "Real time monitoring of thrombin interactions with its aptamers: Insights into the sandwich complex formation". In: *Biosensors and Bioelectronics* 40.1 (2013). Number: 1, pp. 186–192. DOI: 10.1016/j.bios.2012.07.016.

[64] Di Zhang et al. "Quantitative and ultrasensitive detection of multiplex cardiac biomarkers in lateral flow assay with core-shell SERS nanotags". In: *Biosensors and Bioelectronics* 106 (2018), pp. 204–211. DOI: 10.1016/j.bios.2018.01.062.

[65] Frank B. Myers and Luke P. Lee. "Innovations in optical microfluidic technologies for point-of-care diagnostics". In: *Lab on a Chip* 8.12 (2008), pp. 2015–2031. DOI: 10.1039/B812343H.

[66] E. Engvall and P. Perlmann. "Enzyme-linked immunosorbent assay (ELISA). Quantitative assay of immunoglobulin G". In: *Immunochemistry* 8.9 (1971). Number: 9, pp. 871–874. DOI: 10.1016/0019-2791(71)90454-x.

[67] Alexander van Reenen et al. "Analytical performance of a single epitope B-type natriuretic peptide sandwich immunoassay on the Minicare platform for point-of-care diagnostics". In: *Practical Laboratory Medicine* 15 (2019), e00119. DOI: 10.1016/j.plabm.2019.e00119.

[68] Wenwen Jing et al. "Gradient-Based Rapid Digital Immunoassay for High-Sensitivity Cardiac Troponin T (hs-cTnT) Detection in 1 L Plasma". In: *ACS Sensors* 6.2 (2021). Number: 2, pp. 399–407. DOI: 10.1021/acssensors.0c01681.

[69] In Vitrogen. *Human Troponin I ProQuantum Immunoassay Kit - Invitrogen*. URL: https://www.thermofisher.com/elisa/product/Human-Troponin-I-ProQuantum-Immunoassay-Kit/A46074 (visited on 02/28/2023).

[70] Marie Gaillard. "Développement d'un système microfluidique de tri en taille et biomarqueur-spécifique pour l'analyse de vésicules extracellulaires". Theses. Université Grenoble Alpes, Feb. 2022. URL: https://theses.hal.science/tel-03675190.

[71] Masoud Negahdary. "Aptamers in nanostructure-based electrochemical biosensors for cardiac biomarkers and cancer biomarkers: A review". In: *Biosensors and Bioelectronics* 152 (2020), p. 112018. DOI: 10.1016/j.bios.2020.112018.

[72] Panting Sang et al. "Nucleic Acid Amplification Techniques in Immunoassay: An Integrated Approach with Hybrid Performance". In: *Journal of Agricultural and Food Chemistry* 69.21 (2021), pp. 5783–5797. DOI: 10.1021/acs.jafc.0c07980.

[73] Netrapal Singh et al. "Detection of Mycobacterium tuberculosis purified ESAT-6 (Rv3875) by magnetic bead-coupled gold nanoparticle-based immuno-PCR assay". In: *International Journal of Nanomedicine* 13 (2018), pp. 8523–8535. DOI: 10.2147/IJN.S181052.

[74] Guangxin Yang et al. "A gold nanoparticle based immunosorbent bio-barcode assay combined with real-time immuno-PCR for the detection of polychlorinated biphenyls". In: *Sensors and Actuators B: Chemical* 214 (2015), pp. 152–158. DOI: 10.1016/j.snb.2015.02.128.

[75] Pengfei Zhang et al. "Magnetofluidic immuno-PCR for point-of-care COVID-19 serological testing". In: *Biosensors & Bioelectronics* 195 (2022), p. 113656. DOI: 10.1016/j.bios.2021.113656.

[76] S. Sadhasivam et al. "Application of carbon nanotubes layered on silicon wafer for the detection of breast cancer marker carbohydrate antigen 15-3 by immuno-polymerase chain reaction". In: *Journal of Materials Science: Materials in Medicine* 25.1 (2014), pp. 101–111. DOI: 10.1007/s10856-013-5060-9.

[77] Alexandr V. Ivanov et al. "Recombinase polymerase amplification combined with a magnetic nanoparticle-based immunoassay for fluorometric determination of troponin T". In: *Microchimica Acta* 186.8 (2019), p. 549. DOI: 10.1007/s00604-019-3686-0.

[78] Mohammad Pourhassan-Moghaddam et al. "Protein Detection through Different Platforms of Immuno-Loop-Mediated Isothermal Amplifica- tion". In: *Nanoscale research letters* 8 (2013), p. 485. DOI: 10.1186/1556-276X-8-485.

[79] Yi-Je Juang and Yu-Jui Chiu. "Fabrication of Polymer Microfluidics: An Overview". In: *Polymers* 14.10 (2022), p. 2028. DOI: 10.3390/polym14102028.

[80] Sumaira Nishat et al. "Paper-based microfluidics: Simplified fabrication and assay methods". In: *Sensors and Actuators B: Chemical* 336 (2021), p. 129681. DOI: 10.1016/j.snb.2021.129681.

[81] Wei Yin Lim et al. "Paper microfluidic device for early diagnosis and prognosis of acute myocardial infarction via quantitative multiplex cardiac biomarker detection". In: *Biosensors and Bioelectronics* 128 (2019), pp. 176–185. DOI: 10.1016/j.bios.2018.12.049.

[82] Sherif Bayoumy et al. "Sensitive and quantitative detection of cardiac troponin I with upconverting nanoparticle lateral flow test with minimized interference". In: *Scientific Reports* 11.1 (2021), p. 18698. DOI: 10.1038/s41598-021-98199-y.

[83] Laura Magro et al. "Paper-based RNA detection and multiplexed analysis for Ebola virus diagnostics". In: *Scientific Reports* 7.1 (2017-05-02), p. 1347. DOI: 10.1038/s41598-017-00758-9.

[84] Laura Magro et al. "Paper microfluidics for nucleic acid amplification testing (NAAT) of infectious diseases". In: *Lab on a Chip* 17.14 (2017-07-11), pp. 2347–2371. DOI: 10.1039/C7LC00013H.

[85] A. Jaisankar, S. Krishnan, and L. Rangasamy. "Recent developments of aptamer-based lateral flow assays for point-of-care (POC) diagnostics". In: *Analytical Biochemistry* 655 (2022). DOI: 10.1016/j.ab.2022.114874.

[86] Ayokunle Olanrewaju et al. "Capillary microfluidics in microchannels: from microfluidic networks to capillaric circuits". In: *Lab on a Chip* 18.16 (2018), pp. 2323–2347. DOI: 10.1039/C8LC00458G.

[87] Emmanuel Delamarche et al. "Patterned Delivery of Immunoglobulins to Surfaces Using Microfluidic Networks". In: *Science* 276.5313 (1997), pp. 779–781. DOI: 10.1126/science.276.5313.779.

[88] M. I. Mohammed and M. P. Y. Desmulliez. "Autonomous capillary microfluidic system with embedded optics for improved troponin I cardiac biomarker detection". In: *Biosensors and Bioelectronics* 61 (2014), pp. 478–484. DOI: 10.1016/j.bios.2014.05.042.

[89] Jiwoon Park et al. "Lab-on-a-Disc for Fully Integrated Multiplex Immunoassays". In: *Analytical Chemistry* 84.5 (2012), pp. 2133–2140. DOI: 10.1021/ac203163u.

[90] Y. Tang et al. "An immunoassay-based reverse-transcription loop-mediated isothermal amplification assay for the rapid detection of avian influenza H5N1 virus viremia". In: *Biosensors and Bioelectronics* 86 (2016), pp. 255–261. DOI: 10.1016/j.bios.2016.06.063.

[91] Luoran Shang, Yao Cheng, and Yuanjin Zhao. "Emerging Droplet Microfluidics". In: *Chemical Reviews* 117.12 (2017), pp. 7964–8040. DOI: 10.1021/acs.chemrev.6b00848.

[92] Pingan Zhu and Liqiu Wang. "Passive and active droplet generation with microfluidics: a review". In: *Lab on a Chip* 17.1 (2016), pp. 34–75. DOI: 10.1039/C6LC01018K.

[93] A. Rival et al. "An EWOD-based microfluidic chip for single-cell isolation, mRNA purification and subsequent multiplex qPCR". In: *Lab on a Chip* 14.19 (2014), pp. 3739–3749. DOI: 10.1039/C4LC00592A.

[94] Jienan Shen et al. "Digital Microfluidic Thermal Control Chip-Based Multichannel Immunosensor for Noninvasively Detecting Acute Myocardial Infarction". In: *Analytical Chemistry* 93.45 (2021), pp. 15033–15041. DOI: 10.1021/acs.analchem.1c02758.

[95] Todd Thorsen, Sebastian J. Maerkl, and Stephen R. Quake. "Microfluidic large-scale integration". In: *Science (New York, N.Y.)* 298.5593 (2002-10-18), pp. 580–584. DOI: 10.1126/science.1076996.

[96] Anirban Sinha et al. "An integrated microfluidic system with field-effect-transistor sensor arrays for detecting multiple cardiovascular biomarkers from clinical samples". In: *Biosensors and Bioelectronics* 129 (2019), pp. 155–163. DOI: 10.1016/j.bios.2019.01.001.

[97] Charlotte Parent. "Développement d'une plateforme autonome et portable et pour des applications santé". Theses. Université Grenoble Alpes, Oct. 2018. URL: https://theses.hal.science/tel-01996023.

[98] Priya Gopinathan et al. "Optimization of an enzyme linked DNA aptamer assay for cardiac troponin I detection: synchronous multiple sample analysis on an integrated microfluidic platform". In: *Analyst* 144.16 (2019-08-05), pp. 4943–4951. DOI: 10.1039/C9AN00779B.

[99] Quidel. *Quidel Triage Troponin I Test — Quidel*. URL: https://www.quidel.com/immunoassays/triage-test-kits/triage-troponin-i-test (visited on 10/13/2022).

[100] Robert H Christenson et al. "Comparison of 13 Commercially Available Cardiac Troponin Assays in a Multicenter North American Study". In: *The Journal of Applied Laboratory Medicine* 1.5 (2017), pp. 544–561. DOI: 10.1373/jalm.2016.022640.

[101] Durie Suh et al. "Rule-out of non-ST elevation myocardial infarction by five point of care cardiac troponin assays according to the 0 h/3 h algorithm of the European Society of Cardiology". In: *Clinical Chemistry and Laboratory Medicine (CCLM)* 56.4 (2018), pp. 649–657. DOI: 10.1515/cclm-2017-0486.

[102] Mathilde Aubret et al. *Oligonucléotide à double structure tige-boucle et utilisation dans la détection d'analytes d'intêret*. Pat. FR2109667. 2021-09-15.

[103] Mathilde Aubret et al. *Oligonucléotide linéaire et utilisation dans la détection d'analytes d'intêret*. French pat. FR2114556. 2021-12-27.

[104] Mathilde Aubret et al. *Méthode pour contrôler la qualité d'une amplification LAMP et kit utilisé à cet effet*. French pat. FR2214563. 2022-12-27.

[105] Yuanshou Zhu et al. "Nucleic acid testing of SARS-CoV-2: A review of current methods, challenges, and prospects". In: *Frontiers in Microbiology* 13 (2022). URL: https://www.frontiersin.org/articles/10.3389/fmicb.2022.1074289.

[106] Tsugunori Notomi et al. "Loop-mediated isothermal amplification of DNA". In: *Nucleic Acids Research* 28.12 (2000-06-15). Number: 12, e63–e63. DOI: 10.1093/nar/28.12.e63.

[107] Xiang Li et al. "Review in isothermal amplification technology in food microbiological detection". In: *Food Science and Biotechnology* 31.12 (2022-11-01), pp. 1501–1511. DOI: 10.1007/s10068-022-01160-6.

[108] Cassidy Mannier and Jeong-Yeol Yoon. "Progression of LAMP as a Result of the COVID-19 Pandemic: Is PCR Finally Rivaled?" In: *Biosensors* 12.7 (2022-07), p. 492. DOI: 10.3390/bios12070492.

[109] K. Mullis et al. "Specific enzymatic amplification of DNA in vitro: the polymerase chain reaction". In: *Cold Spring Harbor Symposia on Quantitative Biology* 51 Pt 1 (1986), pp. 263–273. DOI: 10.1101/sqb.1986.051.01.032.

[110] Pranab Dey. "Polymerase Chain Reaction: Principle, Technique and Applications in Pathology". In: *Basic and Advanced Laboratory Techniques in Histopathology and Cytology*. Ed. by Pranab Dey. Singapore, 2018, pp. 201–211. ISBN: 978-981-10-8252-8. DOI: 10.1007/978-981-10-8252-8_20. URL: https://doi.org/10.1007/978-981-10-8252-8_20 (visited on 06/24/2021).

[111] Masato Inaba et al. "Diagnostic accuracy of LAMP versus PCR over the course of SARS-CoV-2 infection". In: *International Journal of Infectious Diseases* 107 (2021), pp. 195–200. DOI: 10.1016/j.ijid.2021.04.018.

[112] Patrick Hardinge and James A. H. Murray. "Reduced False Positives and Improved Reporting of Loop-Mediated Isothermal Amplification using Quenched Fluorescent Primers". In: *Scientific Reports* 9.1 (2019), p. 7400. DOI: 10.1038/s41598-019-43817-z.

[113] Lisa Becherer et al. "Loop-mediated isothermal amplification (LAMP) – review and classification of methods for sequence-specific detection". In: *Analytical Methods* 12.6 (2020), pp. 717–746. DOI: 10.1039/C9AY02246E.

[114] Nathan A. Tanner, Yinhua Zhang, and Thomas C. Evans. "Simultaneous multiple target detection in real-time loop-mediated isothermal amplification". In: *BioTechniques* 53.2 (2012-08), pp. 81–89. DOI: 10.2144/0000113902. (Visited on 2022-01-07).

[115] Deguo Wang. "One-pot Detection of COVID-19 with Real-time Reverse-transcription Loop-mediated Isothermal Amplification (RT-LAMP) Assay and Visual RT-LAMP Assay". In: *bioRxiv* (2020), p. 2020.04.21.052530. DOI: 10.1101/2020.04.21.052530.

[116] Ivan Magriñá Lobato and Ciara K. O'Sullivan. "Recombinase polymerase amplification: Basics, applications and recent advances". In: *TrAC Trends in Analytical Chemistry* 98 (2018), pp. 19–35. DOI: 10.1016/j.trac.2017.10.015.

[117] Jayeon Song et al. "A novel method to detect mutation in DNA by utilizing exponential amplification reaction triggered by the CRISPR-Cas9 system". In: *Nanoscale* 13.15 (2021), pp. 7193–7201. DOI: 10.1039/D1NR00438G.

[118] Hongmei Cao et al. "Magnetic-Immuno-Loop-Mediated Isothermal Amplification Based on DNA Encapsulating Liposome for the Ultrasensitive Detection of P-glycoprotein". In: *Scientific Reports* 7.1 (2017), p. 9312. DOI: 10.1038/s41598-017-10133-3.

[119] Huan Li et al. "Establishment of Dual Hairpin Ligation-Induced Isothermal Amplification for Universal, Accurate, and Flexible Nucleic Acid Detection". In: *Analytical Chemistry* 93.6 (2021-02-16), pp. 3315–3323. DOI: 10.1021/acs.analchem.1c00007.

[120] Abdu Ahmed Abdullah AL-maskri et al. "Reverse transcription-based loop-mediated isothermal amplification strategy for real-time miRNA detection with phosphorothioated probes". In: *Analytica Chimica Acta* 1126 (2020-08), pp. 1–6. DOI: 10.1016/j.aca.2020.06.007.

[121] Maud Savonnet et al. *Procédé pour détecter et eventuellement quantifier un analyte avec un oligonucléotde à double structure tige-boucle et ledit oligonucléotide*. French pat. FR3108124. 2020-09-17.

[122] Laura E. Lamb et al. *Rapid Detection of Novel Coronavirus (COVID19) by Reverse Transcription-Loop-Mediated Isothermal Amplification*. SSRN Scholarly Paper ID 3539654. Issue: ID 3539654. Rochester, NY: Social Science Research Network, 2020-02-14. DOI: 10.2139/ssrn.3539654.

[123] Mathilde Aubret et al. "Development of an Innovative Quantification Assay Based on Aptamer Sandwich and Isothermal Dumbbell Exponential Amplification". In: *Analytical Chemistry* 94.7 (2022-02-22), pp. 3376–3385. DOI: 10.1021/acs.analchem.1c05532.

[124] Hunho Jo et al. "Electrochemical Aptasensor of Cardiac Troponin I for the Early Diagnosis of Acute Myocardial Infarction". In: *Analytical Chemistry* 87.19 (2015). Number: 19, pp. 9869–9875. DOI: 10.1021/acs.analchem.5b02312.

[125] Maud Savonnet et al. "Kinetics of Isothermal Dumbbell Exponential Amplification: Effects of Mix Composition on LAMP and Its Derivatives". In: *Biosensors* 12.5 (2022), p. 346. DOI: 10.3390/bios12050346.

[126] T. Sano, C. L. Smith, and C. R. Cantor. "Immuno-PCR: very sensitive antigen detection by means of specific antibody-DNA conjugates". In: *Science* 258.5079 (1992), pp. 120–122. DOI: 10.1126/science.1439758.

[127] Julien Dugal-Tessier, Srinath Thirumalairajan, and Nareshkumar Jain. "Antibody-Oligonucleotide Conjugates: A Twist to Antibody-Drug Conjugates". In: *Journal of Clinical Medicine* 10.4 (2021), p. 838. DOI: 10.3390/jcm10040838.

[128] Alessandro Pinto et al. "Real-time apta-PCR for 20 000-fold improvement in detection limit". In: *Molecular bioSystems* 5.5 (2009-05), pp. 548–553. DOI: 10.1039/b814398f.

[129] Andrew Csordas et al. "Detection of proteins in serum by micromagnetic aptamer PCR (MAP) technology". In: *Angewandte Chemie (International Ed. in English)* 49.2 (2010), pp. 355–358. DOI: 10.1002/anie.200904846.

[130] Yongxi Zhao et al. "Isothermal Amplification of Nucleic Acids". In: *Chemical Reviews* 115.22 (2015-11-25). Number: 22, pp. 12491–12545. DOI: 10.1021/acs.chemrev.5b00428.

[131] Ramón Lorenzo-Gómez et al. "Electrochemical aptamer-based assays coupled to isothermal nucleic acid amplification techniques: New tools for cancer diagnosis". In: *Current Opinion in Electrochemistry*. Bioelectrochemistry Electrocatalysis 14 (2019-04-01), pp. 32–43. DOI: 10.1016/j.coelec.2018.11.008.

[132] Shunbi Xie et al. "Development of an electrochemical method for Ochratoxin A detection based on aptamer and loop-mediated isothermal amplification". In: *Biosensors and Bioelectronics* 55 (2014-05-15), pp. 324–329. DOI: 10.1016/j.bios.2013.11.009.

[133] Guangxin Yang et al. "A gold nanoparticle based immunosorbent bio-barcode assay combined with real-time immuno-PCR for the detection of polychlorinated biphenyls". In: *Sensors and Actuators B: Chemical* 214 (2015), pp. 152–158. DOI: 10.1016/j.snb.2015.02.128.

[134] Yu-Dong Ma et al. "A sample-to-answer, portable platform for rapid detection of pathogens with a smartphone interface". In: *Lab on a Chip* 19.22 (2019-11-05), pp. 3804–3814. DOI: 10.1039/C9LC00797K.

[135] Tingting Zhang et al. "Polymerization nicking-triggered LAMP cascades enable exceptional signal amplification for aptamer-based label-free detection of trace proteins in human serum". In: *Analytica Chimica Acta* 1098 (2020), pp. 164–169. DOI: 10.1016/j.aca.2019.11.044.

[136] Louis C. Bock et al. "Selection of single-stranded DNA molecules that bind and inhibit human thrombin". In: *Nature* 355.6360 (1992-02), pp. 564–566. DOI: 10.1038/355564a0.

[137] Diane M Tasset, Mark F Kubik, and Walter Steiner. "Oligonucleotide inhibitors of human thrombin that bind distinct epitopes11Edited by R. Huber". In: *Journal of Molecular Biology* 272.5 (1997), pp. 688–698. DOI: 10.1006/jmbi.1997.1275.

[138] Camille Daniel et al. "On the use of aptamer microarrays as a platform for the exploration of human prothrombin/thrombin conversion". In: *Analytical Biochemistry* 473 (2015), pp. 66–71. DOI: 10.1016/j.ab.2014.12.015.

[139] Xinyuan Chen et al. "Aptamer-based applications for cardiovascular disease". In: *Frontiers in Bioengineering and Biotechnology* 10 (2022). DOI: 10.3389/fbioe.2022.1002285.

[140] Jean-Jacques Toulmé et al. "Les aptamères : du concept à l'outil". In: *Médecine Nucléaire*. 45ème Colloque de Médecine Nucléaire de Langue Française 31.9 (2007), pp. 478–484. DOI: 10.1016/j.mednuc.2007.07.009.

[141] Kechun Wen et al. "A microfluidic dual-aptamer sandwich assay for rapid and cost-effective detection of recombinant proteins". In: *Microchemical Journal* 188 (2023), p. 108454. DOI: 10.1016/j.microc.2023.108454.

[142] Ho Bin Seo and Man Bock Gu. "Aptamer-based sandwich-type biosensors". In: *Journal of Biological Engineering* 11.1 (2017-03-13), p. 11. DOI: 10.1186/s13036-017-0054-7.

[143] Shiya Qin et al. "Development of Dual-Aptamers for Constructing Sandwich-Type Pancreatic Polypeptide Assay". In: *ACS Sensors* 2.2 (2017), pp. 308–315. DOI: 10.1021/acssensors.6b00836.

[144] Veerappan Mani et al. "Multiplexed sensing techniques for cardiovascular disease biomarkers - A review". In: *Biosensors and Bioelectronics* 216 (2022), p. 114680. DOI: 10.1016/j.bios.2022.114680.

[145] Mengxing Ouyang et al. "A review of biosensor technologies for blood biomarkers toward monitoring cardiovascular diseases at the point-of-care". In: *Biosensors and Bioelectronics* 171 (2021), p. 112621. DOI: 10.1016/j.bios.2020.112621.

[146] Hyoban Lee et al. "Troponin Aptamer on an Atomically Flat Au Nanoplate Platform for Detection of Cardiac Troponin I". In: *Nanomaterials* 10.7 (2020). DOI: 10.3390/nano10071402.

[147] Yujie Han et al. "Electrochemical aptasensor for sensitive detection of Cardiac troponin I based on CuNWs/MoS2/rGO nanocomposite". In: *Microchemical Journal* 169 (2021-10-01), p. 106598. DOI: 10.1016/j.microc.2021.106598.

[148] Anabel Villalonga et al. "Amperometric aptasensor with sandwich-type architecture for troponin I based on carboxyethylsilanetriol-modified graphene oxide coated electrodes". In: *Biosensors and Bioelectronics* 183 (2021), p. 113203. DOI: 10.1016/j.bios.2021.113203.

[149] Shimeles Addisu Kitte et al. "Plasmon-enhanced quantum dots electrochemiluminescence aptasensor for selective and sensitive detection of cardiac troponin I". In: *Talanta* 221 (2021), p. 121674. DOI: 10.1016/j.talanta.2020.121674.

[150] Yi Cen et al. "Development of a novel ssDNA aptamer targeting cardiac troponin I and its clinical applications". In: *Analytical and Bioanalytical Chemistry* 413.28 (2021-11-01), pp. 7043–7053. DOI: 10.1007/s00216-021-03667-z.

[151] Radoslaw Bombera et al. "DNA-directed capture of primary cells from a complex mixture and controlled orthogonal release monitored by SPR imaging". In: *Biosensors and Bioelectronics* 33.1 (2012-03). Number: 1, pp. 10–16. DOI: 10.1016/j.bios.2011.11.034.

[152] Gang Li and Raymond E. Moellering. "A Concise, Modular Antibody–Oligonucleotide Conjugation Strategy Based on Disuccinimidyl Ester Activation Chemistry". In: *ChemBioChem* 20.12 (2019), pp. 1599–1605. DOI: https://doi.org/10.1002/cbic.201900027.

[153] J. Wiener et al. "Preparation of single- and double-oligonucleotide antibody conjugates and their application for protein analytics". In: *Scientific Reports* 10.1 (2020). Number: 1. DOI: 10.1038/s41598-020-58238-6.

[154] Lorena Baranda Pellejero et al. "Protein-Templated Reactions Using DNA-Antibody Conjugates". In: *Small* 19.13 (2023), p. 2200971. DOI: 10.1002/smll.202200971.

[155] John H. T. Luong and Sandeep K. Vashist. "Chemistry of Biotin–Streptavidin and the Growing Concern of an Emerging Biotin Interference in Clinical Immunoassays". In: *ACS Omega* 5.1 (2020), pp. 10–18. DOI: 10.1021/acsomega.9b03013.

[156] Micaela L. Everitt et al. "A critical review of point-of-care diagnostic technologies to combat viral pandemics". In: *Analytica Chimica Acta* 1146 (2021), pp. 184–199. DOI: 10.1016/j.aca.2020.10.009.

[157] Roche. *Automate de biochimie Cobas 6000 c 501 - achat*. URL: http://www.ugap.fr/achat-public/automate-de-biochimie-cobas-6000-c-501-achat_3030369.html (visited on 05/17/2023).

[158] Mais J. Jebrail, Michael S. Bartsch, and Kamlesh D. Patel. "Digital microfluidics: a versatile tool for applications in chemistry, biology and medicine". In: *Lab on a Chip* 12.14 (2012), pp. 2452–2463. DOI: 10.1039/C2LC40318H.

[159] Alfredo Edoardo Ongaro et al. "Engineering a sustainable future for point-of-care diagnostics and single-use microfluidic devices". In: *Lab on a Chip* 22.17 (2022), pp. 3122–3137. DOI: 10.1039/D2LC00380E.

[160] Kaimin Wu et al. "Recent progress of microfluidic chips in immunoassay". In: *Frontiers in Bioengineering and Biotechnology* 10 (2022). URL: https://www.frontiersin.org/articles/10.3389/fbioe.2022.1112327.

[161] Hau Van Nguyen, Vu Minh Phan, and Tae Seok Seo. "Total integrated centrifugal genetic analyzer for point-of-care Covid-19 testing with automatic and high-throughput capability". In: *Sensors and Actuators B: Chemical* 353 (2022), p. 131088. DOI: 10.1016/j.snb.2021.131088.

[162] MIT Technology Review. *10 BREAKTHROUGH TECHNOLOGIES 2001*. MIT Technology Review. URL: https://www.technologyreview.com/10-breakthrough-technologies/2001/ (visited on 06/02/2023).

[163] Lihang Zhu et al. "An integrated microfluidic electrochemiluminescence device for point-of-care testing of acute myocardial infarction". In: *Talanta* 262 (2023), p. 124626. DOI: 10.1016/j.talanta.2023.124626.

[164] The Microfluidic Association. *The Microfluidics Association — The Microfluidics Association promotes the development of the Microfluidics Industry supply chain and positively influences the growth and prosperity of its members.* URL: https://microfluidics-association.org/ (visited on 06/07/2023).

[165] *ISO/TC 48 - Laboratory equipment*. ISO. URL: https://www.iso.org/committee/48908.html.

[166] 14:00-17:00. *ISO 22916:2022*. ISO. URL: https://www.iso.org/standard/74157.html.

[167] Uyen M. N. Cao et al. "Microfluidic Organ-on-A-chip: A Guide to Biomaterial Choice and Fabrication". In: *International Journal of Molecular Sciences* 24.4 (2023), p. 3232. DOI: 10.3390/ijms24043232.

[168] Anthony Tony et al. "The Additive Manufacturing Approach to Polydimethylsiloxane (PDMS) Microfluidic Devices: Review and Future Directions". In: *Polymers* 15.8 (2023), p. 1926. DOI: 10.3390/polym15081926.

[169] Charlotte Parent et al. "A versatile and automated microfluidic platform for a quantitative magnetic bead based protocol: application to gluten detection". In: *Lab on a Chip* (2022). DOI: 10.1039/D2LC00328G.

[170] Shambhulinga Aralekallu, Rajamouli Boddula, and Vijay Singh. "Development of glass-based microfluidic devices: A review on its fabrication and biologic applications". In: *Materials & Design* 225 (2023), p. 111517. DOI: 10.1016/j.matdes.2022.111517.

[171] Vijay Vaishampayan, Ashish Kapoor, and Sarang P. Gumfekar. "Enhancement in the limit of detection of lab-on-chip microfluidic devices using functional nanomaterials". In: *The Canadian Journal of Chemical Engineering* n/a.n/a (2023). DOI: https://doi.org/10.1002/cjce.24915.

[172] Nazente Atceken et al. "Point-of-Care Diagnostic Platforms for Loop-Mediated Isothermal Amplification". In: *Advanced Engineering Materials* n/a (n/a 2023), p. 2201174. DOI: 10.1002/adem.202201174.

[173] Dhrubajyoti Das, Cheng-Wen Lin, and Han-Sheng Chuang. "LAMP-Based Point-of-Care Biosensors for Rapid Pathogen Detection". In: *Biosensors* 12.12 (2022), p. 1068. DOI: 10.3390/bios12121068.

[174] Thi Ngoc Diep Trinh and Nae Yoon Lee. "Advances in Nucleic Acid Amplification-Based Microfluidic Devices for Clinical Microbial Detection". In: *Chemosensors* 10.4 (2022), p. 123. DOI: 10.3390/chemosensors10040123.

[175] Shu-An Hsieh et al. "Digital Droplet Loop-Mediated Isothermal Amplification Featuring a Molecular Beacon Assay, 3D Printed Droplet Generation, and Smartphone Imaging for Sequence-Specific DNA Detection". In: *Analytical Chemistry* 94.34 (2022), pp. 11949–11956. DOI: 10.1021/acs.analchem.2c02979.

[176] M.G. Mauk et al. "Simple approaches to minimally-instrumented, microfluidic-based point-of-care Nucleic Acid Amplification Tests". In: *Biosensors* 8.1 (2018). Number: 1. DOI: 10.3390/bios8010017.

[177] J. F. C. Loo et al. "Sample-to-answer on molecular diagnosis of bacterial infection using integrated lab-on-a-disc". In: *Biosensors and Bioelectronics*. Special Issue Selected papers from the 26th Anniversary World Congress on Biosensors (Part II) 93 (2017), pp. 212–219. DOI: 10.1016/j.bios.2016.09.001.

[178] Hui Wu et al. "Rotary Valve-Assisted Fluidic System Coupling with CRISPR/Cas12a for Fully Integrated Nucleic Acid Detection". In: *ACS Sensors* 6.11 (2021), pp. 4048–4056. DOI: 10.1021/acssensors.1c01468.

[179] Chih-Hung Wang et al. "A magnetic bead-based assay for the rapid detection of methicillin-resistant Staphylococcus aureus by using a microfluidic system with integrated loop-mediated isothermal amplification". In: *Lab on a Chip* 11.8 (2011), pp. 1521–1531. DOI: 10.1039/C0LC00430H.

[180] Zhe Guo et al. "An integrated microfluidic chip for the detection of bacteria – A proof of concept". In: *Molecular and Cellular Probes* 29.4 (2015), pp. 223–227. DOI: 10.1016/j.mcp.2015.05.005.

[181] Yu-Dong Ma, Yi-Sin Chen, and Gwo-Bin Lee. "An integrated self-driven microfluidic device for rapid detection of the influenza A (H1N1) virus by reverse transcription loop-mediated isothermal amplification". In: *Sensors and Actuators B: Chemical* 296 (2019), p. 126647. DOI: 10.1016/j.snb.2019.126647.

[182] Yu-Shiuan Tsai et al. "Electromagnetically-driven integrated microfluidic platform using reverse transcription loop-mediated isothermal amplification for detection of severe acute respiratory syndrome coronavirus 2". In: *Analytica Chimica Acta* 1219 (2022), p. 340036. DOI: 10.1016/j.aca.2022.340036.

[183] Benoit Gilquin et al. "PepS: An Innovative Microfluidic Device for Bedside Whole Blood Processing before Plasma Proteomics Analyses". In: *Analytical Chemistry* 93.2 (2021), pp. 683–690. DOI: 10.1021/acs.analchem.0c02270.

[184] Friedrich Schuler et al. "Digital droplet LAMP as a microfluidic app on standard laboratory devices". In: *Anal. Methods* 8.13 (2016), pp. 2750–2755. DOI: 10.1039/C6AY00600K.

[185] Beatriz Oliveira et al. "Fast Prototyping Microfluidics: Integrating Droplet Digital Lamp for Absolute Quantification of Cancer Biomarkers". In: *Sensors* 20.6 (2020), p. 1624. DOI: 10.3390/s20061624.

[186] Luca Falzone et al. "Sensitivity assessment of droplet digital PCR for SARS-CoV-2 detection". In: *International Journal of Molecular Medicine* 46.3 (2020-09), pp. 957–964. DOI: 10.3892/ijmm.2020.4673.

Appendix A: List of dumbbells, oligonucleotides and primers

Name	Sequence (5'-3')	Length (bases)	Conformation
Dumbbell 1	CGGATCCAAGACGCGGTTTATCGTGCAGTACGCCAACCTTTCTC AATAAACCGCGTCTTGGATCCGCATCTCTGAGTTATATCTTTCCC CCCCTCACTGACCCTCCTTCGGGGGAAAGATATAACTCAGAGAT G	134	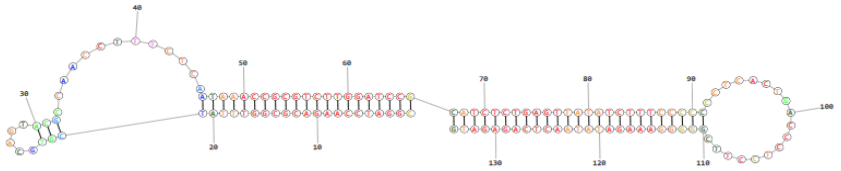
Dumbbell 1*	CGGATCCAAGACGCGGTTTATCGTGCAGTACGCCAACCTTTCTC AATAAACCGCGTCTTGGATCCG**TGA**CATCTCTGAGTTATATCTTT CCCCCCCTCACTGACCCTCCTTCGGGGGAAAGATATAACTCAGA GATG	137	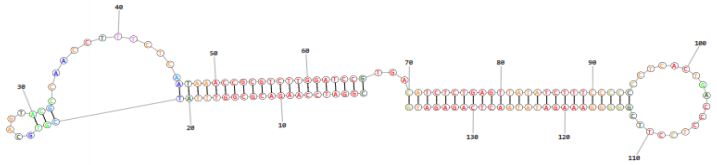
Dumbbell 2	AGAGCAGCAGAAGTGGCACA GGTGATTGTGAAGAAGAAGAG TGTGCCACTTCTGCTGCTCT **TTA** TCAACCTGAAGAAGAGCA GGCAGTGAGGACAATCAGTTCT TGCTCTTCTTCAGGTTGA	122	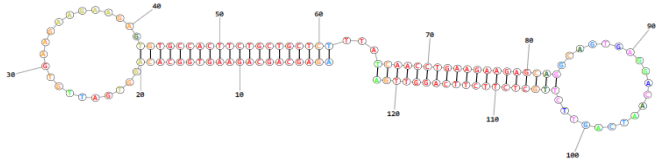
Dumbbell 3	TCCCCTACTGCTGCCTGGAG TTTTCGGCAGTCAAGCCTCTTC CTCCAGGCAGCAGTAGGGGA **TTA** TCCTGCTAGAATGGCTGGCAATT TGAACCAGCTTGAGAGCAAAAAA AATTGCCAGCCATTCTAGCAGGA	134	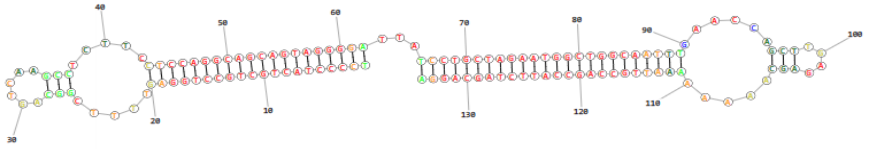
Dumbbell 4	CTGCCCCGACGATAGGCTTAAT CGTGGTCTGGTGAAGTTCTACGG ATTAAGCCTATCGTCGGGGCAG **TGA** TCCAGTGCGACCTGCTGGGTG GTACTGGCGGCGAACAATACC CACCCAGCAGGTCGCACTGGA	133	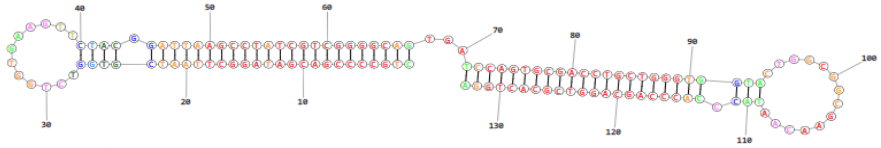

Name	Sequence (5'-3')	Length (bases)	Conformation
L1	CGTGCAGTACGCCAACCTTTCTCAATAAACCGCGTCTTGGATCC GCATCTCTGAGTTATATCTTTCCCCCCCTCACTGACCCTCCTTC	88	
L1-Floop	CGGATCCAAGACGCGGTTTATCGTGCAGTACGCCAACCTTTCTC AATAAACCGCGTCTTGGAT	112	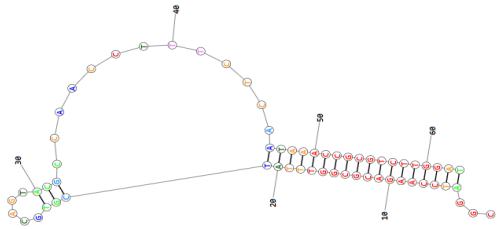
L1-Zip6-DE	**GACCGGTATGCGACCTGGTATGCG**TTTTTTTTTTCGTGCAGTAC GCCAACCTTTCTCAATAAACCGCGTCTTGGATCCGCATCTCTGAG TTATATCTTTCCCCCCCTCACTGACCCTCCTTC	122	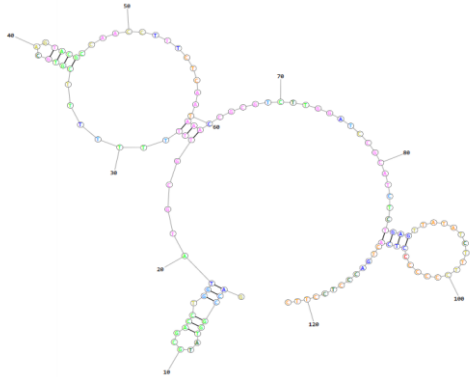
D1-Zip6-DE	**GACCGGTATGCGACCTGGTATGCG**TTTTTTTTTT AGAGCAGCAGAAGTGGCACA GGTGATTGTGAAGAAGAAGAG TGTGCCACTTCTGCTGCTCT TTA TCAACCTGAAGAAGAGCA GGCAGTGAGGACAATCAGTTCT TGCTCTTCTTCAGGTTGA	156	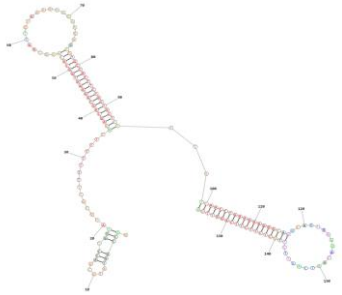

Name	Sequence (5'-3')	Length (bases)	Conformation
D1-THR-C	5’- CGGATCCAAGACGCGGTTTATCGTGCAGTACGCCAACCTTTCTC AATAAACCGCGTCTTGGATCCGT**GGTTGGTGTGGTTGG**GACAT CTCTGAGTTATATCTTTCCCCCCCTCACTGACCCTCCTTCGGGGG AAAGATATAACTCAGAGATG- 3’	152	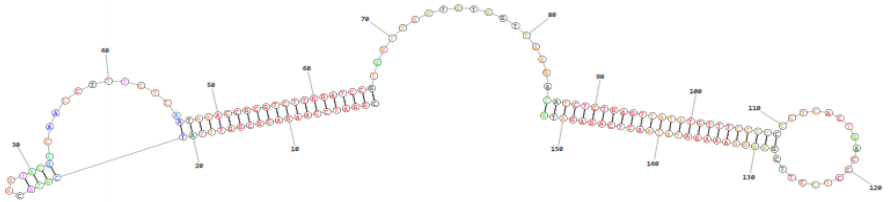
D1-THR-R	5’- CGGATCCAAGACGCGGTTTATCGTGCAGTACGCCAACCTTTCTC AATAAACCGCGTCTTGGATCCGTGACATCTCTGAGTTATATCTTT CCCCC**GGTTGGTGTGGTTGG**CCTCACTGACCCTCCTTCGGGGG AAAGATATAACTCAGAGATG- 3’	152	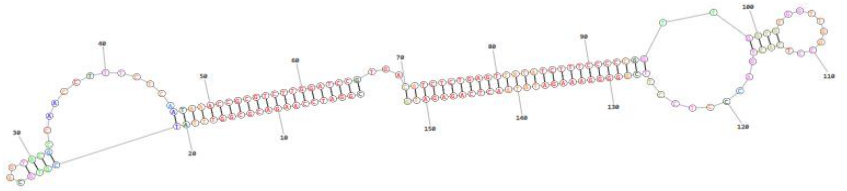
D1-THR-L	5’- CGGATCCAAGACGCGGTTTATCGTGCAGTACGCCAACCTTTCTC A**GGTTGGTGTGGTTGG**ATAAACCGCGTCTTGGATCCGTGACAT CTCTGAGTTATATCTTTCCCCCCCTCACTGACCCTCCTTCGGGGG AAAGATATAACTCAGAGATG- 3’	152	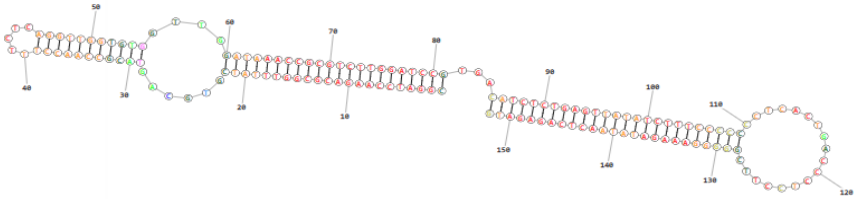
D1-THR-DE5	5’ – **GGTTGGTGTGGTTGG**TTTTTTTTTTCGGATCCAAGACGCGGTTT ATCGTGCAGTACGCCAACCTTTCTCAATAAACCGCGTCTTGGATC CGTGACATCTCTGAGTTATATCTTTCCCCCCCTCACTGACCCTCCT TCGGGGGAAAGATATAACTCAGAGATG – 3’	162	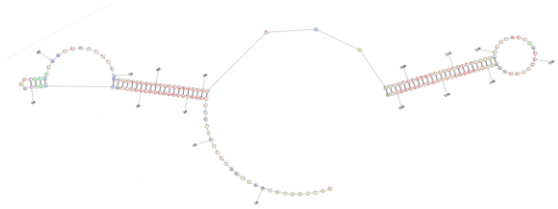
D1-THR-DE3	5'- CGGATCCAAGACGCGGTTTATCGTGCAGTACGCCAACCTTTCTC AATAAACCGCGTCTTGGATCCGTGACATCTCTGAGTTATATCTTT CCCCCCCTCACTGACCCTCCTTCGGGGGAAAGATATAACTCAGA GATGTTTTTTTTTT**GGTTGGTGTGGTTGG** - 3'	162	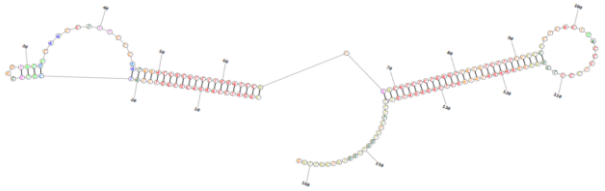

Name	Sequence (5'-3')	Length (bases)	Conformation
D2-TROPO-C	AGAGCAGCAGAAGTGGCACA GGTGATTGTGAAGAAGAAGAG TGTGCCACTTCTGCTGCTCT **CGTGCAGTACGCCAACCTTTCTCATGCGCTGCCCCTCTTA** TCAACCTGAAGAAGAGCA GGCAGTGAGGACAATCAGTTCT TGCTCTTCTTCAGGTTGA	159	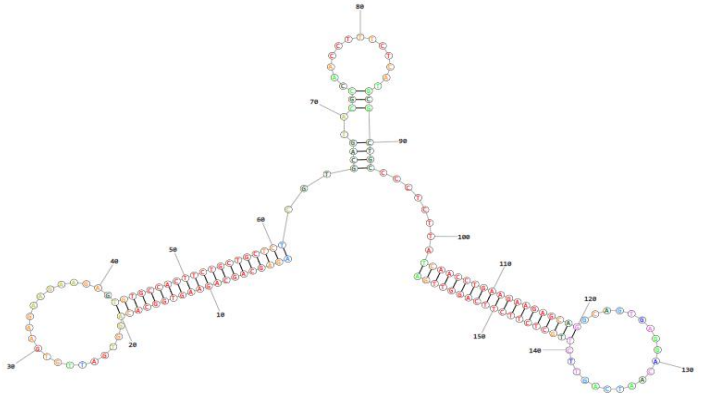
D2-TROPO-DE5	**CGTGCAGTACGCCAACCTTTCTCATGCGCTGCCCCTCTTA** TTTTTTTTTT AGAGCAGCAGAAGTGGCACA GGTGATTGTGAAGAAGAAGAG TGTGCCACTTCTGCTGCTCT TTA TCAACCTGAAGAAGAGCA GGCAGTGAGGACAATCAGTTCT TGCTCTTCTTCAGGTTGA	172	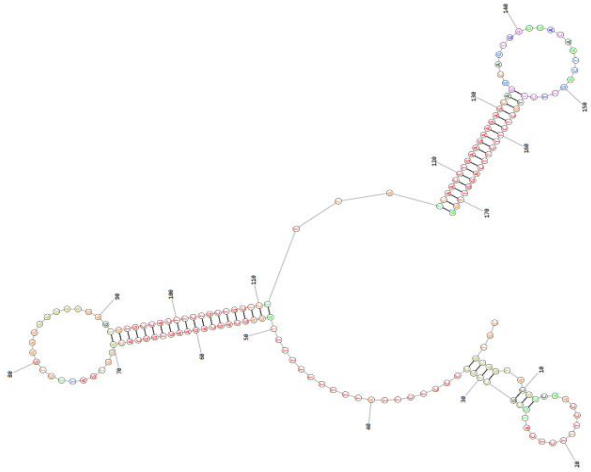

D1-Zip6-DE	GAC CGG TAT GCG ACC TGG TAT GCGTTTTTTTTTT AGAGCAGCAGAAGTGGCACA GGTGATTGTGAAGAAGAAGAG TGTGCCACTTCTGCTGCTCT TTA TCAACCTGAAGAAGAGCA GGCAGTGAGGACAATCAGTTCT TGCTCTTCTTCAGGTTGA	156	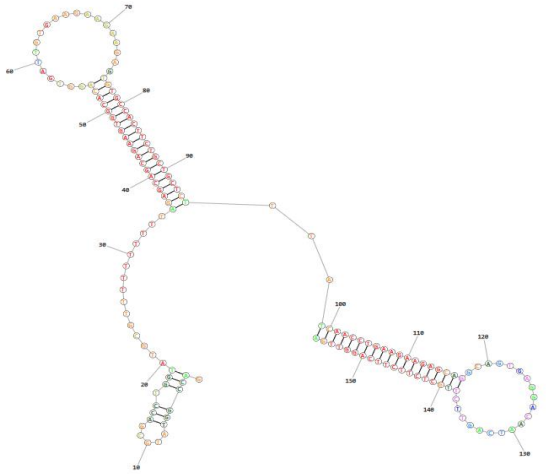
L1-Zip6-DE	GAC CGG TAT GCG ACC TGG TAT GCG TTT TTT TTT TCG TGC AGT ACG CCA ACC TTT CTC AAT AAA CCG CGT CTT GGA TCC GCA TCT CTG AGT TAT ATC TTT CCC CCC CTC ACT GAC CCT CCT TC	122	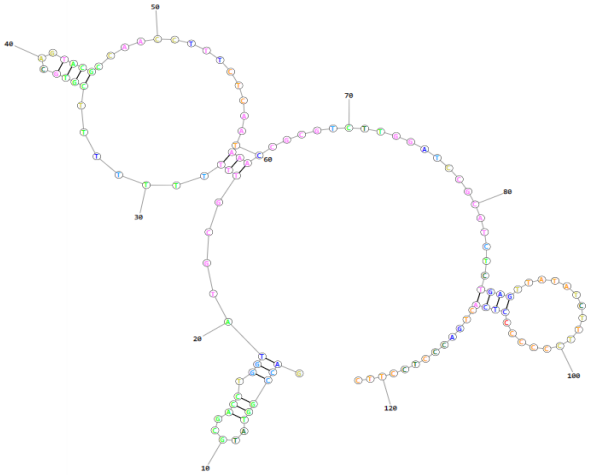

Oligonucleotides

Name	Sequence (5'-3')	Length
Zip6	GACCGGTATGCGACCTGGTATGCG	24
Zip6c	CGCATACCAGGTCGCATACCGGTC	24
Thr1	GGTTGGTGTGGTTGG	15
Thr1c	CCAACCACACCAACC	15
Thr2	AGTCCGTGGTAGGGCAGGTTGGGGTGACT	29
Tro4	CGTGCAGTACGCCAACCTTTCTCATGCGCTGCCCCTCTTA	40
Tro4c	TAAGAGGGGCAGCGCATGAGAAAGGTTGGCGTACTGCACG	40
Zip6c-Tro4	CGCATACCAGGTCGCATACCGGTC TTTTTTTTTT CGTGCAGTACGCCAACCTTTCTCATGCGCTGCCCCTCTTA	74
Zip6-Thr1c	CCAACCACACCAACCGACCGG TATGCGACCTGGTATGCG	39

Primers

Name	Sequence (5'-3')	Length
FIP	CGGATCCAAGACGCGGTTTATCGTGCAGTACGCCAACCTTTCTCA	45
BIP	CATCTCTGAGTTATATCTTTCCCCCGAAGGAGGGTCAGTGAGG	43
FIP2	AGAGCAGCAGAAGTGGCACAGGTGATTGTGAAGAAGAAGAG	41
BIP2	TCAACCTGAAGAAGAGCAAGAACTGATTGTCCTCACTGCC	40
FIP3	TCCCCTACTGCTGCCTGGAGTTTTCGGCAGTCAAGCCTCTTC	42
BIP3	TCCTGCTAGAATGGCTGGCAATTTTTTTTGCTCTCAAGCTGGTTCA	46
FIP4	CTGCCCCGACGATAGGCTTAATCGTGGTCTGGTGAAGTTCTACGG	45
BIP4	TCCAGTGCGACCTGCTGGGTGGGTATTGTTCGCCGCCAGTAC	42

Appendix B: List of buffers

Name	Composition	Chapters
Magnetic beads storage buffer (MB)	PBS 1X, 0.1% BSA, 0.05% Tween 20	3
Magnetic beads washing buffer	10 mM Tris-HCl, 1mM EDTA, 2 M NaCl	3
Hybridization buffer (HB)	PBS 1X, 1.074 NaCl, 0,3% Tween, 20 µg/mL single stranded DNA from Salmon testes, 4% Denhart	3, 5
Rinsing solution (RS)	PBS 1X, 1M NaCl, 0.3 % Tween 20	3, 5
Thrombin aptamer buffer (THAB)	20 mM Tris-HCl, 120 mM NaCl, 1 mM $MgCl_2$, 10 mM KCl pH = 7.4	3
Troponin buffer (TAB)	20 mM Tris-HCl, 300 mM NaCl, 5 mM $MgCl_2$, 0.1 % Tween 20, pH=8	3, 5
Washing buffer (WB)	PBS 1X, 1% BSA, 0.3% Tween 20, 20 µg/mL single stranded DNA from Salmon testes	3, 5
Incubation buffer (IB)	PBS 1X, 1% BSA	3, 5
Dumbbell buffer (DB)	PBS 1X, 1% BSA, 5 mM $MgCl_2$	2, 3, 5

Appendix C : LAMP mix

Mix 1

	Supplier	Final concentration
Isothermal amplification buffer	NEB M0538	1X
$MgSo_4$	NEB M0538	1 mM
dNTPs	Sigma D9156	1.4 mM
Bst 2.0 Polymerase	NEB M0538	0.4 U/mL
Eva Green	JenaBioscience PCR-379	1X
Primers (target dependant)	Eurogenetc	2.4 µM

Mix 2

	Supplier	Final concentration
Isothermal amplification buffer	NEB M0538	1X
$MgSo_4$	NEB M0538	1 mM
dNTPs	Sigma D9156	1.4 mM
Bst 2.0 Polymerase	NEB M0538	0.4 U/mL
Eva Green	JenaBioscience PCR-379	0.25X
Primers (target dependant)	Eurogenetc	2.4 µM

Mix 3

	Supplier	Final concentration
Isothermal amplification buffer	NEB M0374	1X
$MgSo_4$	NEB M0374	1 mM
dNTPs	Sigma D9156	1.4 mM
Bst 3.0 Polymerase	NEB M0374	0.4 U/mL
Eva Green	JenaBioscience PCR-379	0.25X
Primers (target dependant)	Eurogenetc	2.4 µM

Mix 4

	Supplier	Final concentration
LAMP Master Mix	NEB, E1700	1X
LAMP Fluorescent dye	NEB, B1700	1X
Primers (target dependant)	Eurogenetc	2.4 µM

Mix 5

	Supplier	Final concentration
LAMP Master Mix	NEB, E1700	0.75
LAMP Fluorescent dye	NEB, B1700	1X
Primers (target dependant)	Eurogenetc	2.4 µM

Appendix D: Experimental protocols

a. Coupling antibody to NHS-biotin

Material

- Commercial IgG
- NHS-biotin 5mM in DMSO
- UV spectrophotometer (280 nm)
- VivaSpin columns (cutoff threshold 30 kDa)

Protocol

1. Wash the commercial IgG on 30 kDa VivaSpin membrane: wash VivaSpin column
    - Wash VivaSpin column: deposit 200 µL of PBS and centrifuge (15', 15 000g)
    - Deposit 200 µL of commercial IgG (concentration about 0.5 mg/mL) and centrifuge (15', 15 000g)
    - Wash IgG twice: deposit 100 µL of PBS (mix gently), centrifuge (15', 15 000g). Repeat.
    - Resuspend in 100 µL PBS.
    - Evaluate final IgG concentration on spectrophotometer
2. Prepare NHS-biotin at 200 µM in PBS
3. Coupling reaction (raio 10 NHS-biotin : 1 antibody)

Compute the desired volume of NHS-biotin to add to the purified antibody for a coupling ratio 10:1, complete with PBS to qsp 400 µL and mix. Incubate at 4°C for at least 24h.

4. Purification of the coupled IgG
    - Wash VivaSpin column: deposit 200 µL of PBS and centrifuge (15', 15 000g)
    - Deposit 200 µL of sample on column and centrifuge (15', 15 000g)
    - Wash IgG twice: deposit 100 µL of PBS (mix gently), centrifuge (15', 15 000g). Repeat.
    - Resuspend in 100 µL PBS.
    - Evaluate final IgG-biotin concentration on spectrophotometer

b. Grafting of antibodies on Tosylactivated magnetic beads

Material

- Washing/storage buffer: PBS 1X, 0.1% BSA, 0.05% Tween 20, pH=7.4
- Blocking buffer: PBS 1X, 0.5% BSA, 0.05% Tween 20, pH=7.4
- Coating buffer: 0.1 M Sodium Borate pH = 9.5
- 3M Amonium sulfate in coating buffer
- Magnetic beads MyOne Tosylactivated (InVitrogen, 65501) 100 mg/mL
- Antibody
- VivaSpin membrane 50 kDa

Protocol to bind 0.5 mg of antibody to 12.5 mg of magnetic beads

1. Magnetic beads washing
   Withdraw 125µL of Dynabeads and wash thrice with 1 mL washing buffer. Resuspend the magnetic beads in 100 µL of coating buffer (final beads concentration 125 mg/mL)
2. Antibody purification
   - Wash the VivaSpin membrane by adding 500 µL PBS and centrifuge (10', 12 000g)
   - Wash 0.5 mg of antibody on the membrane (10', 12 000g)
   - Check the antibody concentration after purification on spectrophotometer
3. Coating protocol. Coupling volume V_{tot} = 625 µL
   Compute and mix the following quantities of each compound

	Magnetic beads	**Purified antibody**	**Coating buffer**	**Amonium sulfate solution**
V	V_{MB} = 100 µL	V_{IgG}	$V_{buffer} = V_{tot} - (V_{MB} + V_{IgG} + V_{A)}$	V_A = 208 µL
m	12.5 mg	0.5 mg		

   Incubate for 16-24h at 37°C with slow tilt rotation.

4. Blocking
   Place the tube on the magnet for 2 minutes and remove the supernatant.
   Add 625 µL of blocking buffer and incubation at 37°C overnight.
5. Washing and resuspension
   Place the tube on the magnet for 2 minutes and remove the supernatant.
   Add 1 mL of washing buffer and resuspend. Repeat twice.
   Finally resuspend the magnetic beads at the desired concentration in storage buffer.

Appendix E: microfluidic chip assembly thermal study

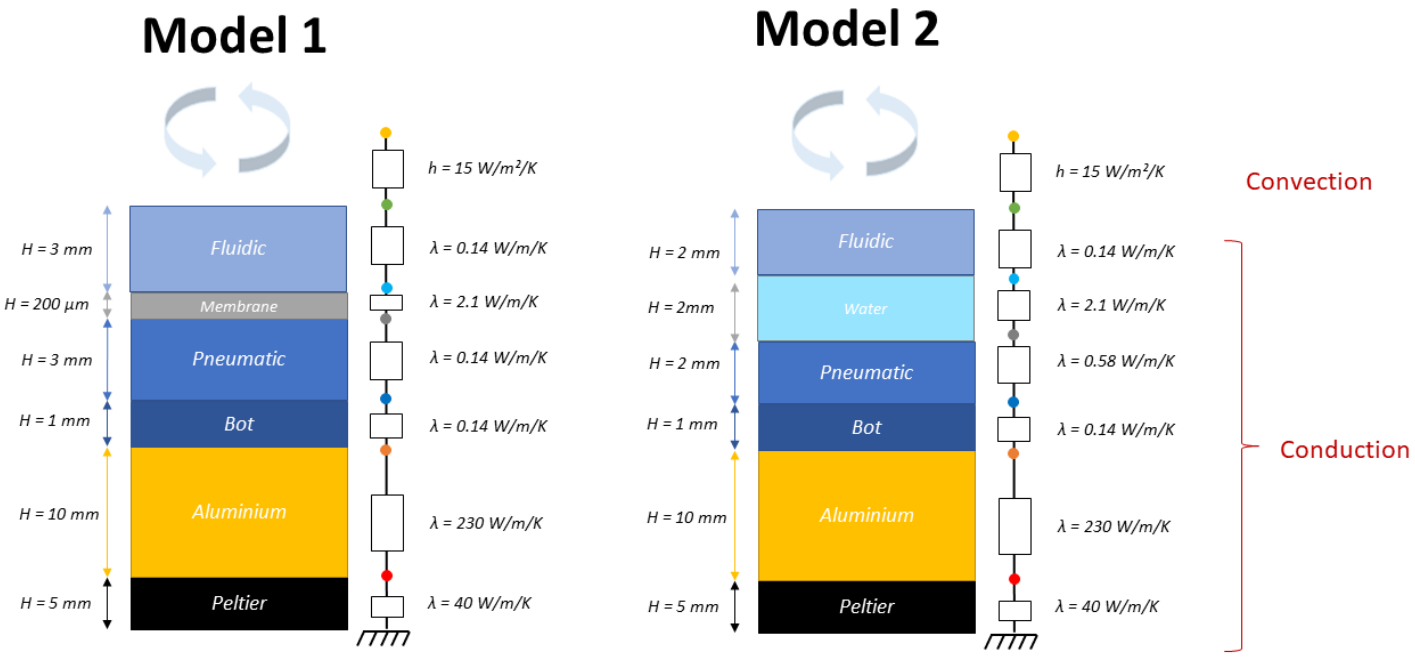

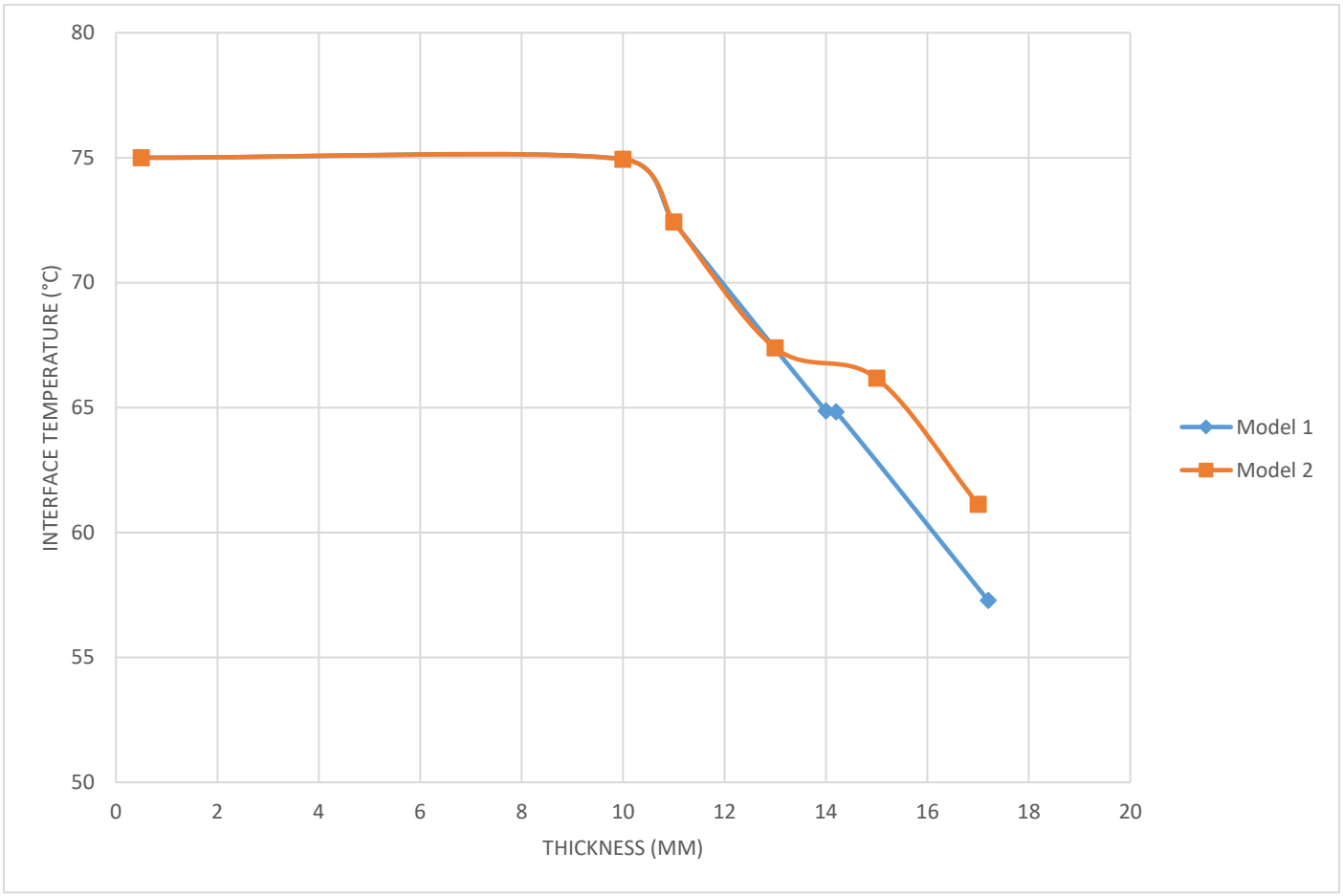

Appendix F: List of designed microfluidic cartridges

Cartridge name	Specificity	SolidWorks CAD
SP.1	8 rows	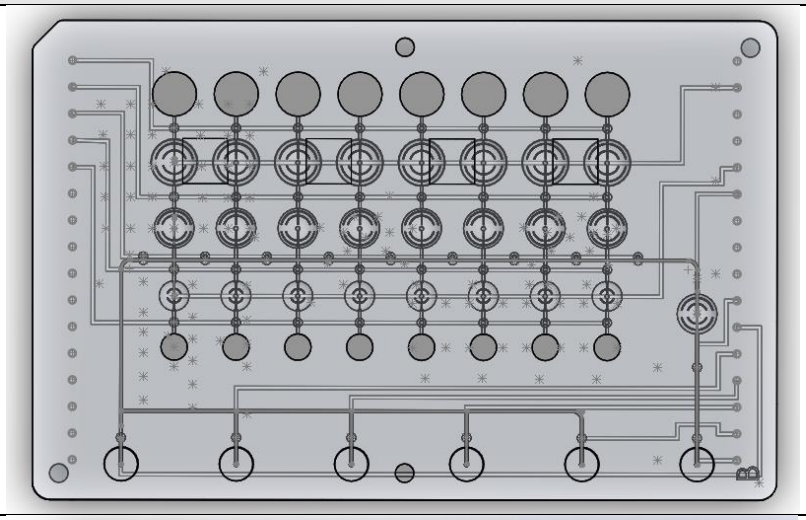
SP.2	10 rows	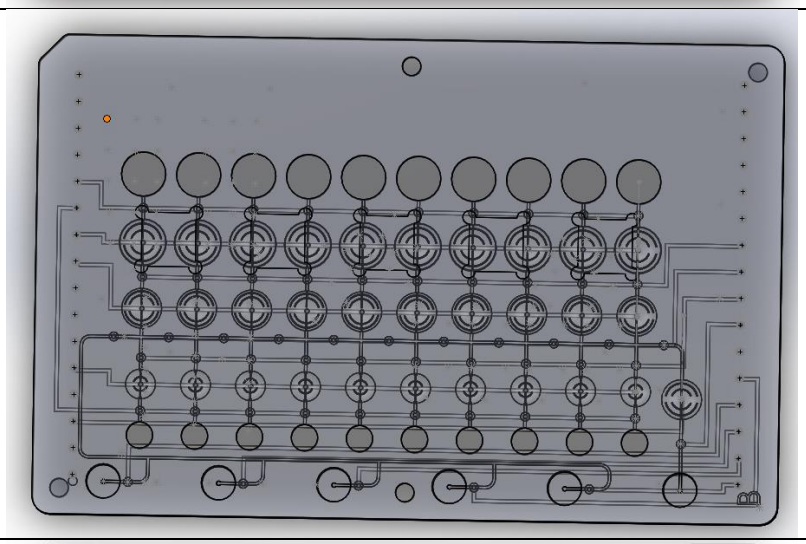
L.1	10 rows + 1 line of LAMP chambers	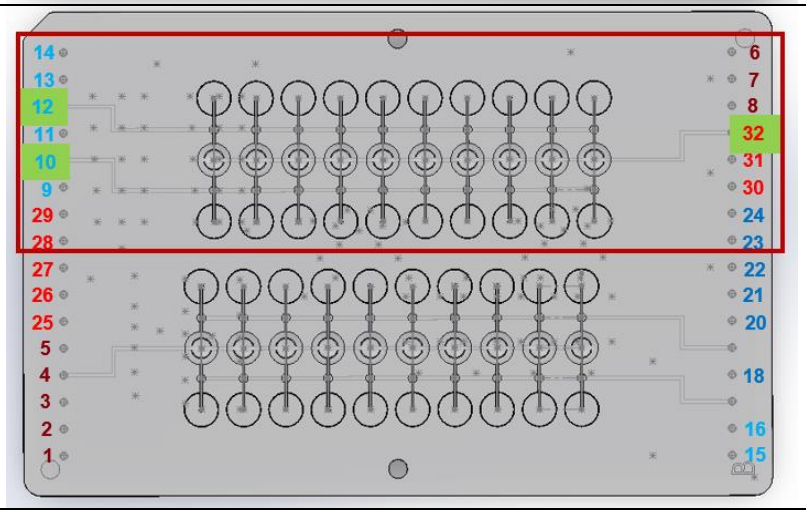

L.2	10 rows + 2 line of LAMP chambers	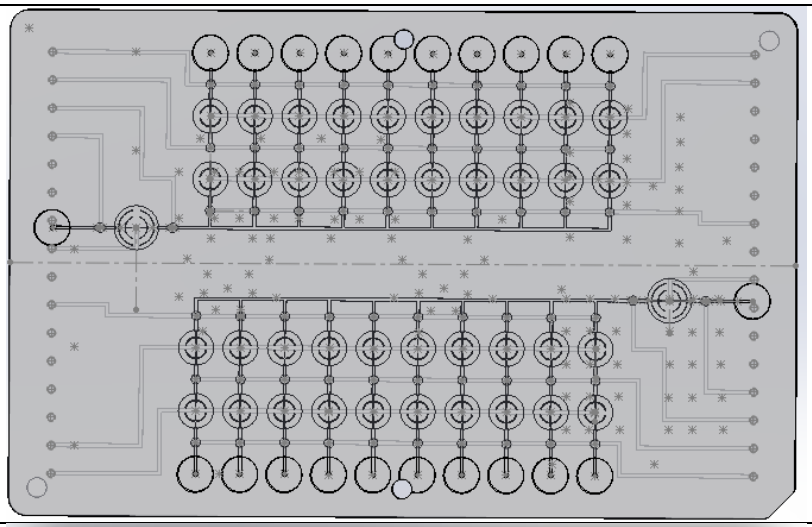
C.1	10 rows + 2 lines of amplification chambers	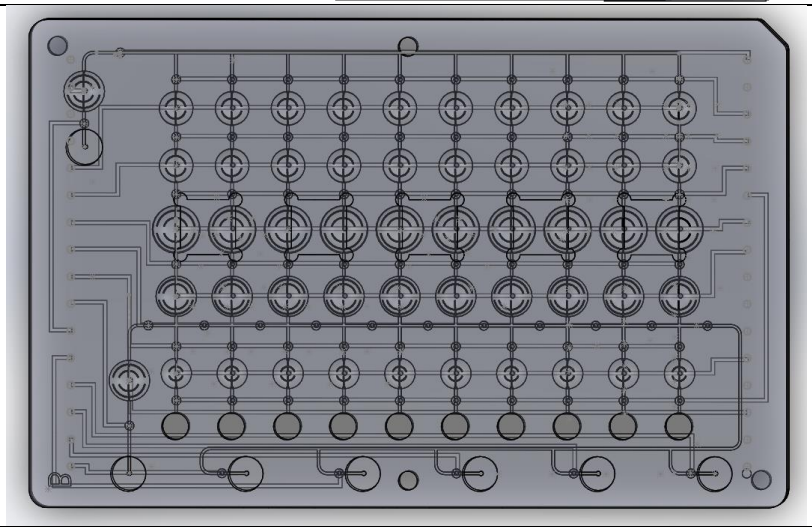
C.2	10 rows + 3 lines of amplification chamber	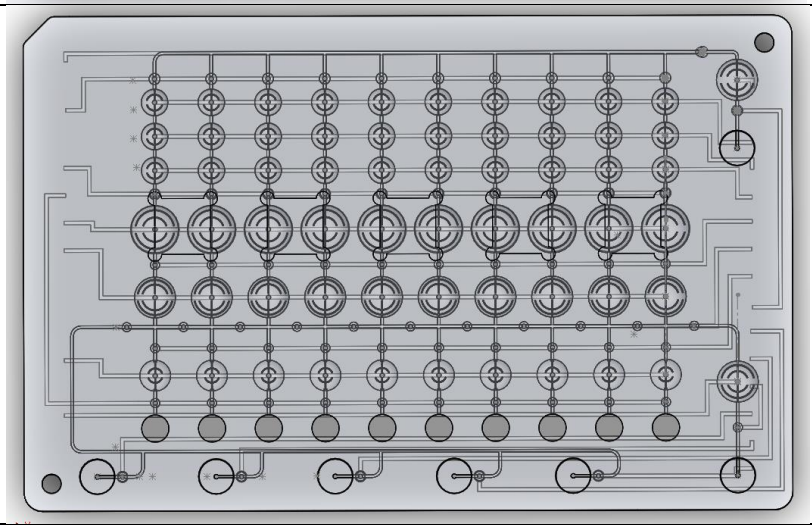

Appendix G: Uflu software functions and scripts

Example of fluid transfer from C3 to C4 and C5:

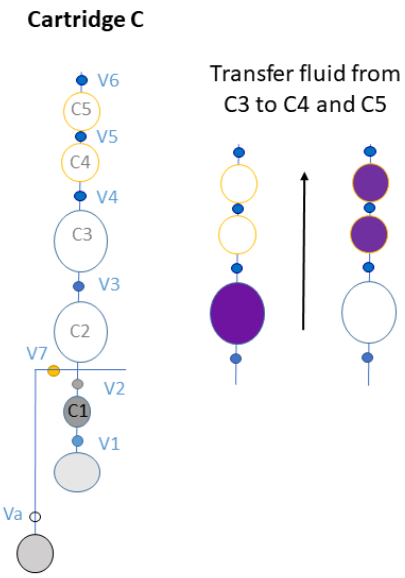

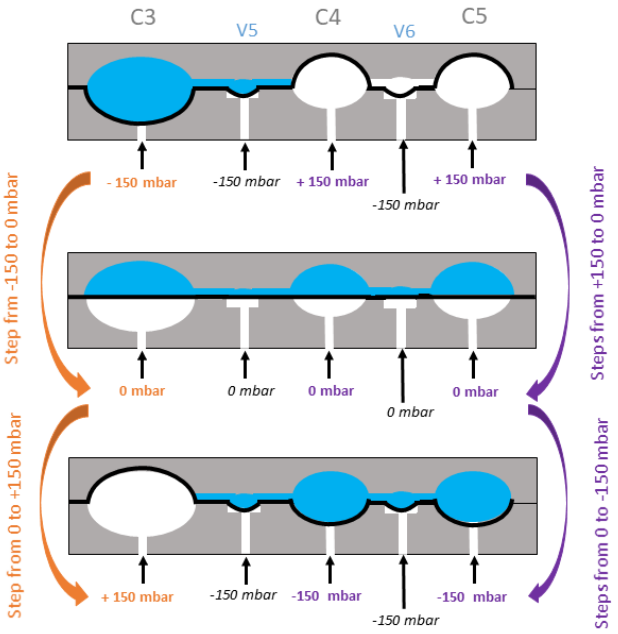

transfer_2chambers(['Ch3','Ch4','Ch5'],['V4','V5'],25)

Function **transfer_2chambers:**

Step	Action
0	Initial step: chamber 1 is ON (-150 mbar) and the two other chambers are OFF (+150 mbar)
1	Open intermediate valves
2	Put all the pressure to 0 with 25 mbar pressure step
3	Switch the first chamber to OFF and the two other chambers to ON
4	Set all the pressure again to +150 mbar (OFF) and -150 mbar (ON) with pressure step 25 mbar
5	Close the intermediate valves

Implementation of the function **transfer_2chambers** in Python script:

```python
import sde
import time
import os
#already defined common functions
from lsmb.base import *
from lsmb.fluidic import *

def pressure_step(Pneg1,Pneg2,Pnegstep,Ppos1,Ppos2,Pposstep):
    """function that implement pressure steps from Pneg2 to Pneg1 with
    Pnegstep and Ppos1 to Ppos2 with Pposstep"""
    NstepN = int(abs(Pneg2-Pneg1)/Pnegstep)
    NstepP = int(abs(Ppos2-Ppos1)/Pposstep)
    if NstepN != NstepP:
        print('The two pressure steps are not equivalent and cannot be run simultaneously')
    else:
        Pneg=Pneg1
        Ppos=Ppos1
        for i in range (NstepN+1):
            sde.execute_sde_command( 'uflu_write_decimal_attribute', '-ctrl', 'Pressure',
            '-attr', 'Target for PNEG', '-read_back', 'TRUE', '-value', str(int(Pneg)))
            Pneg=Pneg+Pnegstep
            sde.execute_sde_command( 'uflu_write_decimal_attribute', '-ctrl', 'Pressure',
            '-attr', 'Target for PC', '-read_back', 'TRUE', '-value', str(int(Ppos)))
            Ppos = Ppos - Pposstep
            time.sleep(1)

def transfer_2chambers(ch,valve,Pstep):
    """function that transfer the fluid between chamber 1 towards 2 successive chambers with
    pressure steps
    ch : list of chamber Ev (x3)
    valve : list of valve Ev (x2)
    Pstep : pressure step in mbar (ex 15 mbar)
    At the begining, one chamber is ON (-P) and the two others are off (+P)"""

    #Open the middle valves
    sde.execute_sde_command( 'uflu_set_some_ev', '-ev_group', 'EV', '-on', valve[0], '-on', valve[1] )
    sde.execute_sde_command( 'wait', '-ms', '1000' )

    #Step 1 : set the pressure to 0 in all chambers
    pressure_step(-150,0,Pstep,150,0,Pstep)
    #Step 2 : shift the chamber values
    sde.execute_sde_command( 'uflu_set_some_ev', '-ev_group', 'EV', '-off', ch[0] )
    sde.execute_sde_command( 'uflu_set_some_ev', '-ev_group', 'EV', '-on', ch[1], '-on', ch[2] )
    sde.execute_sde_command( 'wait', '-ms', '1000' )
    #Step 3 : new pressure rampe
    pressure_step(0,-150,-Pstep,0,150,-Pstep)
    #Close the middle valves
    sde.execute_sde_command( 'uflu_set_some_ev', '-ev_group', 'EV', '-off', valve[0], '-off', valve[1] )
    sde.execute_sde_command( 'wait', '-ms', '1000' )

```

List of contributions

Peer-reviewed papers

- **Mathilde Aubret**, Maud Savonnet, Patricia Laurent, Yoann Roupioz, Myriam Cubizolles, and Arnaud Buhot *Development of an Innovative Quantification Assay Based on Aptamer Sandwich and Isothermal Dumbbell Exponential Amplification* Analytical Chemistry 2022 94 (7), 3376-3385 DOI: 10.1021/acs.analchem.1c05532
- Maud Savonnet, **Mathilde Aubret**, Patricia Laurent, Yoann Roupioz, Myriam Cubizolles, and Arnaud Buhot. 2022. *Kinetics of Isothermal Dumbbell Exponential Amplification: Effects of Mix Composition on LAMP and Its Derivatives* Biosensors 12, no. 5: 346. https://doi.org/10.3390/bios12050346

Patents

- FR2109667 Oligonucléotide à double structure tige-boucle et utilisation dans la détection d'analytes d'intêret
- FR2114556 Oligonucléotide linéaire et utilisation dans la détection d'analytes d'intêret
- FR2214563 Méthode pour contrôler la qualité d'une amplification LAMP et kit utilisé à cet effet
- FR2310266 Procédés d'analyses d'un échantillon liquide dans un dispositif microfluidique
- Système optique de surveillance d'un échantillon par fluorescence

International conferences

- Aubret *et al*, *Developement of an innovative quantification assay based on aptamer sandwich and isothermal dumbbell exponential amplification*, Biosensors 2021
- Aubret *et al*, *Automated microfluidic platform for on field high sensitivity quantification of cardiac troponin I*, NanoBiotech Montreux 2022

Résumé

Français

Les maladies cardiovasculaires représentent la première cause de décès dans le monde. Un diagnostic précis et rapide est primordial pour la prise en charge des patients et la réduction de la mortalité. Plusieurs molécules sont libérées dans le sang avant un accident cardiaque, et leur dosage permet de poser un diagnostic précis. Souvent, ces dosages sont réalisés en laboratoire d'analyse médicales et nécessitent des instruments couteux et des temps d'analyse longs.

Le projet de thèse vise à proposer un dispositif portable pour la détection de marqueurs cardiaques dans le sang, permettant un diagnostic rapide et au plus près du patient. Pour cela, des protocoles biologiques de détection sensibles sont développés et couplés à une plateforme automatisée, intégrant des cartouches microfluidiques pour la gestion des protocoles biologiques, depuis le prélèvement de l'échantillon sanguin jusqu'au résultat.

Cette nouvelle approche de détection biologique ouvre de nombreuses perspectives pour répondre aux besoins de la médecine personnalisée de demain, demandant des protocoles d'analyse sensibles, rapides, robustes et portables.

English

Cardiovascular diseases are the leading cause of death worldwide. A precise and rapid diagnosis is essential for patient care and mortality reduction. Several molecules are released in patient blood prior to a cardiac accident, and testing these molecules allows a precise diagnosis. In most cases, these tests are performed in central medical laboratories, using costly equipment and long analysis times.

The PhD project goal is to develop a portable device for the sensitive detection of cardiac biomarkers in blood, to propose a rapid and delivered diagnostic tool. To do so, sensitive biological detection protocols are developed and integrated into a portable and automated platform. This platform contains microfluidic cartridges that carry out all the operations from sample recovery to result.

This new approach paves the way to many perspectives for the future of healthcare, requiring sensitive, rapid, robust and portable detection devices.